

**Organic Receptors for Chemical Sensors realized on Flexible
Substrates**

**Organische Rezeptoren für Chemische Sensoren realisiert auf
flexiblen Substraten**

Dissertation

der Mathematisch-Naturwissenschaftlichen Fakultät

der Eberhard Karls Universität Tübingen

zur Erlangung des Grades eines

Doktors der Naturwissenschaften

(Dr. rer. nat.)

vorgelegt von

Sudam S. Pandule

aus Shirasgaon Kata (Indien)

Tübingen

2014

Tag der mündlichen Qualifikation:

17.06.2014

Dekan:

Prof. Dr. Wolfgang Rosenstiel

1. Berichterstatter:

Prof. Dr. Udo Weimar

2. Berichterstatter:

Prof. Dr. Krishna Persaud

This doctoral thesis was carried out at the Institut für Physikalische und Theoretische Chemie, der Mathematisch-Naturwissenschaftlichen Fakultät, Eberhard Karls Universität, Tübingen (Germany) under the guidance of Dr. Nicolae Barsan and Prof. Dr. Udo Weimar and in collaboration with the School of Chemical Engineering and Analytical Science, The University of Manchester (UK) under the guidance of Prof. Krishna Persaud during the period from March 2011 to April 2014. This work was carried out in the framework of the European Union Project FlexSmell FP7-People-ITN-2008, Project No. 238454.

..... To My Dear Parents

Acknowledgements

First of all, I would like to express my most sincere appreciation and thanks to my supervisors **Dr. Nicolae Barsan** and **Prof. Dr. Udo Weimar**. I am very grateful to them for providing me the opportunity to work in their research group. I'm thankful not only for the endowed confidence, freedom in the choice of my research and the execution of my own ideas, but also for their competent advice, constant encouragement and limitless patience during the course of my doctoral thesis.

I have no words to thank **Prof. Krishna Persaud** for his unlimited guidance, constant encouragement and practical support during my research work at The University of Manchester, UK. His advice, ideas and encouragement brought real life in my work.

My hearty thanks go to **Dr. Alexandru Oprea** (Sandu) for his constant guidance, patient teaching and help in my work. He has been not only the advisor but also a good friend.

My special thanks to all my colleagues for their very friendly nature and being so supportive in the institute. I am thankful to Peter, Sven, Alex, Ulrike, Elke, Sandra, David, Jens, Susi, Thomas, Julia, Andre, and Benedikt. I must thank Ute Harbusch, Diana Strauss and Egon Merz for their administrative support which made my life easy so that I could focus more on scientific work.

I am thankful to our "FlexSmell" project partners, Dr. Danick Briand, Ehsan, Elena, Andreas, Francisco and Giorgio for their collaborative research and cooperation during the project.

I thank Dr. Anton Khartulyari, Dr. Pramod Sawant and Dr. Sandip Dhayade for their valuable discussion on practical chemistry. My thank goes to Prof. Thomas Chasse, Elke Nadler and Dr. Dorothee Wistuba for their assistance in numerous analytical measurements.

I should thank Prof. Sanjay Madane, Prof. V.V. Chabukswar, Dr. Suresh Shisodia, Prof. L.R. Patil, Prof. D.G. Hingane, Dr. Nawalkishor Mal, Dr. K.S. Nagabhushana, Dr. Uday Avalakki, Suyog Zond, Sandip Sabale, Prashant Jamdar, Prasad Mulay, Kalidas Rasal, Yogesh Gugale,

Acknowledgements

Vijay Hirave, Sandeep Dhavale, Shankar Lade and all my college teachers for encouraging me to learn chemistry and laboratory skills during my studies in India.

I wish to express my sincere feelings to my parents for their great sacrifices and support. Without them, I would not be what I am today. Of course, I thank my wife Rani who stood beside me, also for her infinite love and support to achieve this milestone.

Last but not the least, I gratefully acknowledge European Commission for awarding the Marie-Curie international research fellowship for my doctoral studies on EU project, FlexSmell, FP7-People-ITN-2008, Project No. 238454.

Zusammenfassung

Das Ziel dieser Arbeit war die Synthese und Charakterisierung einer Serie von leitenden Dithienyl Pyrrol basierten Polymeren (SNS) sowie deren Anwendung als chemische Gas-Sensoren. Diese Arbeit wurde mit der Perspektive ein flexibles multisensorisches Radiofrequenz-Identifikationssystem (RFID) für die Überwachung von verderblichen Gütern zu entwickeln durchgeführt, welches das Ziel des EU-Projektes "FlexSmell ist.

In diesem Zusammenhang wurden mehrere Dithienyl Pyrrol - Derivate synthetisiert und durch chemische und elektrochemische Methoden polymerisiert. Die Synthese von SNS-basierten Polymeren unter Anbringung verschiedener funktioneller Gruppen an das Polymerrückgrat wurde unternommen um den Effekt der Elektronen schiebenden / ziehenden Substituenten auf die Polymereigenschaften zu untersuchen. Des Weiteren wurden SNS Polymere mit Halogenatomen (F, Cl, Br und I) hergestellt um deren Effekt auf die Polymereigenschaften zu untersuchen. Flexible chemoresistive Sensoren wurden durch elektrochemische Beschichtung der SNS Polymere auf Substrate mit Interdigitalelektroden (IDE) hergestellt. Die Sensoren wurden bezüglich der Analyte, die für die Verfaulung von verderblichen Gütern verantwortlich sind, wie z.B. Feuchtigkeit, Ammoniak, Ethanol, etc. charakterisiert.

Die optischen Absorptionsspektren für die leitenden SNS Polymere zeigen klar definierte Absorptionsbanden, die einem π - π^* -Übergang, oder den Übergängen zwischen Polaronen, Bipolaronen und Bandzuständen zugeordnet werden können. Diese Merkmale stimmen mit der guten Leitfähigkeit, die die untersuchten Materialien zeigen, überein die man im Rahmen des Leitfähigkeitsmodells für organischen Materialien mit delokalisierten π -Bindungen erwartet. Es wurde der Substituenteneinfluss auf die elektrische Leitfähigkeit der Polymere beobachtet. Die elektrische Leitfähigkeit der Polymere kann mit dem elektronenschiebenden Charakter und der Elektronegativität (gilt für die Polymere mit Halogenatomen) der Substituenten korreliert werden. Die Polymere wurden auch bezüglich ihrer thermischen Stabilität, Morphologie usw. untersucht. Die SNS Polymere, die bezüglich ihrem sensitiven Verhalten gegenüber Feuchtigkeit, Ammoniak und Ethanol untersucht wurden, zeigten eine lineare Zunahme des Widerstandes mit der relativen Feuchtigkeit und eine Potenzfunktion bezüglich den Konzentration der anderen Analyten.

Es wurden auch Versuche unternommen Copolymere bestehend aus Dithienyl Pyrrol-Dialkylbithiazolen herzustellen um leicht lösliche Polymere zu synthetisieren, die unter Umgebungsbedingungen stabil sind. Diese sollten als chemische Sensoren Einsatz finden.

Das Hauptziel des FlexSmell Projektes, Entwicklung eines flexiblen multisensorischen RFID Systems, wurde durch die Zusammenarbeit mit der Ecole Polytechnique Federale de Lausanne (EPFL), Schweiz, der Universität von Manchester (UK) und dem Holst Centre (Niederlanden) erreicht. Die multiSensor Plattform wurde am EPFL entwickelt, während das RFID tag am Holst Centre entwickelt wurde. Die multiSensor Plattform mit Sensoren mit verschiedenen Transduktionsprinzipien wurde mittels Ink-jet-Druck von Ag Nanopartikelintinte auf flexiblen Polyethylen Therephthalat - Folien hergestellt. Die Plattform hat zwei IDE Kondensatoren für die Detektion von Feuchtigkeit, einen Widerstandsdetektor für die Temperaturmessung und zwei IDE Widerstandsvorrichtungen für die Detektion von Ammoniak und VOCs. Die kapazitiven Vorrichtungen wurden mit Cellulose Acetat Butyrat oder Polyether Urethan Schichten an der Universität Tübingen funktionalisiert, während die Widerstandsvorrichtungen an der Universität von Manchester mit Polyanilin und Polypyrrol Schichten funktionalisiert wurden. Das RFID tag wurde in die multiSensor Plattform durch einen hybrid Ansatz integriert. Im Vergleich zu den aktuell erhältlichen sensorischen RFID-Systemen, die auf Siliziumtechnologie basieren, zeigt unser Prototyp bestehend aus einer preisgünstigen, multisensorischen Plattform mit drahtlosen Kommunikationsmöglichkeiten einen sehr vielversprechenden Ansatz für die nächste Generation an intelligenten RFID tags.

Ein anderer Teil dieser Arbeit befasste sich mit der Möglichkeit Schweine Odorant Binding Proteins in die Struktur von Feldeffekt Biosensoren für Gase durch chemische oder physikalische Immobilisierung der biologischen Materialien auf Goldbeschichteten Substraten zu integrieren. Dieses Konzept wurde durch differentielle Kelvin-Sonde Messungen untersucht. Diese Forschung wurde ebenfalls im Rahmen des FlexSmell Projektes getätigt mit dem Ziel Biosensor basierte RFID Systeme zu entwickeln.

Abstract

The aim of this research was to carry out synthesis and characterization of series of dithienyl pyrrole (SNS) based conducting polymers and their applications as chemical gas sensors in the perspective of development of flexible multisensing radio frequency identification (RFID) system for perishable goods monitoring, the aim of the EU project 'FlexSmell'.

In this context, number of dithienyl pyrrole derivatives were synthesized and polymerized by both chemical and electrochemical methods. The synthesis of SNS based polymers with different functionalities on their backbone was undertaken in order to study the effect of electron donating/withdrawing substituents on the properties of the polymers. The SNS polymers with halogen atoms (F, Cl, Br and I) were also prepared and studied for their effects on the properties of the polymers. Flexible chemoresistive sensors were fabricated by electrochemical deposition of the SNS polymers onto interdigitated electrodes (IDE) substrates. The sensors were characterized against the analytes responsible for decay of perishable goods, such as humidity, ammonia, ethanol etc.

The optical absorption spectra of the SNS conducting polymers showed well defined absorption bands due to π - π^* transition or to the transitions among polaron, bipolaron and band states. These features correlate with the good conductivity shown by the investigated compounds when regarded in the frame of the conduction models for organic materials owning delocalised π bonds. The influence of the substituents on the electrical conductivities of the polymers was analysed. The polymers have their electrical conductivity linked to the electron donating character and electronegativity (for the polymers with halogen atoms) of the substituents. The polymers are also studied for their thermal stability, morphology etc. The SNS polymers characterized for their sensing performances against humidity, ammonia and ethanol showed linear increase in their resistances with the relative humidity and a power function one in respect with the concentrations of the other analytes.

Attempts have also been made towards the synthesis of dithienyl pyrrole-dialkylbithiazoles copolymers for the synthesis of easily soluble and environmentally stable polymeric materials intended to be used for chemical sensing.

The main goal of the FlexSmell project, development of flexible multisensing RFID system was achieved by working in collaboration with Ecole Polytechnique Federale de Lausanne (EPFL), Switzerland, The University of Manchester (UK) and Holst Centre (The

Netherlands). The multisensor platform was developed at EPFL whereas RFID tag at Holst Centre. Multisensor platforms with sensors of different transduction principles were fabricated by ink-jet printing of Ag-nanoparticle ink on flexible polyethylene terephthalate foils. The platforms have two IDE capacitors for humidity sensing, one resistive temperature detector for temperature measurement and two IDE resistive devices for ammonia and VOCs detection. The capacitive devices were functionalised with cellulose acetate butyrate or polyether urethane layers at University of Tübingen whereas resistive ones with polyaniline and polypyrrole layers at The University of Manchester. The RFID tag was integrated with the multisensor platform through a hybrid approach. In comparison with the currently available RFID sensing systems based on silicon technology, our prototype of low cost flexible multisensing platform with wireless communication capabilities represents a very promising approach for the next generations of smart RFID tags.

Another part of the work explored the possibility to incorporate porcine odorant binding proteins in the structure of field effect gas biosensors through chemical and physical immobilization of the biological material on gold coated substrates. The concept has been tested by differential Kelvin probe measurements. This investigation was also performed in the frame of FlexSmell project for future developments of biosensor based RFID systems.

Keywords: Conducting polymers, Dithienyl pyrrole, Chemical gas sensors, Smart multisensing RFID, Biosensors.

Table of Contents

Acknowledgements	9
Zusammenfassung	11
Abstract.....	13
Table of Contents	15
List of abbreviations and symbols	20
1. Introduction and Theoretical background	23
1.1 Motivation of the project.....	25
1.2 Chemical sensor	27
1.2.1 Chemical sensor principle	27
1.2.2 Classification of chemical sensors.....	29
1.3 Chemical gas sensor types.....	30
1.3.1 Conducting polymer sensors: Chemoresistors	30
1.3.2 Metal oxide sensors	32
1.4 Conducting polymers as chemical sensors.....	34
1.5 Synthesis of conducting polymers.....	36
1.5.1 Chemical polymerization.....	36
1.5.2 Electrochemical polymerization	37
1.5.2.1 Cyclic Voltammetry.....	39
1.5.2.2 Chronoamperometry	42
1.5.2.3 Mechanism of electrochemical polymerization	43
1.5.3 Functional doping.....	44
1.5.4 Electronic conduction in conducting polymers	44
1.6 Fabrication of flexible polymer sensor.....	47
1.6.1 Electrochemical deposition.....	48

1.6.2 Dip coating	48
1.6.3 Drop casting.....	49
1.6.4 Other methods.....	49
1.7 Sensing principles / detection mechanism	49
1.7.1 Chemical interactions	49
1.7.2 H-bonding and dipole-dipole interaction.....	51
1.8 Aims of the study	51
1.9 Thesis outline	52
2. Poly(dithienyl pyrrole) based chemical gas sensors.....	55
2.1 Monomer Synthesis.....	58
2.1.1 Reason for general synthetic route chosen	58
2.1.2 Friedel-Crafts acylation: Synthesis of 1,4-diketone intermediate	59
2.1.3 Paal-Knorr Pyrrole synthesis: Synthesis of 2,5-di(2-thienyl)-1H-pyrroles	60
2.1.4 Complete reaction scheme.....	62
2.2 Experimental section.....	64
2.2.1 Materials and instrumentation	64
2.2.1.1 Chemicals and working techniques	64
2.2.1.2 NMR spectroscopy.....	64
2.2.1.3 Mass spectroscopy	64
2.2.1.4 FTIR spectroscopy.....	65
2.2.1.5 Chromatographic methods	65
2.2.1.6 Other methods	65
2.2.2 Synthesis of monomers.....	65
2.2.3 Chemical polymerization.....	67
2.2.4 Redox studies and electrochemical polymerization	67
2.2.5 Fabrication of sensors.....	68
2.2.5.1 Polymer pellet sensor.....	68

2.2.5.2 Flexible IDEs Chemoresistor	69
2.2.6 Sensor characterization under controlled conditions	71
2.3 Results and discussions	72
2.3.1 Synthesis of monomers	72
2.3.2 Chemical and electrochemical polymerization	76
2.3.3 UV-Visible spectroscopy	77
2.3.4 FTIR spectroscopy	79
2.3.5 Polymer morphology	81
2.3.6 Thermal stability	84
2.3.7 Electrical conductivity of polymers	86
2.3.8 Sensor Characterization	89
2.3.8.1 Pellet sensors	89
2.3.8.2 IDEs flexible chemoresistors	94
2.4 Conclusion	95
3. Synthesis of Poly(dithenyl pyrrole)-dialkylbithiazole copolymer	97
3.1 Introduction	99
3.2 Experimental	101
3.2.1 Chemical and instrumentations	101
3.2.2 Experimental procedures	102
3.3 Result and discussion	103
3.3.1 Synthesis of 1-bromo ketones (2a, 2b)	103
3.3.2 Synthesis of dialkyl-bithiazoles (3a, 3b)	106
3.3.3 Bromination of dialkylbithiazole	107
3.3.4 Synthesis of SNS-Stannyl intermediate	108
3.3.4.1 Deuterium quenching experiments	110
3.3.4.2 Bromination of SNS	111
3.3.4.3 Me ₃ SnCl reaction on Brominated SNS compound	114

3.4 Conclusion.....	114
4. Flexible Multisensing platform integrated into RFID label.....	117
4.1 Introduction.....	119
4.1.1 RFID Tags	119
4.2 Materials and methods	121
4.2.1 Multisensor platform	121
4.2.2 Functionalization of sensors on the platform	123
4.2.3 Multisensor platform characterization.....	124
4.3 Results and discussion.....	125
4.3.1 Capacitive Humidity sensing.....	125
4.3.2 Resistive Ammonia sensing.....	127
4.3.3 Resistive temperature detector (RTD) measurements	129
4.4 Conclusion.....	131
5. Biosensors based on Pig-odorant binding proteins (OBPs)	133
5.1 Introduction.....	135
5.1.1 Biosensor	135
5.1.2 Classification of biosensors	136
5.1.3 Recognition elements: Bioreceptors.....	136
5.1.4 Immobilization of bio-receptors	137
5.1.5 OBPs as bio-receptors	139
5.1.6 Electrical characterization by Kelvin probe method	140
5.2 Materials and methods	143
5.2.1 Immobilization of Pig-OBPs	143
5.2.1.1 Covalent Immobilization-SAM method	143
5.2.1.2 Physical Immobilization	145
5.2.2 Exposure of the OBPs to pyrazine using gas mixing system	145
5.2.3 Kelvin Probes	145

5.3 Results and discussion.....	146
5.3.1 Data evaluation	146
5.3.2 Measurement of pig-OBP-c sensor.....	148
5.3.3 Measurement of Pig-OBP-m2 sensor	148
5.3.4 Response of gold electrode with 2-isobutyl-3-methoxypyrazine	149
5.3.5 Actual response of Pig-OBP sensors	149
5.3.6 Adsorption of pyrazine gas at gold electrode surface.....	150
5.4 Conclusion.....	151
6. Conclusions and Future work.....	153
6.1 Conclusions	155
6.2 Future Work	157
Appendix.....	159
Analytical data of the compounds	159
References.....	207
List of Publications	218
Curriculum Vitae	220

List of abbreviations and symbols

CDCl ₃	Chloroform deuterated
cm	centimetre
CV	Cyclic Voltammetry
D ₂ O	Deuterium oxide
DCM	Dichloromethane
DMF	Dimethylformamide
FT-IR	Fourier transform infrared spectroscopy
g	Gram (s)
h	Hour(s)
HCl	Hydrochloric acid
HPLC	High performance liquid chromatography
HRMS	High resolution mass spectroscopy
Hz	Hertz
<i>J</i>	Coupling constant
mA	milliampere
mg	milligram
MHz	Megahertz
mL	millilitre
mm	millimeter
mmol	Millimole
mol	mole
mV	millivolt
nm	Nano meter
NMR	Nuclear magnetic resonance
ppm	Parts per million
PTSA	<i>para</i> -toluenesulfonic acid
R _f	Retention factor (TLC)
rt	Room temperature
s	second

List of abbreviations and symbols

S	Siemen
s	Singlet (NMR)
SEM	scanning electron microscopy
T	temperature
t	triplet (NMR)
<i>t</i> -BuLi	<i>tert</i> -Butyl lithium
THF	Tetrahydrofuran
TLC	Thin layer chromatography
UV-vis	ultraviolet-visible
V	volt
δ	Chemical shift
μ L	microlitre
μ m	micrometer
Ω	ohm

1. Introduction and Theoretical background

1.1 Motivation of the project

Food wastage across the world has been subject of concern because of its negative effects on the hunger combat, food security improvement, economic development and the environment protection. Food wastage not only causes a waste of resources used in the production such as water, electricity, harvesting, transportation cost, etc. but also incurs costs on waste disposal and damages the environment. The decomposition of unused food causes methane emission, one of the most harmful gases that contribute to climate change. As a greenhouse gas, methane is 23 times more potent than CO₂, making significant contribution to global warming [1]. There is a large amount of the food wastage at global level: a) approximately 1.3 billion tonnes of food gets wasted in the world every year, which is one third of the food produced annually, b) in the United States 30% of all food is thrown away every year which is worth of US\$ 48.3 billion, etc. [1].

One of the major reasons of food wastage is improper storage during their transportation from producers to consumers. Real-time monitoring of ambient conditions in which goods are transported could potentially reduce this wastage. This should include measurement of basic parameters such as temperature and relative humidity, and more advanced markers that indicate merchandise quality, that is, the gases or volatile organic compounds (VOCs) released by products during its ripening or deterioration. For example, ethylene is an essential plant hormone that stimulates the ripening of fruits, the opening of flowers, etc. [2]. The presence of significant levels of ethylene in fruit transport containers or storage chambers can be responsible for early ripening and significant losses.

Presently available food monitoring systems are based on expensive and bulky sensor equipments, and they can be operated only in laboratory environments. Therefore, there is a great need of new sensing devices which are integrable into food packages and capable of real-time monitoring the quality and freshness of food, from the production site along the logistics chain until arriving into the hands of the consumers. The commercial availability of smart and small monitoring systems would allow producers, logistics groups and customers to trace their perishable goods at any time and take the necessary measures for their storage or sale. Such devices could additionally protect the consumers against frauds as well as from the consumption of unsafe food. In order to implement them in a widespread manner they should be extremely low cost, have reduced dimensions, possess sensing capability to

measure both physical and chemical parameters related to food quality or freshness and should have data storage and communication capabilities.

In this context, the **Marie-Curie Actions European Union project “FlexSmell”** aimed to develop a hybrid very low cost, ultra-low power flexible chemical gas sensing system compatible with RFID read out. These smart sensing RFID tags will be used for monitoring the perishable goods along their transport and storage through a smart packaging solution. Its prototype was jointly developed by the European universities and research organizations, mainly by Ecole Polytechnique Federale de Lausanne (EPFL), Switzerland, University of Tübingen (Germany), The University of Manchester (UK), Holst Centre (The Netherlands) and University of Bari (Italy). The developed sensing system consists of two major components, flexible multisensor platform and RFID tag. The multisensor platform was developed by EPFL by ink-jet printing technique on a flexible plastic foil. The platform includes devices with different transduction principles such as capacitive, resistive, etc. not only for simultaneous monitoring the multiple parameters but also to achieve both low power consumption and high sensitivities. The devices printed on the platform were functionalized with polymer sensing layers at the university of Tübingen and Manchester. The parameters aimed to be evaluated with the platform were relative humidity, temperature, ammonia and VOCs. The RFID tag required for wireless read out was developed at Holst Centre. The multisensor platform and the RFID tag were integrated together to make a complete hybride multisensing RFID system.

I had three major tasks in this multidisciplinary project, a) to carry out synthesis of new polymers or copolymers for their investigation as sensor materials, b) functionalization of multisensor platforms using commercially available or prepared polymers and c) sensing characterization of functionalized multisensor platforms as stand-alone devices or using developed RFID tag. Therefore, the first part of the work was focused on the synthesis of the conducting polymers and their structural and chemical sensing characterizations. The capacitive devices of the platform were functionalized at University of Tübingen for capacitive humidity detection whereas the resistive ones at The University of Manchester (Research group of Prof. Krishna Persaud) for the detection of ammonia and VOCs. My last major task was to perform sensing characterization of fully functionalized multisensor platform integrated on the RFID tag against the foreseen analytes such as relative humidity, ammonia, ethanol etc. and temperature.

The complete system (including platform and RFID tag) successfully monitored/measured humidity, temperature, ammonia and VOCs and transmitted data to the reader. Therefore this work significantly contributed to the development of smart sensing RFID tags opening real perspective for their practical applications.

1.2 Chemical sensor

Nowadays chemical sensors are widely used in various applications such as, in scientific and industrial research, in medical institutions and hospitals for diagnostics, and for foods and drinks processing which use gases such as nitrogen to enhance the shelf life of products by reducing oxidation [3]. They have been largely employed in automobiles to monitor the exhausts gases, in chemical and petrochemical processes to monitor the reactions, for environmental protection including both ambient air and pollutants monitoring. In military applications, they have been used for sensing of different chemical vapours and warfare agents. In agriculture, sensors have increasing importance for the detection of contaminants such as pesticides, drugs, and pathogens in milk, meat, and other foods, and in the determination of product quality by detecting the gases on ripening or spoilage of fruits and vegetables. Therefore, chemical sensors have significant economic impacts and effects on the quality of life.

An early detection and qualitative discrimination of chemical analytes present in the surrounding is absolutely important in every application. Currently, the analysis of chemical analytes requires expensive analytical instrumentation such as GC/MS or HPLC. Moreover, these methods require skilled technicians and analysis can take a matter of days to complete, by which time the chemical ambient will have changed. In this point of view, current research is focused on the development of new materials and new state-of-the-art sensor technology which can provide needed sensitivity and rapid detection of chemical ambient and outcome of the test. For many years, sensor technology, especially machine olfaction called “electronic noses” has successfully simplified the detection of chemical analytes and bacteria or micro-organisms [4-8]. This device provides rapid real-time detection with conclusive results within few minutes compared to the traditional couple of day’s method of analysis.

1.2.1 Chemical sensor principle

The main purpose of a chemical sensor is to translate information from the chemical domain like presence of certain chemical analyte, their concentration in the surrounding into

information which can be interpreted directly or by means of control/data processing unit. The technical definition of a chemical sensor is given as,

“A chemical sensor is a device that transforms chemical information, ranging from the concentration of a specific sample component to total composition analysis, into an analytically useful signal” [9]

The schematic representation of a chemical sensor is shown in the figure 1. The chemical sensor comprises three main components, receptor or sensing layer, transducer and signal processing electronics.

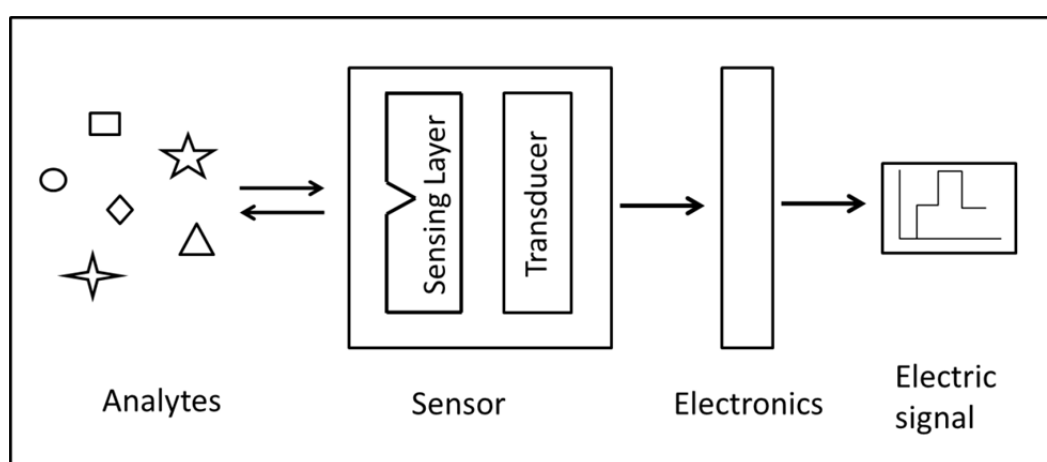


Figure 1. Schematic representation of a chemical sensor

Receptor: The part of a sensor which transforms the chemical information into a form or energy which may be measured by the transducer. In chemical gas sensors, the receptor is often a functionalized layer, named sensing layer. The receptor part of chemical sensor is based on different principles; a physical basis, in which no chemical reaction takes place (based on measurement of absorbance, refractive index, conductivity, temperature, mass change etc.) and a chemical basis in which chemical reaction with participation of the analyte gives rise to the analytical signal, A biochemical basis in which biochemical process is the source of the analytical signal.

Transducer: The sensor building block that transforms the energy delivered by the receptor (carrying the chemical information about the analyte) into a useful analytical signal.

Electronics: The electronic part of a sensor that process the signal provided by transducer into readable output in the specific format to derive complete conclusion.

Often sensor is built of a transducer and on top of that a layer of chemically active material is placed. First of all, a sample or analyte is taken and then filtered or preconcentrated (if required) and afterwards sensor produces a signal as a result of sensing effect. The exposure to an analyte from the environment is usually performed using a pump with controlled sample volume and flow. The exposed target analyte may contain other accompanying compounds, unwanted analytes which may cause interference to a real sensor response. To avoid the problem of interference from other analytes or to protect the sensing device, a filter or separator is being used for most of the sensors. The transducer measures the change of physical properties like temperature, capacitance, mass, resistance, etc. of sensing layer caused by interaction between analyte and sensing layer and converts it into an electrical signal. The response given by the sensor is recorded as either analog or digital signal which can be directly understood or transferred to a computer or data bus system. Electronic signal processing may include amplification of the signal, analog to digital conversion, etc.

1.2.2 Classification of chemical sensors

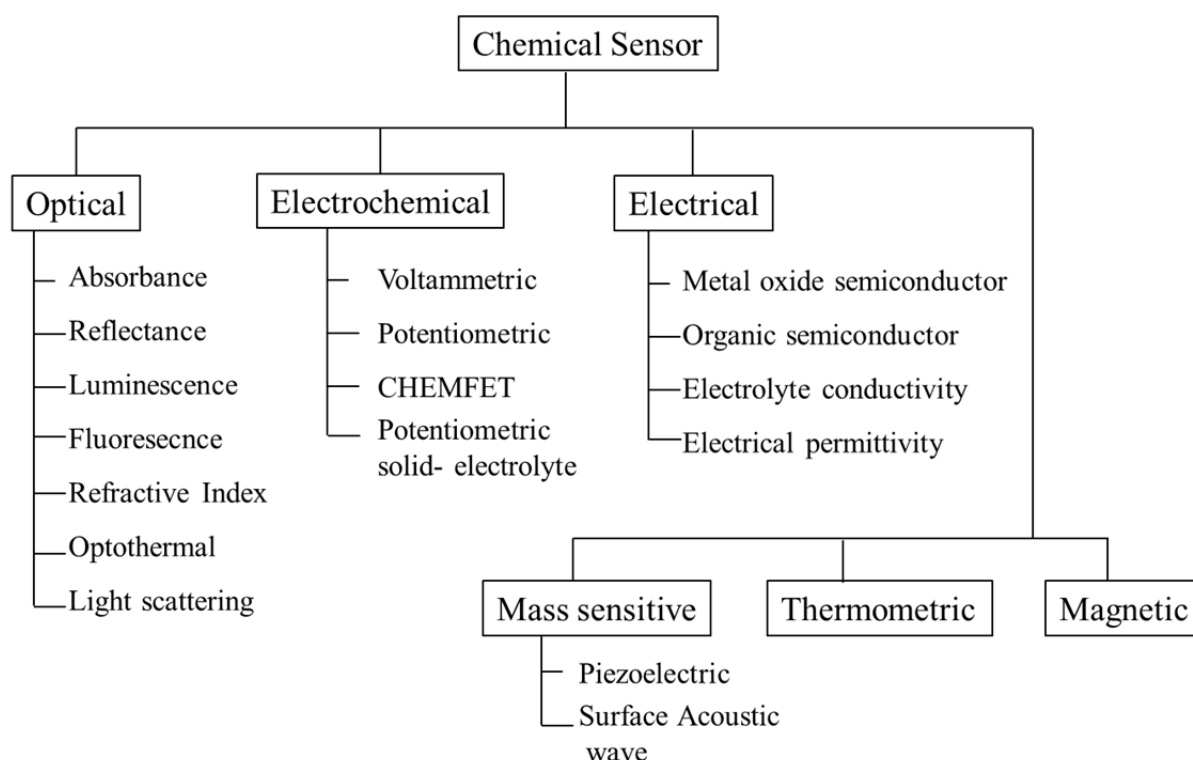


Figure 2. Classification of chemical sensor [9]

The chemical sensors can be classified in many ways. They have been listed on the basis of operating principle of the transducer, application to detect or determine a given analyte e.g. sensors for metal ions, for pH, for determining the oxygen or any other gases, etc. Another basis for the classification of chemical sensor may be according to the mode of application e.g. sensor for process monitoring, for use in vivo, etc. According to the operating principles, Hulanicki A. et al. [9] classified the chemical sensors as schematically presented in the figure 2.

1.3 Chemical gas sensor types

An interaction of sensors with chemical analyte induces a physical and/ or chemical change, which produces a signal in terms of change in resistance, capacitance, etc. There are two distinct types of signals; those where the interaction between the sensor and the chemical analyte is reversible and those where it is irreversible. In the case of a reversible process, the chemical analyte separates away from the sensor without making any permanent changes whereas, in the irreversible type, the chemical analyte undergoes a chemical reaction at the site of the sensor making permanent changes.

There are many different types available that can be used as sensors depending on their transduction principles. The simplest and most commonly used types are conducting polymer based chemoresistors and metal oxide sensors. This section provides an overview of the polymer based chemoresistive sensors and metal oxide sensors.

1.3.1 Conducting polymer sensors: Chemoresistors

Conducting polymer sensors have several advantages over other type of gas sensors. The sensors have rapid absorption and desorption kinetics at room temperature; they are of the reversible type and have high sensitivities being able to detect chemical concentrations in ppb range. Unlike metal oxide sensors, conducting polymer sensors do not require heater elements; therefore, the sensors operate at room temperature and ultimately consume less power. For many decades interdigitated electrodes (IDEs) chemoresistors have been used for the chemical gas sensing [10-14].

Generally pyrrole, thiophene, aniline and their derivatives are used to prepare conducting polymers but the common feature is π -electronic conjugated system in their backbone. According to the specificity of the sensors towards different chemical analytes, polymer properties can be closely tailored by altering the functional group or making their

copolymers. Moreover, conducting polymer sensors are not poisoned by sulphur containing compounds [15], which generally inactivates inorganic semiconductors. One of the major drawbacks of polymeric sensors is the cross sensitivity to humidity while measuring any chemical analyte in a real-time [16, 17]. Chemoresistors can be fabricated by a cheap and conventional process and mainly consists of IDE substrate and polymer sensing layer [18].

Design: Chemoresistive sensor consists of several pairs of electrodes and a layer of conducting polymer in contact with the electrodes as illustrated in Figure 3. IDE transducers are fabricated by depositing comb like metal electrodes onto substrates. A chemical sensitive layer is then deposited onto a transducer to develop a chemical sensor. Usually conducting polymers, copolymers or metal composites are used as a sensing layer. The sensing layer can be easily applied as thin or thick films by a variety of techniques. According to affinity to particular chemical analyte or set of analytes, different polymers can be chosen as sensing layers. The schematics of the configuration of conducting polymer chemoresistor and IDEs transducer are shown in figure 3 and 4 respectively.

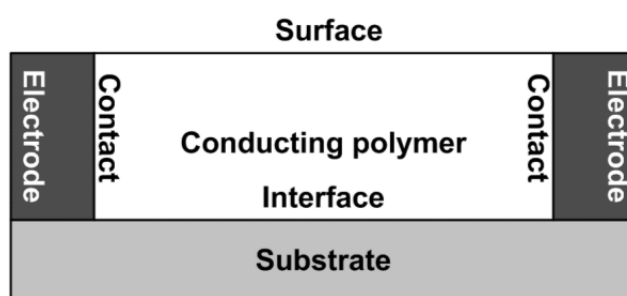


Figure 3. Configuration of chemoresistor showing different components of the sensor [19]



Figure 4. Schematics of interdigitated electrodes (IDEs) substrate. The dark area is comb like metal electrodes and the white part is insulating substrate [19]

The transducers are fabricated by comb like deposition of metal electrodes such as silver, gold, copper, platinum, etc. onto a substrate by peel-off or ink-jet printing method. To fabricate flexible IDE transducers, polyethylene terephthalate (PET), polyethylene naphthalate (PEN) or polyimide (PI) is used as a substrate. The space between two electrodes and width of each electrode are maintained in the range of few tens of μm depending on the applications. The thickness of sensing layer are decided by considering the geometry of the transducers and looking for a trade-off between sensor quick response time (thin layers) and large sensitivity (thick layers). In some applications, the sensing film is obtained by alternative deposition of more than one polymer.

Sensing principle: Generally, a constant potential or current is applied on the sensor and change in current or potential is measured, respectively. The interaction of chemical analytes with the polymer sensing layer induces change in the physical or chemical properties of polymer material and that change is collected as an output of interactions. Therefore, this sensor is very simple, efficient, easy to operate, and even simple ohmmeter is enough to collect the data. Alternating current (AC) also has been used as the signals of chemoresistor sensors [20-23]. Thus, not only resistance, but also capacitance and inductance can be measured to detect gases.

Chemoresistors is very popular device configuration of gas sensors and the required technologies like fabrication of IDE substrates, deposition of sensing layer and the measurement of sensor against various analytes have been maturely developed. Conducting polymers are easy to be synthesized and processed into films by chemical and electrochemical techniques.

1.3.2 Metal oxide sensors

The basic structure of metal oxide sensor consists of planner substrate over which metal electrodes are deposited. A platinum heater is fabricated on the back side of the substrate to give required temperature for sensor operation. The metal oxide materials with dopants are then coated above metal electrodes. Thick or thin metal oxide layers are used in the sensor depending on materials and applications. The metal oxide sensors are thoroughly investigated under operando conditions [24]. The films can be deposited by various methods but for thin films most commonly physical vapour deposition (PVD) [25] whereas for thick films screen-printing methods [25] are used.

Metal oxide sensors usually operate at high temperature, within the range of 200-500 °C. Below this temperature, the reaction rates are too slow resulting in very poor or no sensitivity. The major drawback of this sensor is due to high operation temperature and hence large power consumption of around 800 mW per sensor. The use of thin planner silicon substrates considerably lowered the power consumption. The most commonly used material for the MOX sensor is Tin dioxide (SnO_2), usually doped with Palladium or Platinum [26]. The sensor response and sensitivity have shown to improve when small amounts of noble metal such as Palladium or Platinum is added. Apart from the SnO_2 , oxides such as zinc oxide (ZnO) [27], titanium dioxide (TiO_2) [28] and tungsten oxide (WO_3) [29] have also been used in gas sensors. Eranna *et al.* [30] have discussed a number of materials used in chemical gas sensors.

Although metal oxide sensors have been widely used and studied for decades, the gas sensing mechanisms are not yet fully understood and remain a controversial topic of ongoing debate. Ion sorption theory is commonly used to explain the general mechanism, where absorbed free oxygen ion species are electrostatically stabilised on the surface of sensing layer without forming chemical bonds. Hauffe in the 1950s developed the ion-sorption model from the boundary layer theory of chemisorption [31]. The general mechanism [32, 33] describes chemisorption of oxygen on the surface creates extrinsic acceptor states, immobilises conduction band (CB) electrons from the near-surface region and creates an electron-depleted region for n-type semiconductors. The formation of the potential barrier between the grain boundaries reduces the conductivity by limiting the flow of electrons. Depending on the operating conditions, there can be different oxygen species driving the sensing mechanism which includes molecular O_2^- (superoxide), O^- (charged atomic oxygen) or O^{2-} (peroxide ion). The density of charge carriers (n-type electrons or p-type holes) are affected by the presence of oxidising or reducing gases. In the case of n-type semiconductors, reducing gases abstract the surface oxygen species, releasing immobilised electrons and decreasing the depletion layer thickness, and thus resulting in an increase of conductance, whereas oxidising gases reduce the conductance by creating additional surface acceptor states by immobilising CB electrons and increasing the thickness of depletion layer.

The sensing properties can be adjusted / modified by the change of dopant and/ or operating conditions [34]. Hübner *et al.* have described the influences of Al, Pd and Pt dopants on the

conduction mechanism and the surface and bulk properties of SnO₂ based gas sensor [35]. Sakai and Yamazoe [36] proposed a model describing sensor performance is mainly depend on operating temperature mainly due to the kinetics of reaction between analyte and sensor material and the kinetics of gas diffusion through the sensing layer. Barsan *et al.* [37] also established that the final annealing temperature influences the concentration of the reactive sites for ion sorption. The temperature dependence of the distribution of different oxygen surface species and changing the main reaction route results into alteration of the sensor response and sensitivity (for carbon monoxide). Additionally, film thickness, material porosity, grain size, interconnectivity of grains, the surface-to-volume ratio, and preparation history all influence the sensing properties [38].

1.4 Conducting polymers as chemical sensors

Although, traditionally polymers have been used as insulating materials in the electronic industry and are applied as insulators of metallic conductors or photoresists; since the discovery of conducting polymer in 1977 [39], conducting polymers have attracted immense interest in different applications. The discovery of doping of polyacetylene (PA) resulted into increasing the conductivity of PA by eleven orders of magnitudes [39, 40]. However, the low stability of doped PA when exposed to oxygen or humidity was a limiting factor for their applications. The quest for new structures resulted into synthesis of many novel polymers with improved properties (Figure 5). Then for several decades, polypyrrole (PPy), polythiophene (PTh), polyaniline (PAni), etc. have been studied extensively and implemented in a various applications including in chemical sensors and actuators, Light emitting diodes (LEDs), energy storage devices, rechargeable batteries, electrochromic devices, etc.

The gas sensors or chemically active materials based on conducting polymers have received significant attention for their use in detection, quantification and discrimination of volatile organic compounds (VOCs) [41, 42]. Since early 1980s, conducting polymers such as, PPy, PAni, PTh and their derivatives have been used as active layers in the gas sensors. The electrical conductivity of these polymers changes upon exposure to different kinds of gases [43-47] which gives a simple method to use conducting polymers as sensor materials.

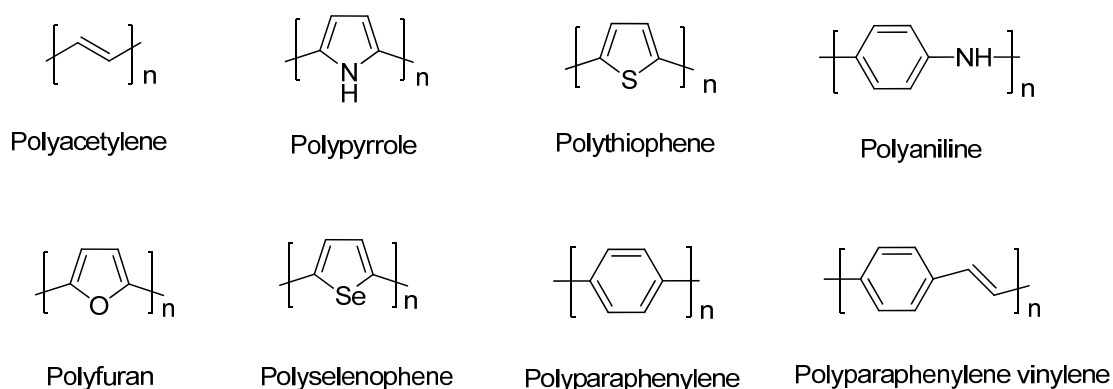


Figure 5. Structures of some common conducting polymers

Conducting polymers can easily be synthesized through chemical or electrochemical processes, and their chemical and physical properties can be easily adjusted by modifying the molecular chain structure by introducing different substituents, or copolymerizing with different monomers. In addition, conducting polymers have many improved characteristics such as mechanical flexibility allowing a facile fabrication of sensors, modifiable electrical conductivity by doping process, reasonably short response time and their ability to operate at room temperatures leading to low device power consumption, etc. [48, 49].

The conjugated systems in the backbone of the conducting polymers are responsible for many unusual electronic properties, for example: electrical conductivity, low ionization potential and high electron affinity etc. These properties of the conducting polymer depend strongly on doping level, ion size of dopant and protonation level, etc. [50]. Moreover, conducting polymer materials are sensitive to a wide range of gases and vapours at room temperature [51] and can be deposited onto the desired area by different techniques such as spray, dip, drop coating, etc.

Conducting polymers can be employed for the development of chemical sensors in two ways [52]. Firstly as a sensitive layer, wherein, electrical conductivity related to redox state of the polymer changes upon interaction with chemical gases. Secondly the conducting polymers can be used as a matrix for specific immobilization. This is usually used during the electrochemical polymerization process, in which, the sensing materials (metals, salts, cells, enzymes etc.) are trapped in the conducting polymers and deposited on the sensor area.

1.5 Synthesis of conducting polymers

Conducting polymers are generally prepared using either chemical or electrochemical oxidative polymerization of monomers [53]. Besides chemical and electrochemical oxidative polymerization, conducting polymers have also been synthesised by methods such as photochemical polymerization [54], plasma polymerization [55], enzyme-catalyzed polymerization [56], organometallic cross-coupling reactions [57], etc. However, most of these techniques are time-consuming and involve the use of costly chemicals.

1.5.1 Chemical polymerization

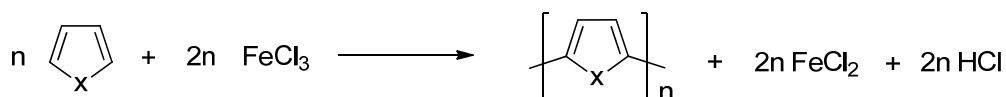
Chemical polymerization is the versatile technique for preparing a wide range of conducting polymers. Chemical polymerization can be achieved by two ways, namely, oxidative coupling method and condensation of the monomeric precursors. Out of these two routes, oxidative coupling method represents the least expensive and most widely exploited means by which conjugated polymers can be prepared [58].

The most widely used chemical oxidants for oxidative polymerisation are ferric chloride (FeCl_3), ammonium persulfate ($(\text{NH}_4)_2\text{S}_2\text{O}_8$), hydrogen peroxide (H_2O_2), potassium dichromate ($\text{K}_2\text{Cr}_2\text{O}_7$), cerium sulphate $\text{Ce}(\text{SO}_4)_2$, and so on [59-61] which simultaneously oxidizes the monomer and provides the dopant anion. Oxidative chemical polymerization results in the formation of the polymers in their doped and conducting state. Isolation of neutral polymer is achieved by exposing the material to strong reducing agents such as ammonia or hydrazine. An advantage of chemical oxidative polymerization is that properly substituted heterocyclic and other aromatic monomers can form soluble polymers. Chemical oxidative polymerization is the most useful method for preparing large amounts of conducting polymer powders and has been extensively used in industry. However, this method suffers from some disadvantages that result in poor quality of polymers e.g. Lewis acid catalysed polymerization can limit the degree of polymerization [62] and resulting in its precipitation from the polymerization medium. Also, the use of strong oxidizing agents can result in the over oxidation and eventual decomposition of the polymer [63].

Thiophene based polymers are generally synthesized by catalytic Grignard reactions in which 2,5 dibromothiophene derivatives are reacted with Mg in THF to produce corresponding -MgBr product. Addition of metal complex catalysts such as $\text{Ni}(\text{bipy})\text{Cl}_2$ initiates self-

coupling reactions leading to PTh derivatives without unwanted 2,3' and 2,4' couplings [64]. Figure 6A and 6B illustrates chemical synthetic routes of polyheterocycles.

6A) Chemical oxidative coupling route



6B) Condensation reaction route

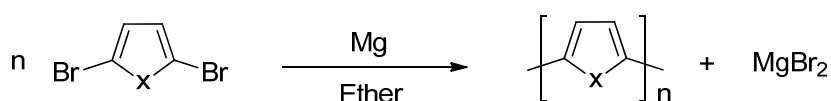


Figure 6. Synthetic routes of polyheterocycles

1.5.2 Electrochemical polymerization

Electrochemical polymerization is a standard oxidative method for preparing electrically conducting conjugated polymers that involve the formation of low molecular weight oligomers that are further oxidised at lower potentials to form a polymer film on the surface of the electrode. Smooth polymeric films can be efficiently synthesized onto conducting materials where their resultant electrical and optical properties can be probed easily by many electrochemical and coupled in situ techniques.

Electrochemical synthesis can be achieved by several techniques [65]: (a) potentiostatic (constant potential) method, (b) galvanostatic (constant current) method, (b) potentiodynamic (potential scanning or cyclic voltammetry) method etc. For all these techniques, a three-electrode cell is the best choice to realize a synthesis. This system comprises a working electrode, a reference electrode, and a counter electrode or auxiliary electrode. The working electrodes used can be of different materials. It exists in various geometries and materials and consists of inert metals, inert carbon or a mercury drop. The commonly used working electrodes are chromium, gold, nickel, copper, palladium, titanium, platinum, indium-tin oxide coated glass plates and stainless steel [66-68]. Semi-conducting materials, such as *n*-doped silicon [69] gallium arsenide [70] cadmium sulphide, and semi-metal graphite [71] can

also be used as a working electrode in electrochemical synthesis. The reference electrode should be non-polarisable and must have a constant potential no matter species used and their concentrations. The most typically used reference electrodes are saturated calomel electrode or Ag/AgCl electrode. The counter electrode or auxiliary electrode is usually made of a gold or platinum wire or foil. A schematic of three-electrode electrochemical set up for the electrical polymerization is shown in figure 7.

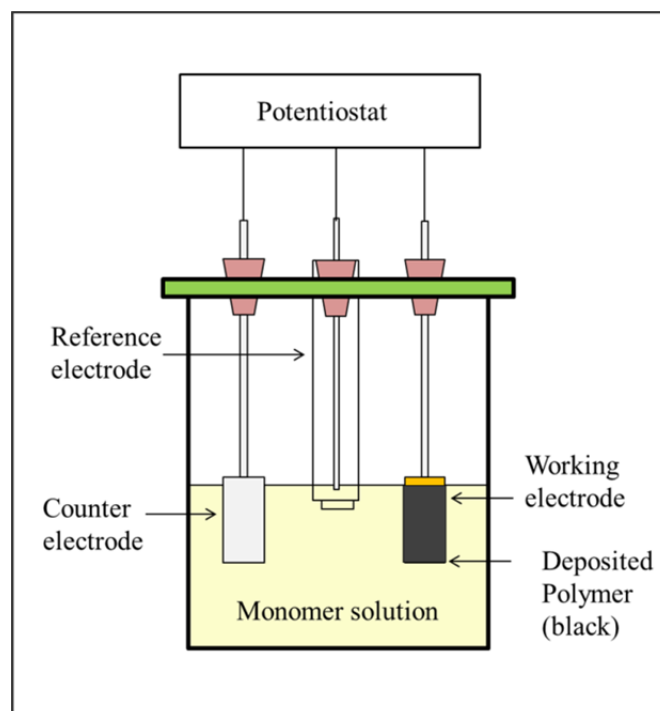
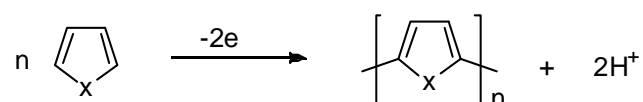


Figure 7. Schematic of three-electrode electrochemical cell

The electrochemical synthesis of polyheterocycles is by anodic and cathodic couplings routes and which is parallel to the chemical oxidative coupling and condensation reactions. Figure 8A and 8B illustrates the electrochemical synthetic routes of polyheterocycles.

8A) Anodic coupling route



8B) Cathodic coupling route

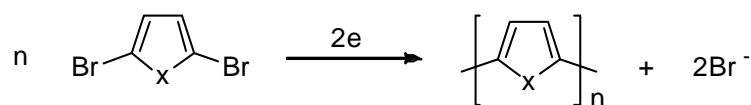


Figure 8. Electrochemical synthetic routes of polyheterocycles

Electrochemical polymerization has many advantages over other techniques that make this approach a good choice for small scale synthesis and characterization of the polymers. These benefits are a) a very small amount of monomer is required (5-50 mg) b) synthesis and characterization takes relatively small duration c) polymer film thickness, morphology & conductivity can be controlled by varying the applied potential, scan rate & polymerization time d) doping of the polymer.

In this study, voltammetry was used for electrochemical polymerization in which time-dependent controlled external potential (or current) is applied to the cell and the current flowing through or dropping on the cell is measured. A plot of current as a function of applied potential is called voltammogram which provides qualitative and quantitative information about the species involved in the oxidation or reduction reaction. Voltammetry techniques can be divided into two main categories; the potential sweep techniques where the potential of the working electrode is linearly scanned (e.g. cyclic voltammetry) and the step or pulse techniques where the potential is stepped, allowing removal of the capacitive current (e.g. chronoamperometry). These kind of electrochemical techniques have number of applications in developing sensors, fuel cells & batteries, environmental protection, corrosion studies, etc.

1.5.2.1 Cyclic Voltammetry

Among various electrochemical methods that can be applied for the synthesis and study of conducting polymers, CV has stood out due to its simplicity, versatility of measurement and its effectiveness in observing redox behaviour over a wide potential window. CV refers to a very common potentiodynamic electrochemical technique where the potential is swept linearly across the electrodes, and the resulting current is measured as a function of applied potential. It is very easy by CV to locate the oxidation or reduction potential of a conducting polymer. An important aspect of the technique is the ability to create a new redox species

during the first potential scan and then probe the future of species on second and subsequent scans. Therefore, CV is very useful technique, both for monitoring the growth of the polymer film on the electrode surface and the following characterization of the polymer within a single set of experiment. Furthermore, the stability of the polymer films can be obtained from CV during multiple redox cycles.

In classical CV experiment, the potential across the working electrode and a counter electrode is increased linearly from a lower limit to an upper limit and the current passing through the working electrode is measured. In the case of freely diffusing species, as the potential is increased, oxidizable species near the electrode surface react, and a current response is measured whereas upon reversing the direction of the scan, the oxidized species near the electrode surface are reduced and again a current response is measured. Data are usually represented as current vs. voltage plots. Redox potentials are identified from the position of the oxidation and reduction current peaks. The linear scanning of potential from an initial lower potential to final higher potential and back to the initial potential again is shown in a triangular waveform in figure 9.

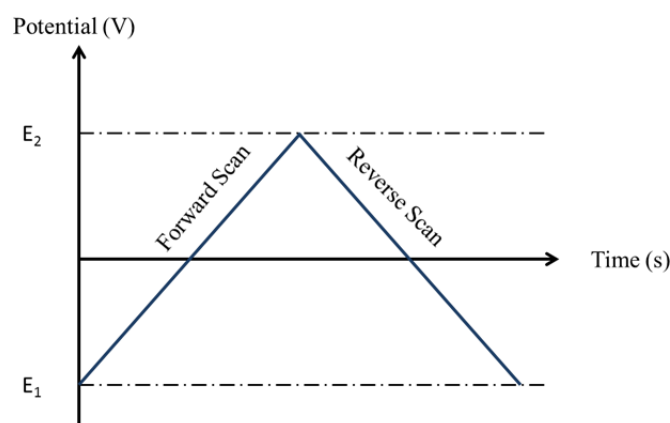


Figure 9. Potential applied to the cell versus time (triangular wave function)

In this case, cyclic voltammetry experiment starts by scanning the voltage at fixed rate, from E_1 to E_2 in a linear fashion and then the scan reverses direction back to the original potential at E_1 .

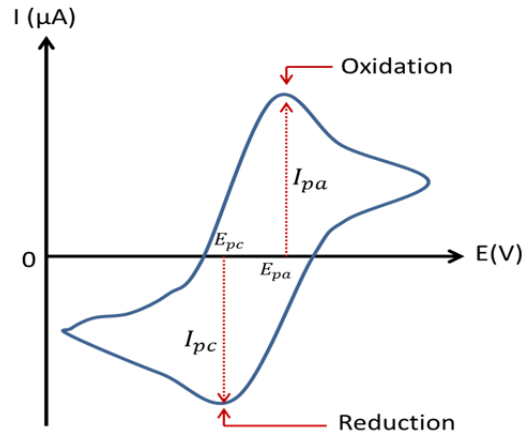


Figure 10. Cyclic voltammogram of a reversible reaction with E_{pc} and E_{pa} are the peak potentials at the cathode and at the anode, respectively. Whereas, I_{pc} and I_{pa} are the maximum current at the cathode and at the anode, respectively.

The cyclic voltammogram recorded for a reversible electrochemical reaction (Figure 10) can be characterised as, when a potential is swept linearly at constant scan rate then the ratio of the peak currents at the anode (I_{pa}) and at the cathode (I_{pc}) is equal to one [72].

$$|I_{pa}/I_{pc}| = 1$$

According to Randles-Sevcik equation, the peak currents are proportional to the square root of the scan rate [73].

$$I_{pa} = 0.4463 nFCA(nFvD/RT)^{1/2}$$

Above equation is simplified as, $I_{pa} = 2.69 \times 10^5 n^{3/2} CAD^{1/2} v^{1/2}$

where n is the number of electrons involved in the reaction, F is the Faraday's constant (96485 C/mol), C is the bulk concentration of electroactive species (mol/cm³), A is the surface area of the electrode (cm²), v is the scan rate (V/s), D is the diffusion coefficient (cm²/s), R is the universal gas constant (8.314 J/mol.K), T is the temperature (K) and I_{pa} is the anodic peak current.

The peak current is proportional to the square root of the scan rate and the size of the diffusion layer at the electrode surface will be different depending on the voltage scan rate.

Since the electroactive polymer adheres to the electrode surface, the process is not diffusion controlled. For surface bound species the peak currents scale linearly with scan rate according to the equation [74, 75].

$$I_{pa} = \frac{n^2 F^2 \Gamma v}{4RT}$$

Where, Γ is the concentration of surface bound electroactive centres (mol/cm^2)

1.5.2.2 Chronoamperometry

Chronoamperometry, an electrochemical technique in which the potential is applied to the working electrode in pulses or steps, and the resulting current from faradic processes occurring at the electrode is monitored as a function of time. Unlike cyclic voltammetry where the potential is swept linearly, in chronoamperometry the potential is applied in pulses or steps from the point where the polymer is not oxidised or reduced (E_1) to the point where it gets oxidised or reduced (E_2) (Figure 11).

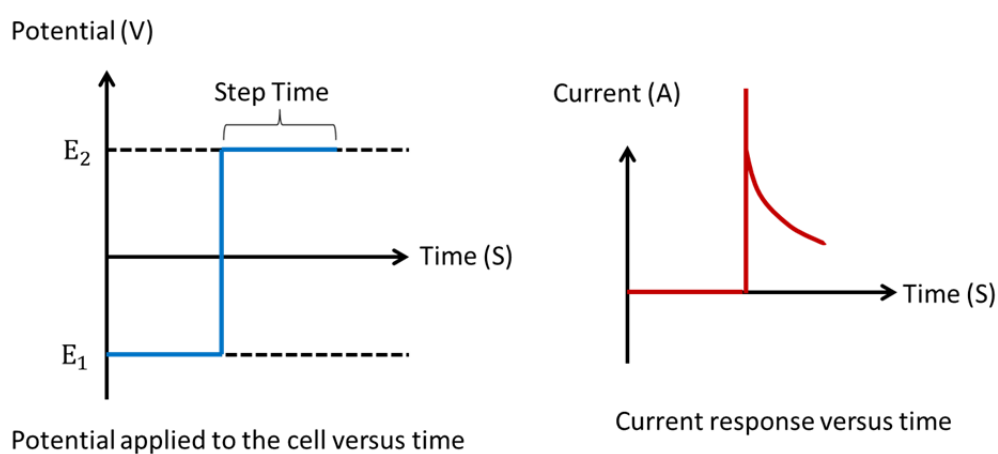


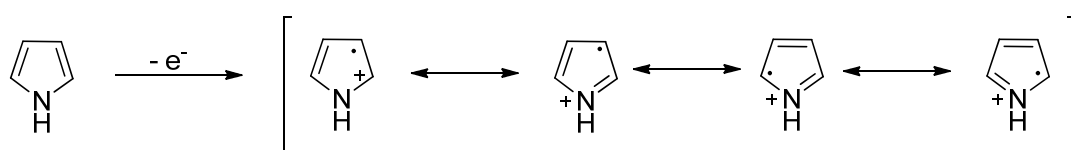
Figure 11. Chronoamperometry technique showing potential applied versus time and current response versus time

The potential is maintained at the same value for a particular time, which should not be very short or very long so that the current remains controlled by diffusion. If the step or pulse time is very short then the charging current is included in the measured current. As the charging current decreases exponentially in time, it is negligible after a few milliseconds.

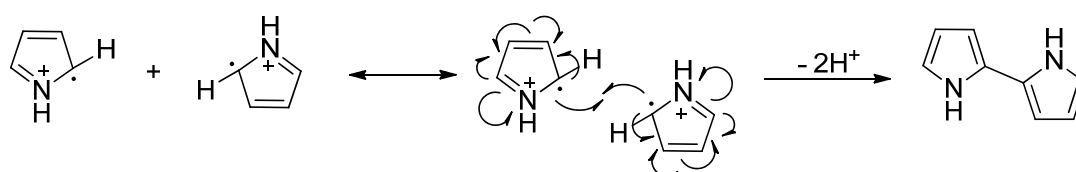
1.5.2.3 Mechanism of electrochemical polymerization

Generally, conducting polymers prepared by electrochemical method follows a similar pathway [76, 77]. Electrochemical polymerization mechanism of heterocycles is shown in figure 12 with pyrrole as a specific example. (a) The first step consists of the formation of radical cation of pyrrole monomer through oxidation at the anode. At this stage, a high concentration of radical cations remains near the electrode surface because diffusion of the monomer is much slower than electron transfer reaction. (b) In the second step, two radical-cations of pyrrole couple to form the dimeric intermediate or a neutral dimer, followed by deprotonation in order to regenerate the aromatic system. (c) Subsequently, since the oxidation of dimer is easier than that of its monomer; the applied potential generates radical cations of the dimers and the resulting radical-cation of dimer reacts with another radical cation of monomer to form the trimer, and the polymer chain propagates with successive oxidations, the coupling reactions, and deprotonations.

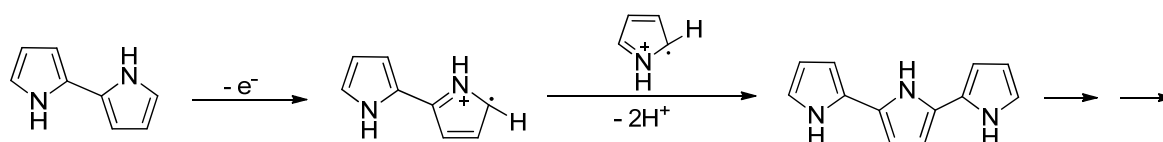
i) Oxidation of monomer



ii) Proton loss and dimerization of radical cation



iii) Oxidation of dimer and reaction with another radical cation



iv) Overall reaction from monomer to polymer

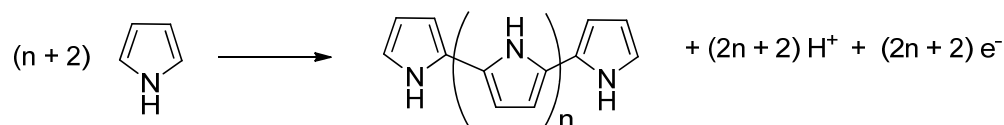


Figure 12. Mechanism of electrochemical polymerization

1.5.3 Functional doping

The electrochemical polymerization reaction occurring at positive potentials produce the polymers in their conductive forms. In their neutral state, conjugated polymers act like a semiconductor. The electronic conductivity of semiconductors can be controlled by introducing small quantities of foreign atoms into the lattice of the host semiconductor. This process is known as “doping” and foreign material is known as “dopant”. A counter ion or anionic species can be incorporated during polymerization to balance the positive charge in the polymer backbone to satisfy electrical neutrality. The dopant can be provided by the oxidant employed during chemical polymerization or can involve electrolyte ions used during the electrochemical polymerization. The dopant incorporated into the conducting polymer during synthesis has a profound effect on its conductivity, and other chemical and physical properties.

A large variety of dopants have been successfully incorporated into conducting polymers. Most commonly, small anions like Cl^- , ClO_4^- and BF_4^- , medium size anions like *p*-toluene sulfonate, dodecylbenzene sulfonate and large polyanions like polystyrene sulfonate, etc. have been utilized as dopants in polymerization process. In addition to these molecules, functional anions, positively charged molecules and oxide particles have been incorporated in conducting polymers to afford various functional materials.

1.5.4 Electronic conduction in conducting polymers

Even though the conventional electronic materials like metals and semiconductors can be explained by band theory, the electrical behaviour in conducting polymers is not really different from them. According to the band model, the highest occupied band (highest range of electron energies where electrons generally exist), which originates from the highest occupied molecular orbital (HOMO) of each monomer unit, is referred to as the valance band

(VB) and the corresponding lowest unoccupied band (lowest range of electron energies that are usually empty), originating from the lowest unoccupied molecular orbitals (LUMO) of monomer is known as the conduction band (CB) [78]. The CB lies above the VB and the energy distance between these two bands is defined as the band gap (E_g).

In their neutral states, conjugated polymers behave as a semiconductor. The incorporation of dopant into a semiconductor produces excess conduction electrons or holes and introduces a new energy level to the band gap and thus facilitates conduction. As larger the concentration of dopant, as higher is the conductivity of the semiconductor. An electrical conductivity of conducting polymers can be controlled in a similar way.

The doping process involves generation of mobile charge carriers (holes or electrons) to the conjugated backbone of polymer chains by oxidation, called *p*-type doping or by reduction, *n*-type doping. These charge carriers move along the polymer backbone via rearrangement of conjugated single and double bonds and enhance the electrical conductivity. In *p*-type doping, the conducting polymers form polymeric cations that are balanced electrically by anionic species, whereas, in *n*-type doping the conducting polymers form polymeric anions that are balanced by cationic species.

The removal of an electron from the π orbital of the backbone produces a free radical and a spinless positive charge. In solid-state physics terminology, the combination of a charge site and a radical is called as a polaron which has a spin of $\frac{1}{2}$. If second electron is removed from the polaron, bipolaron is generated. Low doping levels typically yields polarons, whereas higher doping levels produce bipolarons [79, 80].

The dependence of electronic properties on doping level of conducting polymers has been investigated experimentally and theoretically [81-83]. The explanation of doping level dependent electronic band structure is shown in figure 13. As the doping level of a conducting polymer increases, a large number of localised energy bands associated with polarons and bipolarons are created in the band gap (between VB and CB). At very high doping levels, these bipolaron energy bands overlaps and creates a continuous bipolaron band. The presence of these bipolaron bands reduces the band gap and allows easy access for electrons into the conduction band and hence the conductivities of conducting polymer are very much depending on their doping level i.e. charge carrier density [79].

If a higher doping level is considered (Figure 13e), then both the lower and higher bipolaron bands merge with the VB and CB respectively and the conductivity of a conducting polymer is like partially filled character of the CB, which is similar to the conductivity mechanism of a metal.

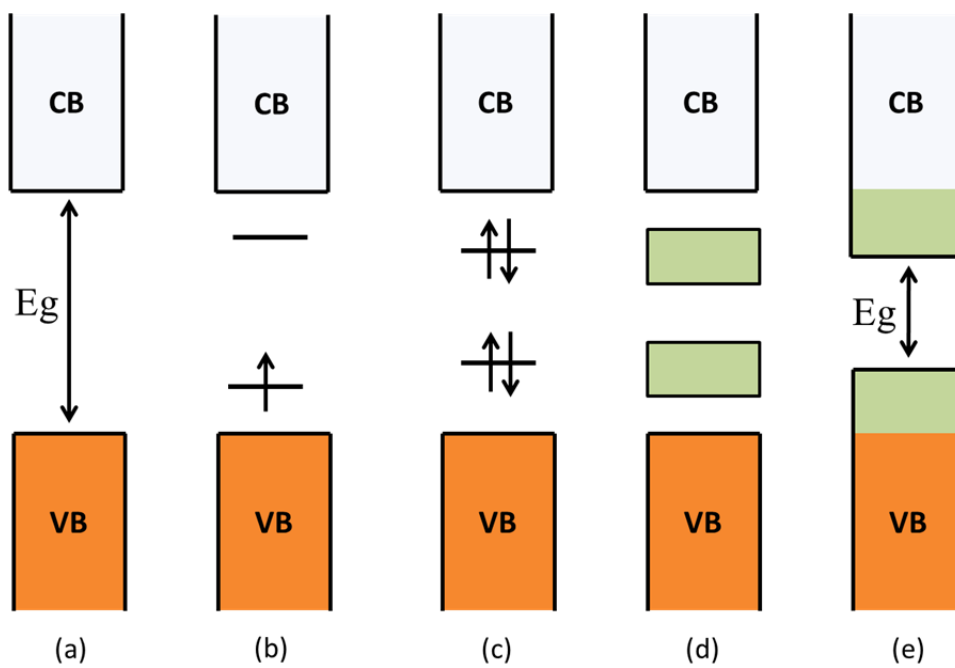


Figure 13. Band structure of CP as a function of doping level: (a) without doping; (b) low doping level, polaron formation; (c) moderate doping level, bipolaron formation; (d) high doping level, formation of bipolaron bands; (e) 100% doping level per monomer. [Adapted from reference [79]]

The doping process results into distortion of polymer structure and formation of the charge on the polymer backbone. The structural changes in the conducting polyheterocycles such as PPy due to oxidative doping process are shown in figure 14. The removal of one electron from the π conjugated backbone of PPy results into formation of quinone type bonds in the polymer chain and a radical-cation pair is formed called a polaron. If a second electron is removed from the polymer then there is a formation of a dication called bipolaron. Both polarons and bipolarons are delocalized serving as a charge carriers. Further oxidation of PPy increase the density of bipolarons (charge carriers) that can move along the π bonded polymer backbones and therefore results in higher conductivity.

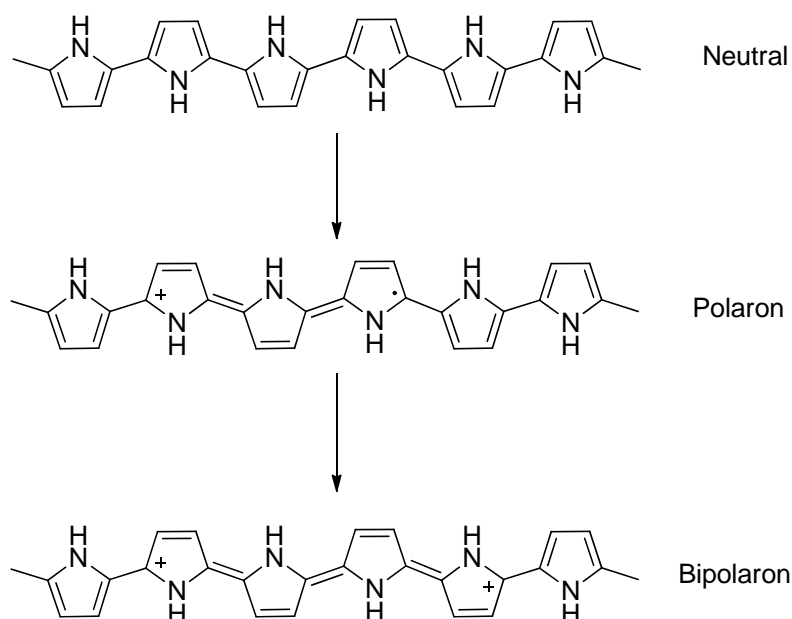


Figure 14. Polaron and bipolaron formation on π -conjugated backbone of polypyrrole

Some common conducting polymers in their neutral form have band gaps of a few electron volts (eV), which results in a conductivity range of 10^{-10} S/cm to 10^{-5} S/cm. The doping of these materials put them in metallic conducting group by increasing their conductivity up to 1 to 10^4 S/cm [84].

1.6 Fabrication of flexible polymer sensor

In this study, flexible IDE transducers were used for the fabrication of chemical gas sensors. The flexible IDEs sensor has three major components namely; flexible substrate, interdigitated electrodes and a sensing layer. The main features of the sensor used in these studies are shown in the figure 15.

The performance of a chemical gas sensor is evaluated using many different criteria but mainly sensitivity, stability, reversibility as well as fast response and recovery. As the deposition of organic material is required in many applications, different methods have been developed for the deposition of conducting polymer film of desired thickness and morphology on different types of transducers. Following are some of the methods used for the deposition of polymeric sensing materials onto IDE substrates.

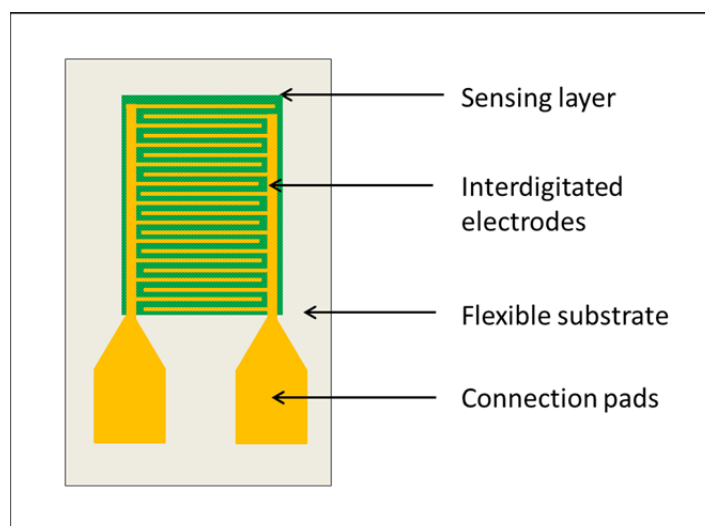


Figure 15. Schematic representation of chemical sensor showing flexible substrate (plastic foil), planner interdigitated electrodes and polymer sensing layer

1.6.1 Electrochemical deposition

Electrochemical deposition is very simple and most convenient method to prepare conducting polymers as well adhering films on the anode surface by potentiostatic, galvanostatic or multi-sweep deposition procedure [65]. The morphology of the polymer can be controlled by experimental conditions such as polymerization potential, monomer concentration, nature of counter or dopant ion, etc. The thickness of the polymer film can be controlled and determined by measuring the total charge passed through the electrochemical cell during film growing process [85]. The conducting polymer films also can be prepared onto patterned microelectrodes [86]. If the insulating gap between two conducting electrodes is close to couple of tens of micrometres then the growing polymer film can fill up the gap and connect the electrodes [87]. A three electrodes electrochemical cell is the best choice to realise electrochemical deposition of polymers as explained in section 1.4.2.

1.6.2 Dip coating

This is very simple and fast technique. If the transducer is dipped into a solution during chemical polymerization then some polymer will be deposited onto its surface [88, 89]. The thickness of the layer depends on the concentration of the polymer solution. So, the samples of different layer thickness can be prepared by dipping in the solution of different concentrations. Another way, alternate immersing of transducer into the monomer and

oxidant solutions will leave thin polymer film on transducer upon drying. In this process the monomer and oxidant reacts on the surface of transducer and forms the polymer layer [90, 91].

1.6.3 Drop casting

If the polymer is soluble then its solution is drop dried [92, 93], and if the polymer is insoluble in organic solvents then few drops of the monomer and oxidant solutions are dropped and reacted onto transducers. If the solution amount is accurately defined, for example, by the use of micropipette, reproducible polymer film can be obtained with the advantage of a very small surface roughness. If wettability of the transducers is not good enough then it results into irregular drying and film of uniform thickness cannot be obtained. The solutions can also be dropped by small metal wire loop. The size of the loop can be taken according to the size of substrates and viscosity of the solutions. This method cannot be used for the substrate of large size.

1.6.4 Other methods

Apart from the above mentioned methods, spray coating, spin coating, Langmuir-Blodgett (LB) technique as well as thermal evaporation and vapour phase polymerization techniques can be used for the deposition of conducting polymer film onto transducers.

1.7 Sensing principles / detection mechanism

1.7.1 Chemical interactions

The conjugated π -electron system and doping levels in the conducting polymers produce fascinating chemical and physical properties in the polymers. Moreover, the doping level or oxidation level of conducting polymers can be altered by oxidation-reduction reactions. The oxidation levels of conducting polymers are easily changed by transferring an electron from or to the analytes at room temperature that results into changes in the resistance. The changes in resistances are generally linear over a wide range of analyte concentration, and this provides a simple technique capable for sensing the chemical analytes. The transfer of an electron can also results in change in the work function of the sensing material. The work function of a conducting polymer is defined as the minimal amount energy needed to remove an electron from bulk to vacuum energy level.

Over the last decade, many working groups have investigated the mechanism of interaction of chemical analyte and polymer sensing layer but still controversy exists over the actual process involved. In the presence of nucleophilic gases such as NH₃, the polymer is reduced, resulting in the increase in resistance due to lower number of positive charges along the backbone of polymer [94-96]. On the other side, in the presence of electrophilic NO₂ gas, the polymer is oxidised resulting in increase in positive charges and ultimately decreases in the resistance of the polymer [97, 98]. However, Li *et al.* found an increase in resistance when emeraldine salt based PANi sensor was exposed to NO₂ gas [94]. When PPy, PTh and in some cases PANi is exposed to NH₃, NO₂, I₂, H₂S and some other redoxing gases, the change in the oxidation level occurs [99-107].

An electron donating and electron withdrawing gases will either enhance or reduce the conductance of the polymers. For example, electron withdrawing gases like NO₂ and I₂, can remove electrons from the aromatic rings of conducting polymers and when this will happen at a p-type conducting polymer, the doping level as well as the electric conductance of the conducting polymer is enhanced. On the contrary, an opposite process will happen when detecting an electron donating gas. The reactions possibly involved in the ammonia sensing process [108, 109] are given in figure 16.

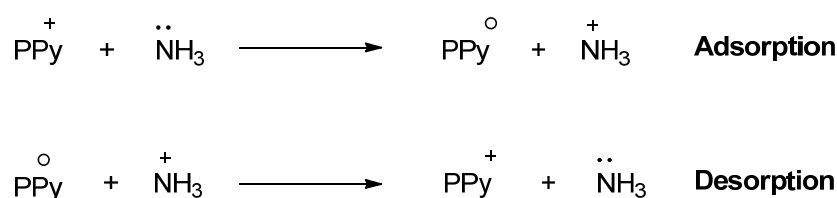


Figure 16. Possible ammonia sensing mechanism with polypyrrole

Based on this mechanism, all *p*-type conducting polymers are expected to de-dope upon exposing to ammonia atmosphere but still the exact mechanism is not very clear and further studies are still needed to make the mechanism more clear. In some cases, the reverse mechanism has been observed, doping of polymer upon interaction with ammonia, resulting in the increase in electrical resistance.

1.7.2 H-bonding and dipole-dipole interaction

It has also been reported that hydrogen bonding and dipole-dipole interactions play important roles in sensing process. The infrared spectra of a PPy film after exposing to acetone indicated the formation of hydrogen bonds (H-bonds) between C=O groups of acetone molecules and N-H groups of pyrrole units [110].

1.8 Aims of the study

As already mentioned, this work was carried out in the framework of EU project FlexSmell, for the development of flexible chemical gas sensing RFID tag for perishable food monitoring. In the collaborative project, this work was mainly focused on a synthesis of new conducting polymers and their chemical sensing investigations. In order to achieve main goal of the FlexSmell project, the multisensor platforms developed by other partner were functionalized with polymer sensing layers. The fully functionalized platforms were integrated on the developed RFID tag and used to monitor humidity, temperature, ammonia and VOCs.

About conducting polymers, they have many improved characteristics but they have not been utilized 100 % in potential applications because of their insolubility and poor mechanical properties. In order to improve these poor properties, their substituted derivatives or copolymers need to be synthesized. Of numerous conducting polymers prepared to date, PTh, PPy and PANi are far more extensively studied than others for sensor investigations. However, introduction of substituents onto the pyrrole and thiophene monomers has a negative effect on the properties of their polymers and often results into material with poor electronic conductivity [111-115]. This is due to high density of functional groups and steric effect that restricts inter-chain electron transfer [116].

The functionalised oligomeric species such as terthiophene [117], 2,5-di(2-thienyl)-1H-pyrrole or dithienyl pyrrole (SNS) [118] and sexithiophene derivatives, in which the ratio of functional groups to the heterocyclic repeating unit is less than one is certainly the best alternative for PPy and PTh. The polymerization of these derivatives results into polymers with a well-defined structure and have less steric interactions, which results into more conjugation length and high electrical conductivity [119]. Moreover, it has been reported that soluble conducting polymers can be prepared from these oligomers and ultimately solution processability, an important property required for the practical applications of polymers.

The aim of the work was to carry out synthesis of series of new SNS based conducting polymers for their investigations as chemical gas sensors on flexible substrates. The preparation of different SNS derivatives was carried out with different substituents on the N-substituted aromatic ring. Different electron donating or electron withdrawing and halogen substituents were used in order to study the effects of these functionalities on the electrical, electrochemical and optical properties of the polymers. The flexible IDE chemoresistive sensors were fabricated using prepared SNS polymers and their sensing characterization against humidity, ammonia, ethanol, etc. was performed.

The work was also focused on the development of the flexible smart chemical sensing system for RFID applications for monitoring perishable goods. This work jointly performed with FlexSmell project partners. In the consortium our task was to functionalise the multisensor platform (developed by partner) with polymer layers and their chemical sensing characterizations against relative humidity, ammonia and VOCs. More details about the scope and aim of the work in the frame of FlexSmell project is already described in the section 1.1.

The last part of the research was focused on investigating another important class of organic receptors, odorant binding proteins (OBPs) obtained from the nasal mucosa of porcine for the construction of biosensors.

1.9 Thesis outline

The work described in this thesis is primarily focused on the synthesis of new conjugated dithienyl pyrrole (SNS) derivative based polymers and their chemical sensing applications. The work also presents the development of a flexible multisensor RFID tag in the later part. The last part of the work was focused on the development of biosensor based on pig odorant binding proteins.

In the first chapter, all the theoretical background has been described. All the details about the chemical sensors in terms of definition, sensor principles, etc. are presented. Thereafter, sensors based on different transduction principles are given with most of the information. The chapter further explains about synthesis of conducting polymers with the mechanisms of chemical and electrochemical polymerizations. The fabrication of chemical sensors using polymeric sensing materials and the deposition methods are explained later on.

Chapter 2 describes the methodology used for synthesis of new SNS derivatives, their structural characterization and property studies by various analytical techniques. The fabrication of sensors by electrochemical deposition of the polymeric layer is given in the later part. The last part of this chapter focuses on sensor characterization against relative humidity, ammonia and ethanol.

In the third chapter, attempts made towards the synthesis of SNS-dialkylbithiazole copolymers have been explained. Synthesis of dialkylbithiazoles is explained in first half part of the chapter whereas later part gives the methods and number of attempts made towards the synthesis of tinylated SNS compounds.

Chapter 4 describes the development of flexible multisensing smart RFID tag for the monitoring of environmental factors such as temperature, humidity, ammonia and VOCs. The chapter gives an overview of the fabrication of multisensor RFID tag and its sensing characterization.

The last chapter is dedicated for the development of biosensor based on pig odorant binding proteins. The chapter is focused on the experimental methods used in the fabrication of the sensors and then electrical characterization of prepared biosensor using Kelvin probes.

2. Poly(dithienyl pyrrole) based chemical gas sensors

This chapter presents the various processes that were used to synthesise different SNS derivatives and their polymerization on the account of manufacture of chemical gas sensors based on conducting polymers. A number of SNS monomers were synthesized using different substituted amine derivatives. Different amine derivatives with electron donating or withdrawing and halogen substituents were used in order to study the effect of these substituents on the properties of resulting polymers. Though the synthesis of many monomers was targeted but not all of them were successfully synthesised. Nevertheless, the experience gained from this study gave understanding into their potential as sensing materials based upon their ease of manufacture. The general structure of dithienyl pyrrole (SNS) is given in figure 17.

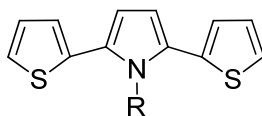


Figure 17. General structure of dithienyl pyrrole

All the synthesized monomers have been polymerized by both chemical and electrochemical methods as explained in the first chapter. To enhance the conductivity of the polymers to be used as sensing layers, they have been doped with oxidizing agents like FeCl_3 , tetraethylammonium-*p*-toluenesulfonate (TEA-PTS) or tetraethylammonium perchlorate. The chemical structures of all the prepared SNS monomers and polymers were confirmed with various analytical techniques. They have been extensively studied in terms of their optical, electrochemical, thermal, electrical, chemical sensing properties, etc.

Two methods were used to prepare the sensing devices; one by depositing the polymers onto IDE substrates electrochemically and secondly by making the pressed pellets out of chemically synthesized polymer powders. The chapter further continues with the characterization of the prepared sensor with chemical analytes such as humidity, ammonia, ethanol, etc. as a change in their resistance upon exposure to chemical analytes. The discussion on the techniques used and the results obtained, as well as the individual studies about the polymer materials or sensors are also discussed therein.

2.1 Monomer Synthesis

For many years, an abundance research has been conducted in the field of conducting polymers as chemical gas sensors. In order to investigate SNS polymer (for the purpose of chemical gas sensing applications) in a systematic way, first part of the study was focused mainly on synthesis of SNS monomers. The SNS derivatives were chosen for the study owing to the fact that the ratio of the functional group in the three member monomer unit is less than one and the polymerization such monomer produce the polymers with much better properties than PTh or PPy. The SNS derivatives can be prepared easily by various methods, while they preserve a fully conjugated π -electrons chain, and they are chemically stable to a wide range of chemicals. Additionally, such derivatives are readily oxidised and show high electrical conductivity. Moreover, they show a good electrochemical reversibility; they can be oxidised and reduced.

The monomers chosen in this study were SNS derivatives with different substituents attached at Pyrrole-N position. They have been prepared by using different amine derivatives namely, *o*-anisidine, *o*-toluidine, 2-aminoacetophenone, 4-fluoroaniline, 4-chloroaniline, 4-bromoaniline, 4-iodoaniline, 1-naphthalamine, 2-aminoacetophenone etc. Apart from these monomers, a few more were attempted but later discontinued due to their poor yield and difficult purification. All the prepared monomers have been later polymerized using both chemical and electrochemical techniques.

2.1.1 Reason for general synthetic route chosen

In general, basic heterocyclic compounds like pyrrole, thiophene or furan are very reactive at their α -protons (2-position or 5-position) compared to other positions like 3-position or 4-position. Considering this benefit, protons of these heterocyclic rings can undergo electrophilic substitution directed almost exclusively to the α -position.

The synthesis of SNS compounds can be achieved by number of ways but not in a single step. They can be easily prepared by reacting respective amine derivatives with 1,4-di(thiophen-2-yl)butane-1,4-dione intermediate. The synthesis of diketone intermediate can be attained by various methods such as: a) Stevens rearrangement of *N,N*-di(2-thienylmethyl)-*N,N*-dimethyl ammonium salts followed by elimination of dimethyl amine and then reduction of the subsequent 2-butene-1,4-diones [120], b) oxidation of the lithium enolate of 2-acetylthiophene with cupric chloride to 1,4-di(2'-thienyl)1,4-butanedione [121], c) the

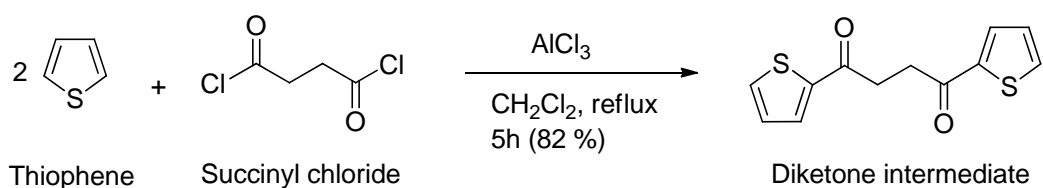
reaction of 2-thiophenealdehyde with 3-dimethylamino-1-(2-thienyl)propanone [122], d) from phenyllithium and N,N,N',N'-tetramethyl succinamide [123] etc. Unfortunately all these synthetic approaches require expensive materials or reagents, lengthy reaction times, harsh conditions, while often result in only modest yields of the products. Therefore, another reported procedure [124] based on cheap starting materials, simple reaction conditions and good yield of the product was selected. The double Friedel-Crafts reaction of thiophene and succinyl chloride in the presence of aluminium chloride as Lewis acid catalyst is a single step procedure with good yield.

The synthesis of monomers was easily achieved via Knorr-Paal pyrrole condensation reaction on 1,4-di(thiophen-2-yl)butane-1,4-dione intermediate. With the diketone intermediate, different aromatic amines were cyclized using *p*-toluenesulfonic acid (PTSA) as a catalyst and under reflux conditions in dry toluene. The condensation of *o*-anisidine, *o*-toluidine, 2-aminoacetophenone, 4-fluoroaniline, 4-chloroaniline, 4-bromoaniline, 4-iodoaniline, 1-naphthalamine, 2-aminoacetophenone with diketone intermediate offered their respective dithienyl pyrroles. However, initially Paal-Knorr reaction gave very poor yield with couple of amines. The yield for these reactions was increased using Dean-Stark apparatus for continuous removal of water forming inside reaction. The reaction was continued until all the starting material was consumed.

2.1.2 Friedel-Crafts acylation: Synthesis of 1,4-diketone intermediate

The Friedel-Crafts method is the reaction developed by C. Friedel and J. Crafts to attach alkyl or acyl substituents to an aromatic ring using strong Lewis acid catalyst. The same procedure has been reliably used to attach an alkyl or acyl group at the 2-position and/or 5-position of thiophene and pyrrole. It is an electrophilic substitution reaction between acyl or alkyl and aromatic ring which uses aluminium chloride (AlCl_3) as Lewis acid catalyst.

In diketone intermediate formation, aluminium chloride first reacts with the acyl groups of succinyl chloride where dissociation of chloride ion forms the electrophile, acyl cation, and AlCl_4^- ion. At this stage, thiophene attacks the electron deficient acyl cation and finally AlCl_4^- anion deprotonate the ring to form HCl and regenerates the AlCl_3 . This process occurs simultaneously at both acyl groups of succinyl chloride and the attack of two thiophenes yield 1,4-di(thiophen-2-yl)butane-1,4-dione. The reaction scheme and mechanism of Friedel-Crafts reaction are given in scheme 1 and figure 18 respectively.



Scheme 1. Synthesis of 1,4-di(thiophen-2-yl)butane-1,4-dione

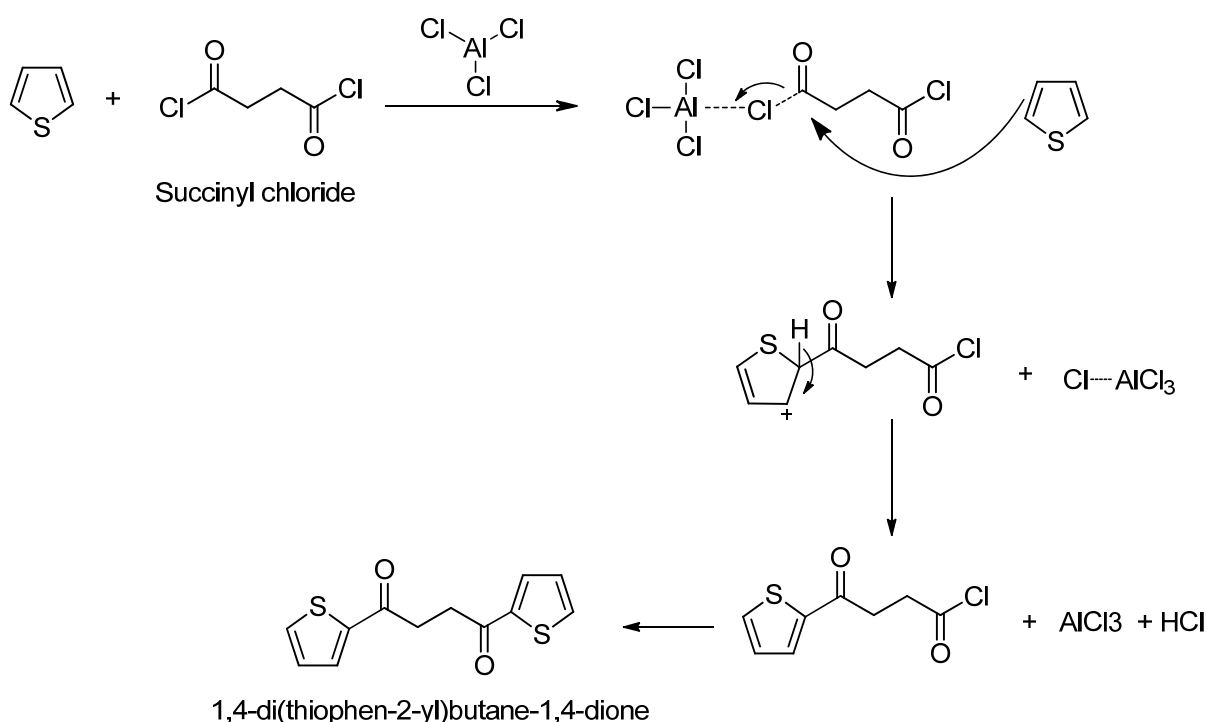


Figure 18. Mechanism of Friedel-Crafts reaction of thiophene and succinyl chloride

2.1.3 Paal-Knorr Pyrrole synthesis: Synthesis of 2,5-di(2-thienyl)-1H-pyrroles

This method of synthesis of pyrroles, furans and thiophenes from 1,4-dicarbonyl compounds was first reported in 1884 by German chemists Carl Paal and Ludwig Knorr. In the case of pyrrole synthesis, diketone compound and amine reacts in a suitable organic solvent, in weakly acidic conditions generally at higher temperature.

Though there are several mechanistic routes have been suggested on mechanism of pyrrole formation but the mechanism suggested by Amarath *et al.* [125] has been widely accepted. They have shown that amine adds to one of the carbonyl groups of the diketone to form a

hemiaminal. Then another lone pair of the nitrogen atom of amine attacks another carbonyl group of diketone to form diol. They also showed that there could be a formation for imine from hemiaminal but it does not lead to pyrrole formation directly. The imine reaches a maximum concentration and tautomerises back to the hemiaminal and diketone. The formation of cyclised diol intermediate has been shown to exist and its cyclisation is considered the rate determining step. An overview of the possible mechanistic route involved in general Paal-Knorr pyrrole synthesis is given in figure 19.

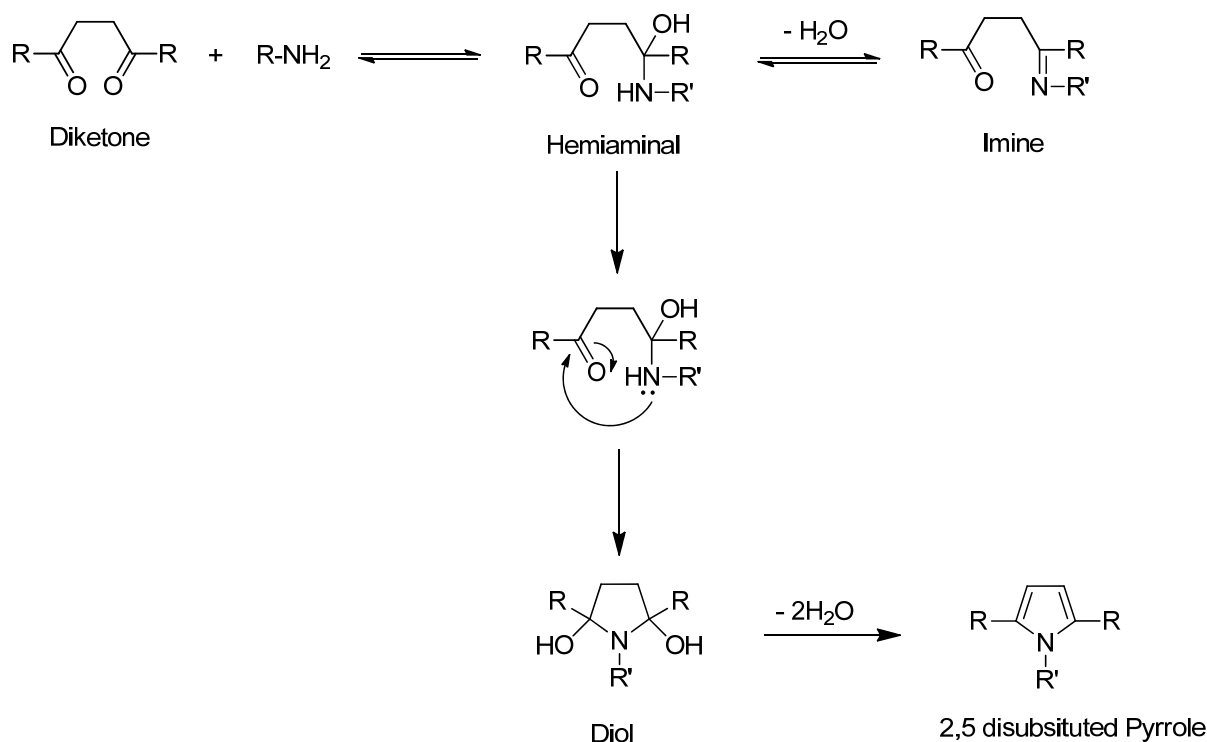
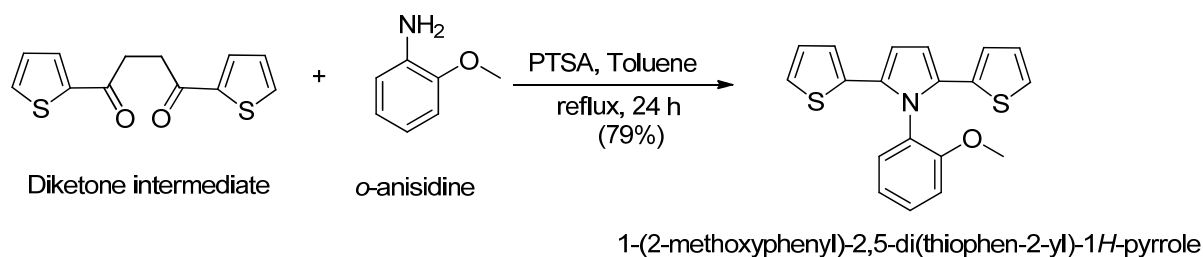


Figure 19. General reaction mechanism of Paal-Knorr pyrrole synthesis

In the case of SNS formation, 1,4-di(thiophen-2-yl)butane-1,4-dione intermediate and amine derivative are reacted at reflux conditions with the catalytic amount of PTSA as a catalyst. The reaction scheme and proposed possible reaction mechanism of 2,5-di(2-thienyl)-1H-pyrrole formation are shown given in scheme 2 and figure 20 respectively.

2. Poly(dithienyl pyrrole) based chemical gas sensors



Scheme 2. Synthesis of SNS by Knorr-Paal synthesis

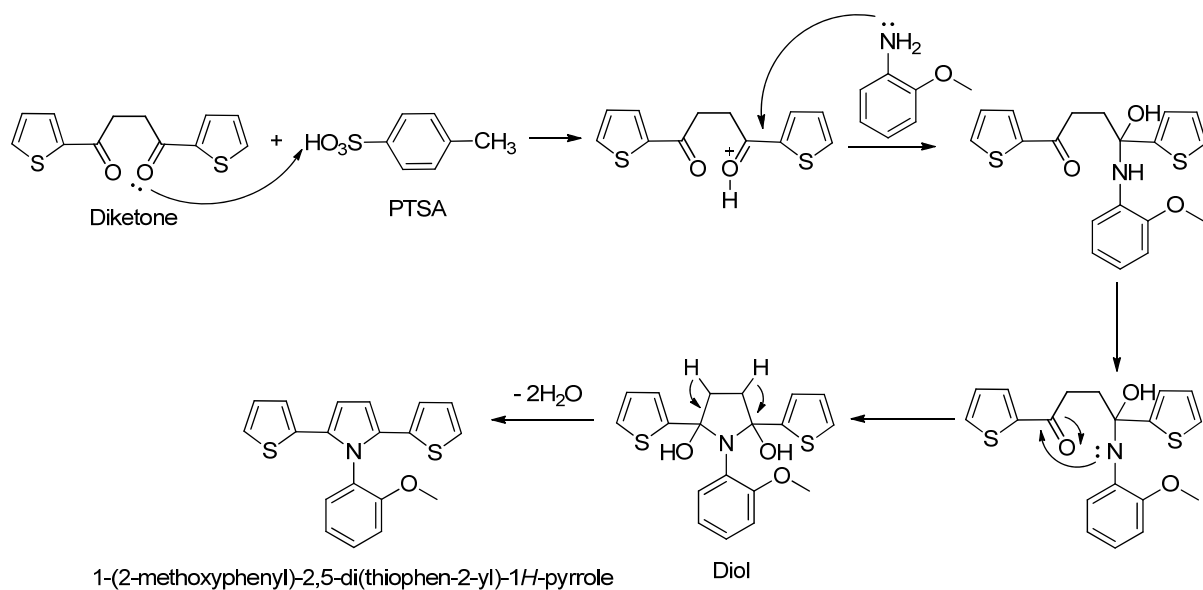
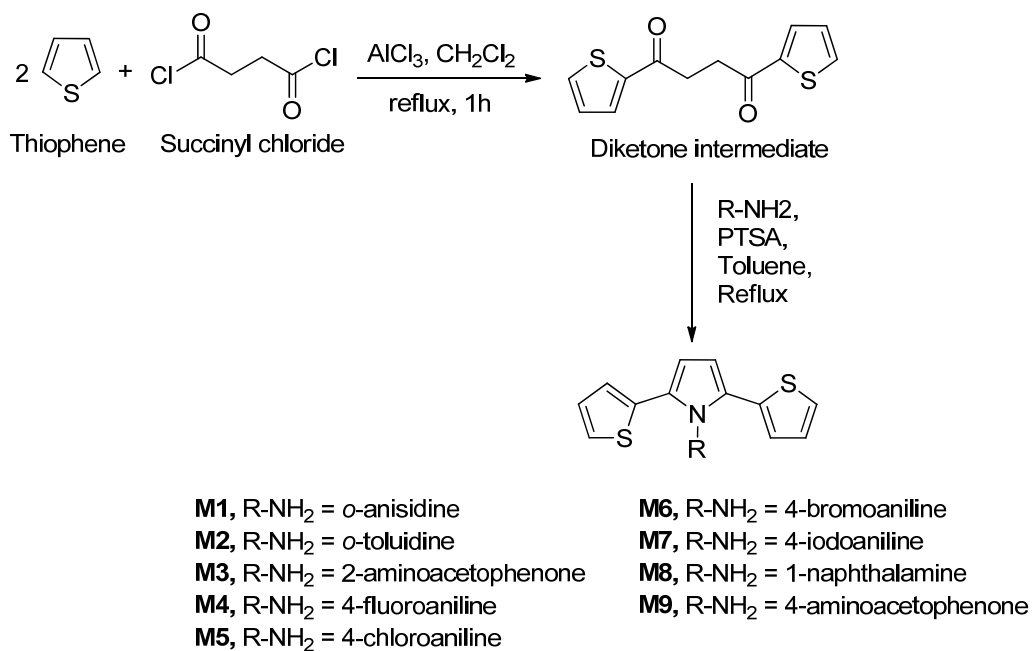


Figure 20. Mechanism of Paal-Knorr pyrrole synthesis

2.1.4 Complete reaction scheme

As mentioned above, a number of SNS derivatives with different N-substituents have been synthesized. They are: 1-(2-methoxyphenyl)-2,5-di(thiophen-2-yl)-1H-pyrrole (**M1**), 2,5-di(thiophene-2-yl)-1-(*o*-tolyl)-1H-pyrrole (**M2**), 1-(2-(2,5-di(thiophen-2-yl)1H-pyrrol-1-yl)phenyl)ethanone (**M3**), 1-(4-fluorophenyl)-2,5-di(thiophen-2-yl)-1H-pyrrole (**M4**), 1-(4-chlorophenyl)-2,5-di(thiophen-2-yl)-1H-pyrrole (**M5**), 1-(4-bromophenyl)-2,5-di(thiophen-2-yl)-1H-pyrrole (**M6**), 1-(4-iodophenyl)-2,5-di(thiophen-2-yl)-1H-pyrrole (**M7**), 1-(naphthalen-1-yl)-2,5-di(thiophen-2-yl)-1H-pyrrole (**M8**) and 1-(4-(2,5-di(thiophen-2-yl)-1H-pyrrol-1-yl)phenyl)ethanone (**M9**). The complete reaction scheme and the structures of the synthesized SNS monomers are presented in scheme 3 and Figure 21 respectively.

2. Poly(dithienyl pyrrole) based chemical gas sensors



Scheme 3. Complete reaction scheme of dithienyl pyrrole derivatives

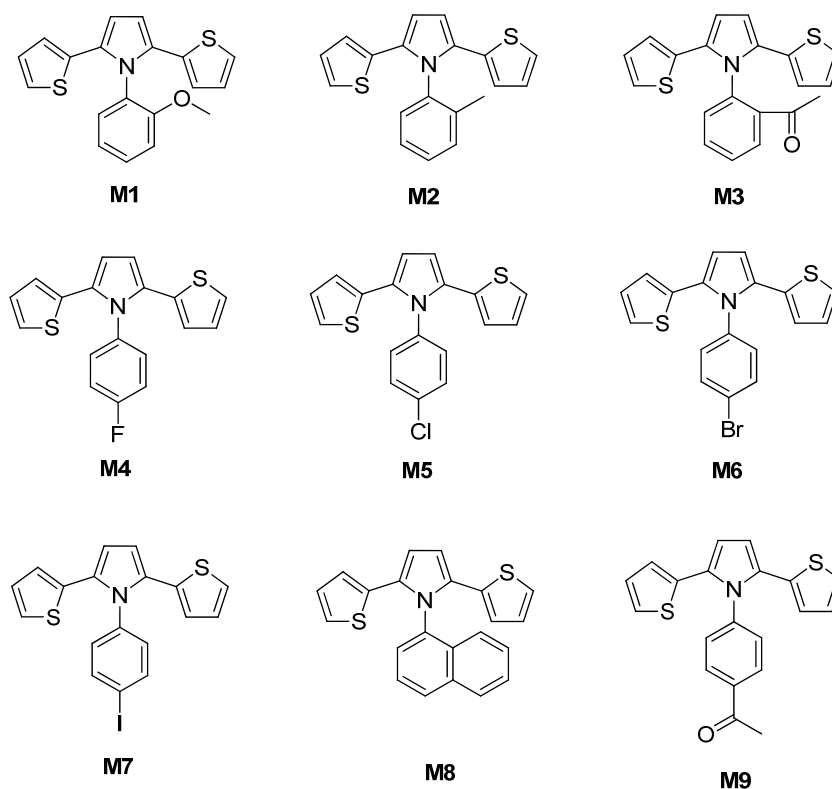


Figure 21: Structures of synthesized SNS monomers

2.2 Experimental section

This section explains about materials and methods, and experimental procedures for the synthesis of SNS monomers and their polymerization by chemical and electrochemical methods. Furthermore, it will describe fabrication of chemical sensors and their operando characterizations against various analytes using gas mixing systems.

2.2.1 Materials and instrumentation

2.2.1.1 Chemicals and working techniques

All chemicals were purchased from commercial suppliers like Acros Organics, Aldrich, Fluka, Merck and Fisher Scientific. All reagents obtained from commercial suppliers were used throughout without further purification unless otherwise stated. Anhydrous solvents for reactions were purchased as follows toluene, ethanol, methanol, glacial acetic acid from Fisher-Scientific; acetonitrile, DMF from Merck; THF from Sigma-Aldrich and DCM from Fluka. Unless and otherwise mentioned, all the reactions were carried out under a nitrogen atmosphere and the reaction flasks were pre-dried with a heat gun under vacuum. All the chemicals, which were air or water sensitive, were stored & used under inert atmosphere.

2.2.1.2 NMR spectroscopy

All the spectra were measured on a Bruker Avance 400 spectrometer, which operates at 400 MHz for ^1H and 100 MHz for ^{13}C nuclei, respectively. ^1H and ^{13}C NMR spectra were recorded at 295 K in deuterated solvent, CDCl_3 . The chemical shifts were assigned by comparison with the residual proton and carbon resonance of the solvent: CDCl_3 ($\delta \text{H} = 7.25$ ppm, $\delta \text{C} = 77.0$ ppm) and tetramethylsilane as the internal reference ($\delta = 0$). Data are reported as follows: chemical shift (multiplicity: s = singlet, d = doublet, t = triplet, dd = doublet of doublet, m = multiplet, J = coupling constant (Hz)).

2.2.1.3 Mass spectroscopy

Mass spectra were recorded on a Finnigan Triple-Stage-Quadrupol Spectrometer (TSQ-70) from Finnigan-Mat. High-resolution mass spectra were measured on a modified AMD Intectra MAT 711A from the same company. The mass spectrometric ionization methods used was electron-impact (EI). HR-FT-ICR mass spectra were measured on an APEX 2 spectrometer from Bruker Daltonic with electrospray ionization method (ESI). The high

resolution mass spectroscopy (HRMS) analysis is reported as calculated mass for the related compound followed by found mass.

2.2.1.4 FTIR spectroscopy

Infrared spectra were recorded on Bruker Vertex 70 spectrometer in the range 400 to 4000 cm^{-1} and the peak positions are given as transmittance (%) against wavenumbers (cm^{-1}). The samples were mixed with KBr (sample-KBr ratio, 2-3:200 mg) and pressed into a pellet for measurement. The background scan of KBr pellet was performed for accurate quantification of sample since it provides a baseline before injecting compounds to be analysed.

2.2.1.5 Chromatographic methods

Flash chromatography was performed using flash silica gel (pore size 60 Å, 230-400 mesh particle size, 40-63 μm particle size) from Sigma-Aldrich. Analytical thin layer chromatography (TLC) was performed on aluminum sheet silica gel plates with 0.2 mm thick silica gel 60 F₂₅₄ from Merck using different solvent mixtures as a mobile phase. The compounds were visualized by UV₂₅₄ light and the chromatography plates were developed in iodine chamber.

2.2.1.6 Other methods

Ultraviolet-visible absorption spectra of the monomers and polymers in DCM were recorded with a Perkin Elmer Lambda 15 double beam spectrophotometer in the range of 190-900 nm. The solutions were prepared by dissolving 2-3 mg sample in 10 mL of DCM. The surface morphology of electrochemically deposited polymer layers was investigated (SEM imaging) with a Hitachi SU8030 FE-SEM microscope. A hydraulic press from Perkin-Elmer was used to press the polymer samples in to pellets for electrical conductivity and sensing measurements. The pellets were obtained by subjecting the polymer samples (~100 mg) to a pressure of 10 tonnes / cm^2 . The thermo-gravimetric analysis of the monomers and polymers was performed with a Netzsch STA 449 F3 Jupiter TGA instrument.

2.2.2 Synthesis of monomers

The monomers were synthesized in two steps. Firstly, 1,4-di(thiophen-2-yl)butane-1,4-dione intermediate was prepared from thiophene as a simple precursor and in the second step diketone intermediate was reacted with different aniline derivatives to produce SNS monomers.

1,4-di(thiophen-2-yl)butane-1,4-dione intermediate

To a suspension of AlCl₃ (31.69 g, 237.70 mmol) in 25 mL of DCM in a three neck round bottom flask under inert gas atmosphere, a solution of thiophene (19.03 mL, 237.70 mmol) and succinyl chloride (13.09 mL, 118.85 mmol) in 20 mL DCM was added drop wise over the period of 1 hour. The reaction mixture was refluxed at 45-50 °C for 1h under constant stirring. The progress of reaction was monitored by TLC. The reaction mixture was then poured into a mixture of ice and concentrated HCl (10 mL). The dark green organic phase was extracted with DCM (3 × 50 mL). The combined organic layers were washed with saturated NaHCO₃ (25 mL) and NaCl (50 mL) solutions, dried over anhydrous Na₂SO₄, filtered and concentrated under reduced pressure. The residue was purified by flash column chromatography (DCM/hexane, 1:9) to yield 1,4-di(thiophen-2-yl)butane-1,4-dione intermediate as a pure white solid.

General experimental procedure for the preparation of monomers (M1-M9)

A mixture of 1,4-di(thiophen-2-yl)butane-1,4-dione intermediate, aromatic amine derivative and PTSA in anhydrous toluene was refluxed under inert gas atmosphere at 120-130 °C using the Dean-Stark apparatus. The progress of the reactions was monitored by TLC. The reaction was performed until the starting material was totally consumed. After completion of reaction, the solvent was evaporated under vacuum and the reaction mixture was extracted with ethyl acetate (50 mL × 3). The combined ethyl acetate layers were washed with saturated NaHCO₃ (25 mL) and NaCl (25 mL) solutions, dried over anhydrous Na₂SO₄ and concentrated under vacuum. The crude compound was subjected to flash column chromatography in DCM/hexane to afford corresponding SNS derivatives.

Reagents and conditions: (M1) Diketone intermediate (5 g, 20 mmol), *o*-anisidine (3.69 g, 30 mmol), PTSA (1.14 g, 6 mmol), toluene (60 mL), reflux, 48h; (M2) Diketone intermediate (5 g, 20 mmol), *o*-toluidine (2.79 g, 26 mmol), PTSA (0.76 g, 4 mmol), toluene (80 mL), reflux, 24h; (M3) Diketone intermediate (5 g, 20 mmol), 2-aminoacetophenone (3.46 g, 24 mmol), PTSA (0.76 g 4 mmol), toluene (80 mL), reflux, 72h; (M4) Diketone intermediate (5 g, 20 mmol), 4-fluoroaniline (2.89 g, 26 mmol), PTSA (0.76 g, 4 mmol), toluene (60 mL), reflux, 48h; (M5) Diketone intermediate (5 g, 20 mmol), 4-chloroaniline (3.31 g, 26 mmol), PTSA (1.52 g, 8 mmol), toluene (80 mL), reflux, 48h; (M6) Diketone intermediate (3 g, 12 mmol), 4-bromoaniline (2.48 g, 14.4 mmol), PTSA (0.46 g, 2.4 mmol), toluene, reflux, 48h; (M7) Diketone intermediate (7 g, 28 mmol), 4-iodoaniline (7.97 g, 36.4 mmol), PTSA (1.07

2. Poly(dithienyl pyrrole) based chemical gas sensors

g, 5.6 mmol), toluene, reflux, 48h; (**M8**) Diketone intermediate (5 g, 20 mmol), 1-naphthalamine (3.437 g, 24 mmol) and PTSA (0.761 g, 4 mmol), toluene (60 mL), reflux, 48h; (**M9**) Diketone intermediate (5 g, 20 mmol), 4-aminoacetophenone (3.25 g, 24 mmol), PTSA (0.76 g, 5.6 mmol), toluene (80 mL), reflux, 48h.

2.2.3 Chemical polymerization

The chemical polymerization of synthesized SNS monomers was achieved using FeCl_3 as oxidizing reagent. The monomers (10 mmol) were dissolved in 60 mL ACN in a round bottom flask under inert gas atmosphere and FeCl_3 (100 mmol) solution in 20 mL ACN was added drop-wise to the solution of monomers while stirring at room temperature. The dark green or blue colour was observed during the addition of oxidant into the monomers. The reaction was carried out overnight at room temperature. The dark precipitated polymer was collected by filtration, washed with methanol to remove the unreacted monomers and dried under vacuum. The table 1 shows the concentration of monomers and oxidant used and some other details about chemical polymerization.

Table 1. Chemical polymerization of SNS derivatives

No	Monomer	Quantity (10 mmol)	Oxidant (100 mmol)	Yield	Polymer colour	Polymer named as
1	M1	202.48 mg	540.6 mg	431 mg	Black	P1
2	M2	192.88 mg	540.6 mg	228mg	Black	P2
3	M3	209.68 mg	540.6 mg	200 mg	Dark green	P3
4	M4	195.25 mg	540.6 mg	206 mg	Black	P4
5	M5	204.88 mg	540.6 mg	216 mg	Dark green	P5
6	M6	231.79 mg	540.6 mg	224 mg	Black	P6
7	M7	259.99 mg	540.6 mg	280 mg	Black	P7
8	M8	214.49 mg	540.6 mg	215 mg	Black	P8
9	M9	209.68 mg	540.6 mg	207 mg	Dark green	P9

2.2.4 Redox studies and electrochemical polymerization

The redox behaviour of the prepared SNS monomers was investigated through CV. The CV measurements have been performed with a scanning potentiostat. The potential ramps have

2. Poly(dithienyl pyrrole) based chemical gas sensors

been supplied to the single compartment electrochemical cell having gold as a working, platinum as a counter and Ag/AgCl (3.0M KCl) as a reference electrodes. The measurements have been performed by sweeping the potential between 0.0V to +1.5V versus Ag/AgCl (3.0 M KCl) at 100 mV/s in a solution of SNS monomer (10 mmol) and TEA-PTS (100 mmol) in 30 mL ACN.

The SNS monomers were electrochemically polymerized in the same cell used for CV. Fully oxidised conducting polymer film on the gold working electrode was obtained by chronoamperometry, by applying the oxidation potential of the monomers for 1 minute. Polymer films prepared on working electrode were washed couple of times by dipping in ACN in order to remove any unreacted monomer or TEA-PTS trapped in the film. Table 2 gives more details about solution preparation for electrochemical deposition of each polymer.

Table 2. SNS monomers and oxidants used for electrochemical depositions

No.	Monomer	Quantity (10 mmol in 60 mL)	Oxidant (100 mmol in 20 mL)	Polymer colour
1	M1	101.24 mg	904.35 mg	Black
2	M2	96.44 mg	904.35 mg	Black
3	M3	104.84 mg	904.35 mg	Dark green
4	M4	97.62 mg	904.35 mg	Black
5	M5	102.44 mg	904.35 mg	Dark green
6	M6	115.90 mg	904.35 mg	Black
7	M7	129.99 mg	904.35 mg	Black
8	M8	107.25 mg	904.35 mg	Black
9	M9	209.68 mg	904.35 mg	Dark green

2.2.5 Fabrication of sensors

2.2.5.1 Polymer pellet sensor

The chemically prepared polymer powders (~150 mg) were pressed into pellets using hydraulic pressure at 10 tonnes / cm² and used as a sensor by connecting with ZIF socket to the electric supply [126]. The prepared pellets had 13 mm diameter and 0.5 mm thickness.

The pellets were mounted in the tight Teflon[®] measuring chamber and used for further characterizations. The pellets made from chemically obtained polymers (**P1-P9**) were named as **Pellet P1-Pellet P9** respectively.

2.2.5.2 Flexible IDEs Chemoresistor

Chemoresistive sensors were fabricated by depositing the SNS polymeric sensing layers on IDE substrates by electrochemical polymerization method using three electrodes electrochemical cell. The IDE substrates used were comb like interdigitated gold electrodes deposited on flexible PET or PI film (film thickness: 125/50 μm) by peel-off technique. The metallic fingers of IDE were 5 mm long and 100 nm thick whereas insulating gap between the two electrodes was 18 μm . The flexible IDE substrates were fabricated and supplied by IMT, SAMLAB, EPFL, Neuchatel, Switzerland.

Electrochemical cell: The electrochemical deposition of SNS polymers was performed using single compartment three electrodes electrochemical cell. The cell consists of thin platinum plate (16 mm long & 5 mm wide) as a counter electrode, Ag/AgCl (3.0M KCl) electrode (Schott Germany) as a reference and IDE substrates as working electrode. The total volume of glass cell was about 30 mL.

Substrate preparation: Prior to electrochemical deposition, IDE transducers were gently cleaned of dust particles and any organic materials traces. The substrates were first kept in the distilled water for few minutes and then rinsed with acetone or ethanol and dried at room temperature. The cleaned substrates were checked under high resolution microscope and with a multimeter for any physical damage.

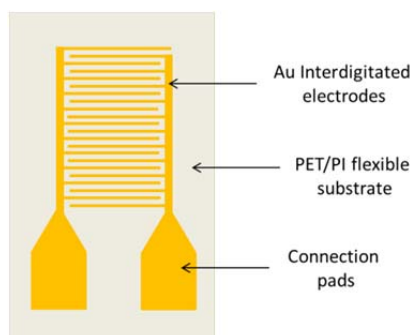


Figure 22. Interdigitated electrodes (IDEs) transducer

Electrochemical deposition: The solutions required for electrochemical polymerization on IDEs were prepared as mentioned in table 2. The SNS monomers (10 mmol) and TEA-PTS (100 mmol) were dissolved in ACN (30 mL) in a glass flask and the three electrodes immersed in the solution. The solutions were kept unstirred in order to favour deposition of the polymer layers on the transducers.

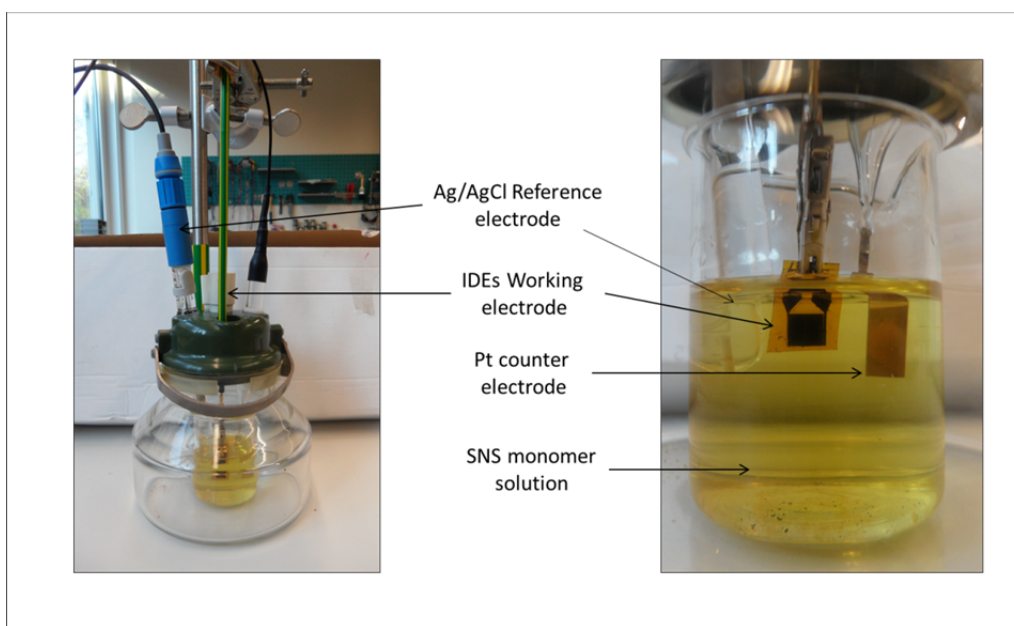


Figure 23. Experimental set up for electrochemical deposition on IDEs

When potential sweeping was performed for redox studies, deposition of the polymer layer occurred at the oxidation potential but fully oxidised conducting polymer films were obtained by oxidising the monomers at their oxidation potentials for one minute through chronoamperometry technique. The polymer films formed were dark green or black coloured. The substrates were then carefully taken out of the cell and washed with ACN several times in order to remove any trapped/unreacted monomers. Four chemoresistive sensors were fabricated from four SNS monomers (schematics in fig. 24).

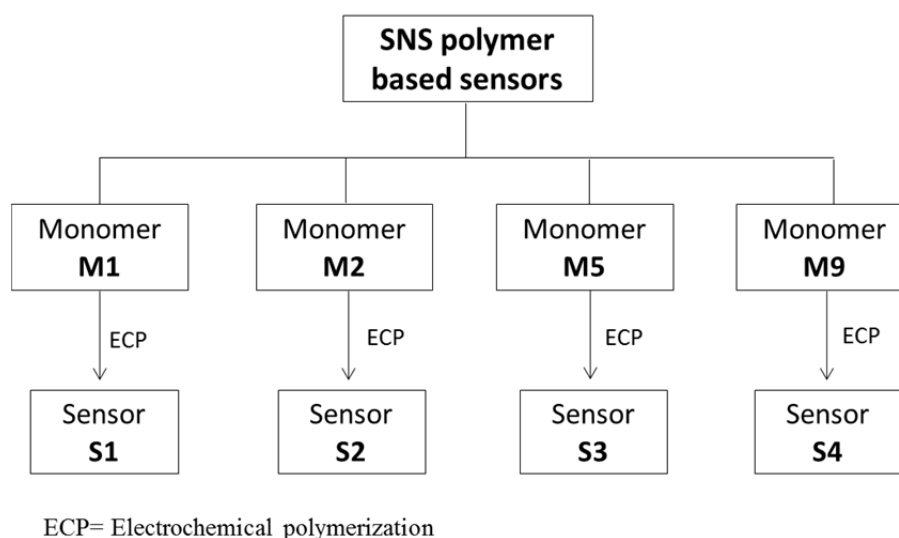


Figure 24. Schematics of IDEs chemoresistive sensors prepared from SNS monomers

2.2.6 Sensor characterization under controlled conditions

In order to perform the required functional tests and characterization under controlled atmosphere, the pellets or IDEs sensors were placed in tight Teflon[®] measuring chamber where desired ambient or exposure conditions were realised. To avoid the effect of not only chemical composition of the environment but also temperature and light, measuring chamber was placed in an environmental test system (Espec Corp. Model: PU-1KTH). The sensors were exposed to gaseous mixtures of target analytes with synthetic air (80% N₂ and 20% O₂, purity 5.5 from Westfalen AG) using suitable devices to ensure required concentration of the analyte. To keep the ambient fresh in the measuring chamber, gaseous mixtures were supplied dynamically (200 sccm test gas flow). The sensor responses were acquired by Agilent 34970A data acquisition/data logger switch unit in order to bring them as readable output.

The computer controlled gas mixing and measurement system (GMMS) (Figure 25) allows the testing and calibration of gas sensors under controlled conditions. It facilitated the exposure of desired analytes with well-defined concentrations and recorded the sensor responses.

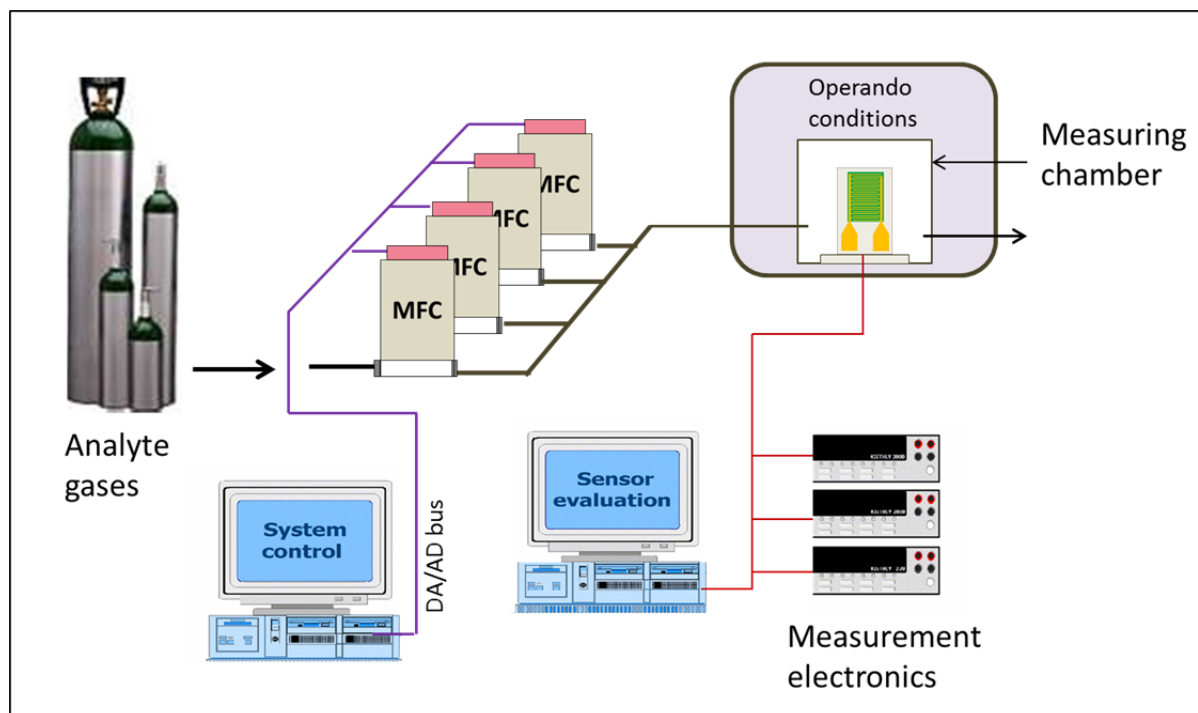


Figure 25. Schematic presentation of gas mixing and measurement system

The first part of the gas mixing system consists of gas bottles or gas generator to supply the chemical analytes, mass flow controller (MFC) to ensure the supply of desired gases with well-defined concentrations which then mixed together to have an expected gaseous mixture. Magnetic valves were installed after the MFCs which switch on or off the gaseous flow through the pipelines. The gas mixing unit was operated by dedicated driving software, 'FlowControl' which operates under HP/Agilent VEE graphical software with Excel XLS instruction files. The next part is the measuring chamber in which sensors are fixed and electrically connected by appropriate sockets. The responses given by the sensors to the analytes were recorded or processed by dedicated measurement software and computer.

2.3 Results and discussions

2.3.1 Synthesis of monomers

The SNS monomers were synthesized in two steps starting with thiophene as a simple precursor as already explained in section 2.1. In the first step, diketone intermediate was synthesized using double Friedel-Crafts reaction on thiophene and succinyl chloride with AlCl_3 as a Lewis acid catalyst. Here the reaction time was considerably reduced from 18h as reported in [124] (reaction at room temperature) to 1h only by refluxing the reaction mixture. The refluxing of the reaction mixture did not cause any loss in the yield of the reaction. After

purification by column chromatography, diketone intermediate was obtained at a very good yield over 80%. In the second step, Paal-Knorr condensation reaction on 1,4-di(thiophen-2-yl)butane-1,4-dione intermediate and corresponding aromatic amines in the presence of PTSA (as a catalyst) produced SNS monomers (**M1-M9**) also with good yields. The diketone intermediate and SNS monomers were characterized using various spectroscopic methods such as ^1H NMR, ^{13}C NMR, HRMS, FTIR, etc. The prepared monomers were then polymerized by both chemical and electrochemical methods.

1,4-di(thiophen-2-yl)butane-1,4-dione intermediate: colourless-white solid; Yield 82%; ^1H NMR (400 MHz, CDCl_3): δ 3.37 (s, 4H, $\text{CH}_2\text{-CH}_2$), 7.13 (t, $J = 3.79, 4.80, 8.59$ Hz, 2H), 7.63 (dd, $J = 1.01, 5.06$ Hz, 2H), 7.80 (dd, $J = 1.01, 3.79$ Hz, 2H); ^{13}C NMR (100 MHz, CDCl_3): δ 33.09, 128.09, 132.06, 133.59, 143.68, 191.32; **FT-IR:** 3100 cm^{-1} (aromatic C-H), 2918 cm^{-1} (aliphatic C-H), 1649 cm^{-1} (carbonyl group), $1405\text{-}1514\text{ cm}^{-1}$ (aromatic C=C), 1351 cm^{-1} , 1315 cm^{-1} , 1055 cm^{-1} (C-H in plane bending), 730 cm^{-1} (C-H α out of plane bending of thiophene); **HRMS** (ESI): $[\text{M}+\text{Na}]^+$ calculated for $\text{C}_{12}\text{H}_{10}\text{O}_2\text{S}_2\text{Na}$: 273.0014, found 273.0011.

1-(2-methoxyphenyl)-2,5-di(thiophen-2-yl)-1H-pyrrole (M1): Yellowish-brown solid; Yield 79%; M. p. $124\text{-}125\text{ }^\circ\text{C}$; ^1H NMR (400 MHz, CDCl_3): δ 3.55 (s, 3H, $-\text{OCH}_3$), 6.49 (s, 2H), 6.55 (dd, $J = 1.01, 3.53$ Hz, 2H), 6.72 (t, $J = 3.78, 5.30, 8.84$ Hz, 2H), 6.88 (m, 2H), 6.92 (dd, $J = 1.27, 5.05$ Hz, 2H), 7.15 (d, $J = 1.77, 7.84$ Hz, 1H, Ar-H), 7.36 (t, $J = 7.83, 15.91$ Hz, 1H, Ar-H); ^{13}C NMR (100 MHz, CDCl_3): δ 55.73 ($-\text{OCH}_3$), 109.44 (CH-CH, pyrrole), 112.25, 120.78, 123.54, 123.62, 126.75, 127.17, 130.07, 130.79, 131.49, 134.97, 157.21; **FT-IR:** 3100 cm^{-1} (aromatic C-H), 2933 cm^{-1} (aliphatic C-H), $1400\text{-}1503\text{ cm}^{-1}$ (aromatic C=C), 1277 cm^{-1} (C-N stretching due to pyrrole and benzene), 1019 cm^{-1} (C-H in plane bending of benzene), 842 cm^{-1} (C-H β of thiophene ring), 760 cm^{-1} (C-H β of pyrrole ring), 691 cm^{-1} (C-H α out of plane bending of thiophene); **HRMS** (ESI): calculated for $\text{C}_{19}\text{H}_{15}\text{NOS}_2$: 337.0590, found 337.0588.

2,5-di(thiophene-2-yl)-1-(*o*-tolyl)-1H-pyrrole (M2): White powder; Yield 84%; M. p. $118\text{-}120\text{ }^\circ\text{C}$; ^1H NMR (400 MHz, CDCl_3), δ (ppm): 1.94 (s, 3H, $-\text{CH}_3$), 6.54 (dd, $J = 1.01, 3.54$ Hz, 2H), 6.61 (s, 2H), 6.80 (t, $J = 3.79, 5.31$ Hz, 2H), 7.01 (dd, $J = 1.26, 5.05$ Hz, 2H), 7.31 (t, $J = 6.32, 14.15$ Hz, 2H, Ar-H), 7.37 (d, $J = 8.59$ Hz, 1H, Ar-H), 7.43 (t, $J = 7.33, 14.65$ Hz, 1H, Ar-H); ^{13}C NMR (100 MHz, CDCl_3), δ (ppm): 17.34 ($-\text{CH}_3$), 109.43 (CH-CH,

pyrrole), 123.16, 123.56, 126.85, 126.92, 129.49, 129.70, 130.46, 131.01, 134.93, 137.60, 138.51; **FTIR**: 3103 cm^{-1} (aromatic C-H), 2920 cm^{-1} (aliphatic C-H), 1406-1493 cm^{-1} (aromatic C=C), 1250 cm^{-1} (C-N stretching due to pyrrole and benzene), 1041 cm^{-1} (C-H in plane bending of benzene), 842 cm^{-1} (C-H $_{\beta}$ of thiophene), 763 cm^{-1} (C-H $_{\beta}$ of pyrrole ring), 725 cm^{-1} (*ortho*-methyl substituted benzene), 687 cm^{-1} (C-H $_{\alpha}$ out of plane bending of thiophene); **HRMS** (ESI): calculated for C₁₉H₁₅NS₂: 321.0640, found 321.0643.

1-(2-(2,5-di(thiophen-2-yl)1H-pyrrol-1-yl)phenyl)ethanone (M3): Yellowish light weight powder; **R_f** = 0.39 (DCM/hexane, 1:1); Yield 76%; M. p. 194-195 °C; **¹H NMR** (400 MHz, CDCl₃), δ (ppm): 2.63 (s, 3H, -COCH₃), 6.51 (dd, J = 1.01, 3.54 Hz, 2H), 6.54 (s, 2H, pyrrole), 6.82 (t, J = 3.79, 5.05, 8.84 Hz, 2H), 7.08 (dd, J = 1.01, 5.05 Hz, 2H), 7.15 (d, J = 1.77, 7.84 Hz, 1H, Ar-*H*), 7.36 (t, J = 7.83, 15.91 Hz, 1H, Ar-*H*), 7.37 (d, J = 8.59 Hz, 2H, Ar-*H*); **¹³C NMR** (100 MHz, CDCl₃), δ (ppm): 26.67 (-COCH₃), 110.67 (CH-CH, pyrrole), 124.52, 124.98, 126.98, 129.05 (2CH, 129.74, 129.98, 134.33, 136.88, 142.54, 197.10 (-COCH₃); **FTIR**: 3086-3104 cm^{-1} (aromatic C-H), 1681 cm^{-1} (carbonyl group), 1410-1500 cm^{-1} (aromatic C=C), 1261 cm^{-1} (C-N stretching due to pyrrole and benzene), 1038 cm^{-1} (C-H in plane bending of benzene), 840 cm^{-1} (C-H $_{\beta}$ of thiophene), 760 cm^{-1} (C-H $_{\beta}$ of pyrrole ring), 700 cm^{-1} (C-H $_{\alpha}$ out of plane bending for thiophene ring); **HRMS** (ESI): calculated for C₂₀H₁₅NOS₂: 349.0590, found 349.0583.

1-(4-fluorophenyl)-2,5-di(thiophen-2-yl)-1H-pyrrole (M4): Yellowish white solid; Yield 69%; M. p. 188 °C; **¹H NMR** (400 MHz, CDCl₃), δ (ppm): 6.46 (s, 2H, pyrrole H), 6.48 (dd, J = 1.01, 3.53 Hz, 2H), 6.76 (t, J = 3.79, 5.06, 8.85 Hz, 2H), 7.00 (dd, J = 1.26, 5.30 Hz, 2H), 7.05 (2H, Ar-*H*), 7.20 (2H, Ar-*H*); **¹³C NMR** (100 MHz, CDCl₃), δ (ppm): 109.93, 116.07, 116.29, 124.21, 124.44, 126.93, 130.16, 131.62, 131.70, 134.36, 134.39, 134.66, 161.50, 163.98; **FT-IR**: 3104 cm^{-1} (C-H stretching of benzene), 3073 cm^{-1} (C-H stretching of thiophene), 1411-1511 cm^{-1} (aromatic C=C), 1222 cm^{-1} (C-N stretching due to pyrrole and benzene), 1036 cm^{-1} (C-H in plane bending of benzene), 842 cm^{-1} (C-H $_{\beta}$ of thiophene ring), 765 cm^{-1} (C-H $_{\beta}$ of pyrrole ring), 693 cm^{-1} (C-H $_{\alpha}$ out of plane bending of thiophene); **HRMS** (ESI): calculated for C₁₈H₁₂FNS₂: 325.038970, found 325.38872.

1-(4-chlorophenyl)-2,5-di(thiophen-2-yl)-1H-pyrrole (M5): Yellow solid; Yield 73%; M. p. 186-187 °C; **¹H NMR** (400 MHz, CDCl₃), δ (ppm): 6.45 (s, 2H, pyrrole H), 6.47 (dd, J = 1.01, 3.54 Hz, 2H), 6.76 (t, J = 3.53, 5.05, 8.84 Hz, 2H), 7.01 (dd, J = 1.01, 5.05 Hz, 2H),

7.16 (2H, Ar-*H*), 7.31 (2H, Ar-*H*); $^{13}\text{C NMR}$ (100 MHz, CDCl_3), δ (ppm): 110.21, 124.34, 124.66, 126.99, 129.38, 129.99, 131.15, 134.51, 134.87, 136.94; **FT-IR**: 3105 cm^{-1} (C-H stretching of benzene), 3087 cm^{-1} (C-H stretching of thiophene), $1410\text{-}1492\text{ cm}^{-1}$ (aromatic C=C), 1197 cm^{-1} (C-N stretching due to pyrrole and benzene), 1035 cm^{-1} (C-H in plane bending of benzene), 833 cm^{-1} (C- H_β of thiophene ring), 762 cm^{-1} (C- H_β of pyrrole ring), 697 cm^{-1} (C- H_α out of plane bending of thiophene); **HRMS** (ESI): calculated for $\text{C}_{18}\text{H}_{12}\text{ClNS}_2$: 341.009420, found 341.009152.

1-(4-bromophenyl)-2,5-di(thiophen-2-yl)-1H-pyrrole (M6): Yellow solid; Yield 76%; M. p. 186-188 °C; $^1\text{H NMR}$ (400 MHz, CDCl_3), δ (ppm): 6.53 (s, 2H, pyrrole H), 6.55 (dd, $J = 1.01, 3.54\text{ Hz}$, 2H), 6.84 (t, $J = 3.79, 5.31, 8.85\text{ Hz}$, 2H), 7.09 (dd, $J = 1.01, 5.06\text{ Hz}$, 2H), 7.17 (2H, Ar-*H*), 7.54 (2H, Ar-*H*); $^{13}\text{C NMR}$ (100 MHz, CDCl_3), δ (ppm): 110.26, 122.93, 124.37, 124.70, 127.0, 129.91, 131.45, 132.36, 134.48, 137.45; **FT-IR**: 3104 cm^{-1} (C-H stretching of benzene), 3084 cm^{-1} (C-H stretching of thiophene), $1411\text{-}1489\text{ cm}^{-1}$ (aromatic C=C), 1192 cm^{-1} (C-N stretching due to pyrrole and benzene), 1037 cm^{-1} (C-H in plane bending of benzene), 844 cm^{-1} (C- H_β of thiophene ring), 760 cm^{-1} (C- H_β of pyrrole ring), 698 cm^{-1} (C- H_α out of plane bending of thiophene); **HRMS** (ESI): calculated for $\text{C}_{18}\text{H}_{12}\text{BrNS}_2$: 384.958905, found 384.959113.

1-(4-iodophenyl)-2,5-di(thiophen-2-yl)-1H-pyrrole (M7): Yellow solid; Yield 78%; M. p. 155-156 °C; $^1\text{H NMR}$ (400 MHz, CDCl_3), δ (ppm): 6.51 (dd, 2H), 6.54 (s, 2H, pyrrole H), 6.79-6.85 (t, $J = 3.79, 5.30, 8.84\text{ Hz}$, 2H), 7.04-7.10 (dd, $J = 1.26, 5.30\text{ Hz}$, 2H), 7.32 (2H, Ar-*H*), 7.40-7.49 (2H, Ar-*H*); $^{13}\text{C NMR}$ (100 MHz, CDCl_3), δ (ppm): 109.80, 123.97, 124.23, 126.87, 129.00, 129.16, 129.97, 131.68, 134.92, 138.34; **FT-IR**: 3104 cm^{-1} (C-H stretching of benzene), 3066 cm^{-1} (C-H stretching of thiophene), $1413\text{-}1496\text{ cm}^{-1}$ (aromatic C=C), 1195 cm^{-1} (C-N stretching due to pyrrole and benzene), 1038 cm^{-1} (C-H in plane bending of benzene), 844 cm^{-1} (C- H_β of thiophene ring), 773 cm^{-1} (C- H_β of pyrrole ring), 694 cm^{-1} (C- H_α out of plane bending of thiophene); **HRMS** (ESI): calculated for $\text{C}_{18}\text{H}_{12}\text{INS}_2$: 432.945580, found 432.940262.

1-(naphthalen-1-yl)-2,5-di(thiophen-2-yl)-1H-pyrrole (M8): white crystalline solid; Yield 79%; $^1\text{H NMR}$ (Fig. 1)(400 MHz, CDCl_3), δ (ppm): 6.32 (dd, $J = 1.27, 3.79\text{ Hz}$, 2H), 6.53 (dd, $J = 3.54, 5.05\text{ Hz}$ 2H), 6.60 (s, 2H, pyrrole H), 6.76 (dd, $J = 1.26, 5.05\text{ Hz}$, 2H), 7.22 (d, 1H, Ar-*H*), 7.26 (t, 1H, Ar-*H*), 7.35 (t, 1H, Ar-*H*), 7.41 (t, 1H, Ar-*H*), 7.48 (dd, $J = 1.26, 8.59\text{ Hz}$, 1H, Ar-*H*), 7.80 (d, $J = 8.08\text{ Hz}$ 1H, Ar-*H*), 7.90 (d, $J = 8.09\text{ Hz}$ 1H, Ar-*H*); $^{13}\text{C NMR}$

(Fig. 2) (100 MHz, CDCl₃), δ (ppm): 109.63, 123.03, 123.55, 123.58, 125.27, 126.68, 126.71, 127.53, 128.02, 128.36, 129.83, 130.98, 132.68, 133.97, 134.60, 135.08; **FT-IR**: 3100 cm⁻¹ (aromatic C-H stretching), 1415-1509 cm⁻¹ (aromatic C=C), 1347 cm⁻¹ (C-S stretching in thiophene), 1197 cm⁻¹ (C-N stretching due to pyrrole and benzene), 1030 cm⁻¹ (C-H in plane bending of naphthalene), 840 cm⁻¹ (C-H _{β} of thiophene ring), 762 cm⁻¹ (C-H _{β} of pyrrole ring), 694 cm⁻¹ (C-H _{α} out of plane bending of thiophene); **HRMS** (ESI): calculated for C₂₂H₁₅NS₂ 357.064042, found 357.064146.

1-(4-(2,5-di-(thiophen-2-yl)-1H-pyrrol-1-yl)phenyl)ethanone (M9): **¹H NMR** (400 MHz, CDCl₃), δ (ppm): 2.63 (s, 3H, -COCH₃), 6.51 (dd, J = 1.01, 3.54 Hz, 2H), 6.54 (s, 2H, pyrrole H), 6.82 (t, J = 3.79, 5.05, 8.84 Hz, 2H), 7.08 (dd, J = 1.01, 5.05 Hz, 2H), 7.37 (d, J = 8.59 Hz, 2H, Ar-H), 7.98 (d, J = 8.59 Hz, 2H, Ar-H); **¹³C NMR** (100 MHz, CDCl₃), δ (ppm): 26.67 (-COCH₃), 110.67 (CH-CH, pyrrole), 124.52, 124.98, 126.98, 129.05, 129.74, 129.98, 134.33, 136.88, 142.54, 197.10 (-COCH₃); **FTIR**: 3104.65 cm⁻¹ (aromatic C-H stretching), 3086.25 cm⁻¹ (C-H _{α} stretching of thiophene), 1681.07 cm⁻¹ (carbonyl group), 1410.5-1500 cm⁻¹ (aromatic C=C), 1261.46 cm⁻¹ (C-N stretching due to pyrrole and benzene), 1038.46 cm⁻¹ (C-H in plane bending of benzene), 762.33 cm⁻¹ (C-H _{α} out of plane bending of thiophene), 699.69 cm⁻¹ (*para*-acetyl substituted benzene ring); **HRMS** (ESI): calculated for C₂₀H₁₅NOS₂ 349.058957, found 349.058890.

2.3.2 Chemical and electrochemical polymerization

The polymerization of all synthesized SNS derivatives was achieved through both chemical and electrochemical methods using FeCl₃ and TEA-PTS as oxidant respectively. The dark green or blue colour observed during the mixing of monomer and oxidant indicated the oxidation of the monomer and formation of polymer. Chemically polymerized material was produced in the form of dark green or blue powder.

Electrochemical polymerization of the SNS derivatives was realized by the anodic deposition of polymers using a three electrodes electrochemical cell. The redox behaviour of the SNS derivatives studied by CV showed that the CV for **M1** contains two peaks (figure 26), the first is associated with the oxidation process at +0.90V, the second associated with the reduction process at +0.52V. The monomer **M2** showed first oxidation peak and a second reduction peak potential at +0.95V and +0.52V respectively (fig. 26). The CV graphs of **M1** and **M2** are given as representative for other monomers.

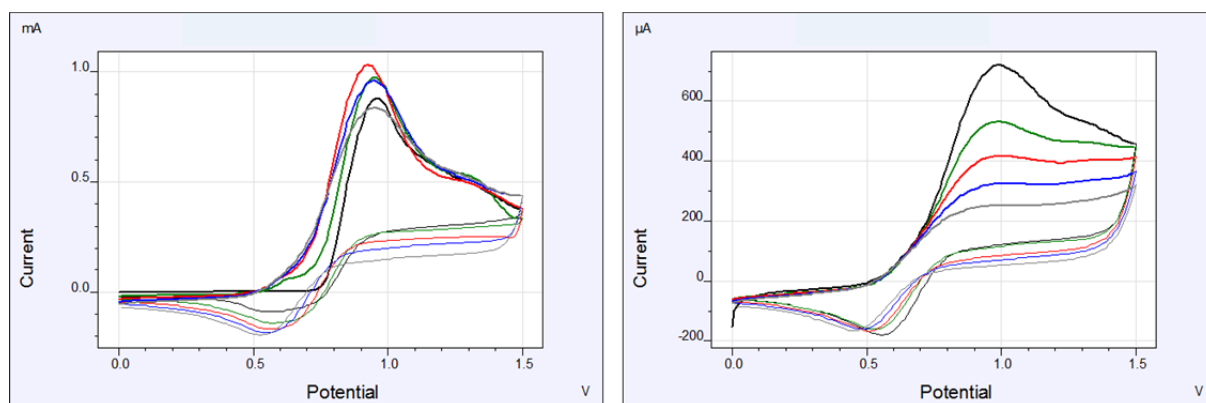


Figure 26. Cyclic voltammogram of monomer **M1** (left) and **M2** (right) in ACN solution swept over the scan range 5 times with scan rate of 100 mV/s.

When repeated potential cycling was performed, a sudden growth of polymer film was observed on the surface of the gold working electrode at the monomer oxidation potential. Under continuous cycling a gradual broadening of the redox peaks and small shifting of anodic potential in the positive direction was observed, indicating the growth of film as reported for other conducting polymers [127-130]. The redox peaks observed cannot be influenced by gold working electrode used for electrochemical polymerization as the effect of metal electrodes in CV has been studied and have no contribution on electrochemical polymerization [131]. Moreover, fully oxidized conducting polymer films were obtained by chronoamperometry, applying the oxidation potential for the corresponding monomer for one min. Polymer films with different thickness were prepared by controlling the time of polymerization.

2.3.3 UV-Visible spectroscopy

The optical behaviour of both SNS monomers and their corresponding polymers was investigated using UV-visible spectroscopy in DCM. The spectra of the monomers and polymer are depicted in figure 27 and 28 respectively. All SNS monomers show one major characteristic absorption peak at ~300 nm. These maximum absorptions at ~300 could be assigned to the π - π^* transition of the π -conjugated segments and the *ter*-heteroaromatic (*thiophene-pyrrole-thiophene*) units of the SNS monomers.

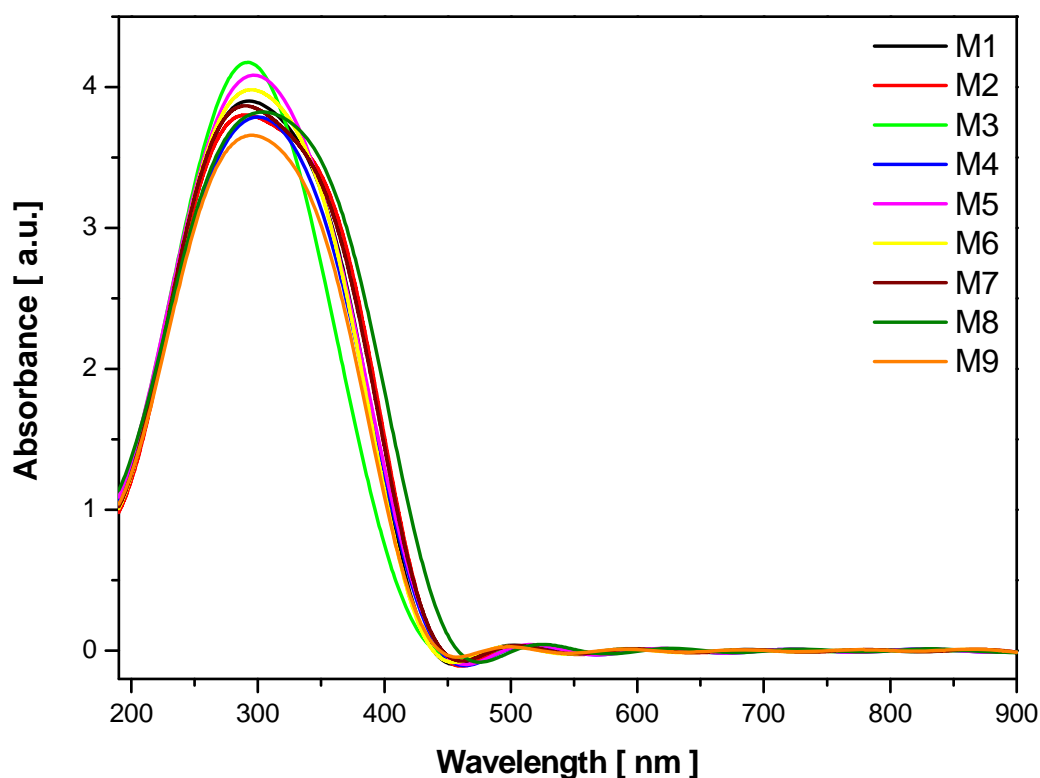


Figure 27. UV-visible absorption spectra of SNS monomers in DCM

The absorption spectra of all SNS polymers showed two major characteristic broad bands at $\sim 250\text{-}450\text{ nm}$ and $\sim 650\text{-}770\text{ nm}$. The maximum absorption at $\sim 250\text{-}450\text{ nm}$ was assigned to the $\pi\text{-}\pi^*$ transition of the π -conjugated benzenoid rings and the *ter*-heteroaromatic systems which relates to the extent of conjugation between adjacent aromatic rings in the polymer chain [132]. The broad band absorption at $\sim 650\text{ nm}$ and $\sim 770\text{ nm}$ appeared due to the electron transfer from the valence band to the polaron and bipolaron level respectively. The appearance of such wide polaron bands is connected to the highly conducting state of the polymers [133].

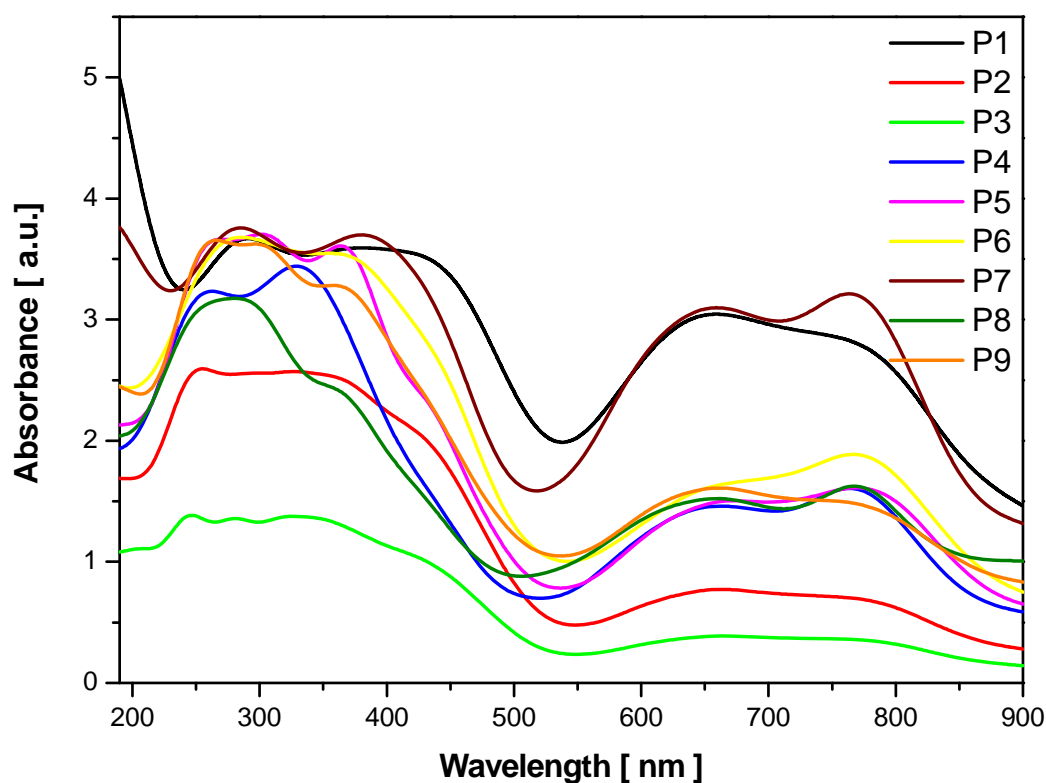


Figure 28. UV-visible absorption spectra of SNS Polymers in DCM

2.3.4 FTIR spectroscopy

All SNS polymers synthesized through chemical oxidative method using FeCl_3 were characterized by FT-IR spectroscopy to confirm their structures. Most of the characteristic peaks of monomers remained unperturbed upon polymerization but the disappearance or appearance of some characteristic peaks confirmed the formation and structure of the polymers. The spectra peak values of selective polymers of SNS compounds are assigned and given in table 3. The major characteristic bands observed in the spectra of each polymer are more or less similar to each other indicating that the chemical structure of the polymer backbone is same.

FT-IR spectral analysis revealed that the polymerization mainly occurred through the α -coupling of the external thiophene rings. For example, the IR spectrum of monomer **M3** had three main peaks at 700 cm^{-1} for α -H of thiophene rings, 760 cm^{-1} for β -H of the pyrrole ring and 840 cm^{-1} for β/β' -H of thiophene rings [134], as shown in figure 29. Due to α -coupling between the external thiophene rings, the peak at 700 cm^{-1} almost disappeared and other

2. Poly(dithienyl pyrrole) based chemical gas sensors

peaks appeared in the polymer spectrum, as expected. The appearance of a new broad band at 796 cm^{-1} due to β -H of thiophene rings additionally confirmed the coupling at α -position [134].

Table 3. Selected FTIR bands (cm^{-1}) of polymer **P1**, **P3**, **P5** and **P8**

P1	P3	P5	P8	Peaks assignment
3062	3060	3075	3100	Aromatic C-H stretching
2835	2842	-	-	Aliphatic C-H stretching of -CH ₃ group
-	1686	-	-	Carbonyl group
1390-1505	1387-1504	1386-1494	1393-1508	Aromatic C=C stretching
1276	1262	1131	1203	C-N stretching due to pyrrole and benzene
1041	1044	1008	1101	C-H in plane bending of benzene rings
845	840	834	845	β/β' -H of thiophene rings
750	760	763	772	β -H of pyrrole rings

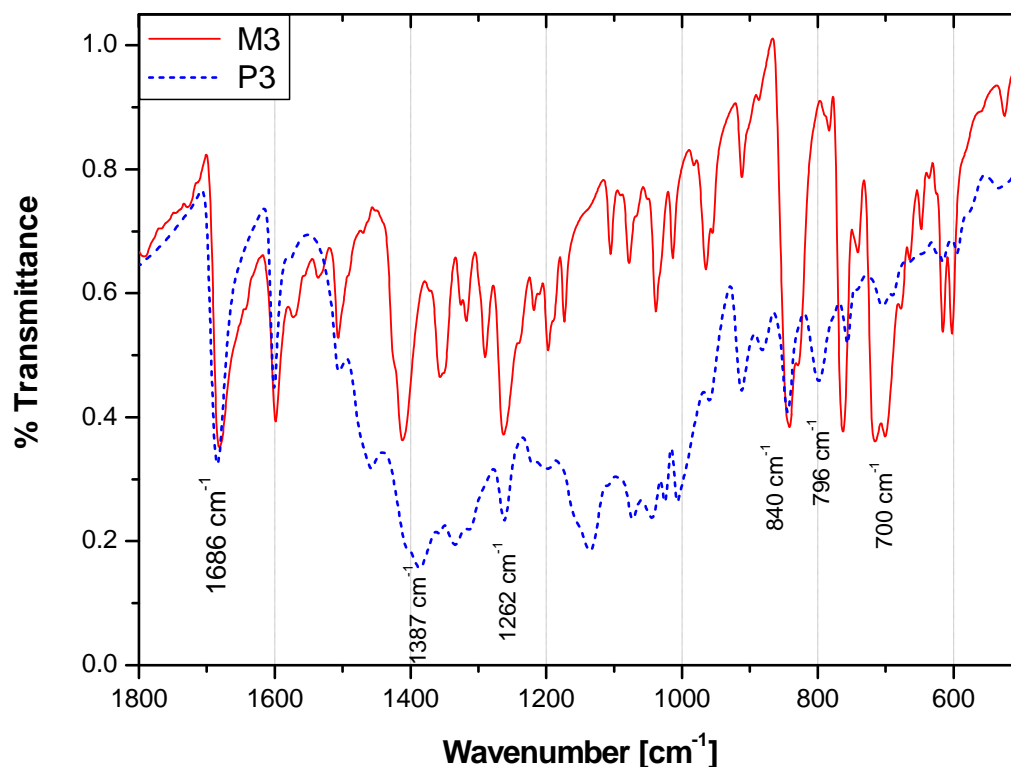


Figure 29. Comparative FT-IR spectrums of **M3** and **P3**

2.3.5 Polymer morphology

The surface morphology of the electrochemically deposited polymer films (**P1-P3**) on gold electrodes were examined by SEM which revealed small spheroid like structures joined together to form homogeneous and compact layers. The SEM images of polymer **P1-P3** films are shown in figure 30.

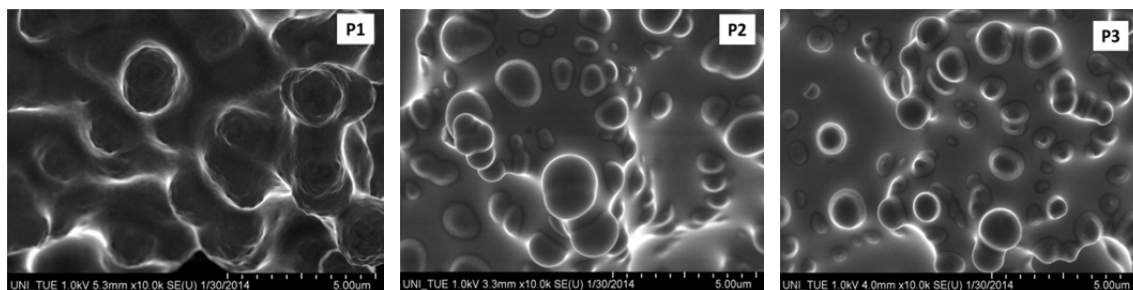


Figure 30. SEM images of electrochemically deposited polymer films (**P1-P3**)

The layer of polymer **P1** showed spheroids of size of $\sim 2 \mu\text{m}$ and the surface of spheroid is observed as rough but in the case of polymers **P2** and **P3**, spheroids are smooth and of $\sim 0.5\text{-}1.5 \mu\text{m}$. When a very thick polymer is prepared, agglomerated deposits over the uniform polymer layer were observed.

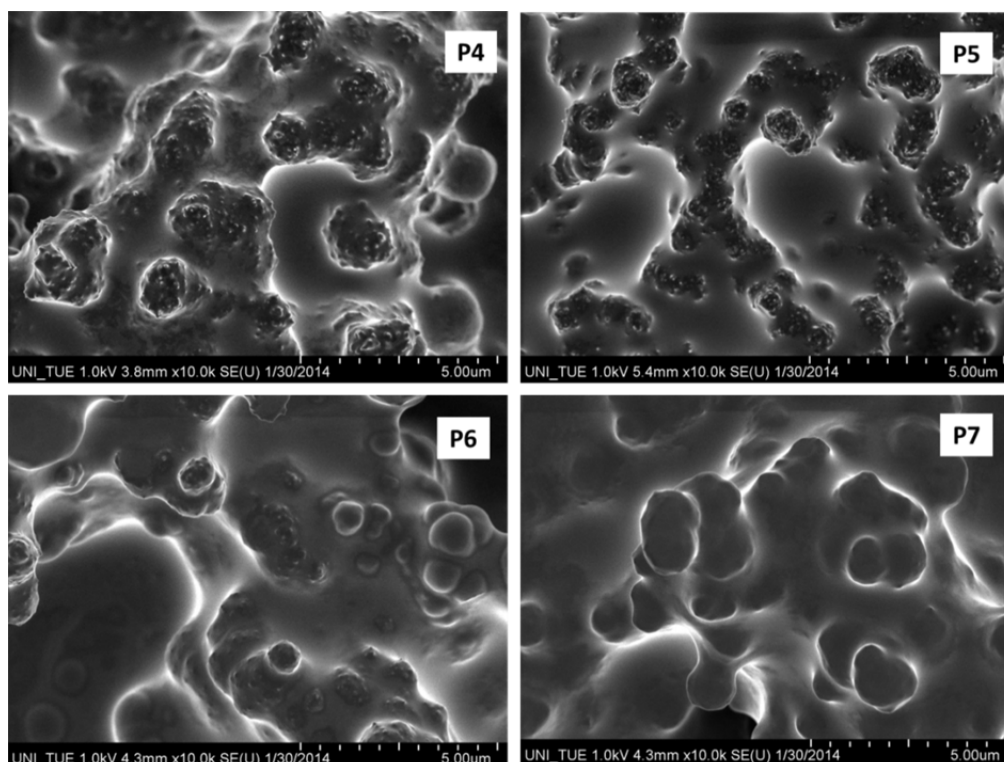


Figure 31. SEM images of electrochemically deposited polymer films **P4-P7**

2. Poly(dithienyl pyrrole) based chemical gas sensors

The SEM images of **P4-P7** films on gold electrodes are shown in figure 31, which also showed small spheroid like structures of $\sim 1-2 \mu\text{m}$ connected together in the compact but rough polymer films. It has been observed that the spheroids have small spikes on their surface. The spikes observed are more in **P4** than **P5** and decrease further in **P6** and disappeared in **P7**. This could be an effect of size or electronegativity of halogen atoms in the polymer chain. As the size of the atoms increased and electronegativity decreased from F to I, the density of spikes on the surface of spheroid decreased. In the case of all polymers, the layer formed are quite compact confirming their capability to form films, one of the important properties required for various practical applications of polymers.

As already described, chemoresistive sensors were manufactured by electrochemically depositing the polymer layers on IDEs transducers. SEM was also employed here to observe the deposited polymer layers. It was observed that, when IDEs transducers were used as working electrodes then the deposited polymer layers were very porous and with much more spheroids than when the layers deposited on plane gold electrodes. The SEM images of **P1** and **P9** layers deposited on IDEs are given in figure 32. The size of the spheroids observed for these polymers were nearly $1-2 \mu\text{m}$.

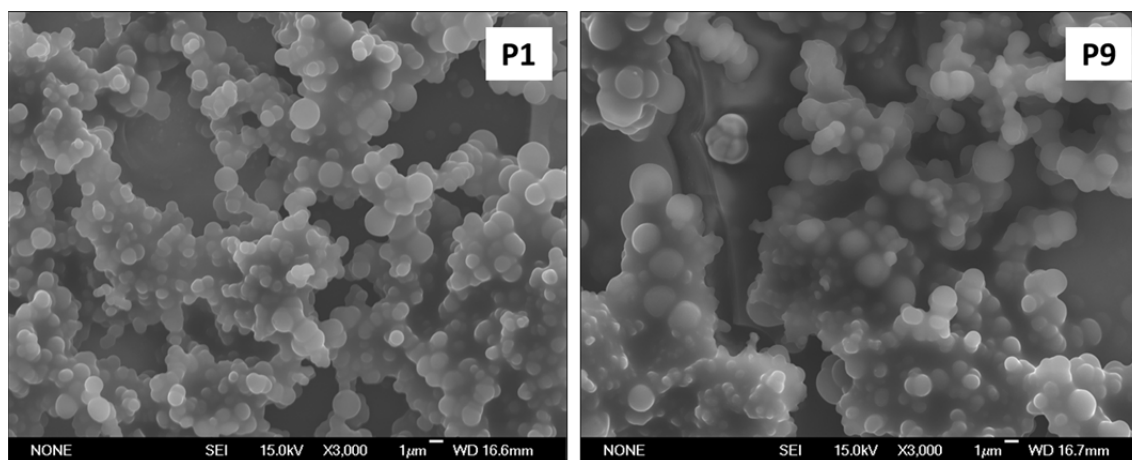


Figure 32. SEM images electrochemically deposited polymer layers on IDEs

For the successful fabrication of chemoresistive sensors, it was important to fill the insulating gap between the two IDEs with a layer of polymer to connect them. An electron dispersive X-ray spectroscopy (EDX) was employed to confirm the formation polymer film in the insulating gap between two IDEs electrodes. Two EDX spectra were recorded, one over the polymer film on the electrode (figure 33) and the other on insulating area between the electrodes (figure 34).

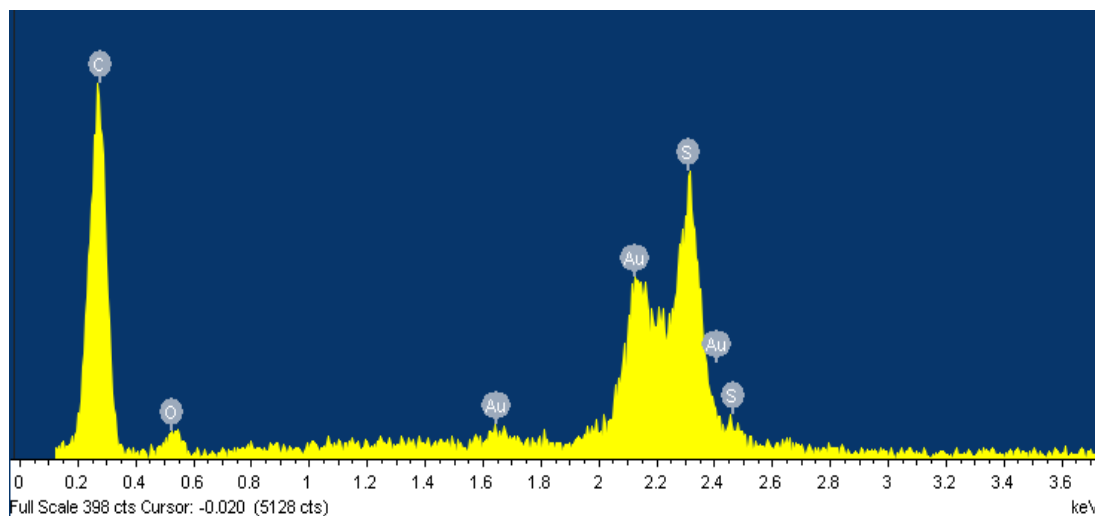


Figure 33. EDX spectrum on the polymer film over the electrode

In figure 33, the spectrum showed the atoms detected for the polymer and the electrode. The strong carbon peak at 0.3 keV is from the contribution of polymer as well as PET substrate. The peak at 2.15 keV is of gold metal electrodes whereas a strong peak at around 2.3 keV is only from the sulphur atom of SNS polymer film.

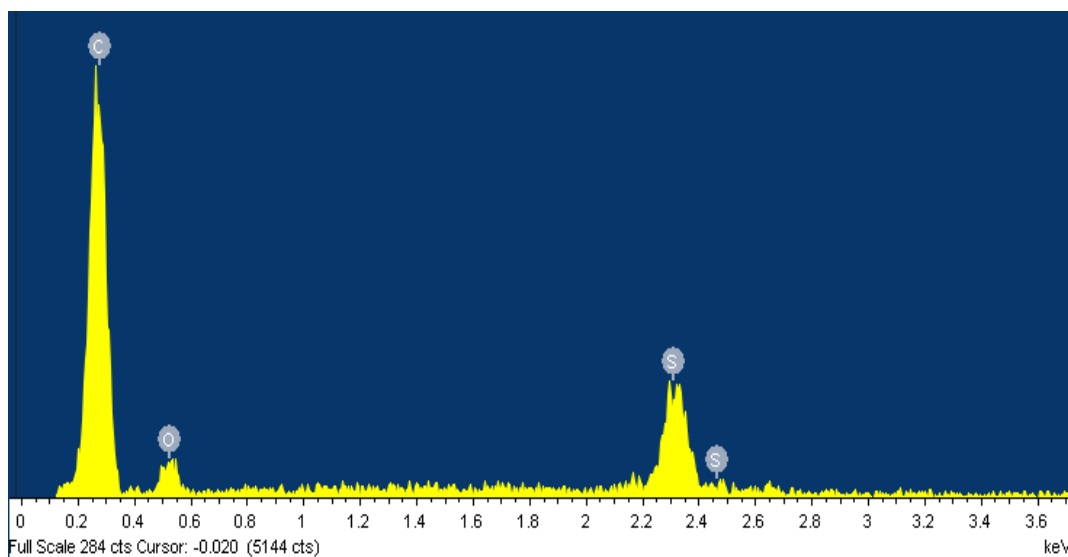


Figure 34. EDX spectrum recorded on insulating area in between the electrodes

The spectrum presented in figure 34 showed strong carbon peak at 0.3 keV from the contribution of polymer film and PET substrate foil. The peak at 2.32 keV is of sulphur atoms that come only from the SNS polymer film. The EDX spectrum 1 (figure 33) and 2 (figure

34) confirms the formation of polymer films not only on the electrodes but also on the insulating gap in between the electrodes.

2.3.6 Thermal stability

Thermal stability of the monomers **M1-M8** and their corresponding polymers **P1-P8** was evaluated by means of TGA measurements carried out under argon atmosphere at a heating rate of 2 °C per minute in the temperature range 20 °C to 1000 °C. The thermo gravimetric results for the monomers are displayed in figure 35. They show more or less similar evolution trends. The thermal degradation starts at ~200 °C in the case of all monomers and with all them, major loss of weight was observed in the range of ~200-400°C.

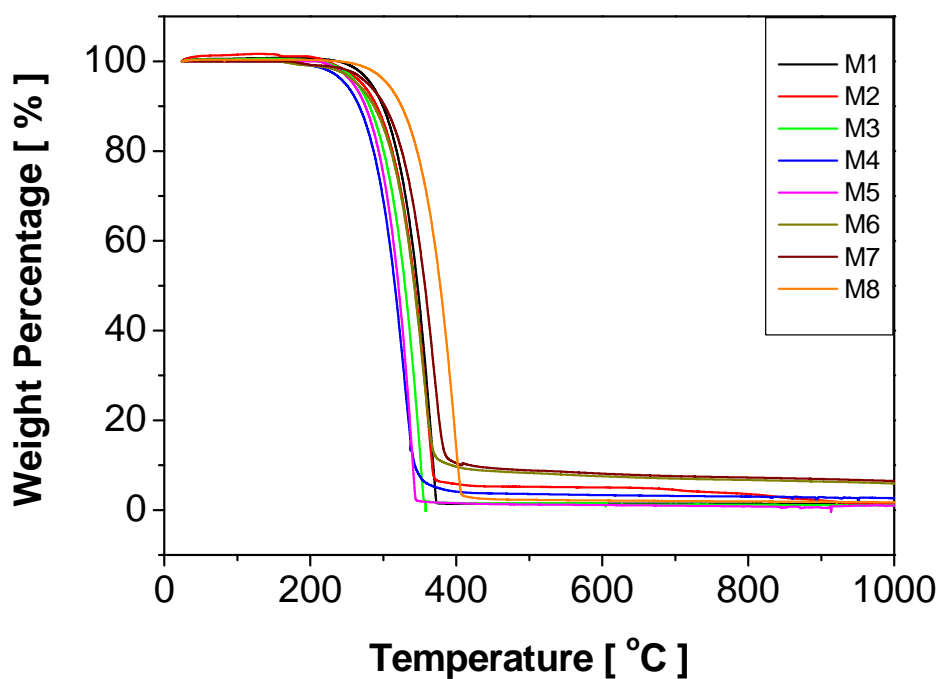


Figure 35. Thermal degradation of monomers

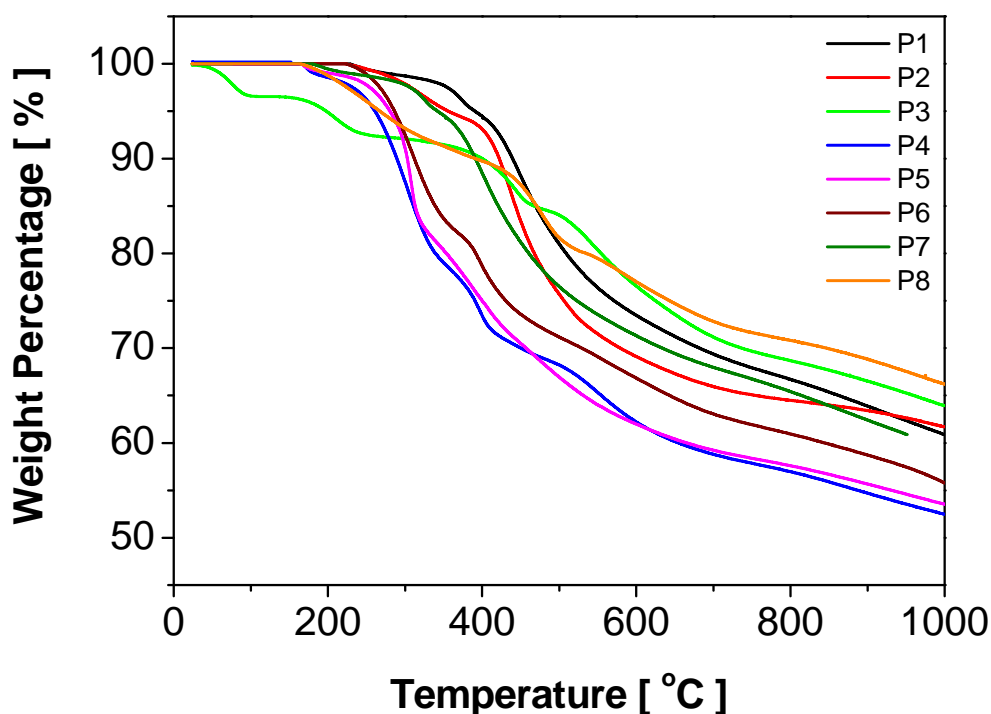


Figure 36. Thermal degradation of polymers

Thermal degradation graphs shown in figure 36 confirmed good thermal stability of SNS polymers. The degradation starts at 200 °C for almost all polymers but further increase in temperature resulted in to unequal loss in weight of the polymer. All polymers showed 10% loss in weight in wide temperature range ~300-500 °C. The weight left after increasing the temperature up to 1000 °C was ~55-65% for all polymers.

The effects of the substituents and their positions on the thermal properties of polymers have been reported in the past [135-137]. The results showed that the polymers with electron donating groups have higher thermal stability than the ones with electron withdrawing nature. The polymer **P1**, with strong electron donating methoxy group, showed higher thermal stability than polymer **P2**, with mild electron donating methyl group, whereas polymer **P3** which has electron withdrawing acetyl group, showed comparatively lower thermal stability.

Similarly, polymers having halogen atoms with different electronegativity showed different thermal stability. Polymer **P4-P7** has F, Cl, Br, and I atoms, which showed increased thermal stability with decrease in electronegativity of the halogen atoms. The polymer **P4** with

highest electronegative F atom showed lower thermal stability compared to **P7** which has an I substituent. There could also be the influence of size of halogen atom on the thermal stability of the polymers. The size of halogen increases from F to I. The polymer **P8** also showed similar kind of evolution trend like other polymers over the specified temperature range. From the performed investigation, it was not possible to establish if a connection between electrical properties and the thermal stability actually exists or not.

2.3.7 Electrical conductivity of polymers

Electrical conductivity of the polymers was measured at room temperature by the two probe method using a pressed pellet. The pellets were prepared by subjecting ~100-150 mg polymer powder to 10 tonnes / cm² for 15 minutes. The pellets obtained had a 13 mm diameter and ~0.5 mm thickness. Electrical conductivities measured for the SNS polymers are listed in table 4.

It was seen that there is an influence of electron donating / withdrawing substituents or halogen atoms attached to the aromatic rings of N-substituted pyrrole on the electrical conduction of the SNS polymers. Reynolds et al. have reported an increase in electrical conductivity when electron donating substituents were used on poly[1,4-bis(2-furanyl)phenylenes] [138].

Table 4. Electrical conductivity of polymers

No.	Material	Conductivity (S/cm ⁻¹)
1.	Polymer P1	1.13×10^{-4}
2.	Polymer P2	0.41×10^{-4}
3.	Polymer P3	0.17×10^{-4}
4.	Polymer P4	0.57×10^{-4}
5.	Polymer P5	1.11×10^{-4}
6.	Polymer P6	3.97×10^{-4}
7.	Polymer P7	4.37×10^{-4}
8.	Polymer P8	5.20×10^{-4}
9.	Polymer P9	0.57×10^{-4}

In the case of the first three polymers **P1-P3**, it was observed that the polymer **P1** which has good electron donating methoxy group shows higher electrical conductivity than **P2** (-methyl group). On the other hand in the case of polymer **P3**, with an electron withdrawing acetyl

substituent, lower electrical conductivity than the polymers of monomer **P1** and **P2** has been measured. The polymer with halogen substituents, that is **P4-P7** have F, Cl, Br and I substituents respectively on their N-substituted aromatic rings. Electronegativity of these halogens decreases with the increase in their size. The order of their electronegativity is $F > Cl > Br > I$. It was observed that these halogen substituents also have an influence on the electrical conductivity of the polymers. The electrical conductivity for polymer **P8** and **P9** was observed 5.20×10^{-4} and 0.57×10^{-4} respectively. Table 4 shows that, as electronegativity of the halogen atom decreased, electrical conductivity of the polymers increased.

The effect of the temperature on the electrical conductivity of the prepared SNS polymers was investigated under dry synthetic air. The polymer pellets were kept at each selected temperature step (10, 20, 30, 40, 50 and 60 °C) for 45 minutes (wherein a constant resistance was attained) and the steady resistance value was considered. Figure 37 and 38 shows the thermally activated polymer conductance of polymers **P1-P3** and **P4-P9** respectively. It increases with the temperature increase roughly 3 to 4 times over the specified temperature interval. The conductivity activation energy inferred from the experimental data for all synthesized polymers is given in table 5.

$$S = S_0 \cdot \exp\left[-\frac{E_a}{k_B T}\right]$$

Where, E_a is the activation energy and k_B the Boltzmann constant.

Table 5. Energies of activation of the polymers

No.	Material	S_0	E_a (meV)
1.	Polymer P1	0.0203	212
2.	Polymer P2	0.0145	236
3.	Polymer P3	0.0044	227
4.	Polymer P4	0.0046	198
5.	Polymer P5	0.0184	216
6.	Polymer P6	0.0058	155
7.	Polymer P7	0.0504	207
8.	Polymer P8	0.0500	204
9.	Polymer P9	0.0276	243

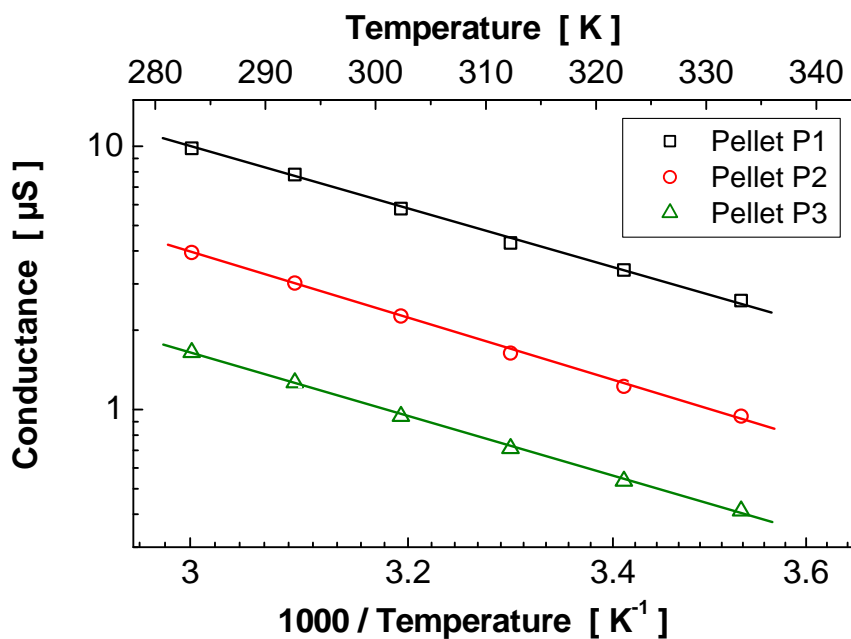


Figure 37. Temperature dependence of the polymers conductance for P1-P3. The pellets were measured only once for the specified temperature range.

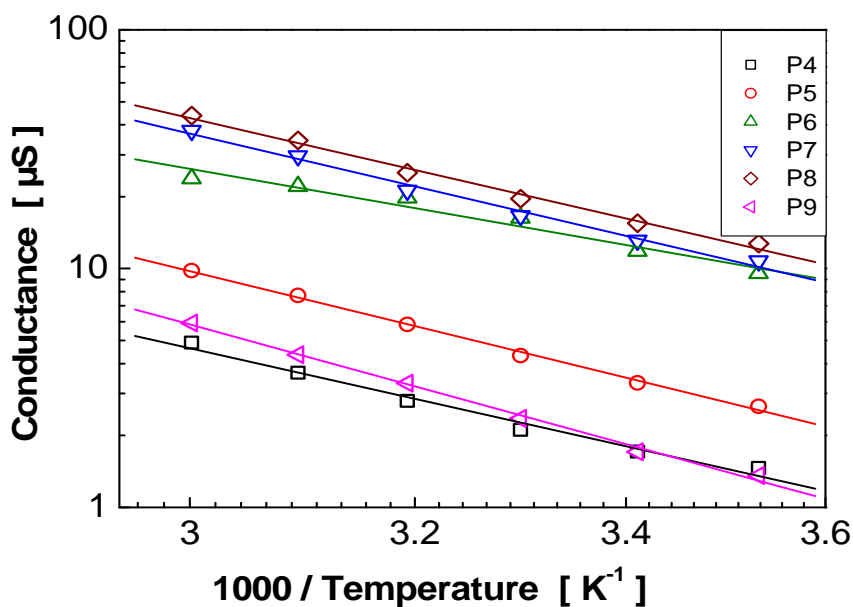


Figure 38. Temperature dependence of electrical conductance for P4-P9. The pellets were measured for only once for the specified temperature range.

From the acquired data, it is not possible to identify whether the activation is due to charge carrier concentration or their mobility because no additional measurement (Hall, Seebeck or field effect transconductance) has been performed yet.

2.3.8 Sensor Characterization

As mentioned in the experimental section, polymers were characterized for their sensing performances by two ways; one by making pressed pellets of chemically prepared polymers and another by fabricating IDEs chemoresistive sensors. The pellet sensors were characterized for different relative humidity steps and different concentrations of ammonia whereas IDEs sensors against ammonia and ethanol.

2.3.8.1 Pellet sensors

A) Humidity sensing

The polymer pellets were subjected to different steps of relative humidity as 0, 10, 30, 50 and 70%. The exposure protocol includes purging of pellets with synthetic air for 2 h and then each humidity step for 1 h (Figure 39).

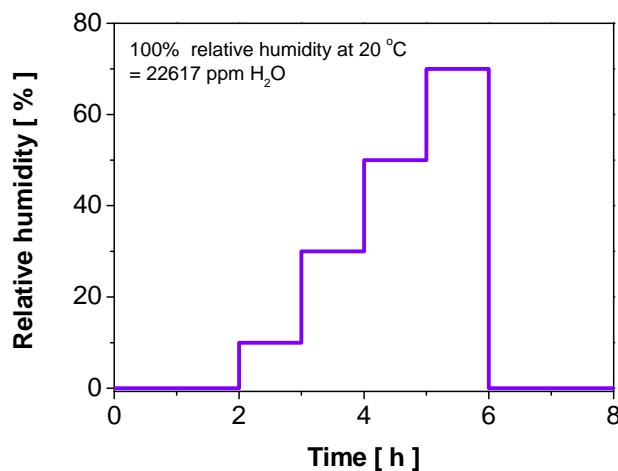


Figure 39. Relative humidity protocol used for pellet sensors

The SNS polymers present a linear increase in their resistances with the increase in RH, as shown in figure 40 for polymer P1-P3. They have electron donating or withdrawing substituents in their structures. Relative change in the resistance has been preferred in order to better compare the three polymers under observation. The effect might come from the polymers swelling as far as the water molecules are not able to modify the charge carrier

concentration (to modify the polymer oxidation degree) but not investigated yet. In figure 41, the change in resistance for polymers P4-P7 is given. They have different halogen substituents in their chemical structures. The responses of remaining two polymers P8 and P9 are given in figure 42.

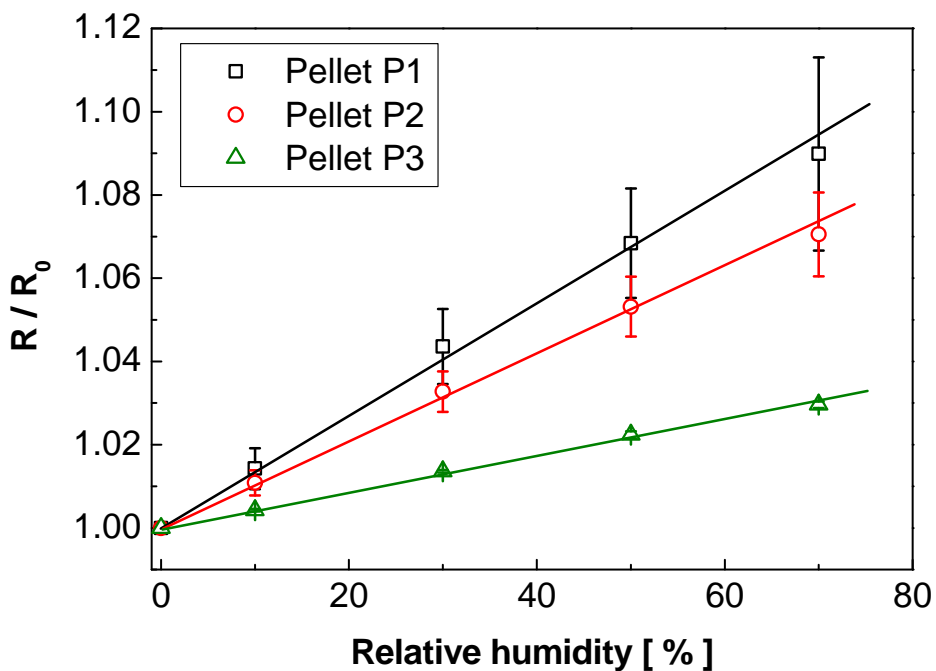


Figure 40. Responses of SNS polymers (P1-P3) to different humidity levels

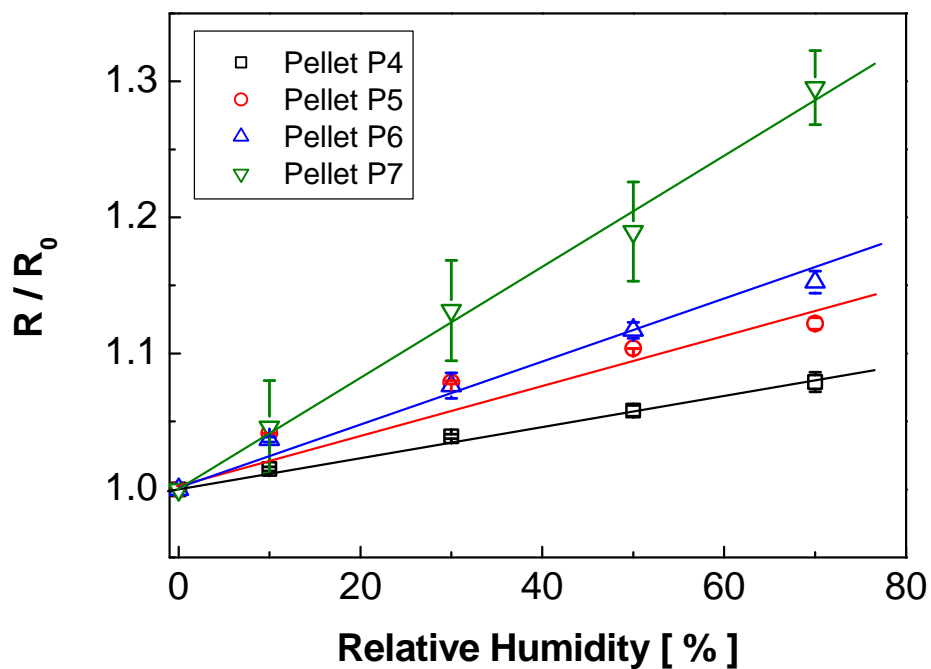


Figure 41. Responses of SNS polymers P4-P7 to different humidity levels

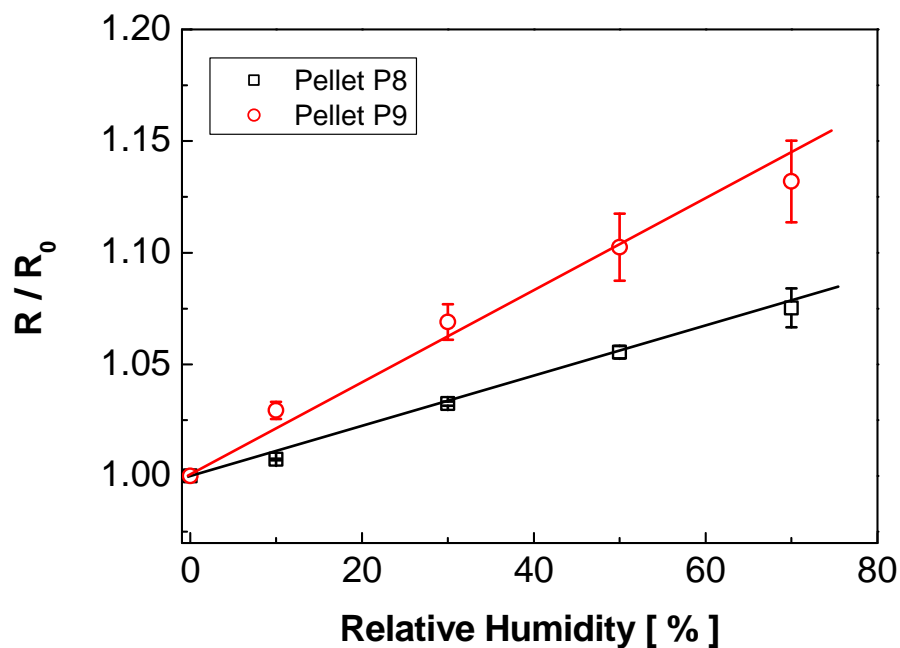


Figure 42. Responses of SNS polymers P8 and P9 to different humidity levels

B) Ammonia sensing

Figure 43 shows the responses (calibration curves) of the prepared SNS polymers P1-P3 to different ammonia concentrations from 10 to 300 ppm. The signals are given as relative shifts in the sample resistances ($[R-R_0]/R_0$). In double logarithmic scales, their resistances are a power function with the ammonia concentration. The responses of polymers with halogen substituents (P4-P7) are shown in figure 44 and the responses of P8-P9 are depicted in figure 45.

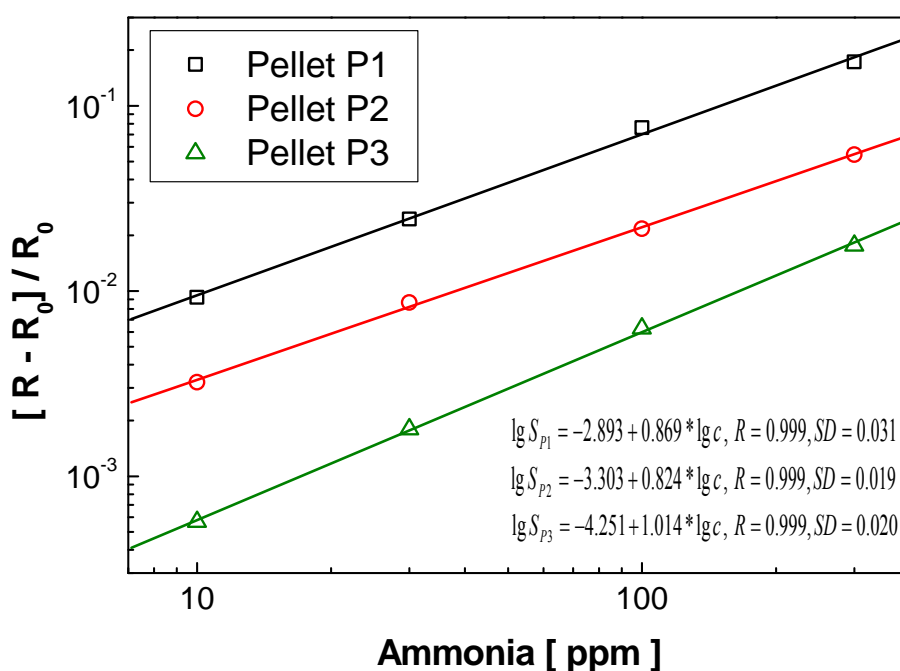


Figure 43. Responses of polymers **P1-P3** to different ammonia concentrations. Three measurements were performed but the data for only one was obtained on proper order. (in the graph statistics, S is pellet sensor signal)

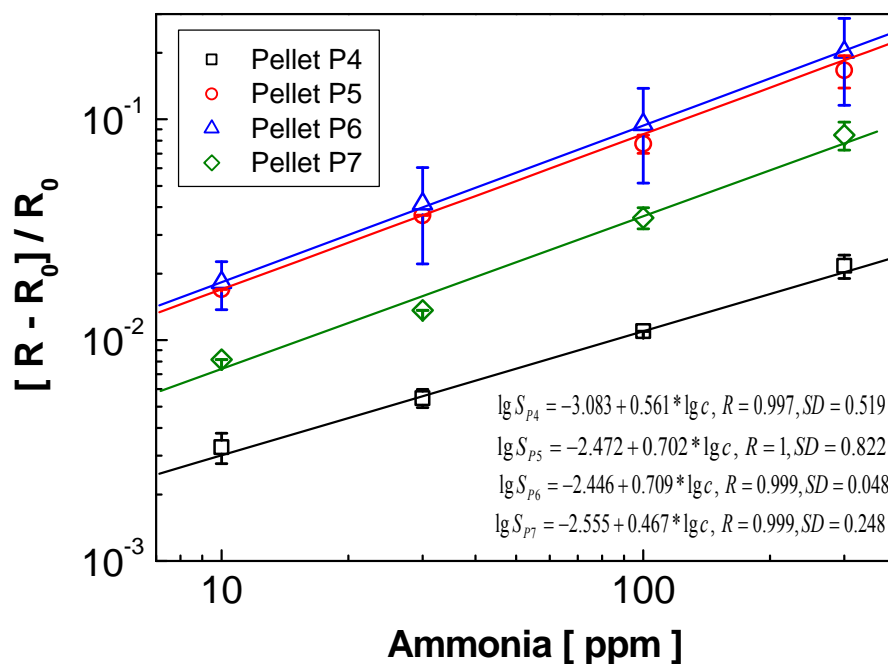


Figure 44. Responses of polymers **P4-P7** to different ammonia concentrations, measured two times for the given protocol. (in the graph statistics, S is pellet signal)

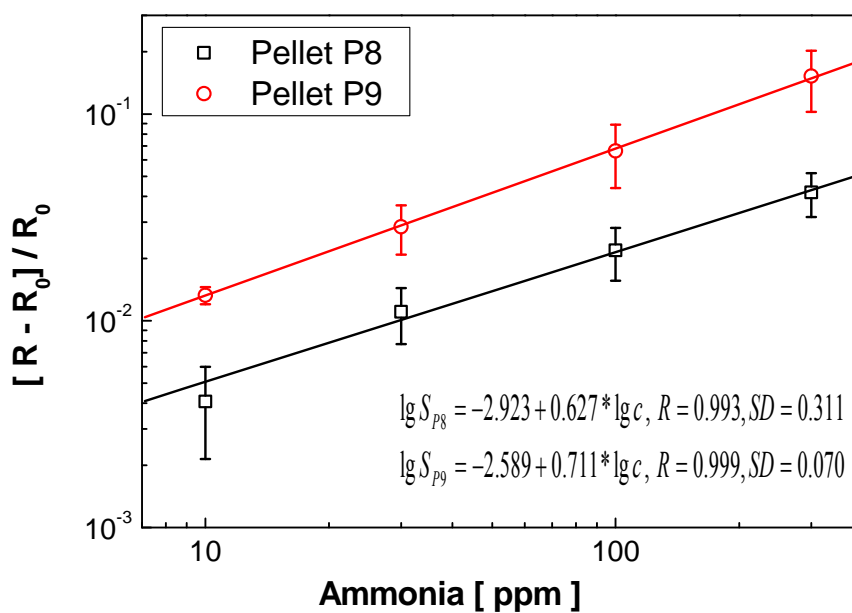


Figure 45. Responses of polymers **P8-P9** to different ammonia concentrations

For the moment no thorough investigations on the ammonia sensing mechanisms have been made so that one cannot ascertain on the significance of the shape of the calibration curves.

2.3.8.2 IDEs flexible chemoresistors

A) Ammonia sensing

The responses of prepared SNS polymer based IDE sensors against different ammonia concentrations were investigated. The exposure protocol for ammonia includes 0.3, 1, 3, 10 and 30 ppm steps/pulses. After purging the sensors with synthetic air for 2 h, each ammonia concentration was given for 30 min. The calibration curves of SNS sensors against ammonia are presented in figure 46. The responses are presented as relative shifts in the sensor resistances ($[R-R_0]/R_0$). In double logarithmic scales they are a power function on the ammonia concentration.

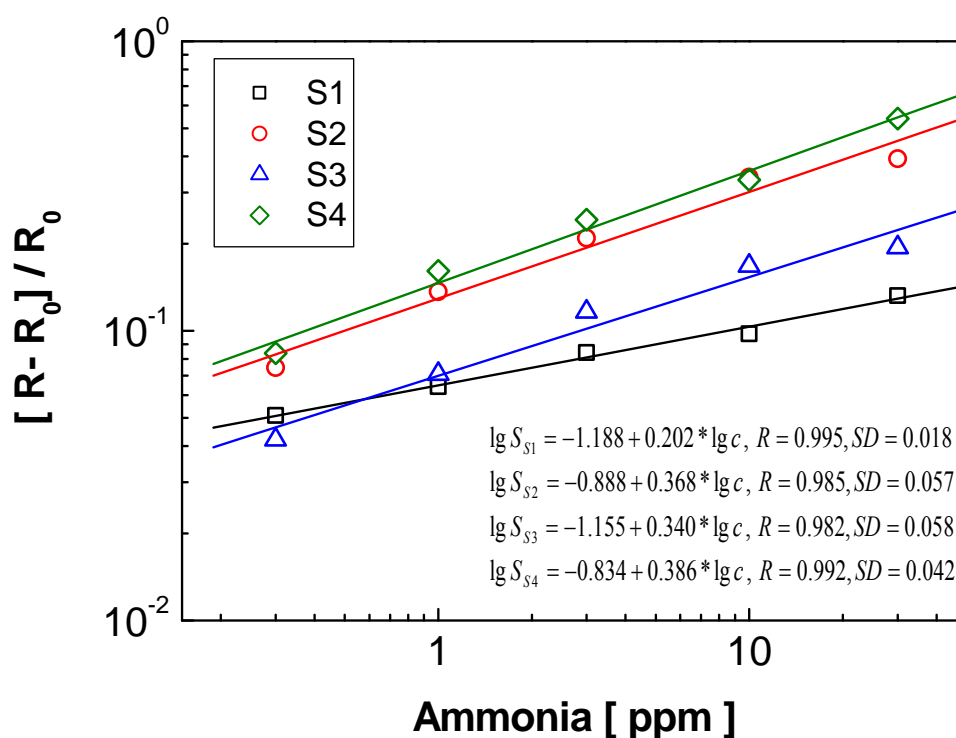


Figure 46. Calibration curves of SNS polymer based IDEs sensors **S1-S4** against ammonia. The S1-S4 sensors were manufactured by electrochemical polymerization of monomer M1, M2, M5 and M9 respectively on IDEs transducers. (S is sensor signal)

B) Ethanol sensing

The calibration curves of SNS polymer based IDE sensor characterized for ethanol are depicted in figure 47. Here as well the sensors were purged with synthetic air for 2 h and then each ethanol concentration was given for 30 min. The ethanol exposure protocol was 10, 30, 100, 300 and 750 ppm of ethanol. Here as well the signals of sensors against different ethanol concentrations are presented as relative shifts in the sensor resistances ($[R-R_0]/R_0$). In double logarithmic scales they are also a power function on the ethanol concentrations.

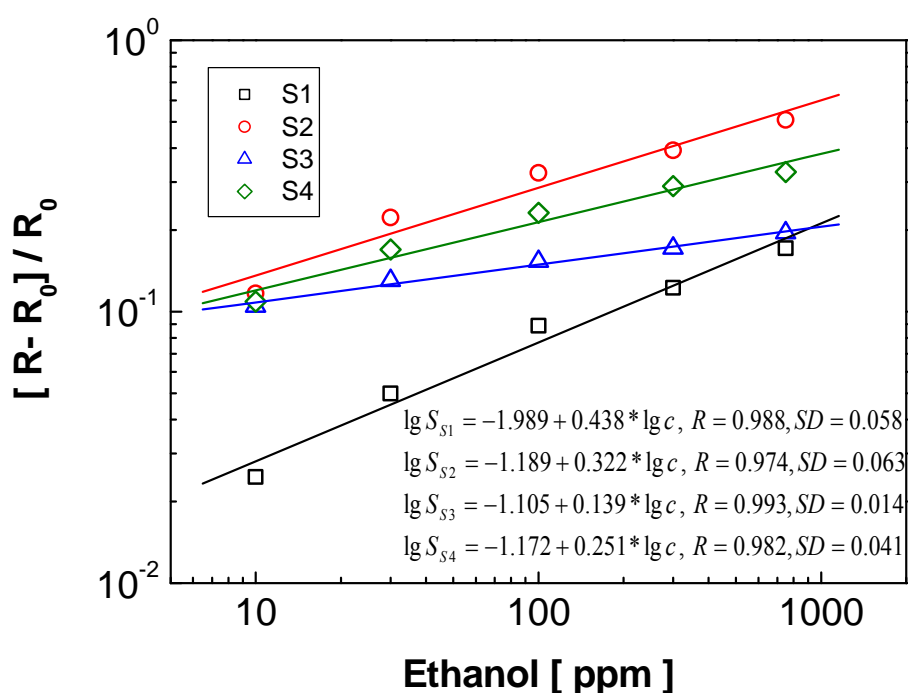


Figure 47. Calibration curves of SNS polymer based IDEs sensors (S1-S4) against ethanol. The S1-S4 sensors were manufactured by electrochemical polymerization of monomer M1, M2, M5 and M9 respectively on IDEs transducers. (S given in the statistics is sensor signal)

2.4 Conclusion

A series of conducting polymers based on 2, 5-di(thiophen-2-yl)-1*H*-pyrrole (SNS) having an electron donating or withdrawing and halogen group on N-substituted aromatic rings was synthesized by chemical and electrochemical polymerization techniques. The literature reported procedure for the 1,4-di(thiophen-2-yl)butane-1,4-dione intermediate synthesis have been modified resulting in a significant reduction of the complete reaction time from 18 h to

1h. FT-IR spectra put in evidence the polymerization of the monomers through the coupling of α -H of external thiophene rings. The polymers **P1**, **P2** and **P3** showed an electrical conductivity correlated with the electron donating character of the substituents and **P4-P7** correlated to their electronegativity. Moreover, the UV-visible spectra for all the prepared polymers contain well defined absorption bands due to polaron and bipolaron states, in agreement with the standard conduction model for organic materials owning delocalised π bonds. The influence of temperature on the electrical conductivity of the polymers is thermally activated. Morphological characterizations of polymers by SEM proved their capability to form continuous, thick / thin layers, which is a property important for many practical applications. The polymers exhibited very good thermal stability by withstanding up to 400 °C with less than 10% loss of weight. The polymers having N-substituted aromatic ring with electron donating groups showed higher electrical conductivity and thermal stability than the ones having electron withdrawing groups. The pellets and IDE chemoresistive sensors characterized for relative humidity, ammonia and ethanol showed a linear increase in their resistance with the concentration of the analytes.

3. Synthesis of Poly(dithenyl pyrrole)- dialkylbithiazole copolymer

3.1 Introduction

This chapter describes the attempts made towards the synthesis of copolymers based on dithienyl pyrrole (SNS) and dialkylbithiazole. After synthesizing the number of SNS derivatives as already explained in the previous chapter, I decided to make copolymers using SNS derivatives with dialkylbithiazole. The copolymer synthesis was attempted with the objectives of making new polymer materials for better solution processability and environmental stability.

The sensitivity of conducting polymer is alone not enough to enable the polymer to be used as chemical sensor material. Additionally the polymer should have solution processability and environmental stability. Though a wide range of polymers is cheaply available, only a few of them have been used in real sensor applications. Most of the polymers need to be modified in order to make them useful as a sensor material. The electronic and optical properties of conjugated polymers can be easily modified by use of functional dopants, by controlling the π -conjugation, making their substituted derivatives, attaching long chain aliphatic groups on the polymer chain or making copolymers [139]. When a polymer to be used for the fabrication of chemical sensor is solution processable then deposition techniques such as spray coating, spin coating, inkjet printing, and screen printing allow large area fabrication, important in terms of industrial scaling up process [139-145]. Moreover, on the account of the applications of any sensor in real life, the sensor has to deal with many environmental factors such as humidity, temperature, etc. and compositions (number of gases present in the air) can interfere in the proper functioning of the sensors. In order to dominate such interfering environmental factors, the polymer materials used in the sensors must have enough environmental stability.

Unfortunately, only few polymers or copolymers fulfil all the above mentioned requirements in terms of sensitivity, solubility and environmental stability. Thus, designing and synthesizing novel semiconducting or conducting polymers with good sensitivity and solubility as well as understanding structure and morphology is still an important area of research in chemical sensor field. So I attempted to synthesise a new class of copolymers based on SNS and dialkylbithiazole. The general structure of the copolymer aimed for is given in figure 48.

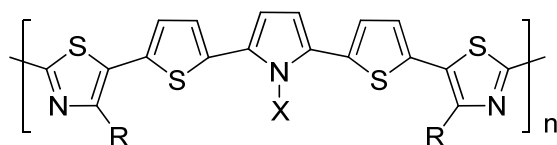
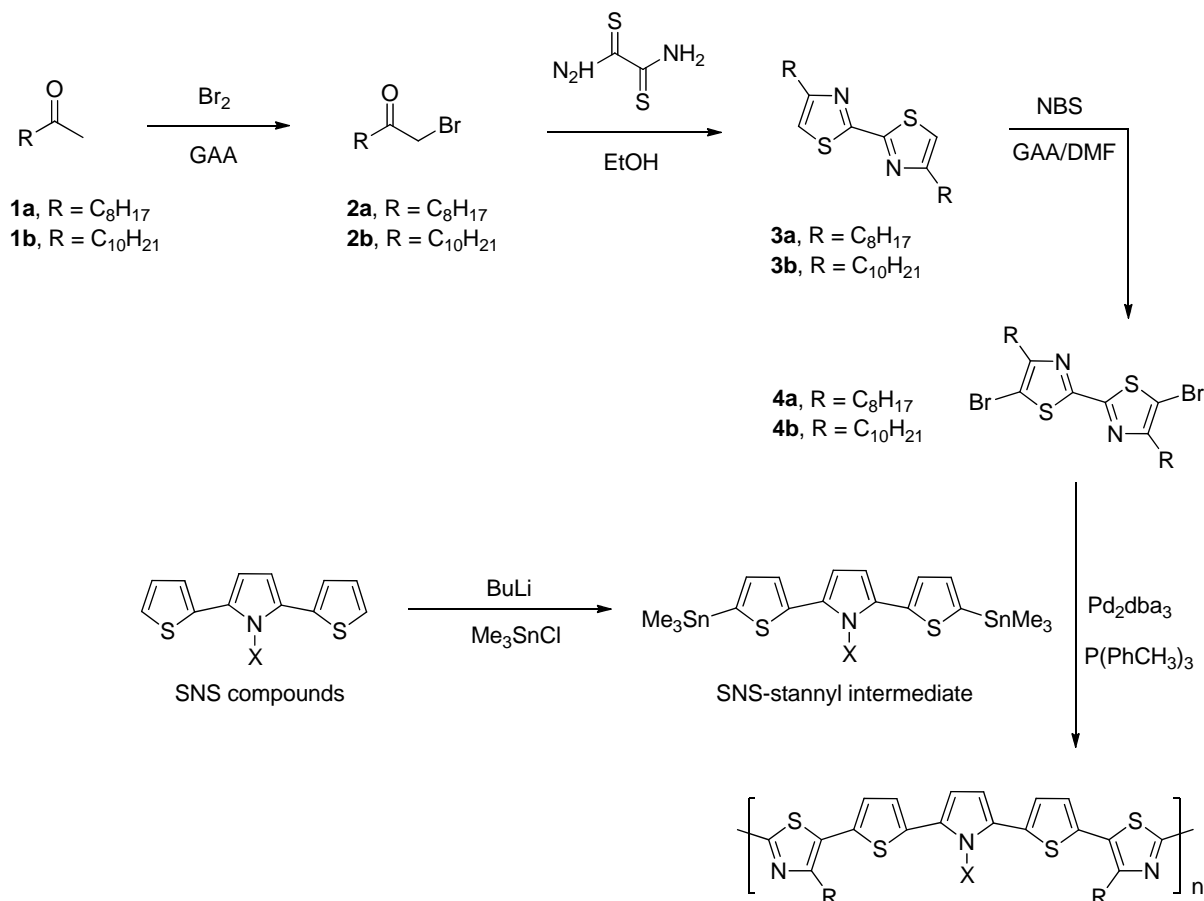


Figure 48. General structure of planned dithienyl pyrrole-dialkylbithiazole copolymer



Scheme 4. Planned synthesis scheme for preparation of SNS-dialkylbithiazole copolymers

Solution processability of the polymer materials could be improved by an incorporation of long alkyl chains into the polymers whereas the environmental stability by deepening the highest occupied molecular orbital (HOMO) level, which means by increasing the ionization potential (IP) of the polymers. The IP of the polymers have been increased by shortening the conjugation length by introducing fused aromatic rings [146-151] and by increasing the rotational freedom of the backbone [152]. Additionally, IP can be increased by introducing comparatively electron deficient unit in the polymer [153-156]. I planned to incorporate a

long alkyl chain to increase solubility and electron deficient bithiazole units to increase the IP. The dialkylbithiazole units have been successfully introduced in the thiophene based polymers and oligomers in the past. Comparatively, bithiazole units are more electrons deficient and more rigid than central SNS unit. Therefore, the design of copolymer with SNS unit and long chain alkyl attached bithiazole can lead to polymer with chemical sensitivity, good solution processability and better environmental stability. The planned synthetic routes for the synthesis of SNS-dialkylbithiazole copolymer is given in scheme 4.

Two different long chain alkyl groups were planned on the thiazole ring in order to confer the solubility to the polymers. The strategy to put n-octyl and n-decyl groups on thiazoles ring produce 5,5'-dibromo-4,4'-dioctyl-2,2'-bithiazole **4a** and 5,5'-dibromo-4,4'-decyl-2,2'-bithiazole **4b**. As shown in the scheme, two dialkylbithiazole derivatives were reacted with the trimethyl tin intermediate of SNS to synthesise final copolymers.

3.2 Experimental

3.2.1 Chemical and instrumentations

All chemicals were purchased from commercial suppliers Acros, Aldrich, Fluka, Merck and Fisher Scientific. All reagents obtained from commercial suppliers were used throughout without further purification unless otherwise stated. Anhydrous solvents for reactions were purchased; toluene, ethanol, methanol, glacial acetic acid from Fisher-Scientific; acetonitrile, DMF from Merck; THF from Sigma-Aldrich and DCM from Fluka. The reaction were performed in the pre-dried flasks (with a heat gun) and under inert gas atmosphere. The air or water sensitive chemicals and solvents were stored and used under inert atmosphere.

The ^1H , ^{13}C NMR spectra were recorded on a Bruker Avance 400 spectrometer operating at 400 MHz for ^1H and 100 MHz for ^{13}C nuclei, respectively at 295 K in CDCl_3 . The chemical shifts were assigned in comparison with the residual proton and carbon resonance of the solvent CDCl_3 ($\delta \text{H}=7.25$ ppm, $\delta \text{C}=77.0$ ppm) and tetramethylsilane (TMS) as the internal reference ($\delta=0$ ppm). The assigned protons are written in italic form. HRMS analysis was done on an APEX 2 spectrometer from Bruker Daltonic with electrospray ionization (ESI) method.

3.2.2 Experimental procedures

1-bromodecan-2-one (2a): A mixture of 2-decanone (10 g, 63.992 mmol), urea (6.379 g, 106.23 mmol) and glacial acetic acid (40 mL) in 500 mL was taken into a two necked round bottom flask under inert gas atmosphere and cooled to 0 °C with an ice bath. A solution of bromine (3.607 mL, 70.391 mmol) in glacial acetic acid (15 mL) was added dropwise to the above solution while continuous stirring. The resulting reaction mixture was stirred overnight at room temperature. The reaction was monitored by TLC. Water (100 mL) was then added to the reaction mixture and the solution was extracted with DCM (50 mL × 3). The combined organic layers were washed with saturated NaHCO₃ and NaCl solution, dried over anhydrous Na₂SO₄ and filtered. The filtrate was concentrated and the residue was purified by flash column chromatography (EtOAc/Hexane, 1:50 & then 1:30) to yield α-brominated ketone, 1-bromodecan-2-one **2a** as colourless thick oil.

1-bromododecan-2-one (2b): 2-dodecanone (10 g, 54.253 mmol), urea (5.041 g, 90.06 mmol) and glacial acetic acid (40 mL) in 500 mL was placed in two necked round bottom flask under inert gas atmosphere with an ice bath for cooling to 0 °C. Then, a solution of bromine (3.057 mL, 59.679 mmol) in glacial acetic acid (15 mL) was added dropwise. The reaction mixture was stirred overnight at room temperature, and the completion of reaction was checked by TLC. The reaction was quenched with water (100 mL), and the solution was extracted with DCM (50 mL × 3). The combined DCM layers were washed with saturated NaHCO₃ and NaCl solution, dried over anhydrous Na₂SO₄ and filtered. The filtrate was concentrated in vacuum, and the residue was subjected to flash column chromatography purification (EtOAc/Hexane, 1:50 & then 1:30) to furnish 1-bromododecan-2-one **2b** as colourless thick oil.

4,4'-dioctyl-2,2'-bithiazole (3a): A mixture of 1-bromodecan-2-one **2a** (8.61 g, 36.613 mmol), dithiooxamide (2.2 g, 18.307 mmol) in absolute ethanol (120 mL) was refluxed in round bottom flask equipped with reflux condenser for 4-5 h. After confirming the completion of the reaction by TLC, the reaction solvent was evaporated in vacuum, and the residue was added in ice-water mixture (25 mL). The mixture was extracted with DCM (50 mL × 3) and washed with saturated NaHCO₃ solution. The combined organic layers were dried over anhydrous Na₂SO₄, filtered and concentrated in vacuo. After the evaporation of the solvent, the cyclized bithiazole product **3a** was obtained as brown crystalline residue.

4,4'-didecyl-2,2'-bithiazole (3b): Two necked round bottom flask equipped with reflux condenser was charged with 1-bromododecan-2-one **2b** (9.747 g, 37.031 mmol), dithiooxamide (2.226 g, 18.512 mmol) and absolute ethanol (130 mL). The orange coloured reaction mixture was refluxed for 5 h. The completion of the reaction was checked by TLC. The reaction mixture was concentrated in vacuum and the residue was added in ice-water mixture (25 mL). The mixture was extracted with DCM (50 mL × 3), washed with saturated NaHCO₃ solution, combined organic layers dried over anhydrous Na₂SO₄, filtered and concentrated in vacuo. After the evaporation of the solvent, the cyclized bithiazole product **3b** was obtained as a brown crystalline residue.

5,5'-dibromo-4,4'-dioctyl-2,2'-bithiazole (4a): A solution of 4,4'-dioctyl-2,2'-bithiazole **3a** (6.265 g, 15 mmol) and N-bromosuccinimide (6.674 g, 37.5 mmol) in a mixture of glacial acetic acid (65 mL) and DMF (65 mL) was stirred in the dark for 2 h. The grey-brown solid precipitate formed in the reaction mixture was filtered and washed with methanol. The obtained residue was purified by flash column chromatography (EtOAc/Hexane, 1:20) to produce brominated dialkylbithiazole compound **4a** as yellowish powder.

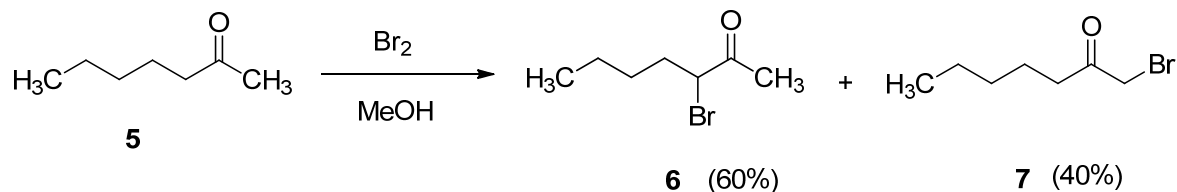
5,5'-dibromo-4,4'-didecyl-2,2'-bithiazole (4b): 4,4'-didecyl-2,2'-bithiazole **3b** (8.8 g, 19 mmol) and N-bromosuccinimide (8.454 g, 47.5 mmol) were dissolved in a mixture of glacial acetic acid (90 mL) and DMF (90 mL) and stirred in the dark for 2 h. The precipitated grey-brown solid formed in the reaction mixture was filtered and washed with methanol. The obtained residue was subjected to flash column chromatography purification (EtOAc/Hexane, 1:20) to produce brominated dialkylbithiazole product **4b** as yellowish powder.

3.3 Result and discussion

3.3.1 Synthesis of 1-bromo ketones (2a, 2b)

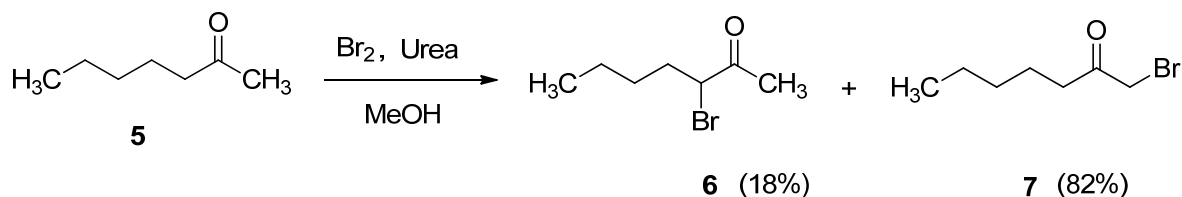
In general, α -bromination of ketone is realized by N-bromosuccinimide (NBS) [157-159], cupric bromide [160] and molecular bromine [161-163]. Additionally, during last years, a number of methods have been reported using NBS-NH₄OAc [160], NBS-photochemical [164], NBS-PTSA [165], NBS-silica supported sodium hydrogen sulphate [166], NBS-Amberlyst-15 [167], NBS-Lewis acids [168], NBS-ionic liquids [169], MgBr₂-(hydroxy(tosyloxy)iodo) benzene-MW [170], N-methylpyrrolidin-2-one hydrotribromide (MPHT) [171], (CH₃)₃SiBr-KNO₃ [172], BDMS [173], NaBr [174]. Among these reagents, bromination of acyclic ketones is generally achieved using NBS-NH₄OAc [160] NBS-

photochemical [164] and NBS-PTSA [165]. One major problem with these methods is that all these methods provide a mixture of 1-bromo (terminal) and 3-bromo ketones with predominant formation of 3-bromo product [175] (scheme 5).



Scheme 5. Bromination of 2-heptanone

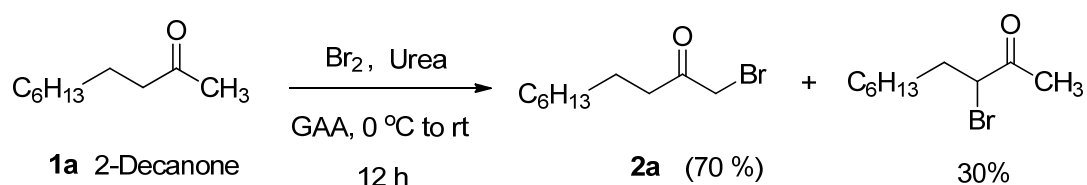
Gaudry and Marquet in 1970 reported a method [176] for the selective terminal bromination of acyclic ketone. They found that use of urea in α -bromination of ketones makes huge difference on the position of bromine offering maximum α -brominated product.



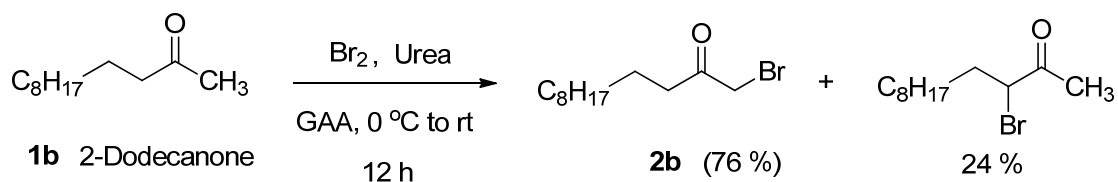
Scheme 6. Bromination of 2-heptanone in the presence of urea

The bromination of 2-decanone **1a** and 2-dodecanone **1b** was performed using liquid Br_2 in the presence of urea as reported by Gaudry and Marquet. Glacial acetic acid was used to catalyse the reaction. The reported method uses elemental bromine in MeOH as a solvent but I did not use any solvent but the reaction was performed only with the mixture of ketone, liquid Br_2 , urea and glacial acetic acid. The reaction performed in this way produced major α -brominated product than 3-bromo product. The brominated ketones **2a** and **2b** were confirmed with ^1H NMR, ^{13}C MR and HRMS. The possible mechanism for acid catalysed bromination of 2-decanone is given in figure 49.

3. Synthesis of Poly(dithenyl pyrrole)-dialkylbithiazole copolymer



Scheme 7. Bromination of 2-Decanone



Scheme 8. Bromination of 2-Dodecanone

1-bromodecan-2-one (2a): Colourless thick oil; Yield 10.5 g, 70%; $R_f = 0.57$ (EtoAc/hexane, 1:9); $^1\text{H NMR}$ (400 MHz, CDCl_3), δ (ppm): 0.86 (t, 3H, $-\text{CH}_3$), 1.25-1.30 (m, 10H), 1.59 (m, 2H), 2.63 (t, 2H), 3.86 (s, 2H); $^{13}\text{C NMR}$ (100 MHz, CDCl_3), δ (ppm): 14.05 (CH_3), 22.59, 23.84, 29.01, 29.06, 29.25, 31.75, 34.27, 39.82, 202.23 ($\text{C}=\text{O}$); **HRMS** (ESI): $[\text{M}+\text{Na}]^+$ calculated for $\text{C}_{10}\text{H}_{19}\text{BrONa}$ 257.051149, found 257.051115.

1-bromododecan-2-one (2b): Colourless thick oil, Yield 10.8 g, 76%; $R_f = 0.53$ (EtoAc/hexane, 1:9); $^1\text{H NMR}$ (400 MHz, CDCl_3), δ (ppm): 0.85 (t, 3H, $-\text{CH}_3$), 1.23-1.29 (m, 14H), 1.59 (m, 2H), 2.62 (t, 2H), 3.86 (s, 2H); $^{13}\text{C NMR}$ (100 MHz, CDCl_3), δ (ppm): 14.05 (CH_3), 22.62, 23.81, 28.99, 29.24, 29.26, 29.38, 29.49, 31.83, 34.26, 39.79, 202.17 ($\text{C}=\text{O}$); **HRMS** (ESI): $[\text{M}+\text{Na}]^+$ calculated for $\text{C}_{12}\text{H}_{23}\text{BrONa}$ 285.082449, found 285.082549.

3. Synthesis of Poly(dithenyl pyrrole)-dialkylbithiazole copolymer

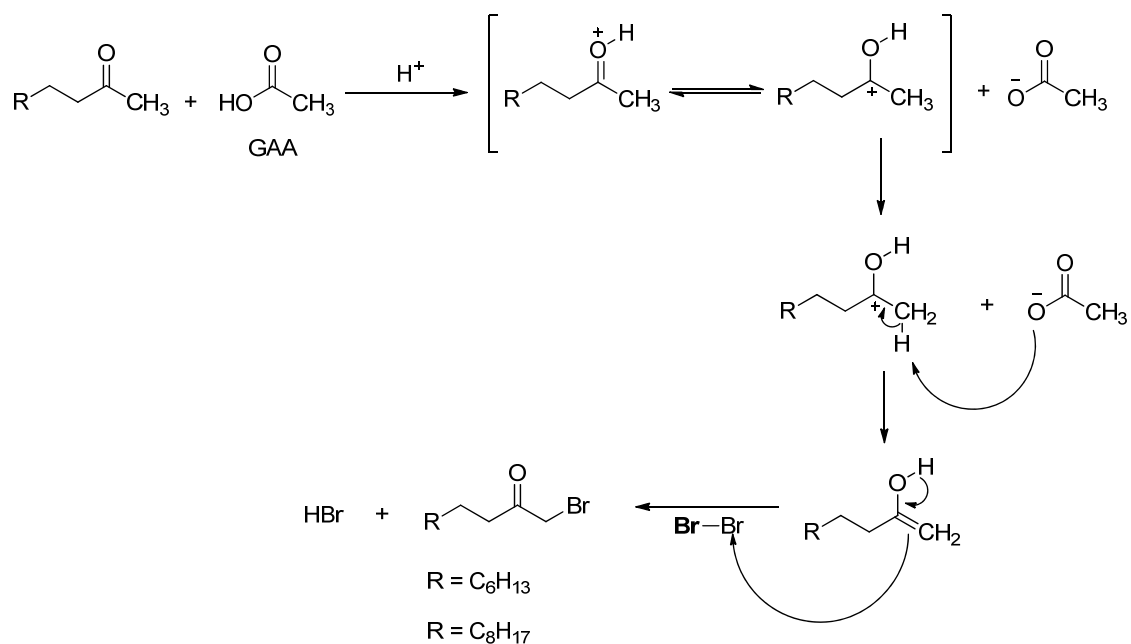
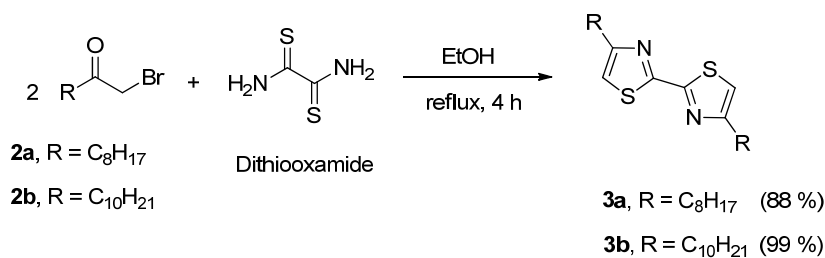


Figure 49. Possible mechanism of bromination of 2-decanone & 2-dodecanone

3.3.2 Synthesis of dialkyl-bithiazoles (3a, 3b)

In second step, α -brominated ketones **2a** and **2b** were cyclized with dithiooxamide to produce corresponding dialkylbithiazole products. The process reported by Curtis M. and co-workers in 1994 for synthesis of bithiazoles was followed [177]. They used dithiooxamide for cyclization with α -bromo ketone to produce bithiazole. Bromo ketones were refluxed with dithiooxamide for 4 hours in absolute ethanol. After confirming the completion of the reaction by TLC, ethanol was evaporated and the composition was extracted with DCM, which on evaporation offered bithiazoles. The products were not purified by any methods as they were pure enough to be taken ahead for next reactions. The reaction of cyclization brominated decanone and dodecanone is given in scheme 9. The possible reaction mechanism of cyclization of α -bromo ketones and dithiooxamide is given in figure 50.



Scheme 9. Synthesis of dialkyl bithiazoles

3. Synthesis of Poly(dithenyl pyrrole)-dialkylbithiazole copolymer

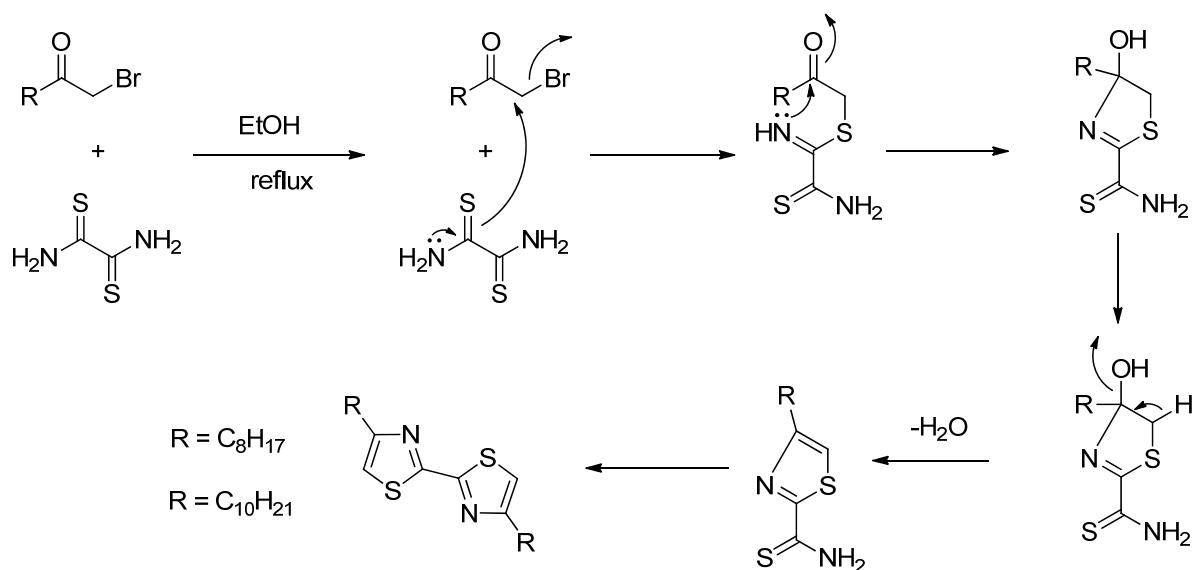
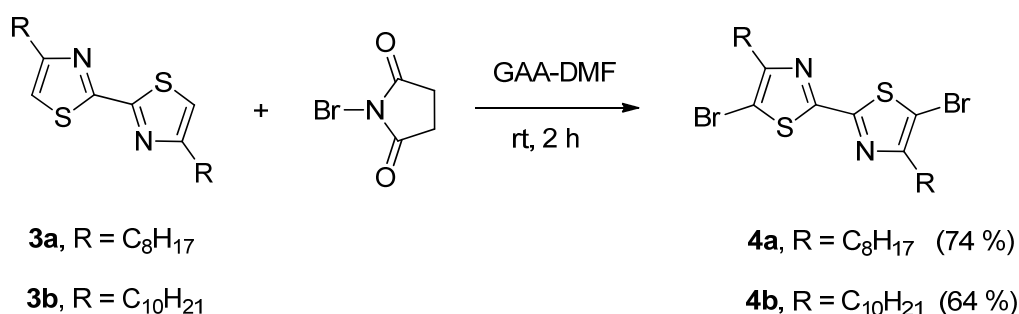


Figure 50. Possible reaction mechanism of dialkylbithiazole formation

3.3.3 Bromination of dialkylbithiazole

The bromination of dialkylbithiazole product was easily performed using NBS (scheme 10). The dialkylbithiazole compounds **3a** or **3b**, NBS were stirred in the mixture of GAA and DMF in the dark for 1-2 hours at room temperature. The formation of yellowish solid precipitate was observed during the reaction. Filtration of the products and washing with methanol gave brominated dialkylbithiazole compounds with good yields. The possible reaction mechanism of bromination of dialkyl-bithiazole is shown in figure 51.



Scheme 10. Bromination of alkylated bithiazoles

5,5'-dibromo-4,4'-dioctyl-2,2'-bithiazole (4a): Yellowish while solid; Yield 6.466 g, 74 %; $R_f = 0.86$ (EtoAc/hexane, 1:9); $^1\text{H NMR}$ (400 MHz, CDCl_3), δ (ppm): 0.86 (t, 6H, $2 \times \text{CH}_3$), 1.26-1.32 (m, br, 20H), 1.69 (m, 4H), 2.73 (t, 4H); $^{13}\text{C NMR}$ (100 MHz, CDCl_3), δ (ppm): 14.10, 22.65, 28.67, 29.13, 29.21, 29.31, 29.31, 29.47, 106.79, 157.36, 159.91. **HRMS** (ESI): $[\text{M}+\text{H}]^+$ calculated for $\text{C}_{22}\text{H}_{35}\text{Br}_2\text{N}_2\text{S}_2$ 549.060292, found 549.060576.

5,5'-dibromo-4,4'-didecyl-2,2'-bithiazole (4b): Yellowish white solid; Yield 7.049 g, 64 %; $R_f = 0.88$ (EtoAc/hexane, 1:9); $^1\text{H NMR}$ (400 MHz, CDCl_3), δ (ppm): 0.87 (t, 6H, $2 \times \text{CH}_3$), 1.25-1.32 (m, br, 28H), 1.69 (m, 4H), 2.73 (t, 4H); $^{13}\text{C NMR}$ (100 MHz, CDCl_3), δ (ppm): 14.12, 22.69, 28.67, 29.12, 29.33, 29.35, 29.48, 29.55, 29.59, 31.91, 106.80, 157.39, 159.92. **HRMS** (ESI): $[\text{M}+\text{H}]^+$ calculated for $\text{C}_{26}\text{H}_{44}\text{Br}_2\text{N}_2\text{S}_2$ 605.122892, found 605.122560.

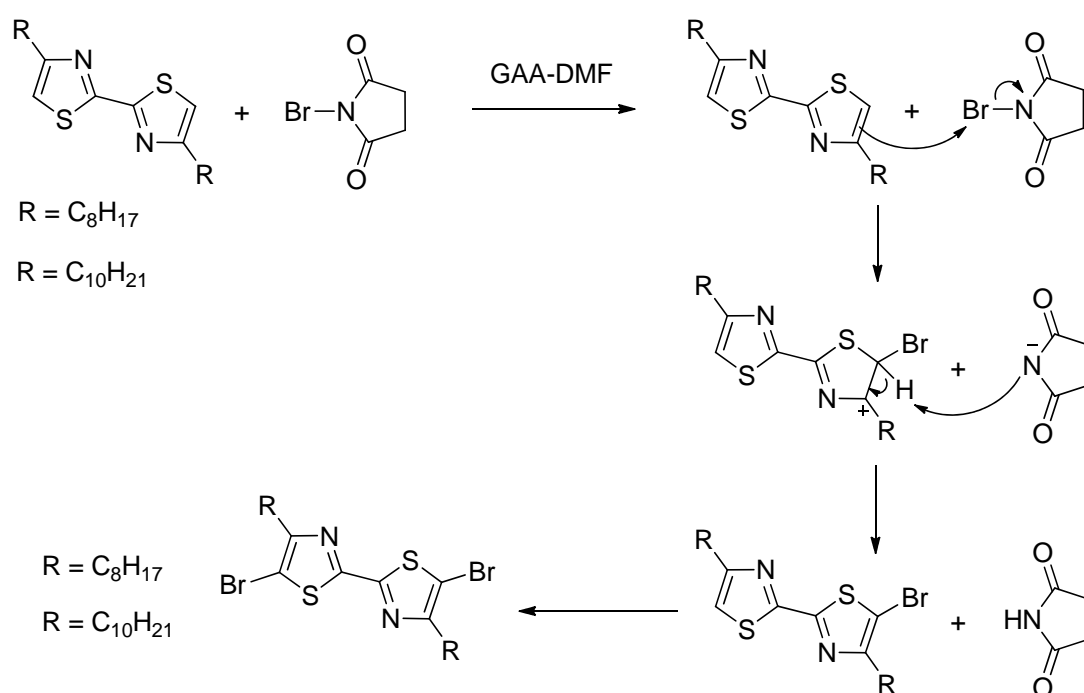


Figure 51. Mechanism of bromination of alkylated bithiazoles by NBS

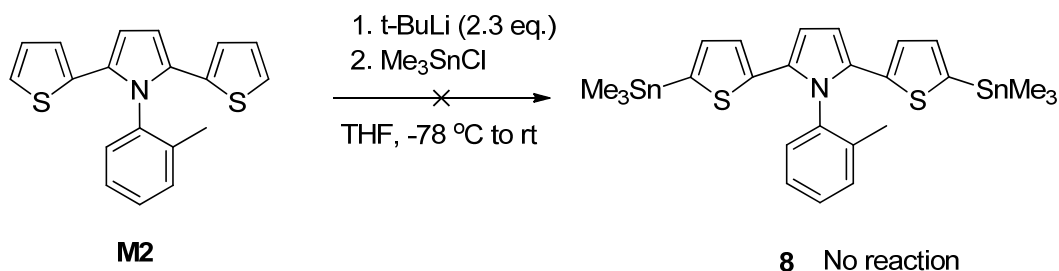
3.3.4 Synthesis of SNS-Stannyl intermediate

In order to put together the brominated dialkylbithiazoles with SNS compounds, it was necessary to put trimethyl tin groups on both side of the SNS compound. Trimethyl tin

3. Synthesis of Poly(dithenyl pyrrole)-dialkylbithiazole copolymer

groups are expected to easily attach with bromo thiazoles through metal (Sn)-halogen (Br) exchange mechanism. Although there are several reports on trimethyl tin metallation of different aromatic or heterocyclic compounds but not a single on the SNS compounds (to the best of my knowledge). Therefore, the process reported by Liu and co-workers for tin metallation of 4-(2-hexyldecyl)-4H-dithieno [3,2-b:2',3'-d]pyrrole [178] (somewhat similar compound as SNS) was tried for one of the SNS derivatives **M2**.

The SNS compound **M2** was dissolved in dry THF under inert atmosphere and the resulting yellowish solution was then cooled to $-78\text{ }^{\circ}\text{C}$ using liquid N_2 and ethyl acetate mixture cooling bath. $t\text{-BuLi}$ (2.3 eq.) was added dropwise to generate a nucleophile at 5 and 5' position of thiophene rings of **M2**. The orange coloured solution was stirred under the same conditions for 1 h before slowly raising it to room temperature. The mixture was again cooled to $-78\text{ }^{\circ}\text{C}$ to add Me_3SnCl -THF solution in one lot. After addition of Me_3SnCl , the reaction was slowly brought to room temperature for stirring another 2 h. The reaction was checked by TLC but it was found that the reaction did not proceed.



Scheme 11. Attempt made for attaching Me_3Sn group on **M2**

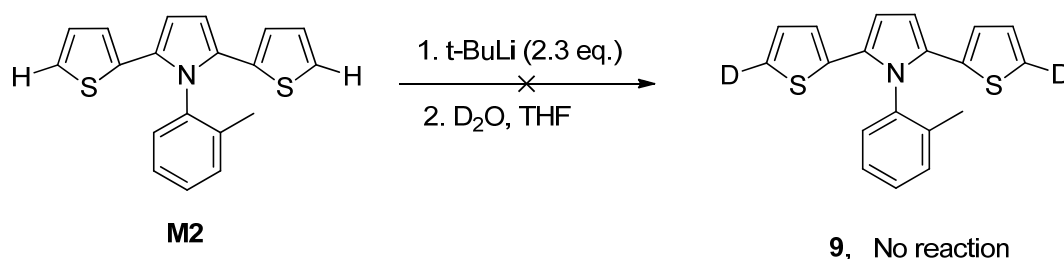
Afterwards, the same reaction was tried again with higher equivalents of $t\text{-BuLi}$, thinking that previously used 2.3 eq. was not enough to abstract H from thiophene system (to generate nucleophile) but again no attempt was successful.

Table 6. Attempts made for attaching Me₃Sn group on **M2**

No.	Comp.	Conditions	Results
1	M2	2.5 eq. t-BuLi, Me ₃ SnCl, THF, -78 °C to rt, 2 h	No reaction
2	M2	3.0 eq. t-BuLi, Me ₃ SnCl, THF, -78 °C to rt, 2 h	No reaction
3	M2	3.5 eq. t-BuLi, Me ₃ SnCl, THF, -78 °C to rt, 2 h	No reaction
4	M2	4.0 eq. t-BuLi, Me ₃ SnCl, THF, -78 °C to rt, 2 h	No reaction
5	M2	5.0 eq. t-BuLi, Me ₃ SnCl, THF, -78 °C to rt, 2 h	No reaction

3.3.4.1 Deuterium quenching experiments

In order to check whether 5 and 5' positions of thiophene rings of **M2** are getting deprotonated or not, deuterium quenching experiment was performed. Three reactions were performed on SNS derivative **M2**.

**Scheme 12.** Deuterium quenching experiment**Table 7.** Deuterium quenching experiments (additions of D₂O at different temperature)

No.	Comp.	Conditions	D ₂ O addition temp.	Results
1	M2	2.5 eq. t-BuLi, THF	-80 °C	No reaction
2	M2	2.5 eq. t-BuLi, THF	-50 °C	No reaction
3	M2	2.5 eq. t-BuLi, THF	-30 °C	No reaction

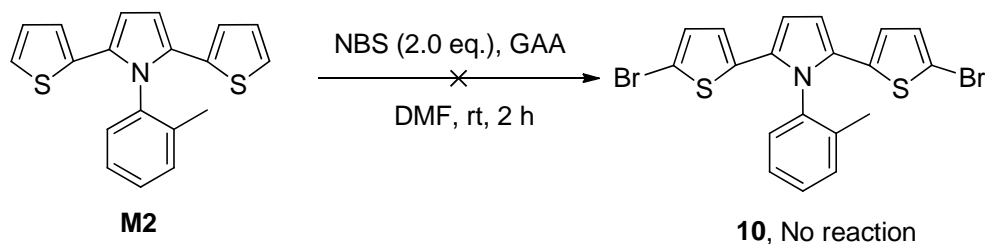
The SNS compound was dissolved in dry THF under inert atmosphere and the solutions were degassed by purging N₂ gas for 30 min. The solution was cooled to -80 °C and 2.5 eq. t-BuLi was added dropwise and stirred for 1h allowing formation of deprotonated (nucleophile) entity. All three reactions were quenched with D₂O at different temperatures. The reactions

3. Synthesis of Poly(dithenyl pyrrole)-dialkylbithiazole copolymer

were then brought to room temperature, THF was evaporated and NMR was taken to see if targeted protons have been replaced by deuterium or not. The ^1H NMR shows that there was no deprotonation in any reaction.

3.3.4.2 Bromination of SNS

Afterwards, not having successful attachment of Me_3Sn group on **M2**, the synthetic approach was changed to put bromine at 5 and 5' position of thiophene rings of **M2**, where Me_3Sn group was expected to come. A new approach was chosen because if those positions would have bromine atoms then metal (Sn)-halogen (Br) exchange becomes easy. Initially bromination was tried using NBS and GAA in DMF at room temperature (scheme 13). The SNS monomer **M2** was subjected to 2.0 eq. NBS as two Br groups were expected on **M2** but no bromination has been observed. Therefore, many reactions were tried with different equivalents of NBS.



Scheme 13. Bromination of monomer **M2**

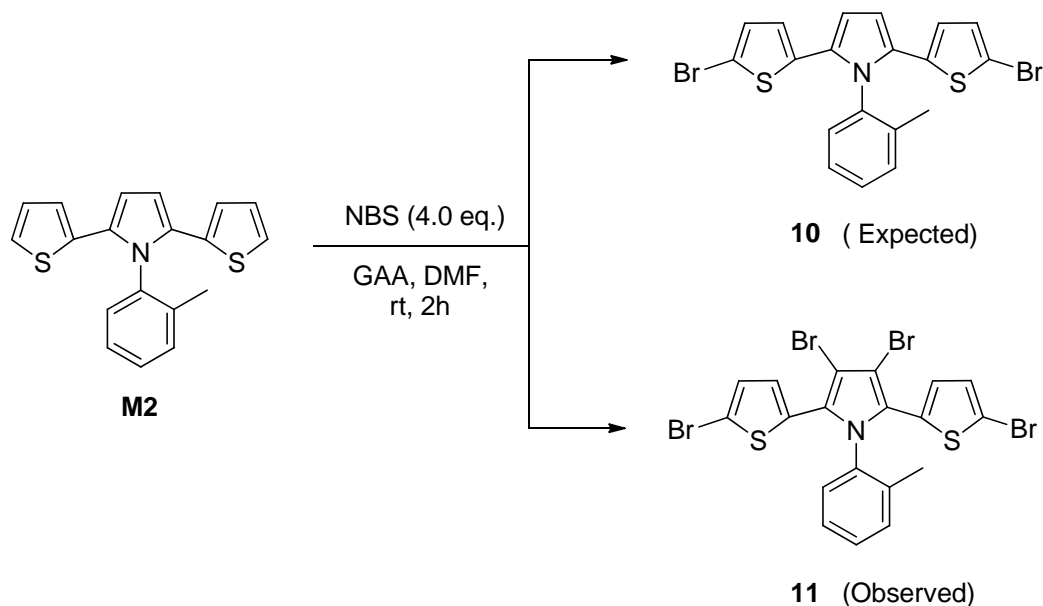
Table 8. Bromination of **M2** performed using different equivalents of NBS

No.	Compound	NBS (eq.)	Results
1	M2	2.5	Incomplete reaction
2	M2	3.0	Incomplete reaction
3	M2	3.5	Incomplete reaction
4	M2	4.0	Reaction seen complete on TLC

Although all the starting material had been consumed as analysed by TLC, when NBS amount was increased to 4.0 eq. (Table 8, entry 4) (scheme 14), the ^1H NMR analysis showed that the bromination has taken place not only on thiophene rings but also on pyrrole ones as well (figure 53). 4 hydrogen atoms (protons) were found missing on the NMR confirming the

3. Synthesis of Poly(dithenyl pyrrole)-dialkylbithiazole copolymer

bromination on thiophene as well as on pyrrole ring. This means that the bromination was not selective at 5 and 5' position of thiophene rings of **M2**. The ^1H NMR of **M2** and pyrrole brominated compound (resulted from bromination on **M2**) are given in figure 52 and figure 53 respectively.



Scheme 14. Bromination of SNS derivative (**M2**) by NBS

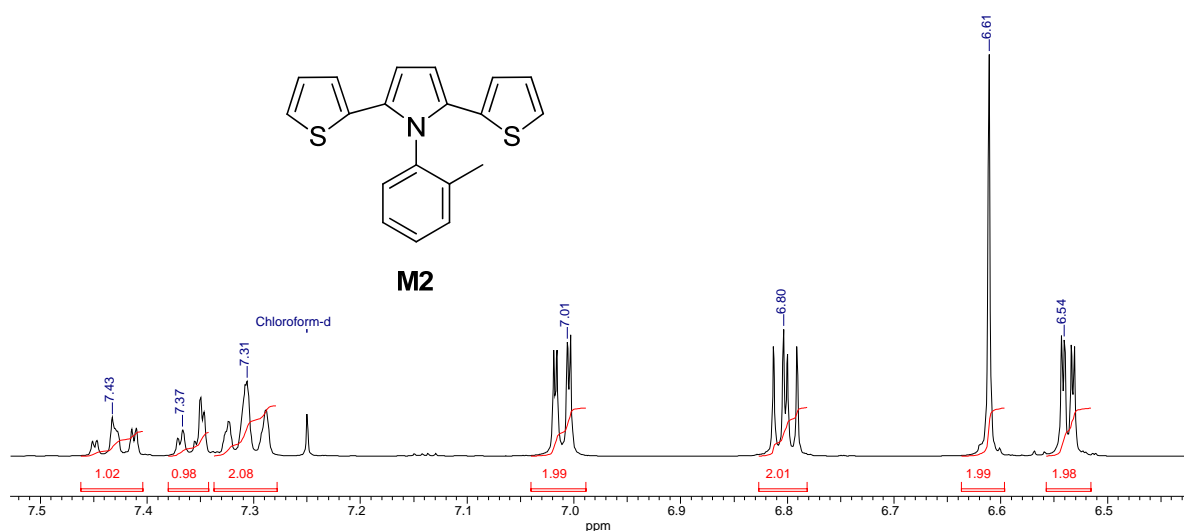


Figure 52. NMR spectra of monomer **M2**

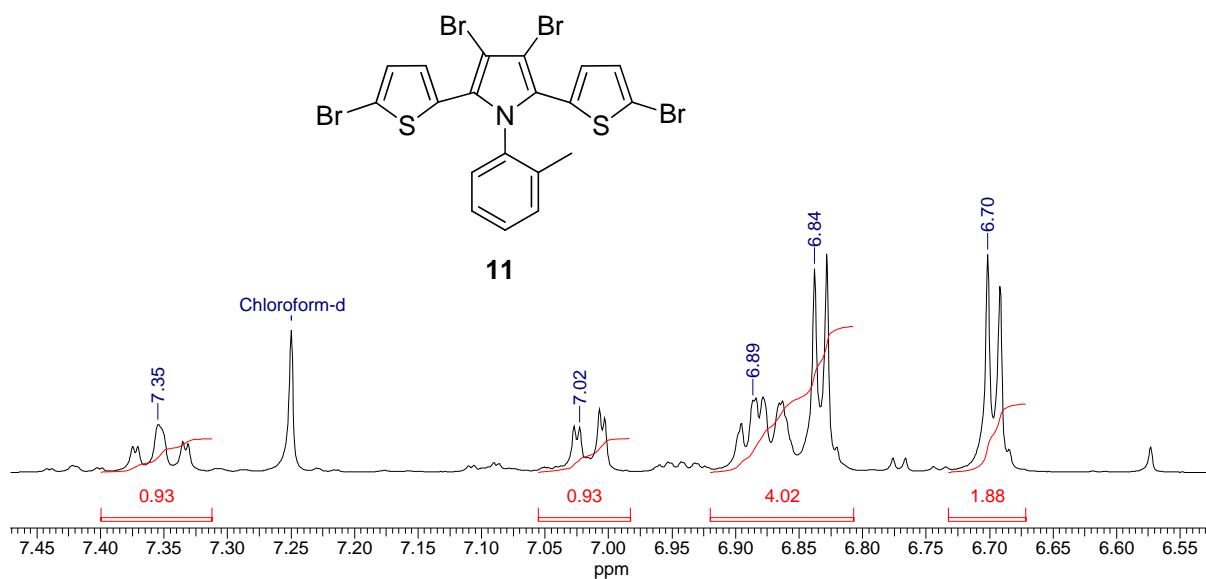
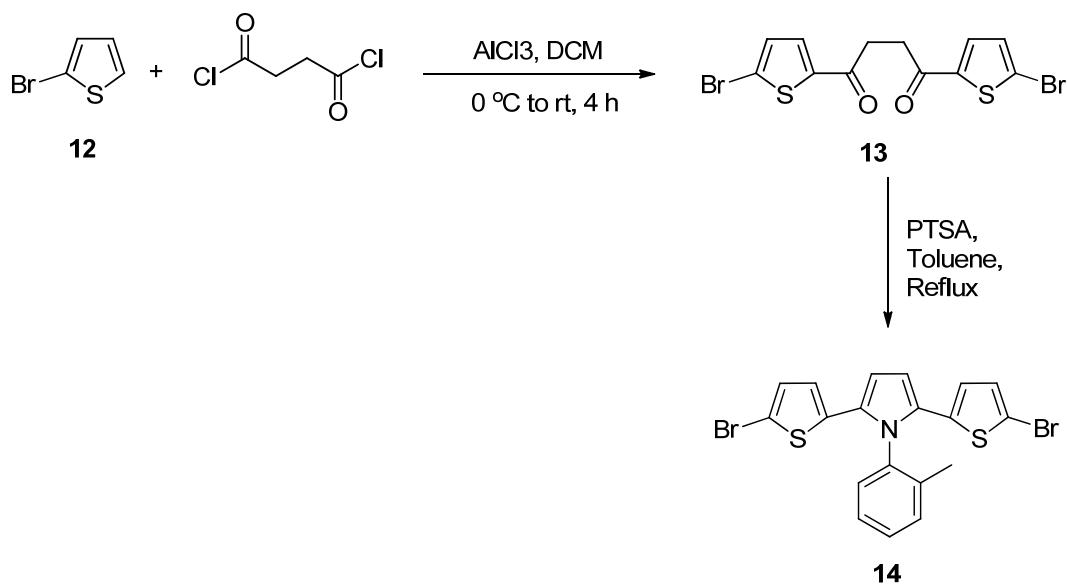


Figure 53. NMR spectra of extra brominated SNS compound **11**

After realizing that bromination was not going to be selective on thiophene ring, another synthetic approach was adapted for selective bromination. I decided to try the synthesis of Br-SNS starting right from 2-bromothiophene instead of thiophene. The new synthetic route adapted is shown in scheme 15.



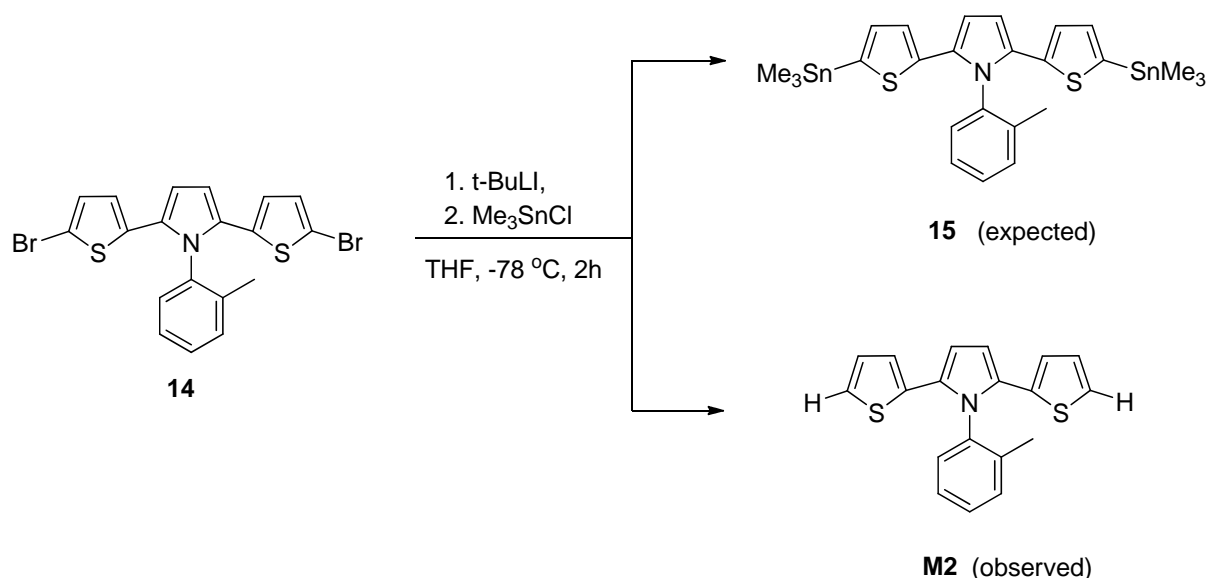
Scheme 15. New synthetic plan for bromination of SNS

3. Synthesis of Poly(dithienyl pyrrole)-dialkylbithiazole copolymer

With the new bromination approach, firstly 2-bromothiophene **12** was reacted with succinyl chloride in the presence of aluminium chloride as a Lewis acid catalyst. Once bromothieryl diketone was in hand, the intermediate was subjected to the Paal-Knorr pyrrole reaction with *o*-toluidine to successfully produce brominated SNS compound **14** with good yield.

3.3.4.3 Me₃SnCl reaction on Brominated SNS compound

According to the modified plan, the synthesis of tynylated SNS using newly brominated SNS derivative **14** was attempted. First, *t*-BuLi was added to THF solution of brominated SNS derivative **14** at -80 °C and then after stirring for 1h, Me₃SnCl solution in THF was added in one portion. Though it was seen on TLC that total starting compound was consumed and new moiety has formed, ¹H NMR confirms that the moiety is nothing but the debrominated SNS meaning bromine atoms were replaced by H and this is back to same compound as **M2**.



Scheme 16. Tynylation of brominated SNS compound (**14**)

3.4 Conclusion

The synthesis of dithienyl pyrroles (as explain in previous chapter) and dialkylbithiazoles with long aliphatic chains were successfully achieved but the synthesis of dithienyl pyrrole-dialkylbithiazoles was not successful. The use of higher concentrations of *t*-BuLi (up to 5 eq.) did not help to connect both molecules. The deuterium quenching experiment showed that either there was no generation of nucleophile or the stability of the nucleophile was very low. The attempt to put Me₃Sn groups on the brominated SNS compounds produced debrominated

3. Synthesis of Poly(dithenyl pyrrole)-dialkylbithiazole copolymer

SNS compounds showed that there could be a generation of nucleophile but the moisture present in the reaction quenched the nucleophile before reacting it to the Me_3SnCl . This reaction may proceed positively under total dry (moisture free) conditions.



4. Flexible Multisensing platform integrated into RFID label

This work has been developed in the framework of the European Union project: FlexSmell. The aim of the project was to develop a low cost, low power, flexible multisensing system compatible with wireless communication for smart packaging of perishable foods. The main contributors for this work were Ecole Polytechnique Fédérale de Lausanne (EPFL), Neuchâtel (Switzerland), The University of Manchester (UK) and the Holst Centre/ TNO (The Netherlands) and Institute of Physical Chemistry, University of Tübingen (Germany).

4.1 Introduction

Radio frequency identification (RFID) sensors have attracted immense interest in the number of applications ranging from detection of chemical analytes, environment monitoring, and healthcare to safety and security [179-181]. In many applications real time monitoring of environmental factors such as temperature, humidity, etc. and detection of chemical analytes present in the surrounding is very important in a social, economic and environmental context. For example, a) Temperature stands second in the list of factors causing foodborne health problems b) 300 million tonnes of produce are wasted annually in the world due to improper transport and deficient storage, etc. The gases emitted during the ripening or decay of fruits, foods and vegetable can be used to monitor in real-time for proper transport and storage of the products. Multisensors platforms on RFID tags are expected to significantly reduce these problems by means of real-time monitoring of ambient.

Therefore, current research in scientific communities is very much focused on developing a multisensing RFID system for monitoring perishable goods. As reported in the literature, such RFID systems have been used to monitor the temperature for perishable food storage only [182]. Multi-gas detection with on-tag metal oxide gas sensor [183] and mixed vapour detections with polymer electrolyte membrane using RFID [184] are also reported. Though there are many RFID sensing systems that have been reported, flexible multisensing RFID system with multi-parametric detection such as temperature, humidity, and various chemical analytes on a single platform are rare to find. This chapter presents the development of a flexible multisensing smart RFID system for monitoring of perishable foods.

4.1.1 RFID Tags

An RFID sensing system encompasses a tag with sensors and a reader (base station), which communicate with each other by means of radio frequency electromagnetic waves. The reader emits modulated electromagnetic waves to which tag is designed to respond. When recognizing the inquiry signal from the reader, the data stored in the microchip of tag is

transmitted to the reader. RFID tags can be classified into following three classes: passive, active and semi-passive. a) **Passive tags**: These tags have no power source on board and rely on the power transferred from the reader wirelessly. When the radio waves from the reader cross the passive tag, antenna coil there in generate RF currents which are used for both, to transfer information between the reader and tag and to operate the circuits in the tag. b) **Active tags**: Active tags rely on a battery power for tag operation instead of being powers wirelessly from the reader. c) **Semi-passive tags**: These systems fall in between above mentioned types, being powered from a reader with an additional battery on board. They use the passive RFID interface allowing wireless communication to the device without using the internal power source. The battery is used to enable the tag to function in the absence of a reader. The preferred RFID embodiments for environmental monitoring would be a passive one but because of power demanding resistive sensors included the other two versions, semi-passive or active, have to be practically implemented.

The schematic representation of sensing tag used in the study is shown in figure 54, which includes four major components such as: a multisensor platform, processing electronics, battery power supply and high frequency antenna for wireless communication.

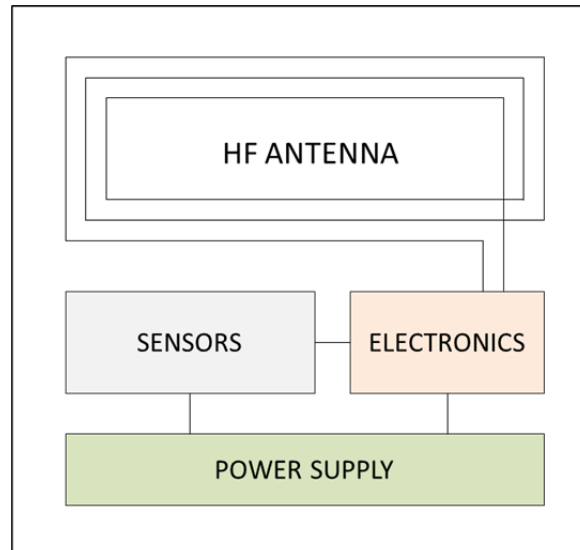


Figure 54. Schematic representation of the tag with sensor platform, electronics, battery and HF antenna

The multisensing platform and the RFID tag used in this study were fabricated on a flexible substrate. The components of the tag such as antenna, electrical connection lines, etc. are

fully printed on flexible plastic. The multisensing platform and RFID tag have been integrated using a zero insertion force (ZIF) connector. The multisensor platforms include sensors with different transduction principles (mainly resistive and capacitive) on a single substrate for simultaneous detection of environmental parameters such as temperature, humidity and chemical analytes such as ammonia, ethanol and other VOCs.

This chapter will describe low-cost multisensing systems consisting of two IDE capacitors for humidity sensing, resistive temperature detector (RTD) to measure the temperature and two IDE resistors for detection of ammonia and VOCs. The multisensor platform was developed and manufactured by SAMLAB, EPFL, Neuchatel (Switzerland). I have functionalized the capacitive transducers at IPC, University of Tübingen (Germany) whereas the resistive ones at The University of Manchester. A flexible printed RFID label (compatible with developed multisensor platform) was developed at Holst Centre (The Netherlands). The chapter will present the sensing characterization of the multisensor platforms with RFID communication system.

4.2 Materials and methods

4.2.1 Multisensor platform

A multisensing platform with the sensors of different transduction principles was fabricated by using inkjet printing techniques at EPFL, IMT, SAMLAB, Neuchatel Switzerland. The platforms have been prepared on 250 μm -thick polyethylene terephthalate (PET) film with silver nanoparticle ink. An optical image of a close view of the multisensor platform showing the different types of transducers is shown in Figure 55A. The platform consists two capacitive sensors, two resistive sensors and one resistive temperature detector (RTD). The ink-jet printed flexible arrays of transducing platforms for the multisensing system is shown in the optical image view in figure 55B.

The comparatively large size IDE capacitive structures visible on top of figure 55A were to be used for the capacitive humidity sensing. One of these two structures is used as a reference to remove the parasitic effect of the substrate through differential measurements [11].

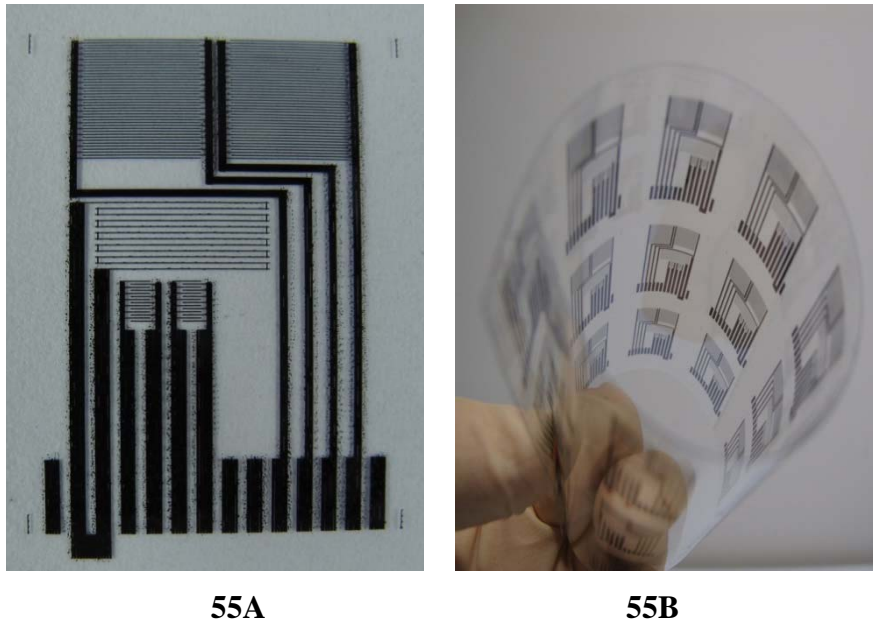


Figure 55. A) Optical image of a close view of the transducers platform including (from top to bottom and left to right): Two large combed electrode structures for capacitive gas detection, a meander-shaped resistor for temperature detection and two small comb electrode structures for resistive gas detection. B) Optical image depicting a flexible array of transducing platforms for the multisensing systems fabricated by inkjet-printed silver nanoparticles on PET foil (by courtesy of F. M. Lopez, SAMLAB EPFL).

The IDE capacitors are 5 mm in length and have 120 μm insulating gap between the two neighbouring electrodes. The total number of electrodes in each capacitor is 36 and together with insulating gaps makes a total effective surface area of $5.1 \times 4.2 \text{ mm}^2$. In the middle of the image, a meander-shaped RTD is placed. The RTD is electroplated with Ni to improve its temperature coefficient of resistance (TCR). The RTD is 6.7 mm long and contains 6 meanders having 240 μm gaps between the lines. The total effective surface area of RTD is $7.3 \times 2.7 \text{ mm}^2$. Finally, at the bottom, two small combs like structures are placed for resistive gas detection. The IDE resistor consists of 14 fingers with a total surface area of $1.2 \times 1.6 \text{ mm}^2$.

The IDE capacitors are targeted to a nominal capacitance of 3.5 pF before the deposition of the polymer sensing layer. The RTD should be 1 k Ω before plating with Ni and $\sim 500 \Omega$ after 1 μm -thick layer plating. The small IDE to be used as chemoresistor was foreseen for sensing layer having a resistance in the range of 10 k Ω to 1M Ω . The resistive sensors are devoted to

the conductive, polymer based, ammonia and VOCs detection. The number of analytes that could be measured may be increased by changing the nature of the conducting polymer, copolymer or using mixtures of polymers.

4.2.2 Functionalization of sensors on the platform

A) Capacitive humidity sensors: One of the two capacitive parts of the platform was deposited at IPC by me with cellulose acetate butyrate (CAB) or polyether urethane (PEUT) using spray coating techniques. The solution of CAB (from Aldrich) was prepared by dissolving 500 mg of polymer in 200 mL of 2-butanone (0.25% w/v). The PEUT solution was prepared by dissolving 500 mg of the polymer in 200 mL of THF (0.25% w/v). The area of the platform that needs to be protected / uncoated was covered with shadow masks. Alternatively, at EPFL, CAB layers have been printed from inks prepared at IPC, University of Tübingen.

B) Resistive ammonia sensors: The sensing layers for resistive ammonia detection were deposited by vapour phase deposition polymerization (VDP) technique by E. Danesh at The University of Manchester, UK. On the left resistive transducer (Figure 56, lower part) the PANi layer was deposited in two steps, firstly the transducer area was coated with an oxidant/dopant mixture containing ammonium persulfate (APS) and poly(4-styrenesulfonic acid) (PSSA) by drop casting, and then the platform was exposed to aniline vapours (the monomer) in a home-made VDP chamber. Similar method was followed for the right side transducer, where the layer of PPy doped with ferric chloride (FeCl_3) was deposited. In-situ polymerized layers were rinsed with water to remove any unreacted matter still present in the layer. The sensors have been then annealed at 60 °C.

Figure 56 clearly shows polymer sensing layers deposited on the platform coated with CAB on capacitive transducer and polyaniline (PANi) and polypyrrole (PPy) layers on resistive parts.

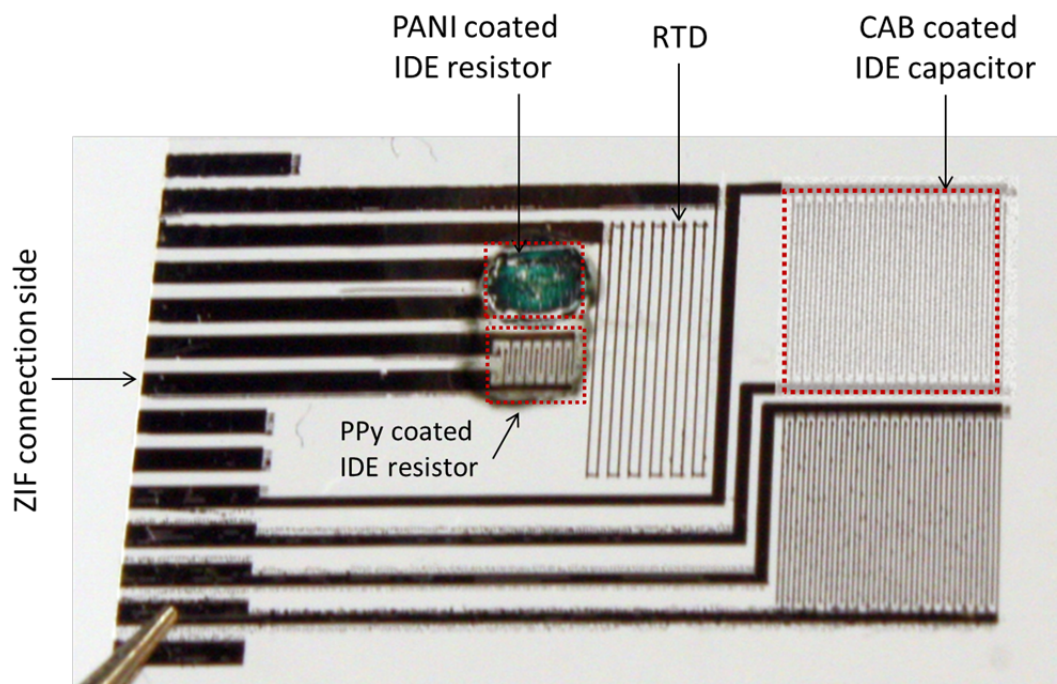


Figure 56. Optical image of a multisensing platform with sensing layers deposited on devices: One of the capacitors is coated with a polymeric layer (CAB in this case) and two small IDE functionalized with PANi (left) for ammonia detection and PPy (right) for VOCs detection. PANI and PPy layer were deposited by E. Danesh at The University of Manchester, UK.

4.2.3 Multisensor platform characterization

The platforms were characterized by using the flexible RFID tags and software (developed by Holst center) and a commercially available reader (from STM Microelectronics). The flexible RFID label includes screen printed high frequency antenna, analog to digital converter silicon chip for the capacitors, microcontroller for the readout of the resistors and a RFID chip for wireless communication. The measurements of the platforms were performed in a measuring chamber where the chemical analytes have been delivered. The multisensing platforms were exposed gaseous mixtures of target analytes with synthetic air (80% N₂ and 20% O₂, purity 5.5 from Westfalen AG) using computer controlled gas mixing system provided with mass flow controller as explained in section 2.2.6. The gaseous mixtures were given under dynamic exposure (200 sccm test gas flow) to keep the ambient with constant composition. The relative humidity pulses were obtained by bubbling synthetic air through a column of double deionised water. For the resistive characterization of PANi and PPy, different

ammonia concentrations were obtained by mixing of analytical ammonia (3.8 NH₃ in 5.5 synthetic air) from Westfalen AG with synthetic air. The set-up picture showing the multisensor platform with flexible RFID label mounted in the measuring chamber is shown in figure 57.

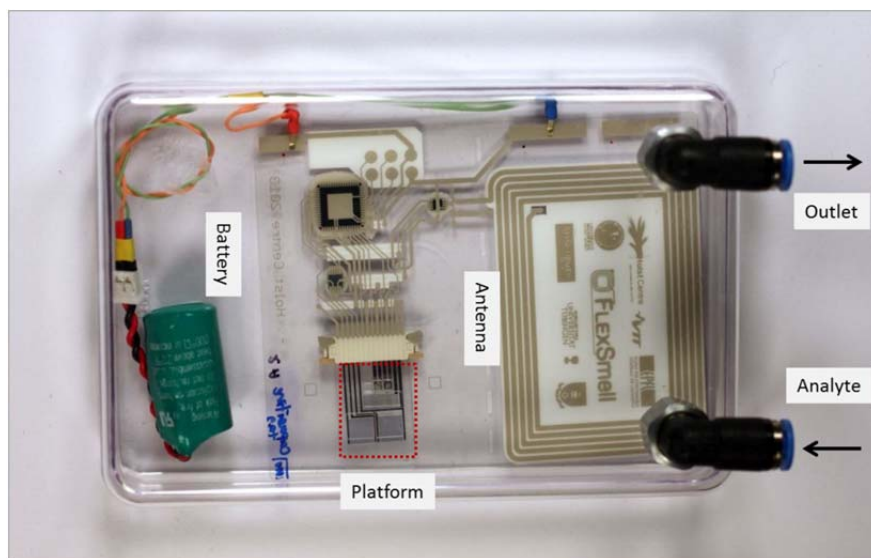


Figure 57. Optical image of measuring chamber containing the multisensor platform, RFID label with antenna, battery for power supply and inlet-outlet connections for the analytes mixtures.

4.3 Results and discussion

4.3.1 Capacitive Humidity sensing

Cellulose acetate butyrate and PEUT coated platforms were subjected to different levels of relative humidity: 0, 10, 30, 50 and 70% RH. The exposure protocol includes 20 min purging with synthetic air and then each level of RH for 10 min. (Figure 58). The responses of the humidity sensors are given as shift in their capacitance upon exposure to different humidity levels. Figure 59 and 60 shows the calibration curves of CAB and PEUT respectively against different humidity levels. The graph shows a linear increase in the capacitance with humidity.

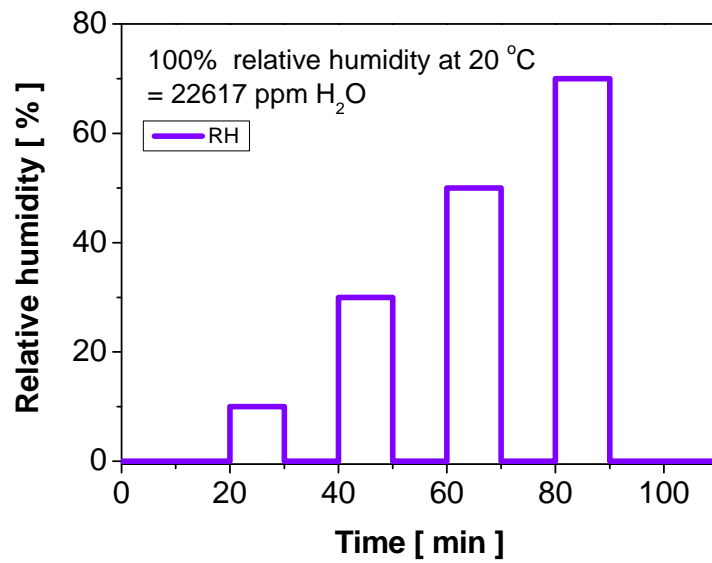


Figure 58. The exposure protocol of humidity sensing

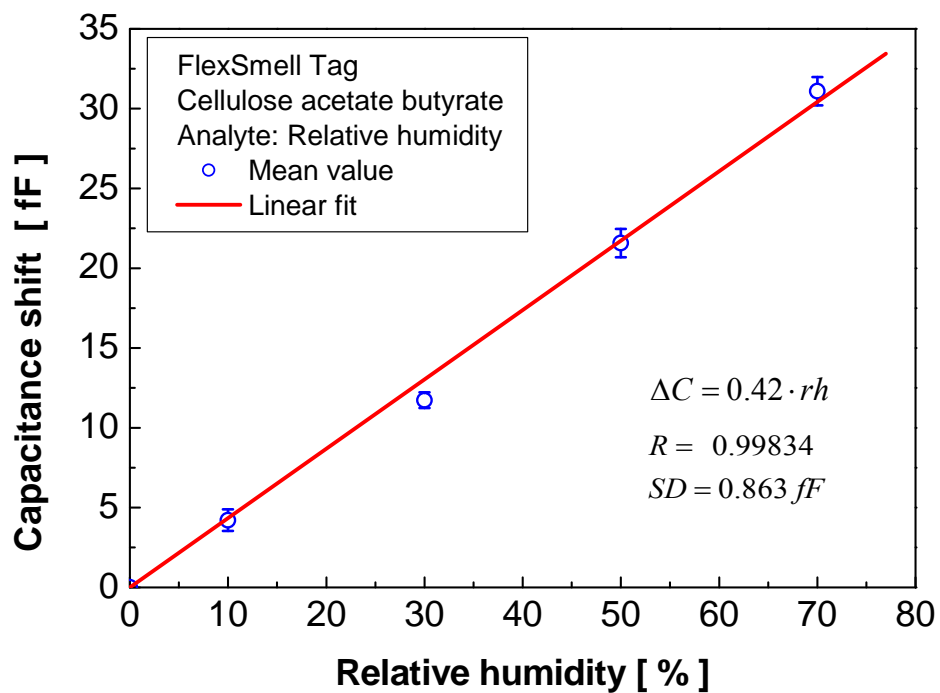


Figure 59. The response of CAB coated capacitive sensor to different RH levels. The measurement was performed six times with given exposure protocol.

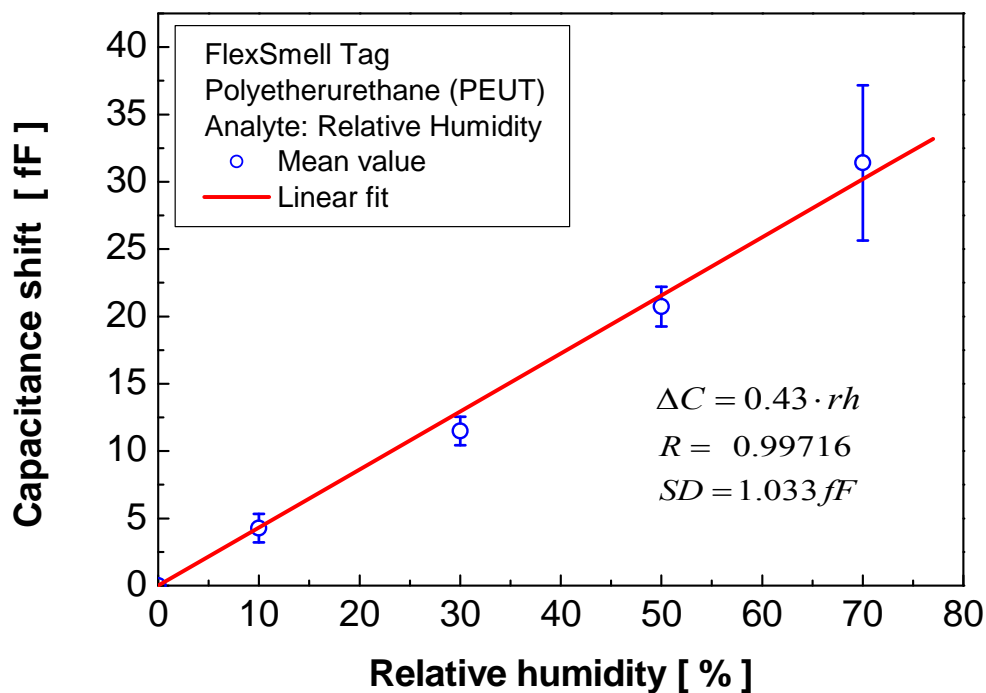


Figure 60. The response of polyether urethane (PEUT) coated capacitive sensor to different relative humidity levels. The measurement was performed six times with given exposure protocol.

4.3.2 Resistive Ammonia sensing

The multisensor platform with PANi and PPy layers on their resistive transducers were characterized against ammonia. The evaluation of the sensors towards ammonia included 20 min of synthetic air purging and then exposures of 10 min each at ammonia concentration steps (10, 30, 100, 300 and 1000 ppm). The measurements were performed twice, first in dry air (0% RH) and another with 50% RH in background. The calibration curves of PANi and PPy against different ammonia concentrations are shown in figure 61 and 62 respectively.

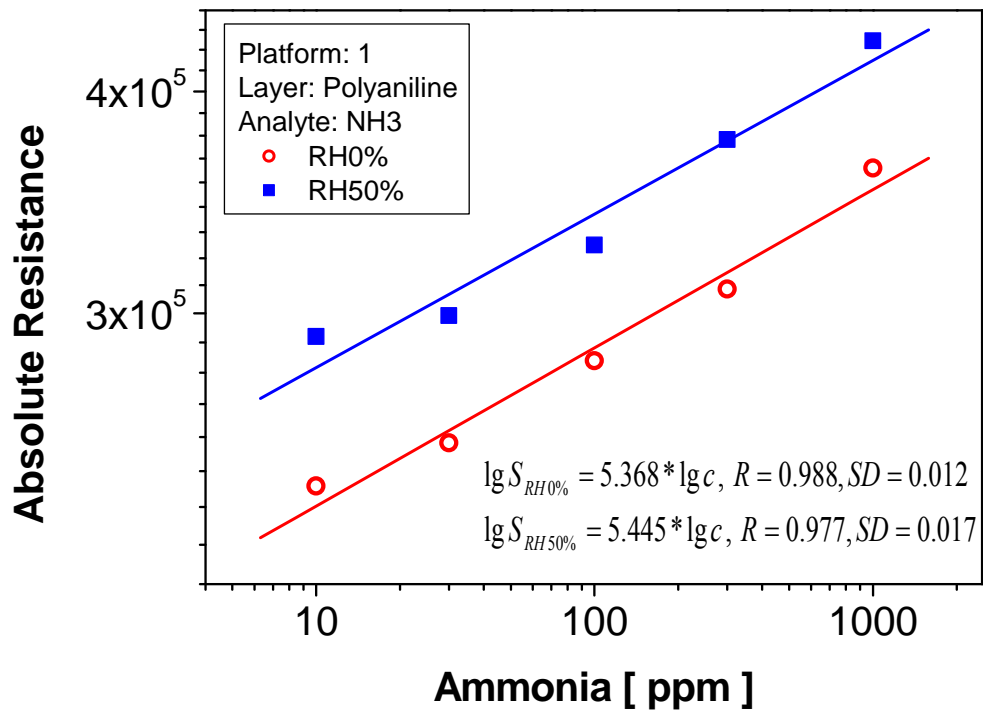


Figure 61. The change in resistance of the PANi sensor against different concentrations of ammonia in the absence of RH (red open symbols) and in the presence of 50% RH (blue fill symbols). The measurements were performed three times but data for only one exposure was obtained proper order. The straight lines are linear fits. In the statistics S is sensor signal.

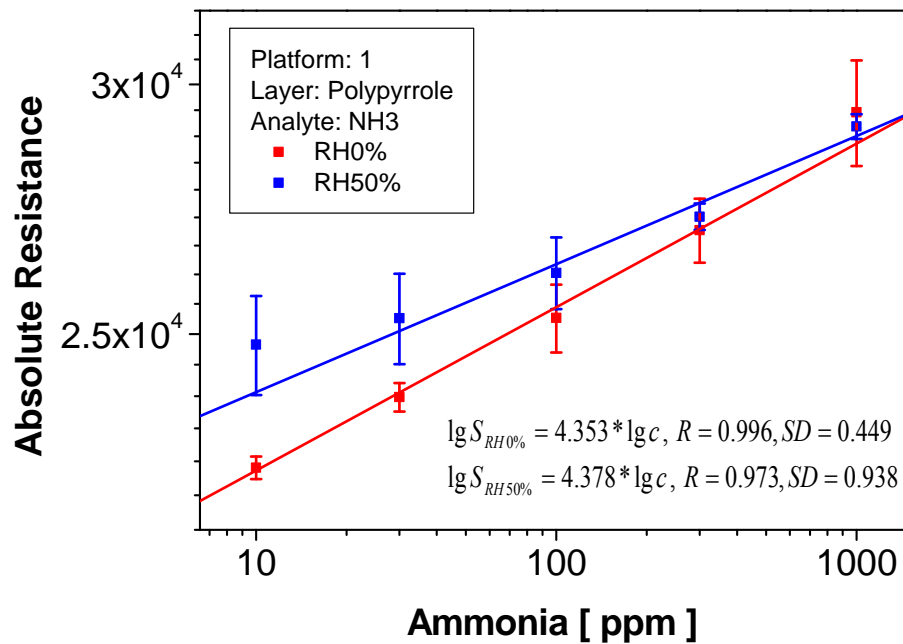


Figure 62. The change in resistance of the PPy sensor against different concentrations of ammonia in the absence of RH (red symbols) and in the presence of 50% RH (blue symbols). The straight lines are linear fits. The measurement was performed two times with given exposure protocol. In the statistics, S is sensor signal.

4.3.3 Resistive temperature detector (RTD) measurements

The characterization of the RTD device of the platform was performed by subjecting the platform to different temperatures (10, 20, 30, 40, 50 and 60 °C) in an environmental test system (Espec Corp. Model: PU-1KTH) and each temperature step for 15 min. The RTD showed $\sim 2 \Omega$ increase in its resistance at each step (Figure 63). The RTD device was also measured for relative humidity levels (10, 30, 50, 70% RH) at different temperatures (60, 35 and 10 °C).

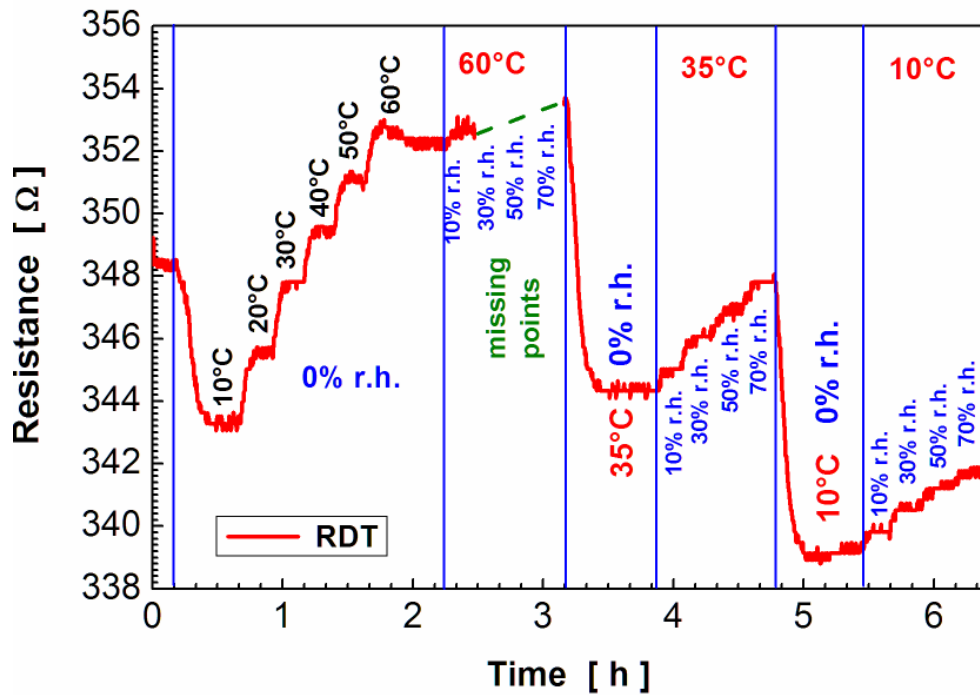


Figure 63. The shift in resistance of RTD with the temperature measured in dry air, and for different RH levels at different temperatures

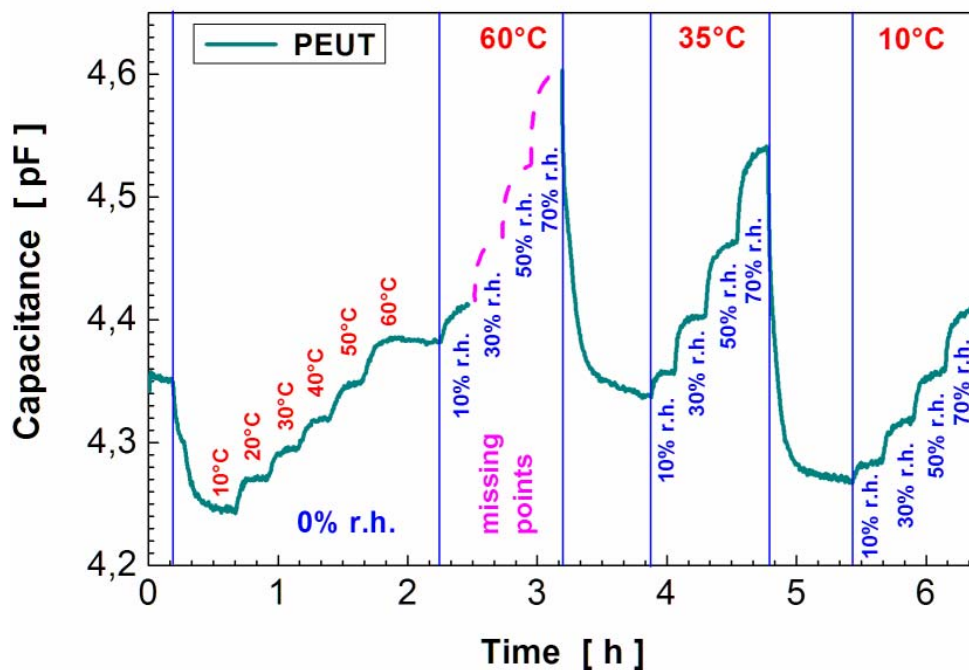


Figure 64. The response of PEUT deposited capacitive devices when exposed to different temperature steps and RH levels (at different temperatures)

When the multisensing platform was subjected to different for RTD characterizations, PEUT coated capacitive device also responded to the variations of the temperatures. The graphics depicted in figure 64 shows capacitive response of PEUT layers to temperatures steps and the humidity steps (10, 30, 50 and 70% RH) characterized at different temperatures (60, 35 and 10 °C).

4.4 Conclusion

This chapter presented a development of the smart multisensing RFID label in terms of multisensor platform fabrication, functionalization of each device of the platform and their sensing characterization. The smart label with multisensor platform (comprising sensor of different transduction principles) and flexible RFID label have been successfully fabricated and integrated. The devices had been functionalized with various polymer sensing layers for monitoring the humidity, ammonia and VOCs at the universities of Tübingen and Manchester. The functionalized multisensing platforms are readily integrable in a flexible RFID label with sensing capabilities. The multisensing platform included two IDE capacitive devices for humidity sensing, two for resistive devices for ammonia and VOCs detection and a resistive temperature detector (RTD) for environmental temperature detection. The main task assigned to the IPC-University of Tübingen, functionalization of multisensing platforms and their sensing characterization using flexible RFID label have been done successfully.



5. Biosensors based on Pig-odorant binding proteins (OBPs)

The work presented in this chapter was carried to explore the possibility to use porcine odorant binding proteins in the construction of biosensor and their characterization using Kelvin probe method. This work was performed within the frame of the FlexSmell project for building the platform for future developments of biosensor based RFID systems.

5.1 Introduction

5.1.1 Biosensor

A biosensor is an analytical device which integrates a biological recognition element with a physical transducer to generate a measurable signal proportional to the concentration of the analytes [185, 186].

The detection of chemical analytes using biosensor involves two steps; a recognition step and a transduction step. In recognition, biological sensing element or receptors are involved which interact or recognize biological or chemical analyte in surrounding atmosphere or solution medium. A biosensor is made up of a bio receptor surface, transducer, signal process and output display unit [187] (Figure 65). The receptors can be of biological proteins such as enzyme, antibody, DNA, peptide sequences or whole cells. The receptors or biological sensing elements are in close contact with the transducer which converts the analyte-receptor interaction into measurable output.

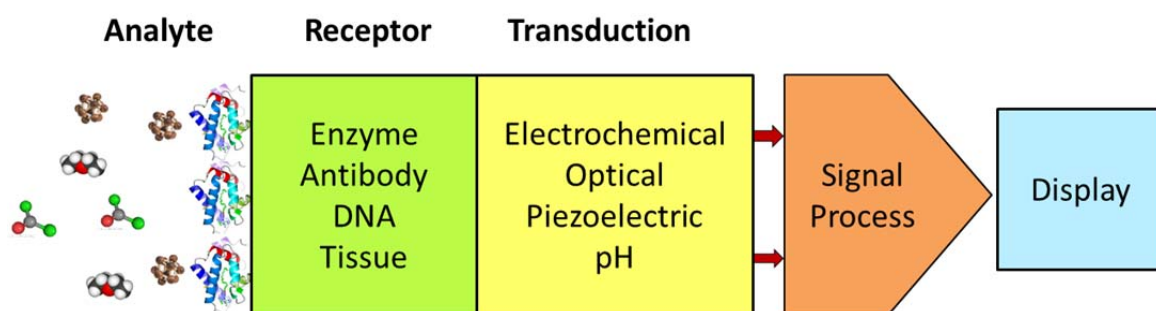


Figure 65. Schematic presentation of biosensor components

5.1.2 Classification of biosensors

Since the bioreceptor and transducer are the main components of the biosensors, they are generally classified based on the type of receptor and transducer used to build the sensor [188] (Figure 66).

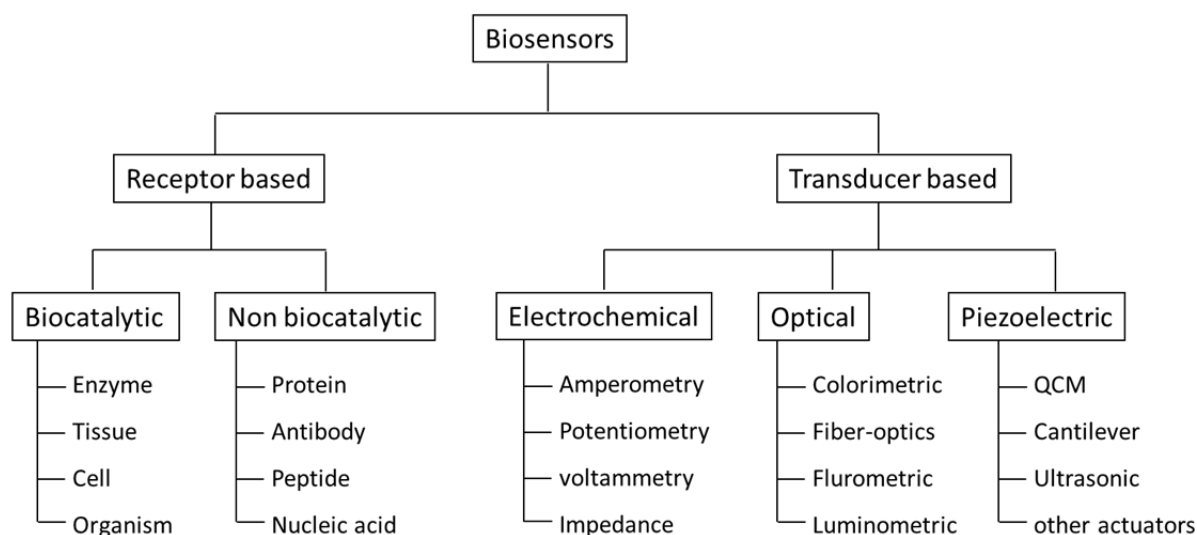


Figure 66. Classification of biosensors

5.1.3 Recognition elements: Bioreceptors

A recognition element is a biological part of the sensor which interacts with chemical analyte and produces a signal to be read by transducer. The bio-receptors can be from various biological parts of the living organisms such as cells, tissues, peptides or even organisms. All these receptors can be divided into catalytic and non-catalytic receptors based on their functions [189].

Catalytic receptors include enzymes, cells, tissues and organisms. They are employed in indirect detection sensors where the interaction between the biological component and the target analyte releases a detectable second molecule. Since the enzymes have a high level of amplification in bio-recognition processes and specific selectivity, they have been widely used as catalytic detectors.

Non-catalytic receptors, such as proteins, antibodies, nucleic acids, antibodies, DNA, etc. are very common to be used in the direct biosensors where the interaction between receptor

and analyte is monitored in real time. Antibodies are very common in use as non-catalytic receptors because of their specificity, stability and versatility.

5.1.4 Immobilization of bio-receptors

To develop an immobilization method for stabilizing of biomolecules to the surface of the transducer is one of the important factors in the construction of a biosensor. The method should be easy to implement, should not change the activity or function of the biomolecules and offer long term stability to the bioactive layer even in different environmental conditions [189]. The bio-recognition elements of the biosensor and transducer can be coupled together in one of the four possible ways that are schematically shown in Figure 67: 1) Membrane entrapment, 2) physical or chemical adsorption, 3) matrix entrapment/porous encapsulation, and 4) covalent bonding. The method to be selected for immobilization is generally based on the chemical or structural nature of the biomolecules, sensor surface or matrix, purpose of the sensor, etc.

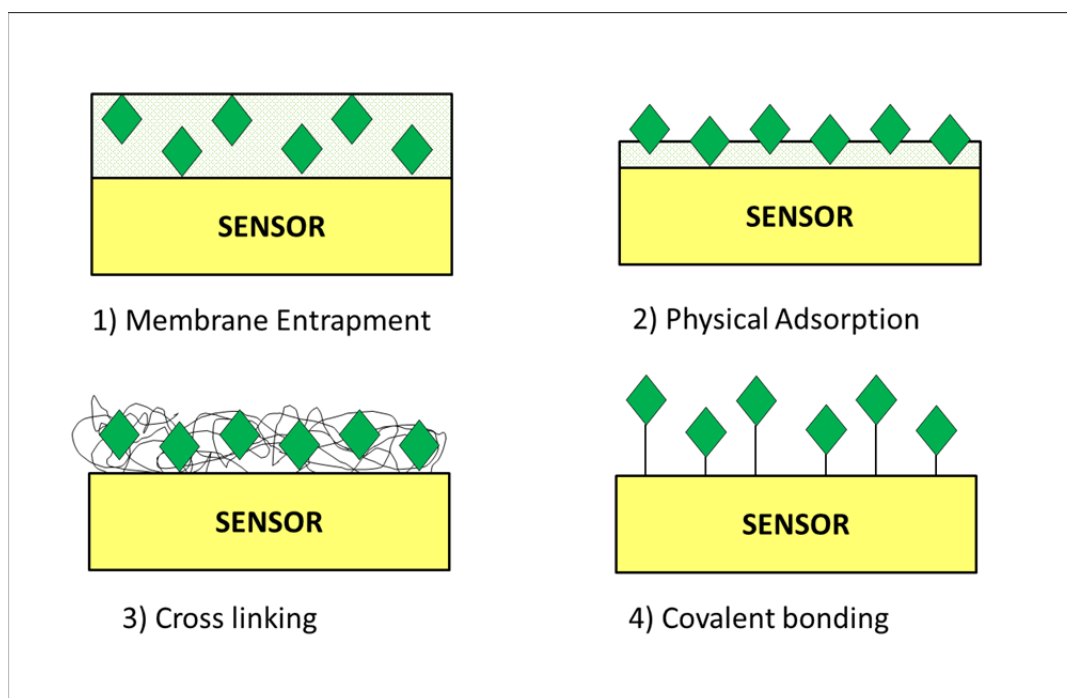


Figure 67. Schematics of different methods for biomolecule deposition

Membrane entrapment: Entrapment of biomolecules or enzymes in the polymeric gels or surfactant matrices has been used widely in the past [190]. Polymers such as polyvinyl alcohol, polyvinyl chloride and polycarbonate are generally used in this method. Loss of activity due to leakage of biological species is a major limitation of this method.

Physical adsorption: This is very simple and easy method to deposit biomolecules onto solid surface. The solution of biomolecules is just dropped onto electrode surface. Natural evaporation of solvent leaves behind the bio-molecular layer. Adsorption of biomolecules takes place via either chemical bonding or physical adsorption involving Van der Waal's forces, ionic bonding or hydrophobic forces, etc. [191].

Cross coupling: Cross linking of bio-molecules using multi-functional group reagents is another method of immobilization. Glutaraldehyde is the most common cross linking agent used in biosensor applications. This method has many limitations like loss of activity, diffusion, etc. [192].

Covalent bonding: In covalent immobilization method, biomolecules are attached to the surface of the transducer by covalent bond. The structural analysis of biomolecules such as OBPs and enzymes reveals that, they have many different functional groups in their structures e.g. amino group, carboxylic acid group, sulfhydryl group, which can be used for covalent immobilization. The functional group involved in the immobilization should not reduce the activity of the biomolecules. Metal surfaces such as gold or silver can be modified by reaction with hydroxyalkanethiols to generate hydroxyl, carboxyl or amino groups which may react with enzymes and proteins [193]. The hydroxyalkanethiols forms a well-ordered assembly on the metal surface and offers sites to OBPs to connect through a covalent bond formation. This technique is called as self-assembled monolayers (SAMs) method.

Sulfides (R-S-R), disulfides (R-S-S-R) and thiols (R-SH) are strongly adsorbed on gold, platinum and silver layers and provides a strong platform for the formation of monolayers [194]. Gold is a metal very commonly used for growing SAMs since gold thin film can be obtained by thermal evaporation, they are easy to clean and inert in atmospheric gases. Thiols are chemisorbed on gold through the oxidation of S-H bond, followed by reductive elimination of hydrogen and formation of thiolate ions. The adsorption of disulfides is due to simple oxidation of the S-S bond on the gold surface. Alkylthiols used in SAM often carry carboxylic acid functional groups which can be activated by carbodiimide and forms stable amide bond with an amino group of protein. This method offers the bio-molecular sensing layer with great uniformity and stability. It does not make any aggregation, diffusion or inactivation of biomolecules on the metal surface.

5.1.5 OBPs as bio-receptors

For the survival of most animals and insects it is necessary to detect the chemical signals in the environment which provides the information about food, danger, predator, mate, etc. Animals have highly developed olfactory system which can distinguish thousands of diverse volatile compounds. In insects and vertebrates, the olfactory neurons are separated from the air by a protective layer of hydrophobic secretion, nasal mucus and sensillar lymph resp. To reach the olfactory receptor neurons the odorants have to cross the hydrophilic barrier. The sensillar lymph and nasal mucus of vertebrates contain large amounts of small soluble proteins called odorant binding proteins (OBPs), which specifically and reversibly bind odours or pheromones [195].

Odorant binding proteins belongs to the family of proteins called lipocalin which act as a carrier for small lipophilic molecules in other body fluids. The structural analysis reveals that OBPs contain polypeptide chain folded into eight anti-parallel β -sheets with α -helical domain located near the carboxyl terminal. The β -sheets continuously form a β -barrel by hydrogen bonding and can carry odorant molecule in it. Several distinct OBPs have been identified and each OBP has unique ligand binding profile. Based on the diversity of OBPs, it seems that they are involved in preselecting those volatile compounds which finally interact with olfactory sensory cells [196].

Porcine-OBPs as bio-receptors: Odorant binding proteins of vertebrates, porcine OBPs were investigated as possible choice as sensing layer for biosensor. Porcine OBP is a monomer of amino acids and shows wide specificity towards medium size hydrophobic molecules such as alkyl substituted pyrazines and thiazoles (Nutty to green smelling derivatives), terpenoids such as menthol & thymol and medium size alcohols and aldehydes [197-199]. Pig OBP binds these odorants by weak Van der Waal forces.

Two mutated porcine OBPs, pig OBP-C and Pig OBPM2 were studied as possible bio-sensitive material. The pig OBP-C has additional cysteine group at position 2 which makes the covalent immobilization of proteins easier onto gold electrode surface. This protein shows good affinity to several aromatic compounds e.g. 2-isobutyl-3-methoxypyrazine. Pig OBPM2 has tryptophan at the place of phenylalanine 88. The three dimensional structures of both the OBPs are given below (figure 68).

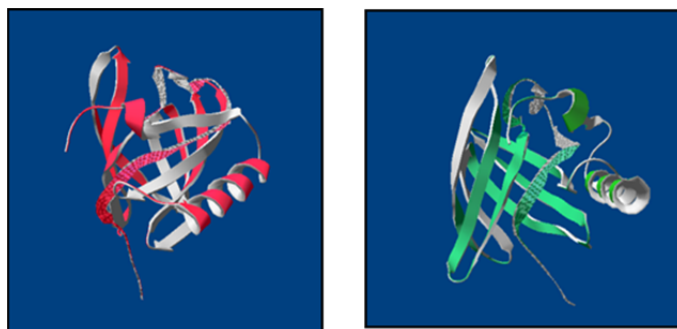


Figure 68. 3D structures of Porcine OBP-C and OBP-m2 (Pictures from Tuccori, E. The University of Manchester, UK)

5.1.6 Electrical characterization by Kelvin probe method

The sensors are characterised by exposing them to wished chemical analytes. Upon interaction, the physical or chemical parameters of the sensors such as work function, resistance, capacitance, photoluminescence, etc. are changed. Among these, work function measurement by kelvin probe method is very sensitive and well known method of characterization of sensors.

In 1861, William Thomson, the renowned Scottish scientist and Professor of natural philosophy at the University of Glasgow, firstly employed capacitor technique to measure the change in the work function of metals and the semiconductors. The original apparatus used by Lord Kelvin is given in figure 69.

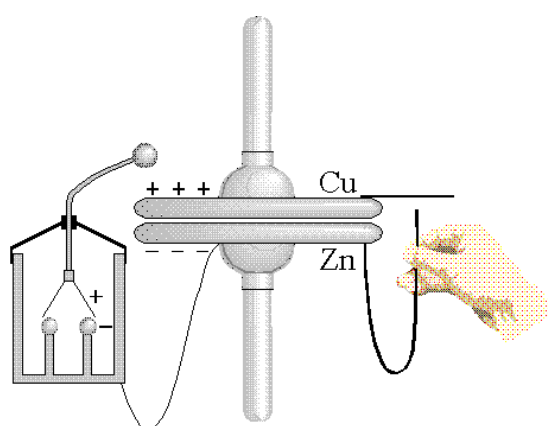


Figure 69. The original apparatus used by Lord Kelvin

The Kelvin Probe is an extremely sensitive, non-contact, non-destructive measurement device used to investigate properties of materials. It is based on a vibrating capacitor electrometer which measures the contact potential difference between the reference material and a sample with a resolution of $\sim 1\text{mV}$.

Work Function: The work function is described as “the least amount of energy required to remove an electron from conducting material to a point just outside of its surface with zero kinetic energy known as vacuum level.” When an electron moves through the surface region, its energy is influenced by the characteristics of the region. The ab/adsorption of gases or other species, surface contamination, surface charging, etc. may induce substantial variation of the energy required to remove an electron from the Fermi level [200]. Therefore, work function is an extremely sensitive indicator of surface condition. This advantage of Kelvin probe can be used to for evaluation of Pig-OBP sensors. The interaction of biological receptors with target analyte or any other species can bring changes in material work function if conducting or on the metallic electrode is insulating.

Technique/Operation: Kelvin Probe (KP) measures the contact potential difference (CPD) when two conducting materials with different work functions are brought together by an external wire contact, electrons in the material with a lower work function flow to the one with a higher work function. If these materials are made into a parallel plate capacitor, equal and opposite surface charges forms. Measuring the contact potential is then very simple: an external potential is applied to the capacitor until the surface charges disappear, and at this point the external potential equals the contact potential.

The traditional Kelvin Probe method consists of two electrodes: flat circular electrode or vibrating reference electrode hanging above and parallel to a stationary electrode e.g. sample with pig-odorant binding proteins immobilized on it and thus creating a simple capacitor. The figures 70A to 70C show various electron energy diagrams for two conducting specimens.

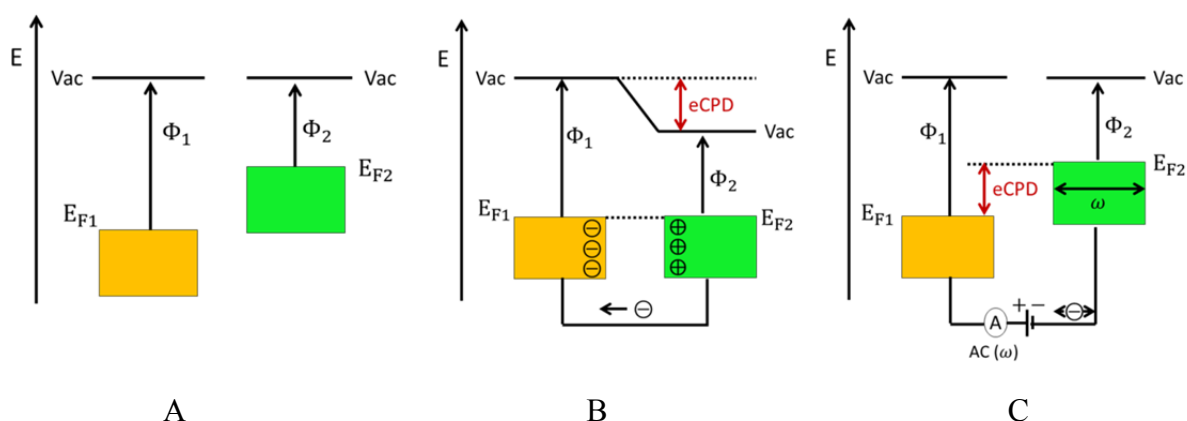


Figure 70. Electron energy diagrams

Figure 70A: The electron energy level diagram shows two separated metals without any electrical contact between them. Their vacuum levels are aligned but Fermi levels not, because of the different nature resulting in different work functions. In the figure Φ_1 and Φ_2 and E_{F1} & E_{F2} designate work functions and their Fermi levels respectively.

Figure 70B: When both metals are connected by an external electric wire then their Fermi levels equalises due to the flow of the electrons from the metal with the smaller work function to the metal with the larger work function. Then metal with large work function charges negatively whereas metal with smaller work function positively. The equally but oppositely charged metals develop an electrical potential gradient. As soon as the electric field compensates for the work function difference, the electron transfer process stops. In this equilibrated state, the potential associated with the electric field exactly equals CPD between the two metals.

Figure 70C: The gradual application of a counter potential (V_b) to the CPD and monitoring the charge on one of the metals allows the determination of charge free point where the average electric field vanishes, resulting in a null output signal. The counter potential V_b that achieves this state is exactly -CPD.

Practically, in the Kelvin probe one of the electrodes is vibrated at a certain frequency ω and using a lock-in amplifier, the AC (ω) current generated by the oscillation is monitored. The current appears because capacitor charge has to adjust itself to the instant value of the capacitance (electrode distance) the potential on the capacitor being just the CPD, which is constant or almost constant on time intervals of the order of $1/\omega$. Slowly tuning of the

counter potential and finding zero AC current yields CPD. Since small currents are difficult to detect, usually an I/V curve is measured and the I=0 point is found through a curve fit.

By using a vibrating probe, a varying capacitance is produced. This is given by:

$$C = \frac{Q}{V} = \frac{\epsilon_0 A}{d}$$

Where C is the capacitance, Q is the Charge, V is the Potential, ϵ_0 is the permittivity of the dielectric (in an air probe the dielectric is air). A is the surface area of the capacitor and d is the separation between the plates. Therefore, as the separation d increases the capacitance C decreases. As the voltage remains constant, the charge must change.

5.2 Materials and methods

All chemicals and reagents used were purchased from Sigma-Aldrich and were used as received. The porcine odorant binding proteins, Porcine-OBP m2 and Porcine-OBP C used for fabrication of biosensors were provided by The University of Manchester (UK). Unless and otherwise stated, all the procedures were carried out at room temperature.

5.2.1 Immobilization of Pig-OBPs

Among the various possible methods for immobilization of OBPs, physical immobilization and covalent immobilization-self assembled monolayer (SAM) method were chosen. Two different pig OBPs used in the present studies are Pig OBP-C and Pig OBP-m2. In order to ensure proper immobilization of OBPs, the gold surface was cleaned by rinsing with absolute ethanol and double distilled water, in case of new gold electrodes whereas the used electrodes were cleaned by dipping the electrode in the piranha solution (3:1=H₂SO₄: 30% H₂O₂) for a couple of minutes to remove all organic residues from the surface.

5.2.1.1 Covalent Immobilization-SAM method

Thioctic acid (0.1M) solution in absolute ethanol was dropped on the surface of the electrode repeatedly at every 20 minute for 2 hours and then gold electrode was washed gently with distilled water and dried in the air. The carboxylic acid group of thioctic acid was activated by 20 μ L solution consisting of a mixture of Ethyl(dimethylaminopropyl)carbodiimide (EDC) (0.3M) and N-hydroxysuccinimide (NHS) (0.6M). The solution was placed over the electrode for 2 hours and then gently rinsed with distilled water and dried in the air. OBPs were immobilised on the activated SAM layer by placing the 10 μ g OBP solution onto the gold surface for 1 hour. The surface was rinsed with distilled water and dried in the air.

5. Biosensors based on Pig-odorant binding proteins (OBPs)

The process and possible detailed reaction mechanism involved in the immobilization of OBPs via SAM method is shown in figure 71 and figure 72 respectively. The covalent immobilization method is very reliable and widely used for OBP immobilization on gold electrodes.

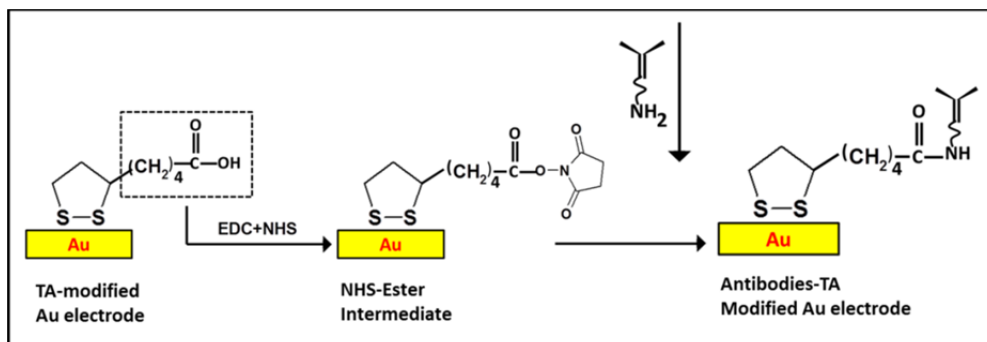


Figure 71. Immobilization of OBPs by SAM of thioctic acid

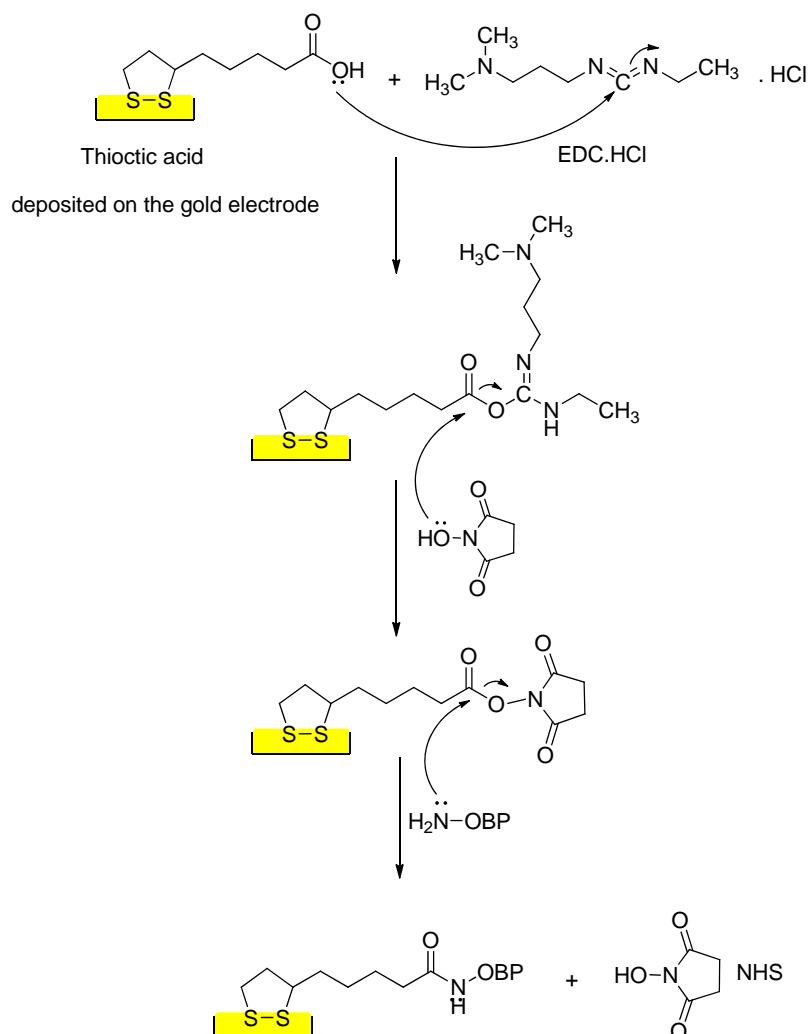


Figure 72. Possible reaction mechanism-covalent immobilization of OBPs on gold electrode

5.2.1.2 Physical Immobilization

In this simple method, OBPs are just spread over the electrode surface. The Pig-OBP-C was immobilized by this method on the gold electrode surface. The proteins are mutated at the amine terminal by adding a cysteine. The immobilization was carried out by spreading 5 μ L of proteins (2.3 mg/mL) onto gold surface. The proteins were added at every two hours four times and then surface was rinsed with distilled water and dried at room conditions. This method forms a stable bond between the thiol of the cysteine and gold surface.

5.2.2 Exposure of the OBPs to pyrazine using gas mixing system

As explained in the section 2.2.6, a GMMS system was used for characterization of pig-OBPs sensors where desired analyte was delivered to the sensors. To avoid the effect of not only chemical composition of environment but also temperature and light, the Kelvin probes were kept in controlled atmospheric conditions.

The sensors, pig-OBP-C and Pig-OBP-m₂ were measured against different concentrations of 2-isobutyl-3-methoxypyrazine with the background of different relative humidity levels. The 2-isobutyl-3-methoxypyrazine was dosed in ascending and descending concentrations as 0, 2, 5, 10, 20, 30, 20, 10, 5, 2, 0 ppm. The complete set of concentrations was repeated with the background of 0 (dry air), 20, 40, and 60% relative humidity.

5.2.3 Kelvin Probes

The Pig-OBP-C and Pig-OBP-m₂ were measured against 2-isobutyl-3-methoxypyrazine using two kelvin probes simultaneously, one for sensor and another for reference. The passivated sample was made by coating boron nitrite over a metallized substrate and used as reference. The heads of the Kelvin probes used for the measurements are given in figure 73. Two versions of electronics named Kelvin probe 05 and Kelvin probe 07 were used for this study.

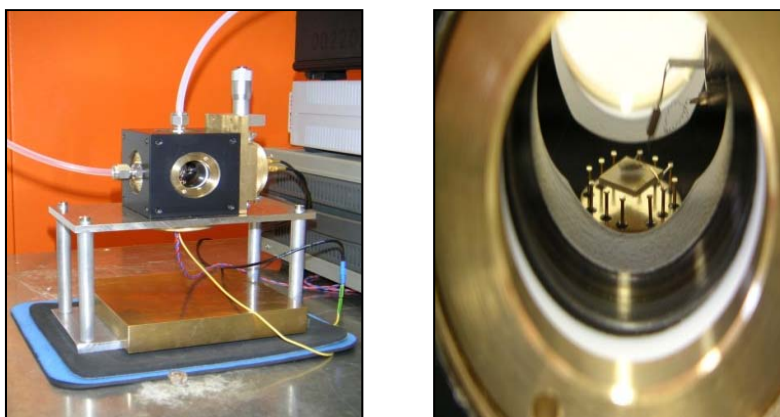


Figure 73. Pictures of heads of Kelvin probe used in the study

5.3 Results and discussion

5.3.1 Data evaluation

Two Kelvin probes were simultaneously used to characterise the prepared biosensors. The measurements were carried out with interchanging of the sample and reference between two Kelvin probes. E.g. in first measurement, Kelvin-05 has sensor and Kelvin-07 has reference then in second measurement Kelvin-05 has reference and Kelvin-07 has sensor. The response given by each sensor in both kelvin probes was calculated separately. The actual response of each sensor was obtained by subtracting the reference signal from sensor signal (figure 74).

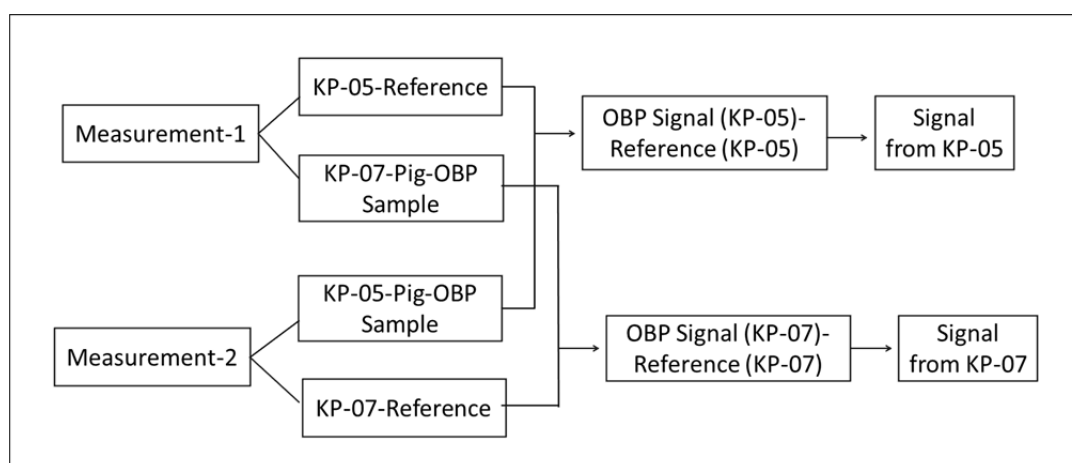


Figure 74. Graphical representation of data evaluation where sensor is measured using two Kelvin probes

5. Biosensors based on Pig-odorant binding proteins (OBPs)

Figure 75 shows Pig-OBP-c (Pig-OBP-4) sensor and reference measured in Kelvin probe-05 with different concentration of pyrazine vapour with variable percentage of relative humidity in background. The signal of both OBP sensor and reference at 0% relative humidity is magnified in order calculate contact potential difference (CPD).

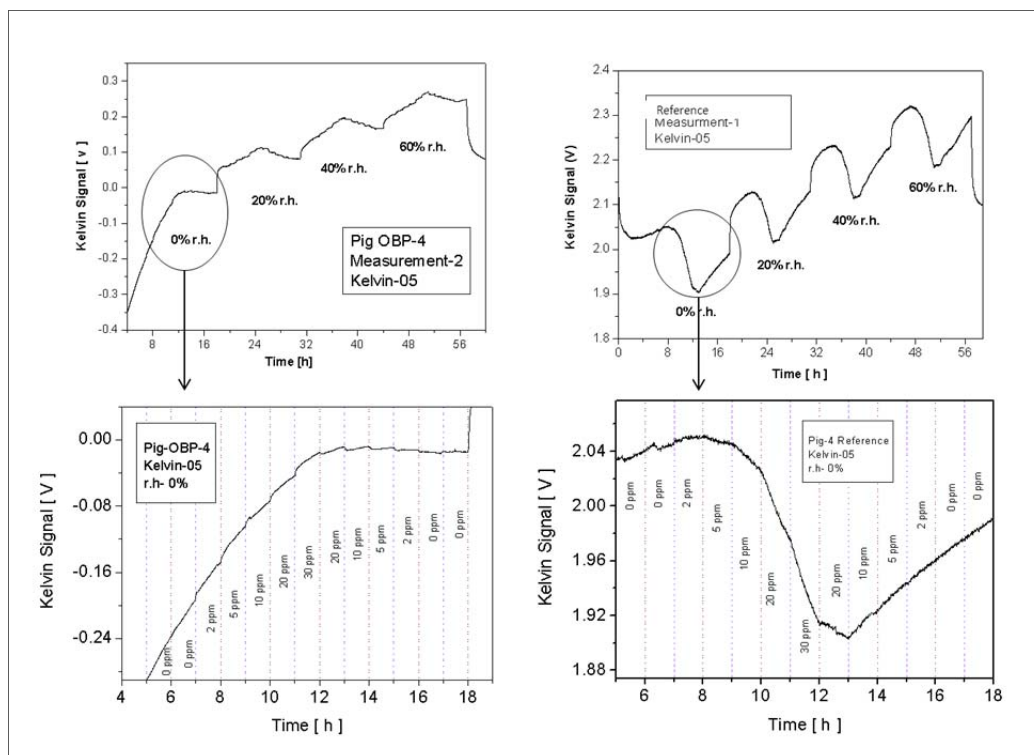


Figure 75. Unprocessed data obtained for Pig-OBP-4 and reference in Kelvin probe-05

The subtraction of reference signal (Kelvin-05) from pig-OBP-4 sensor signal (Kelvin-05) against different concentrations of pyrazine gas with no humidity in background is shown in figure 76.

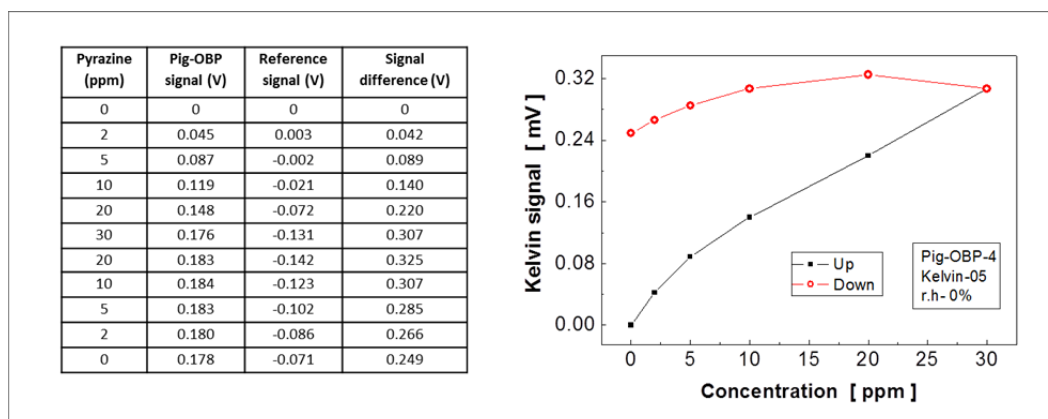


Figure 76. The response of pig-OBP-4 sensor against pyrazine vapour

5.3.2 Measurement of pig-OBP-c sensor

As shown above, responses of Pig-OBP-C against 2-isobutyl-3-methoxypyrazine with the background of 0, 20, 40, 60% relative humidity using Kelvin probe-05 and Kelvin probe-07 were obtained (figure 77). The sensor measured in both kelvin probes kelvin-05 and 07 shows similar response, near about 150 mV.

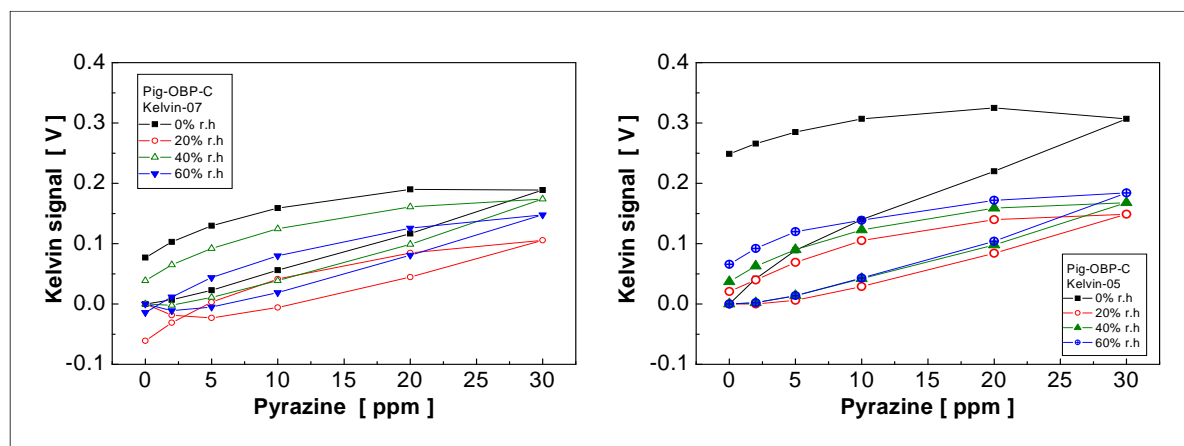


Figure 77. Response of Pig-OBP-C sensor against pyrazine vapour with different humidity levels in background, measured by Kelvin probe-07 (left) and Kelvin probe-05 (right)

5.3.3 Measurement of Pig-OBP-m2 sensor

The response of Pig-OBP-m2 sensor with 2-isobutyl-3-methoxypyrazine recorded using both Kelvin probe-05 and Kelvin probe-07 is shown in figure 78. This sensor showed similar signal intensity in both the Kelvin probes, which is nearly 150 mV.

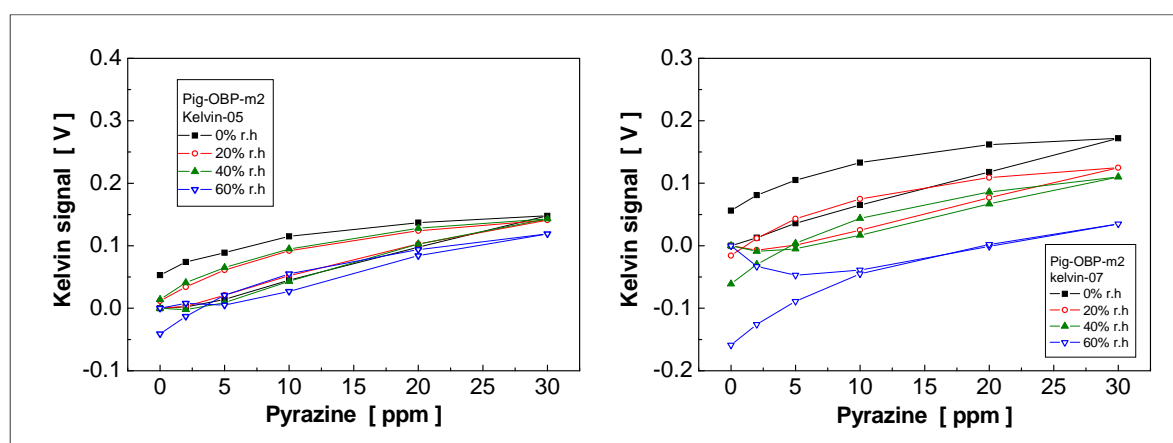


Figure 78. Response of Pig-OBP-m2 sensor against pyrazine gas with different humidity levels in background, measured using Kelvin probe-05 (left) and Kelvin probe-07 (right)

5.3.4 Response of gold electrode with 2-isobutyl-3-methoxypyrazine

In order to be sure about the pig-OBP response, gold electrode used for OBP immobilization was measured with 2-isobutyl-3-methoxypyrazine with same parameters used for pig-OBP sample measurement. The response given by gold electrode with pyrazine gas is shown in the graphs in figure 79. It seems that gold electrode is strongly responding to pyrazine vapour and the intensity of the signal is nearly equal to that of Pig-OBP samples.

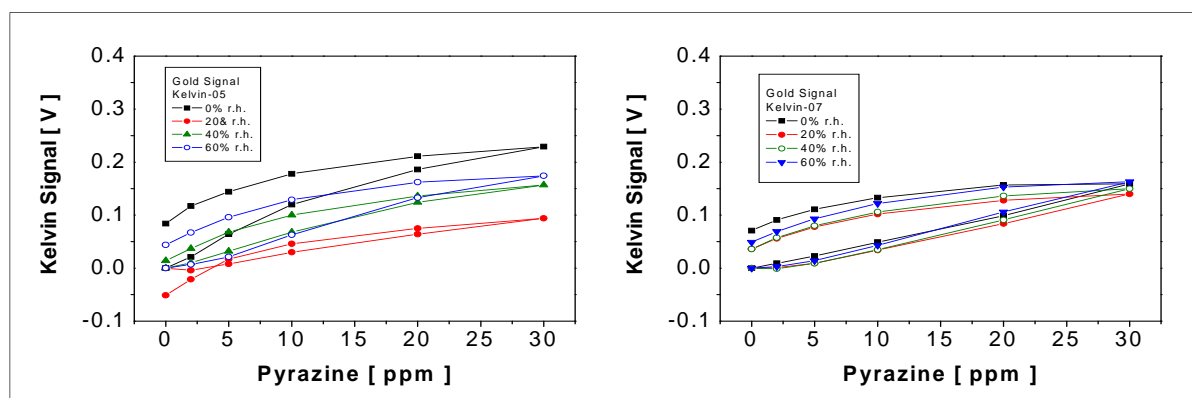


Figure 79. Response of gold electrode (used for sensor fabrication) against pyrazine gas with different humidity levels in background, measured using Kelvin probe-05 (left) and Kelvin probe-07 (right)

5.3.5 Actual response of Pig-OBP sensors

The actual sensor response is obtained by subtracting the gold electrode signal from pig-OBP sample. The graph shows very small response from OBP and most of the response is coming from gold electrode (Figure 80 and 81). From all the measurements it seems that gold is showing strong non-specific interaction with pyrazine vapour.

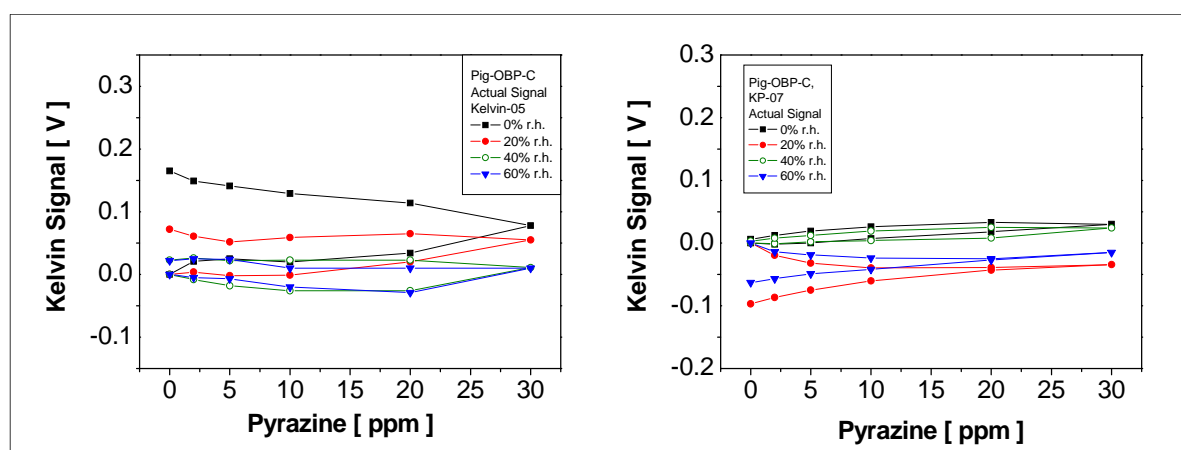


Figure 80. Actual response of Pig-OBP-C sensor against 2-isobutyl-3-methoxypyrazine with different humidity levels in background, measured using Kelvin probe-05 (left) and Kelvin probe-07 (right)

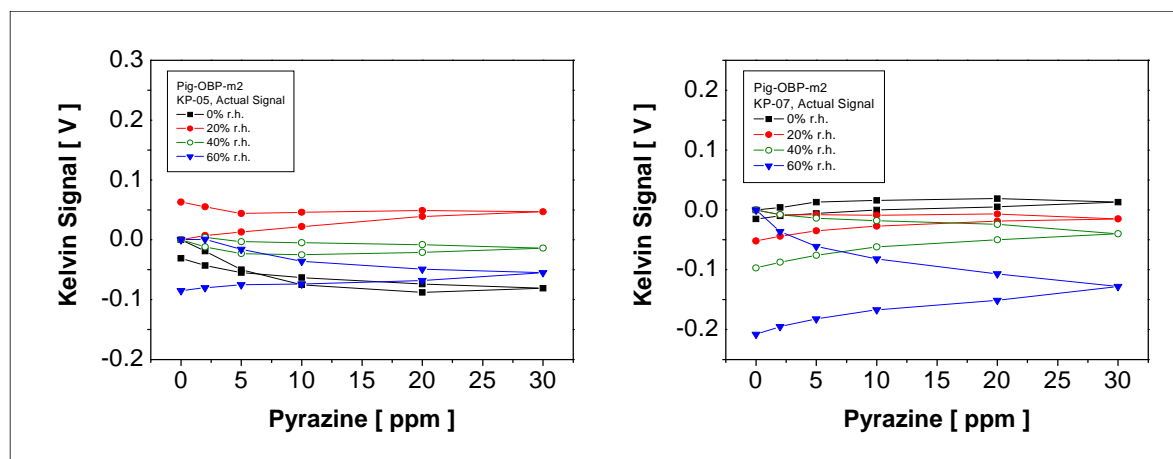


Figure 81. Actual response of Pig-OBP-C sensor against 2-isobutyl-3-methoxypyrazine with different humidity levels in background, measured by Kelvin probe-05 (left) and Kelvin probe-07 (right)

5.3.6 Adsorption of pyrazine gas at gold electrode surface

Above measurements has shown that the gold electrode used for pig-OBPs deposition is showing quite strong interaction with pyrazine vapour. The adsorption of organic compound from solution onto an electrode is rather complex process and involves direct interaction of the adsorbed molecules with the metal electrode surface, interaction with the solvent molecules, displacement/substitution of the previously adsorbed molecules and lateral interaction between the adsorbate molecule and their modified cospheres [201]. The adsorption is controlled by competition between the forces involved in the metal-solute and metal-solvent interactions. In any adsorption process not only the interaction between metal and solute & solvent occurs but also the electronic factor plays an important role; the electric field may considerably influence the metal as well as the adsorbate electronic states bringing changes in the adsorption energetics [202].

The chemisorption process taking place at the metal surface vapour interface can be described with the simplest model usually used considering the metal surface-adsorbate interaction in terms of simple Lewis acid-base chemistry [202]. As far as 2-isobutyl-3-

methoxypyrazine adsorption onto gold is concerned, the molecule has two nitrogen atoms with lone pair of electrons can act as an electron donor whereas the gold metal as acceptor. The pyrazine molecule can adsorbed on gold with one nitrogen atom in vertically directed and second the nitrogen atom can participate to the formation of hydrogen binding with solvent molecules [203].

5.4 Conclusion

The work has explored the possibility of use of porcine odorant binding proteins (OBPs) as possible bio-receptor material for real sensing applications to detect volatile organic compounds such as 2-isobutyl-3-methoxypyrazine.

Two different Porcine OBPs (Pig-OBP-c & Pig-OBP-m2) were immobilized onto gold electrodes by physical adsorption and covalent immobilization (self-assembled method) respectively. The sensors were characterized against 2-isobutyl-3-methoxypyrazine as work function change. This work has shown that biosensors based on odorant binding proteins can be measured by using Kelvin probe method. Pig-OBP-c and Pig-OBP-m2 showed some affinity for 2-isobutyl-3-methoxypyrazine therefore such biosensors can be used to detect small hydrophobic molecules like pyrazine and thiophene. A non-specific interaction of 2-isobutyl-3-methoxypyrazine with gold electrode surface was observed which shows large work function change. The non-specific interaction of pyrazine and gold electrode surface can be avoided by an adequate coverage with OBPs.



6. Conclusions and Future work

6.1 Conclusions

The aim of the work was to carry out synthesis of a series of conducting polymers / copolymers and to investigate their characteristics as chemical gas sensor materials. The work was performed within the frame of the Marie Curie Action European Union project “FlexSmell”. The project aimed the development of flexible multisensing RFID system for perishable goods monitoring during their logistics and transportation.

The development of conducting polymers included the synthesis of a series of 2, 5-di(thiophen-2-yl)-1*H*-pyrrole (SNS) monomers, their chemical and electrochemical polymerization, characterization of the resulted polymers. The SNS monomers have different substituents on the aromatic ring attached to central pyrrole N-atom. They are of electron donating or withdrawing nature, and halogen atoms of different electronegativity such as F, Cl, Br or I. The monomers with different substituents in their structures were chosen in order to study the effects of these substituents on the properties of the resulting polymers. The synthesis of SNS monomers using long chain alkyl substituted thiophenes (e.g. 3-hexylthiophene) was also attempted but later discontinued due to difficult purification and poor yields of the product.

The prepared SNS monomers were successfully polymerized by both chemical and electrochemical polymerization methods. The protocol for both polymerization methods was successfully developed in terms of suitable dopant/counter ion, concentrations of monomer and oxidant etc. The electrochemical polymerization was performed by anodic deposition of thin or thick polymer layers onto gold working electrodes. The SNS polymers prepared were thoroughly studied for their optical, electrochemical, thermal and electrical properties. The SNS polymers studied for their optical properties clearly showed absorption bands for π - π^* transition and for polaron and bipolaron conductive states. It was confirmed by FTIR spectroscopy that polymerization of SNS monomers takes place through α -H coupling of external thiophene rings. The thermo gravimetric analysis confirmed the polymer suitability even at high temperature. The electrical conductivity of the polymers is correlated with the nature and character of the substituents attached on the N-substituted aromatic ring.

The chemical gas sensing ability of the prepared SNS polymers was studied using two methods, a) by making pressed pellets of the chemically prepared polymer powders. The pellets characterized by exposing to different relative humidity levels and ammonia concentrations showed linear increase in their resistances with the concentrations of the

analytes. b) the flexible chemoresistive sensors were fabricated by electrochemical deposition of polymer layers onto IDE transducers and characterized by exposing to different relative humidity, ammonia and ethanol concentrations. They also showed linear responses with the concentration of these analytes. In spite of moderate sensitivities of the SNS polymers, they could be used for chemical gas sensor applications.

After successful synthesis of SNS monomers and their polymers, the preparation of copolymers based on SNS monomers and dialkylbithiazoles were attempted. The synthesis of the copolymer was attempted with the intention of bringing solubility to the polymer materials in common organic solvents in order to effectively use them in the fabrication of the sensors. Therefore, bithiazoles with long chain aliphatic substituents such as n-octyl and n-decyl groups were prepared. Dialkylbithiazoles were chosen also to improve the environmental stability of the copolymer. The synthesis of dialkylbithiazoles was obtained successfully but it was not possible to put them together with SNS monomers, mainly due very critical reaction conditions.

The aim of the FlexSmell project was achieved through collaborative work with other partners. The flexible multisensor platforms developed at EPFL has two IDE capacitive devices, two IDE resistors and one RTD. The capacitive devices of the platform were successfully functionalized with cellulose acetate butyrate or polyether urethane for humidity detection at University of Tübingen and with PANi and PPy for ammonia and VOCs detection at The University of Manchester. The sensing platforms developed by EPFL were readily integrable on the RFID tag developed by another partner, Holst Centre. The complete sensing RFID system was characterized under controlled conditions, which successfully monitored the targeted parameters, relative humidity, ammonia and VOCs. Although synthesis of SNS polymers was carried out with the intentions of using them as resistive materials on the multisensor platform, it was not possible due to their poor solubility in common organic solvents. An electrochemical deposition of the SNS polymers onto resistive parts of the platform was attempted but large insulating gap between the printed electrodes did not allowed to form polymer to connecting the electrodes. When flexible chemoresistive sensors were prepared by electrochemical deposition of the SNS polymers onto IDE transducers, the insulating gap between neighbouring electrodes was maintained in the range of 15-20 μm (section 2.2.5.2). The drop coating method was attempted by alternating addition of monomer and oxidant solutions did not work effectively as the polymers layer developed several cracks upon evaporation of the solvent.

The porcine odorant binding proteins (OBPs) were also investigated as possible organic receptor in the construction of an intergrable biosensor. The porcine OBPs were successfully immobilised on gold substrates by physical adsorption and self-assembled monolayer (SAM) methods. The OBPs sensors characterized with 2-isobutyl-3-methoxypyrazine using the Kelvin probe method showed that pyrazine vapour's non-specific binding with gold electrode used for OBPs immobilization. The study showed that biosensors can be characterized by Kelvin probe method but the electrodes should be fully covered with OBPs to avoid interaction of pyrazine vapours with gold.

To shortly summarise, this thesis has covered number of areas such as synthesis of series of SNS monomers, their polymerization, fabrication of sensors and their sensing characterizations against number of analytes. The thesis also presented the work carried out in collaborations with the project partners towards successful development of flexible chemical gas sensing system with RFID read out, the main goal of the FlexSmell project. The work also explored the possibility to use of porcine OBPs for chemical detection using Kelvin probe method.

6.2 Future Work

The main future improvements required of the SNS polymers presented in this thesis would be their solubility in organic solvents. Due to the insolubility of the reported SNS polymers, there is not much space to choose various methods for the deposition as sensing layers. Therefore, in order to prepare soluble SNS polymers, several ways could be tried, such as:

- a) The development of new synthetic approach which will allow preparing SNS monomers with long aliphatic chain on it.
- b) Use of different dopants / oxidants
- c) Copolymerization of SNS monomers with other monomers
- d) Polymerization of SNS monomers in the presence of metal salts or nano-particles to make polymer-metal composite.

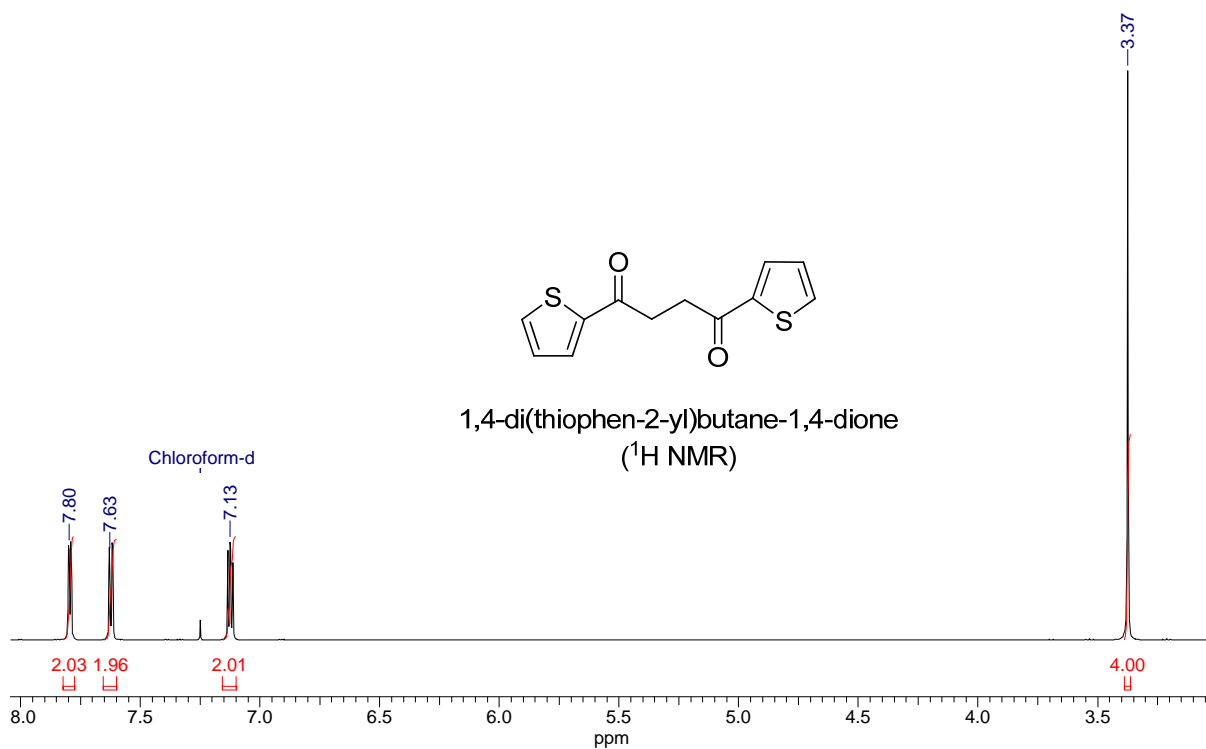
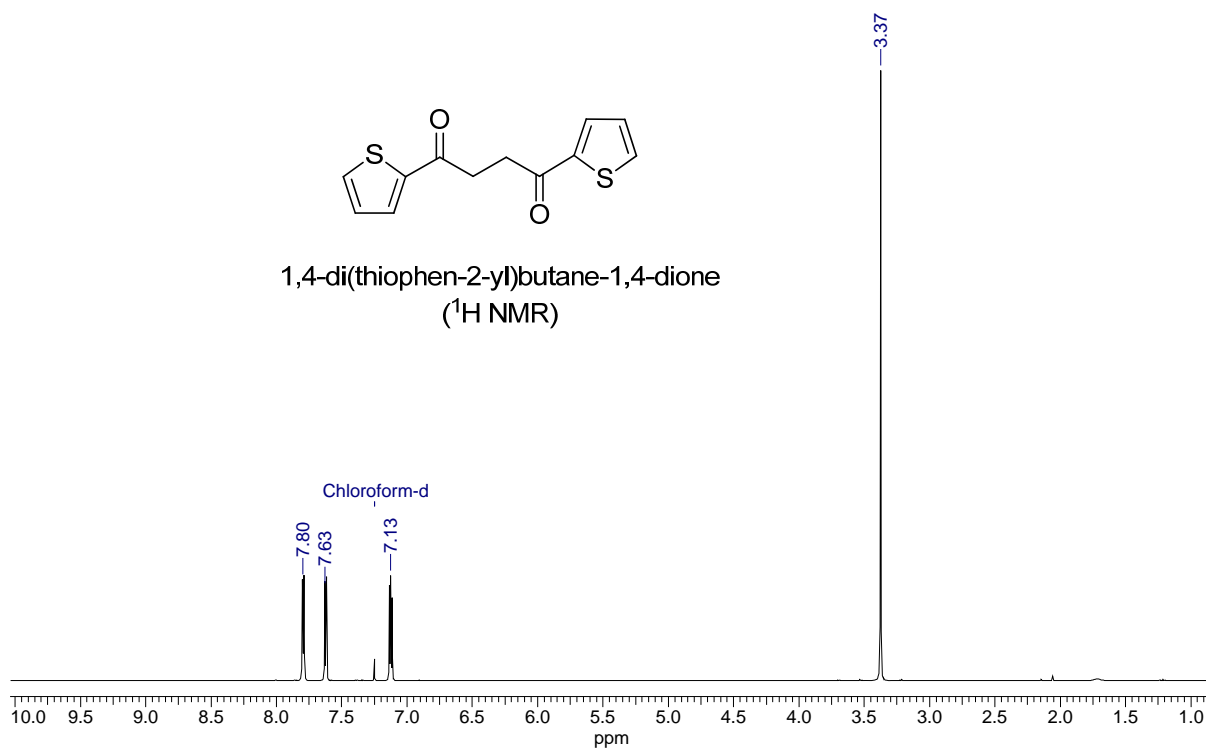
The synthesis of SNS-dialkylbithiazole copolymer was attempted for the purpose of preparing the soluble materials but was failed at the final stage because of difficulties in maintaining the critical reaction conditions. It was necessary to attach Me_3Sn groups on SNS monomers to be able to react with brominated dialkylbithiazole. The reaction of putting Me_3Sn groups on SNS is moisture sensitive and can proceed if complete dry conditions are

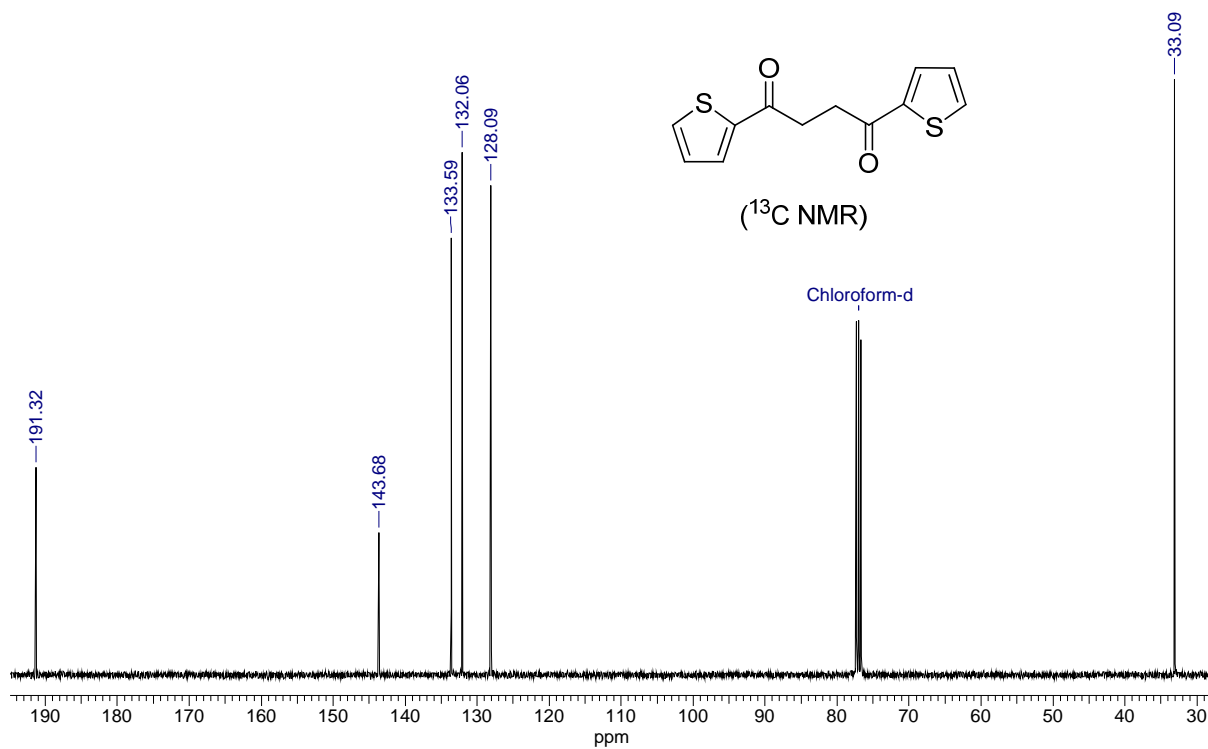
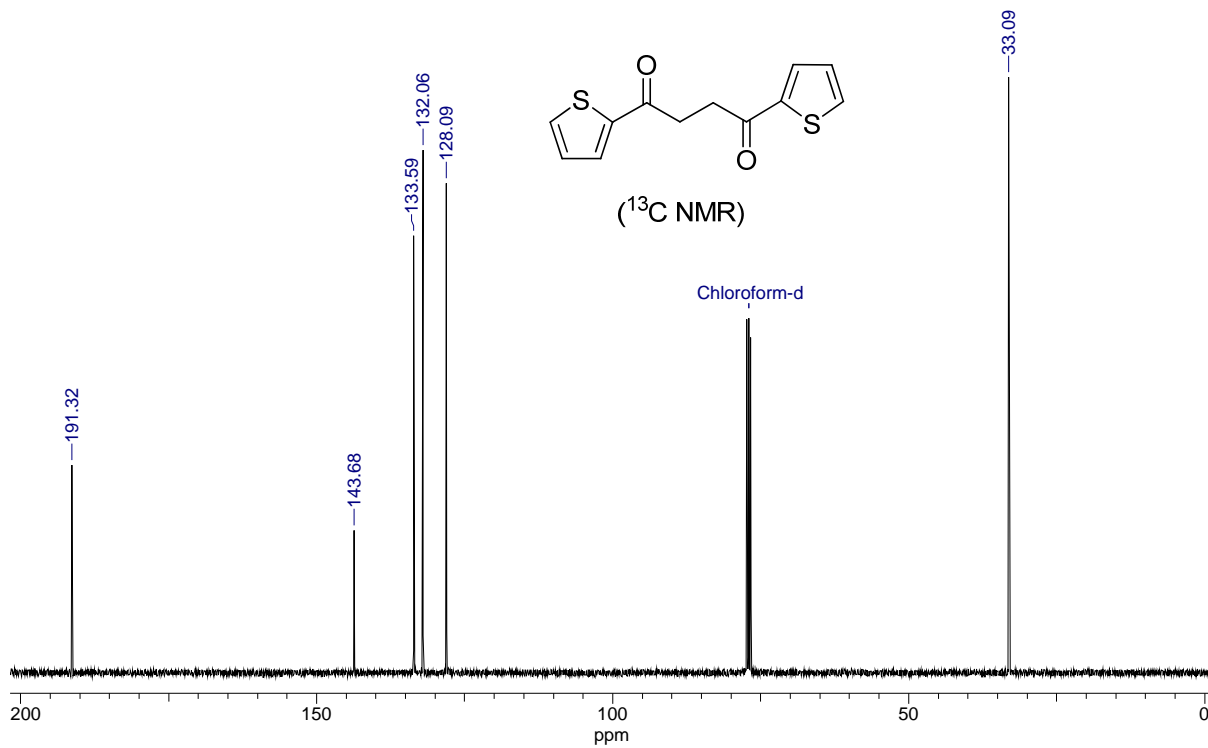
provided. This can be achieved by using freshly dried THF. For this, THF should be refluxed over sodium metal and in the presence of benzophenone as an indicator under inert conditions. Refluxing in this way, sodium metal will take out moistures dissolved in the THF giving blue/violet colouration to the solvent. Then THF should be distilled out and used within few hours. Secondly, Me_3SnCl is also moisture sensitive and need to be freshly distilled out before using it for the reaction. This reaction could proceed if THF and Me_3SnCl are freshly distilled and if the reaction is performed under completely inert atmosphere. The standardised procedures for the synthesis of SNS and dialkylbithiazole compounds is presented in this thesis but there is need of a new approach to put them together to make the targeted copolymers.

Regarding the functionalization of resistive parts of the platform with the SNS polymer layers, the platforms should be designed with the resistive IDEs having their insulating gap in the range of 15-20 μm . The electrochemical deposition SNS monomers can form layers of different thicknesses if the platforms are designed in this way.

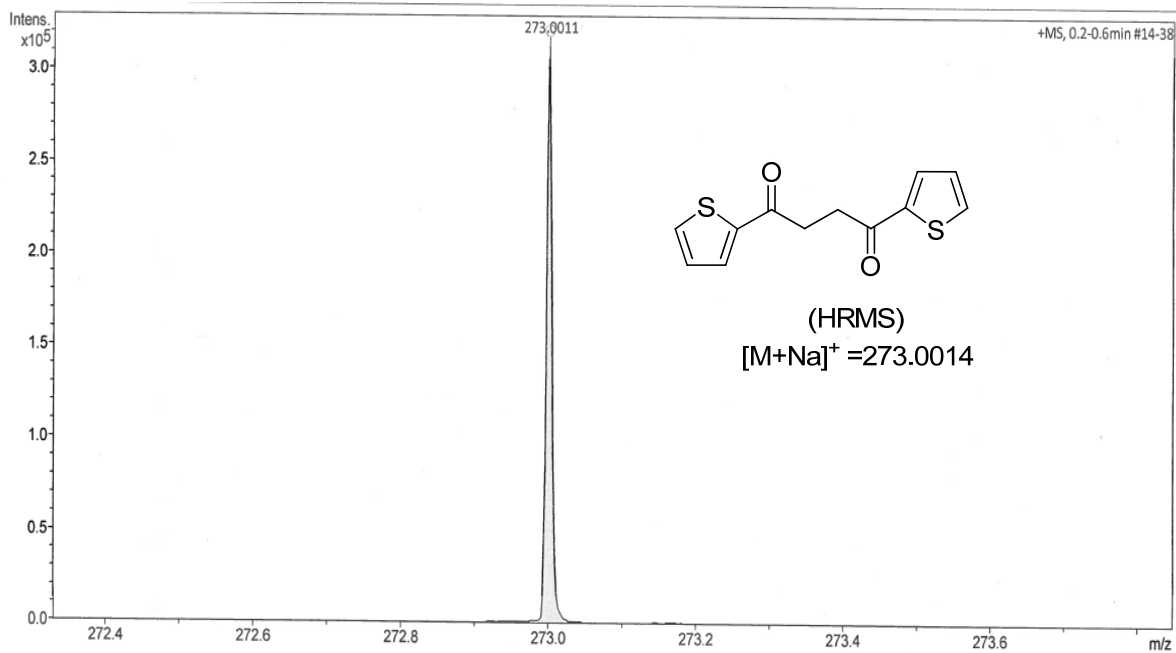
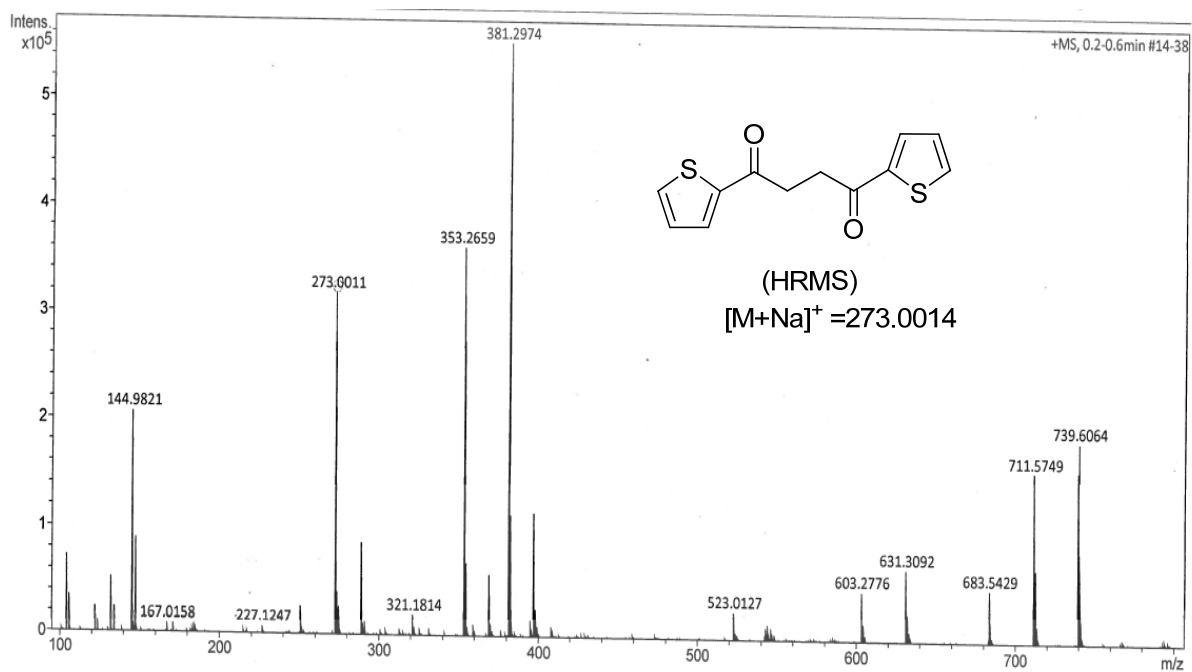
Appendix

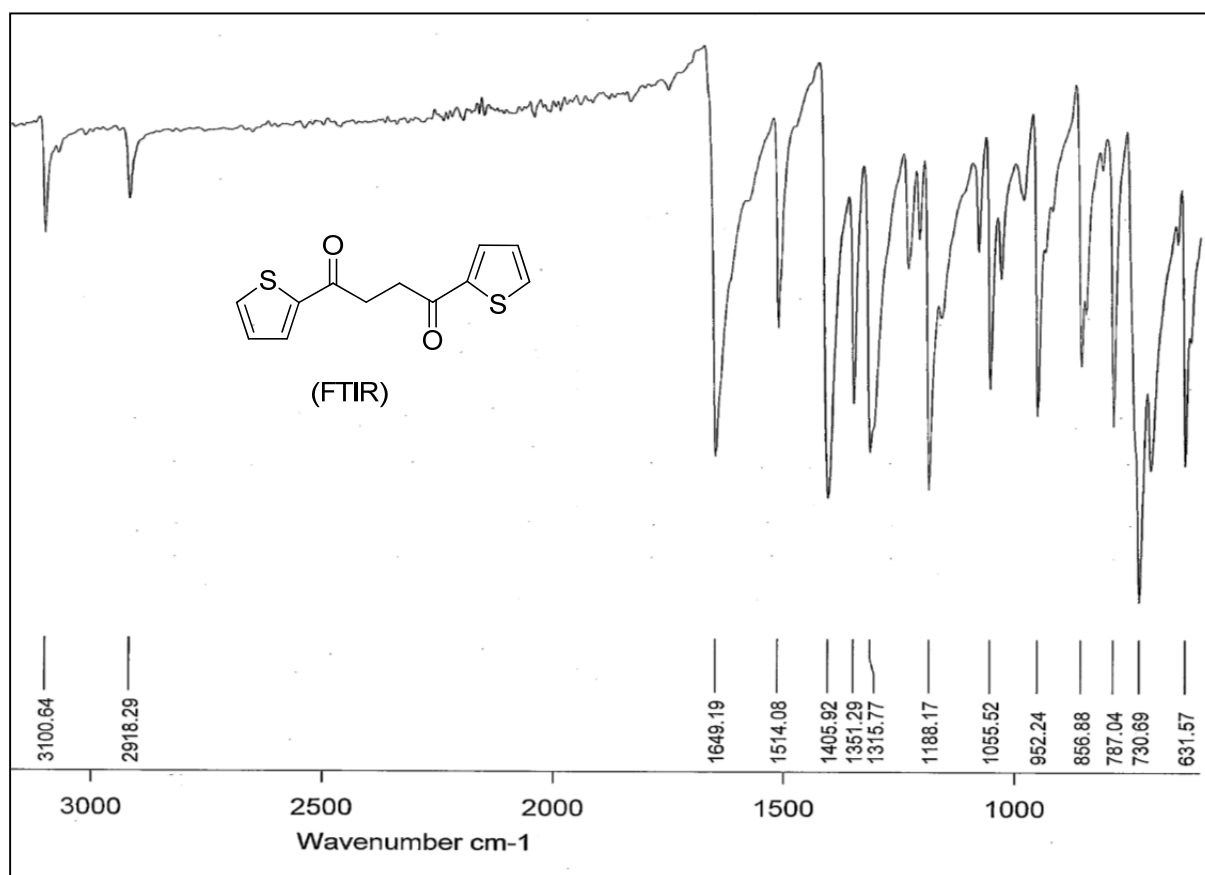
Analytical data of the compounds

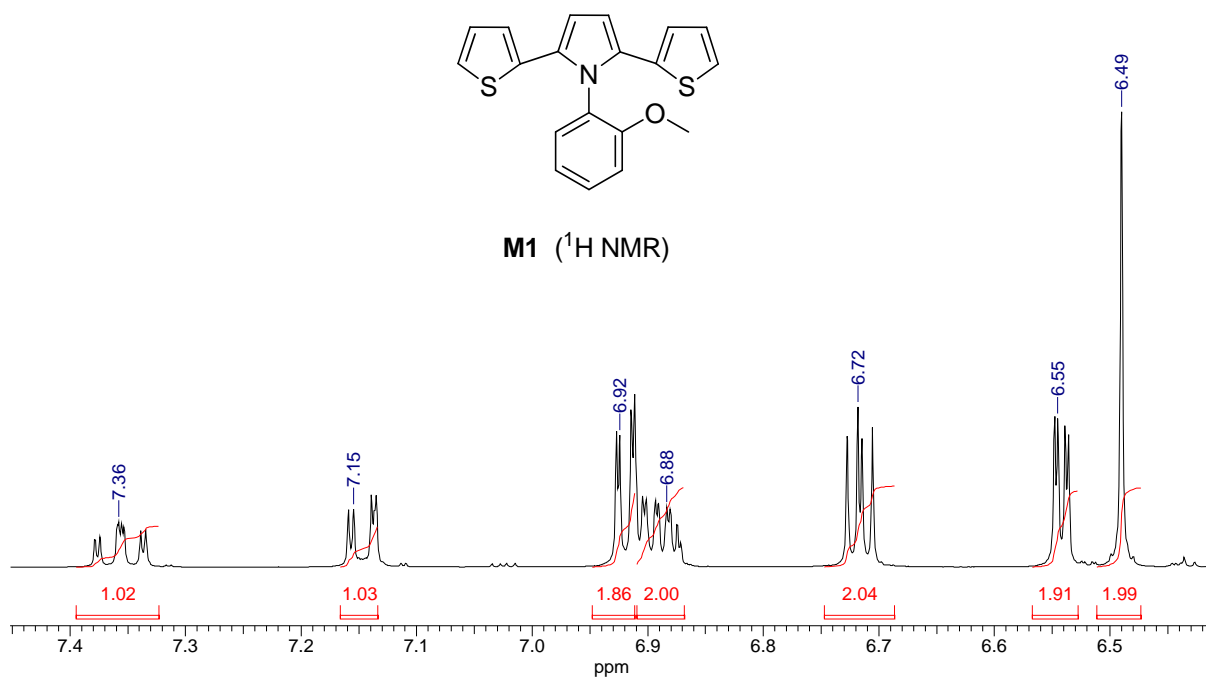
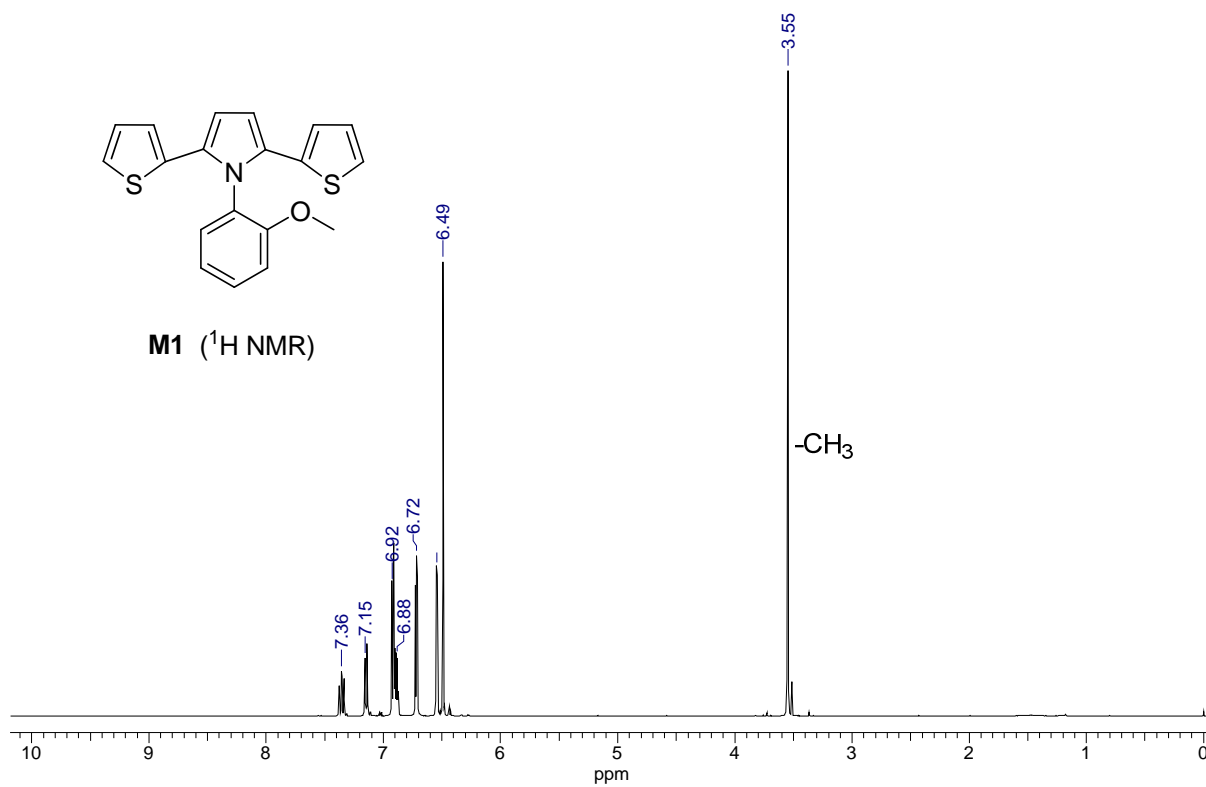


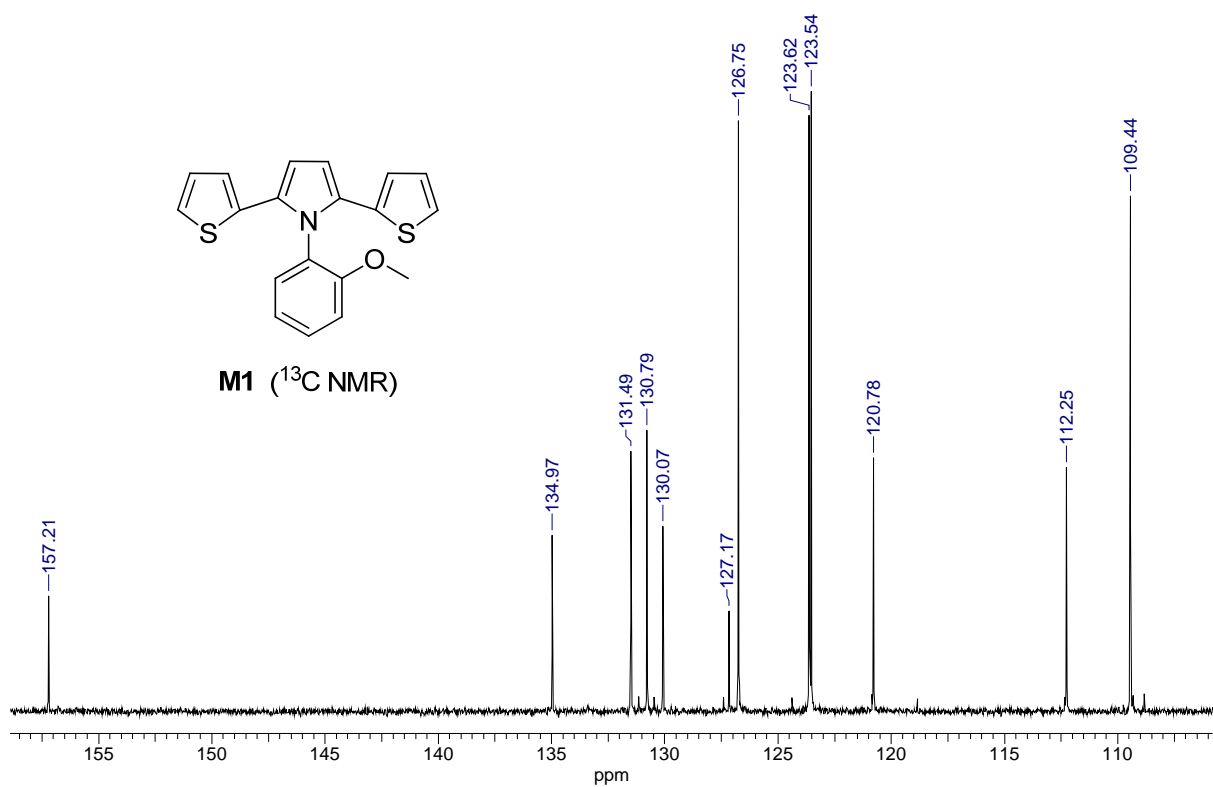
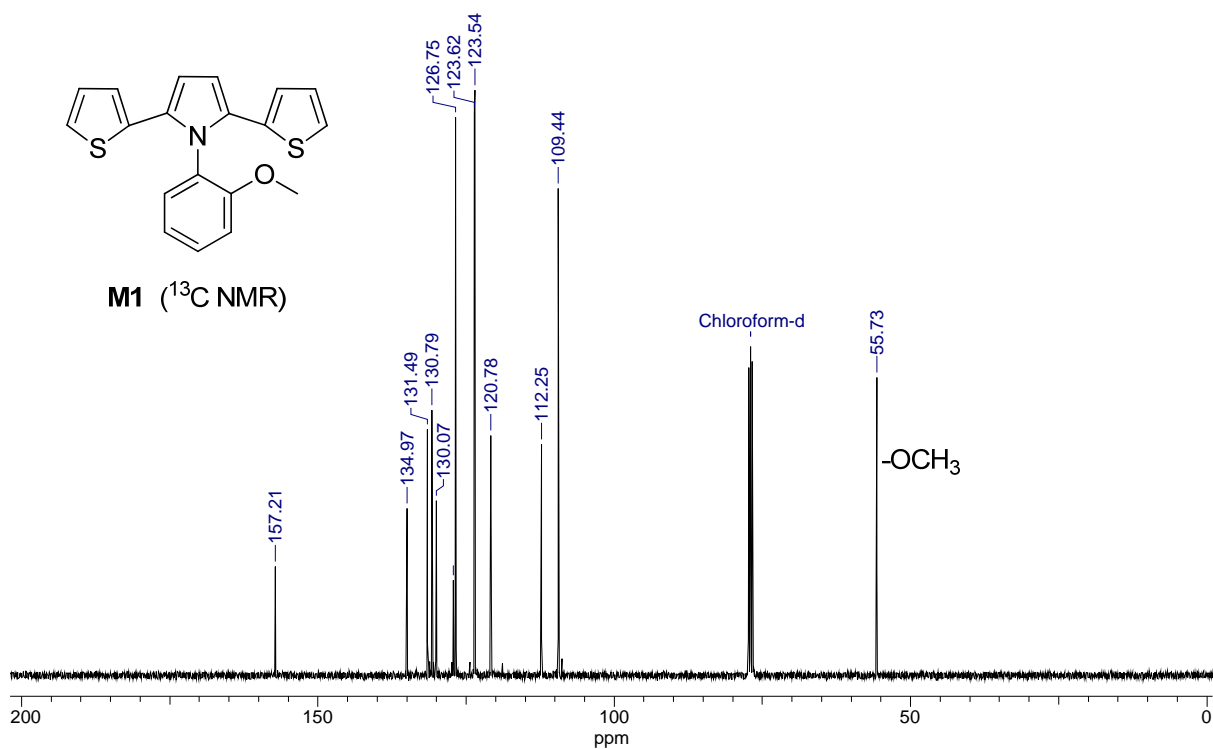


Analytical data of the compounds

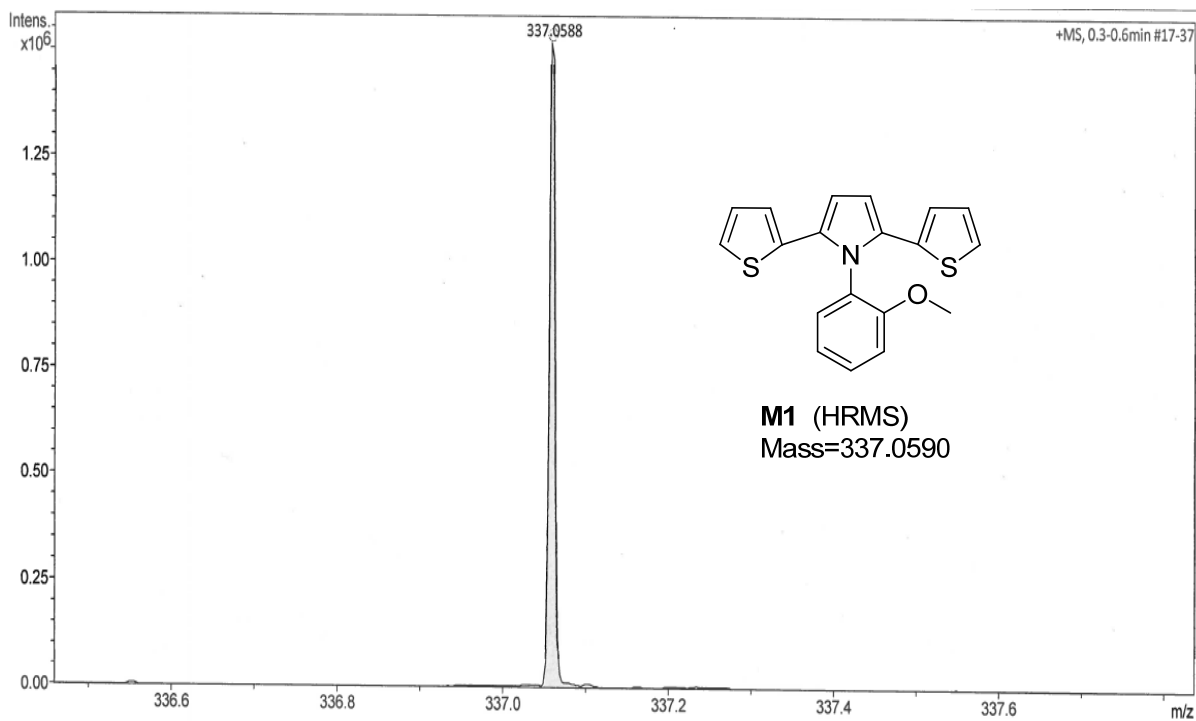
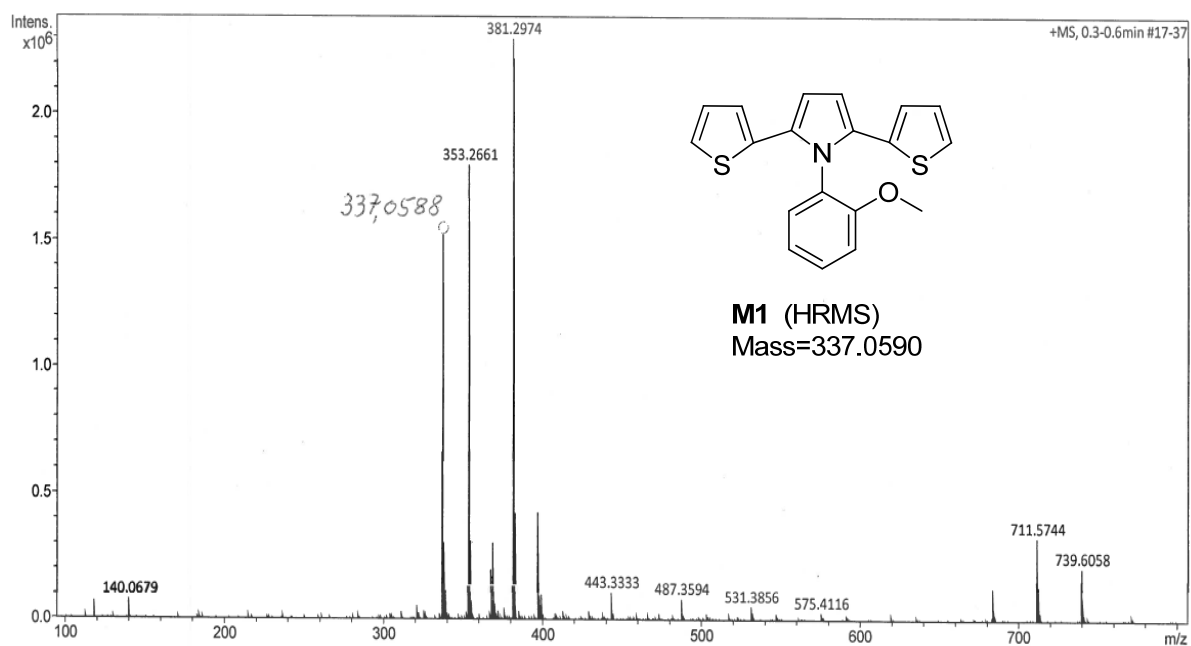


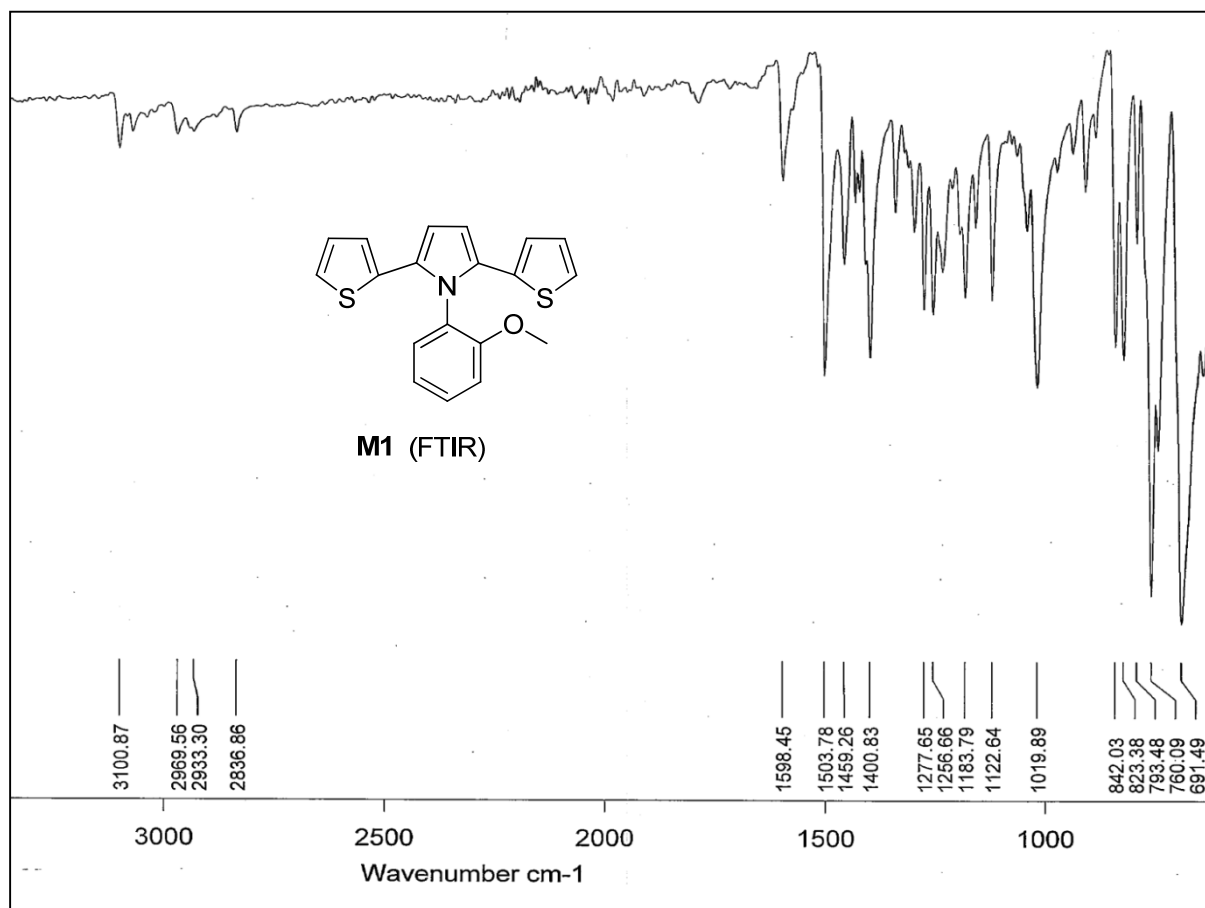


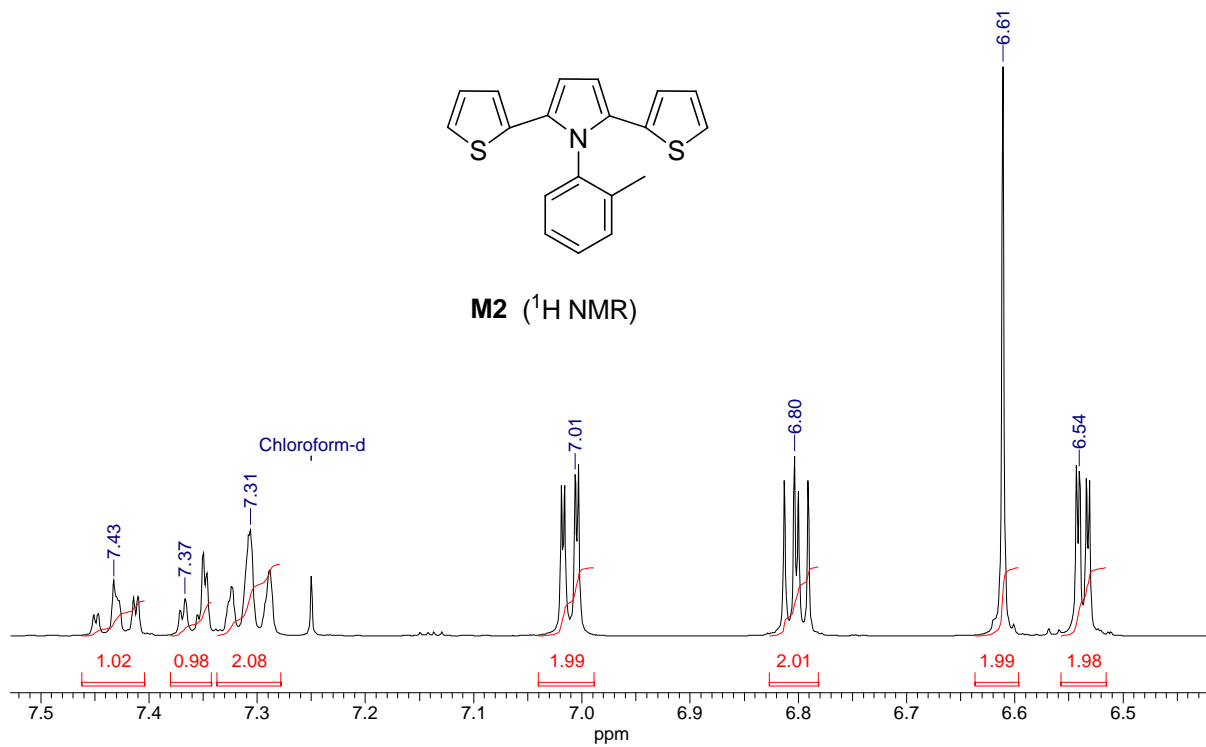
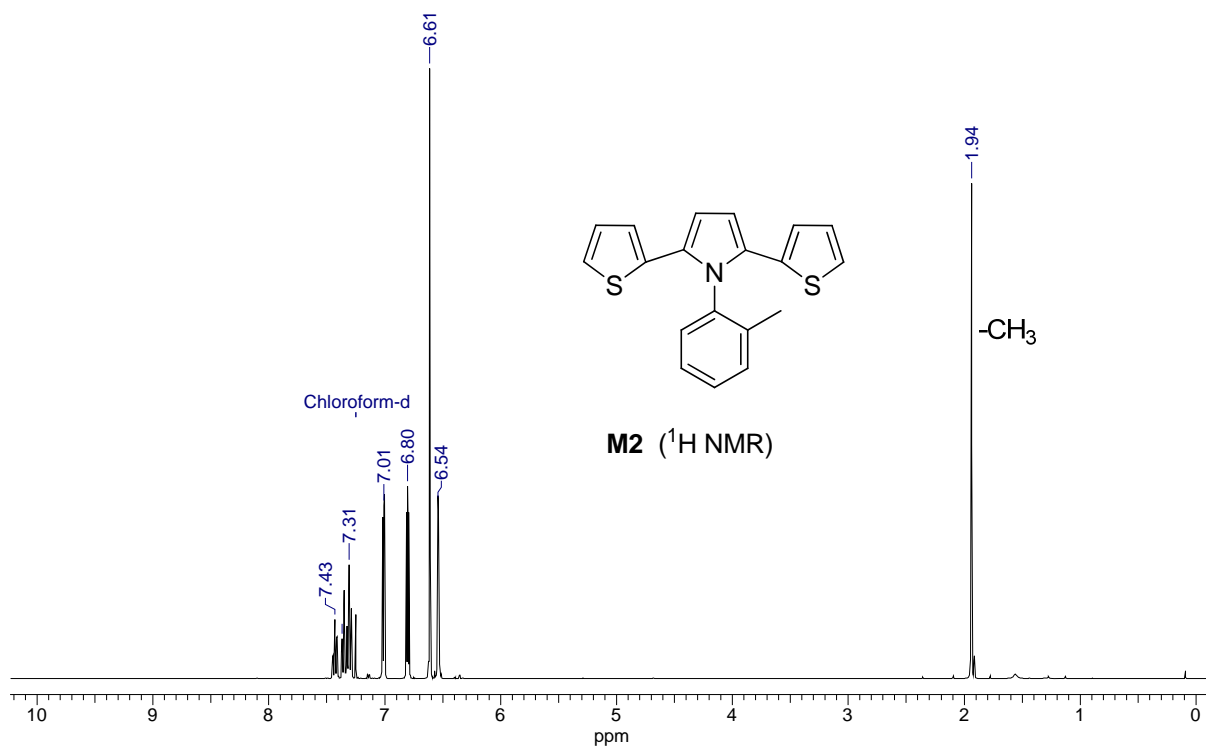


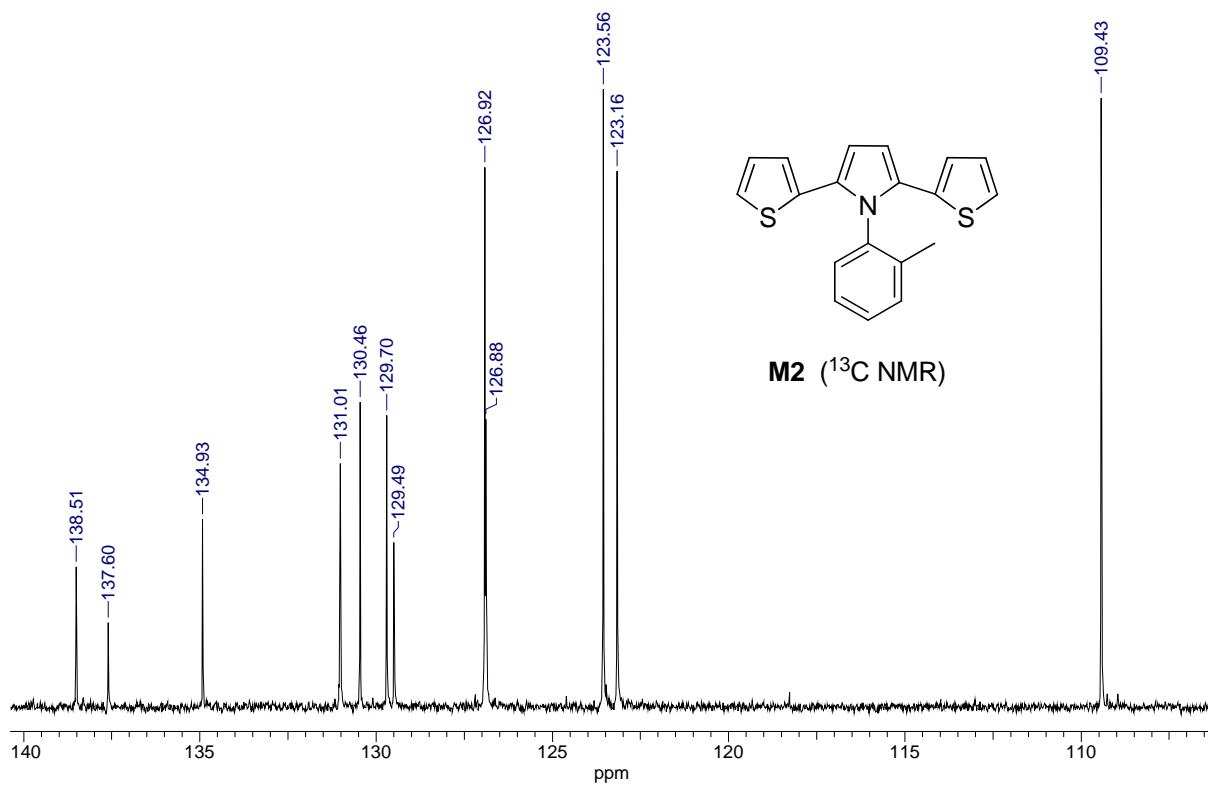
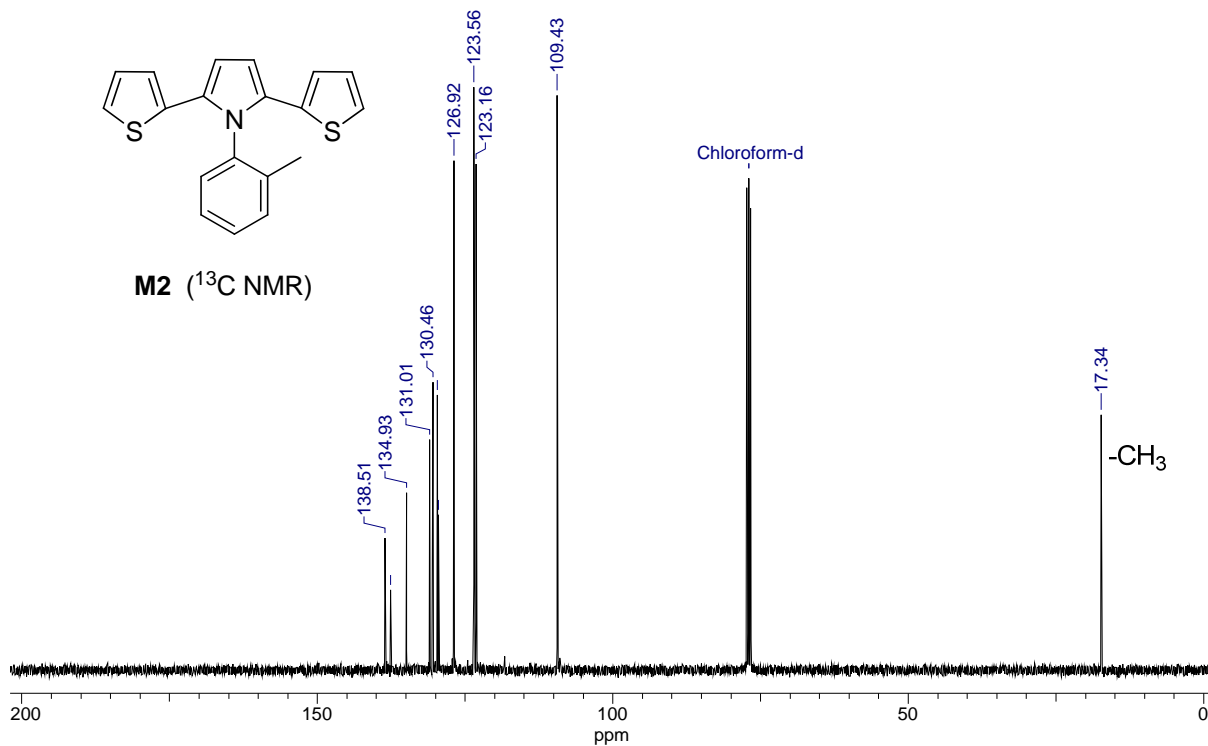


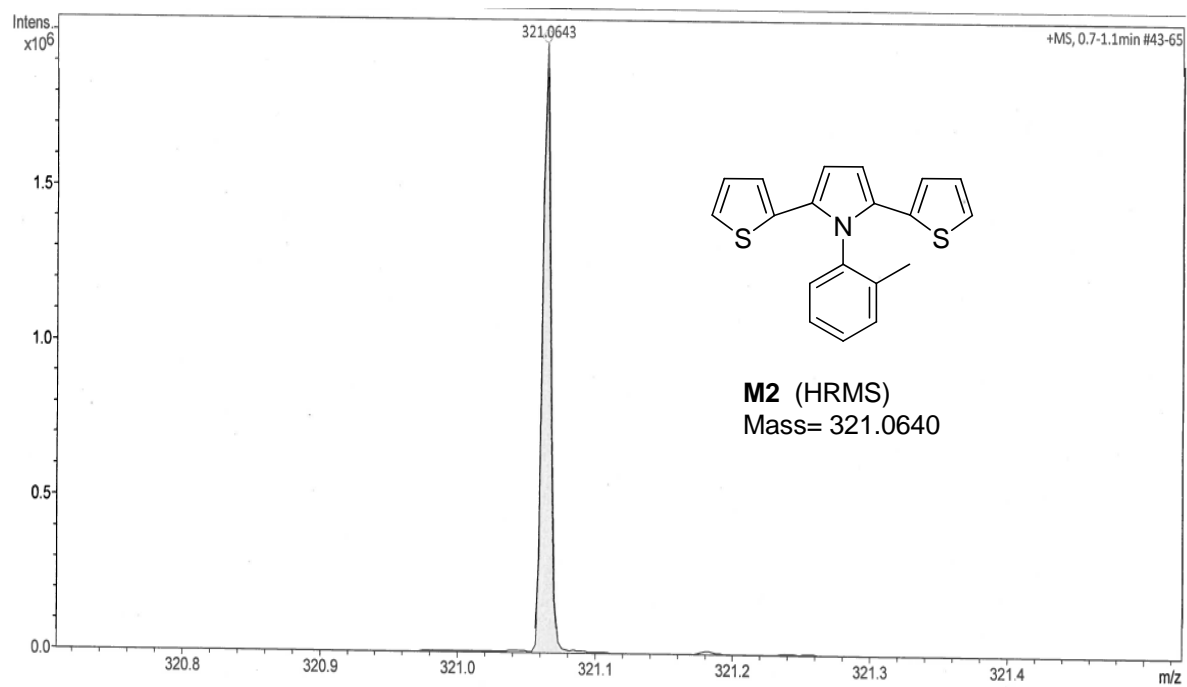
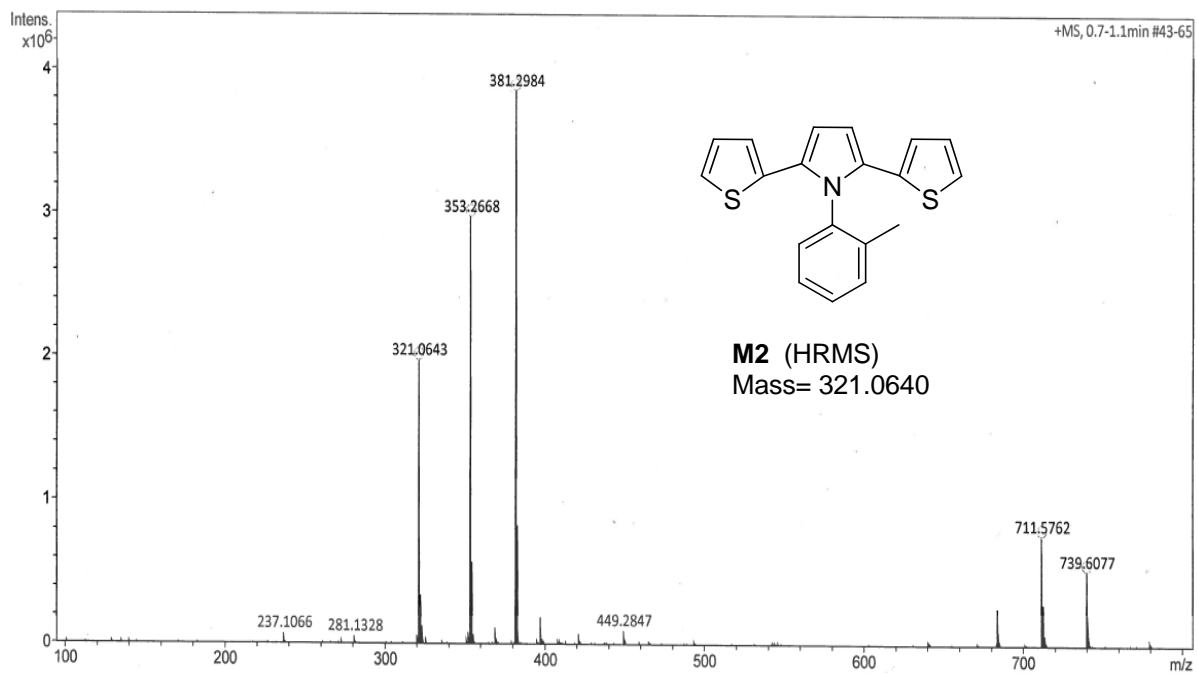
Analytical data of the compounds

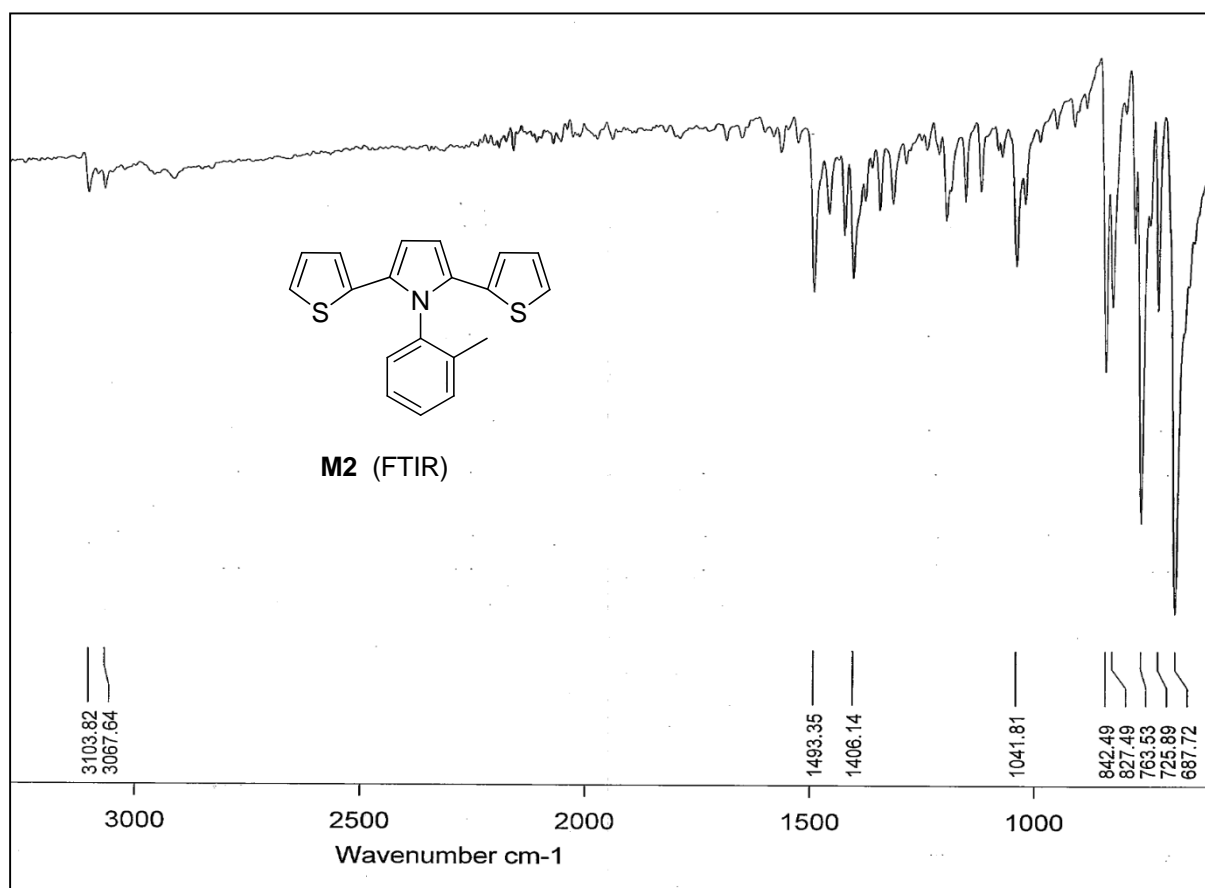


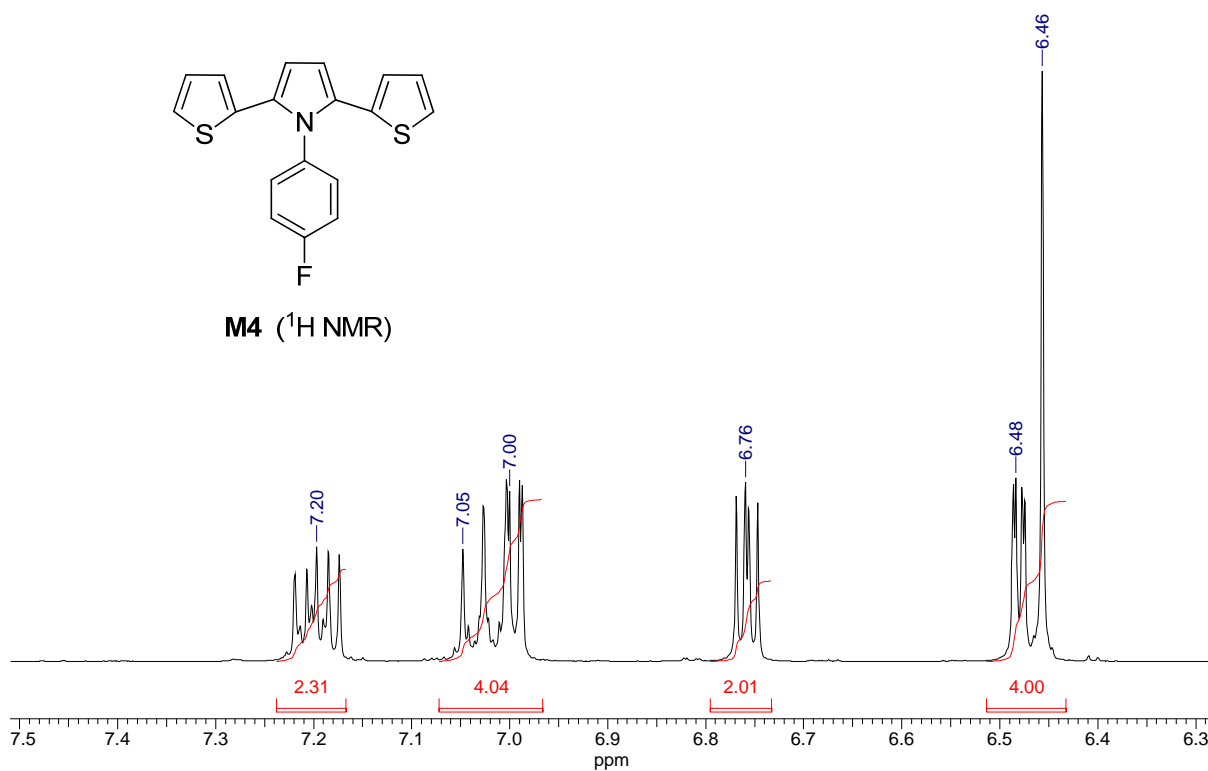
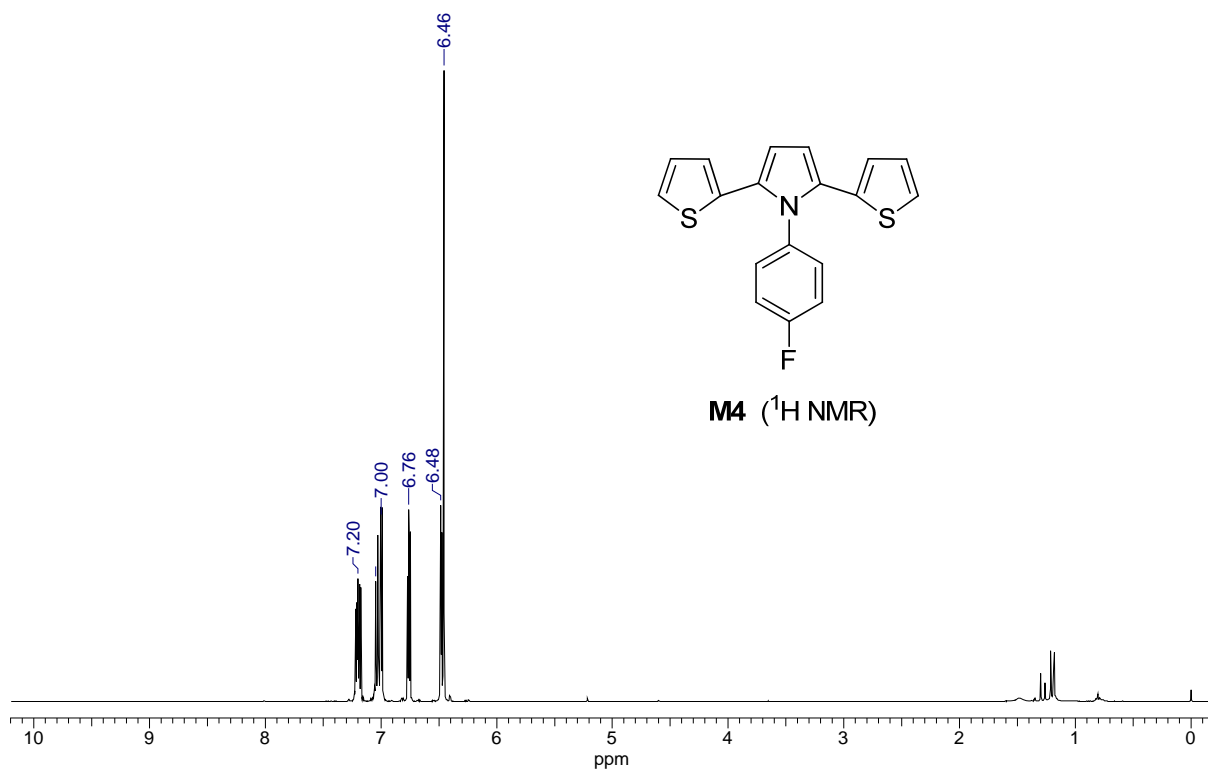


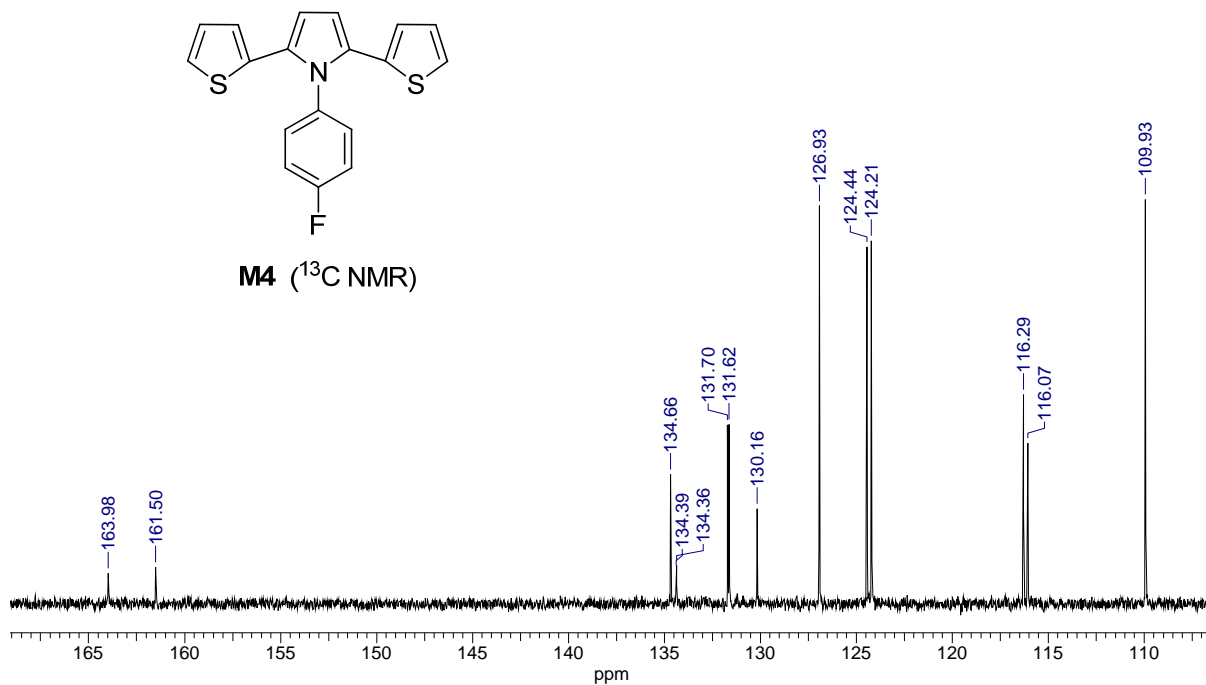
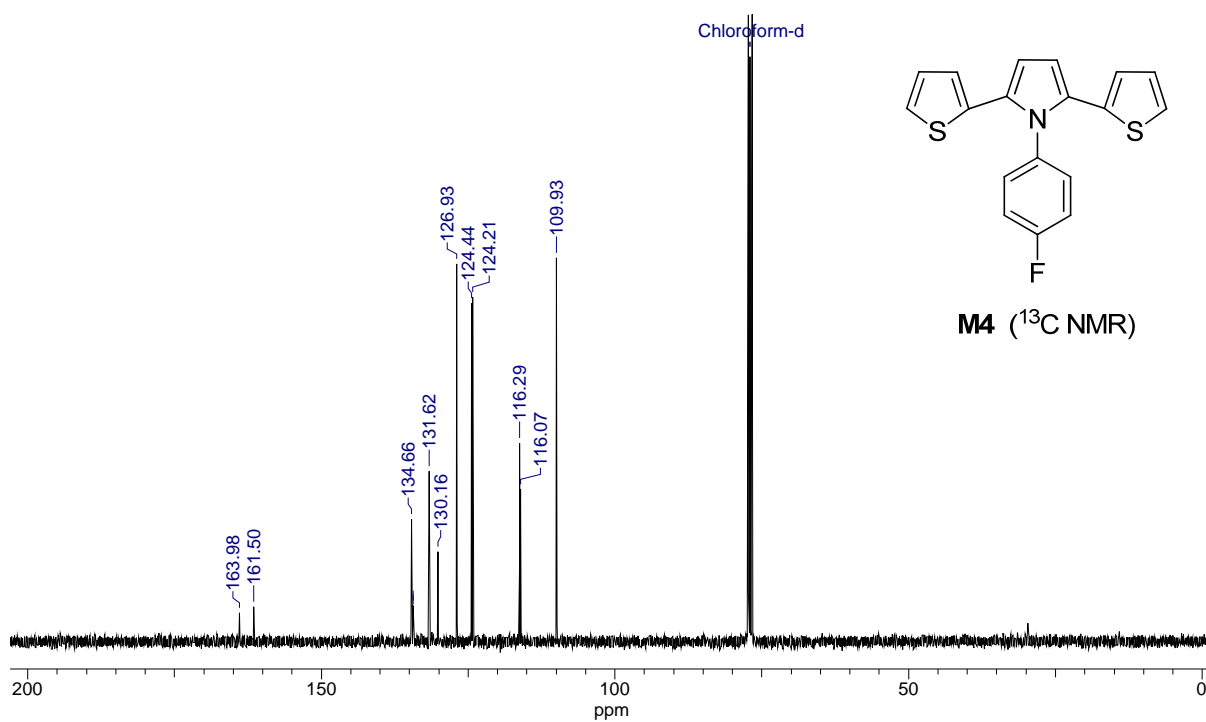




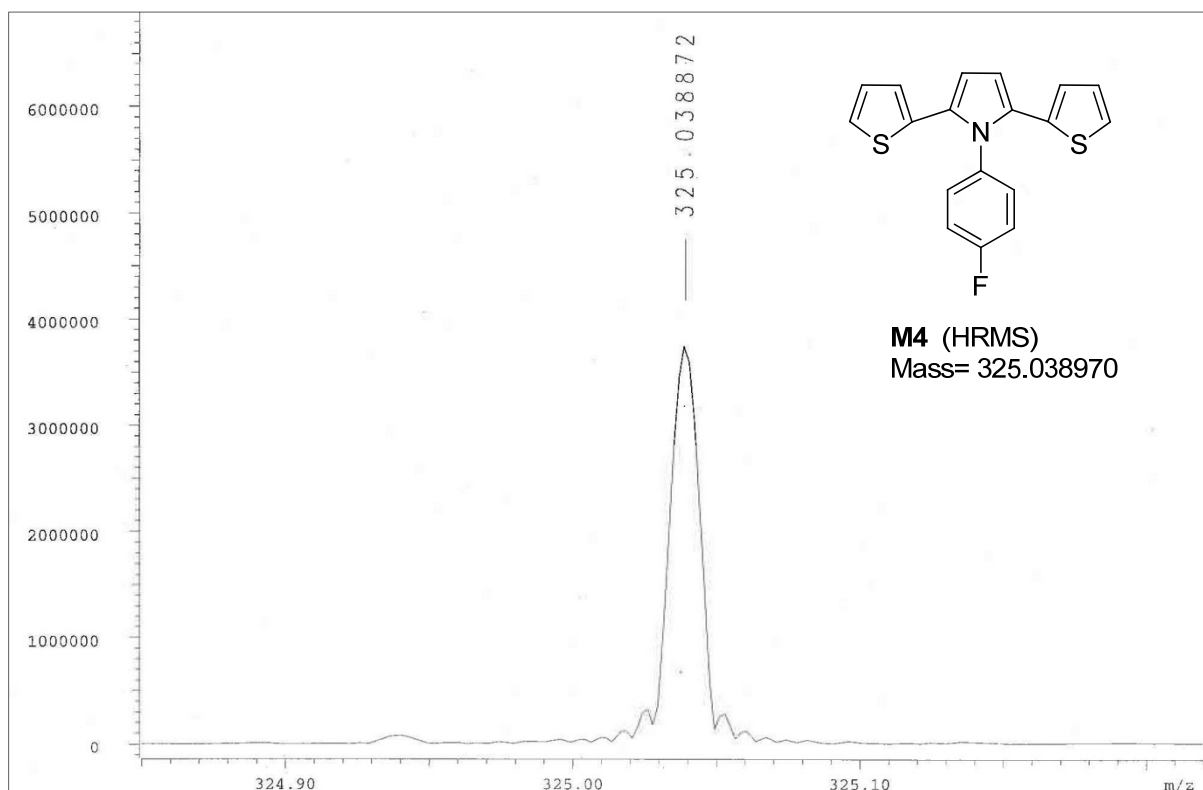
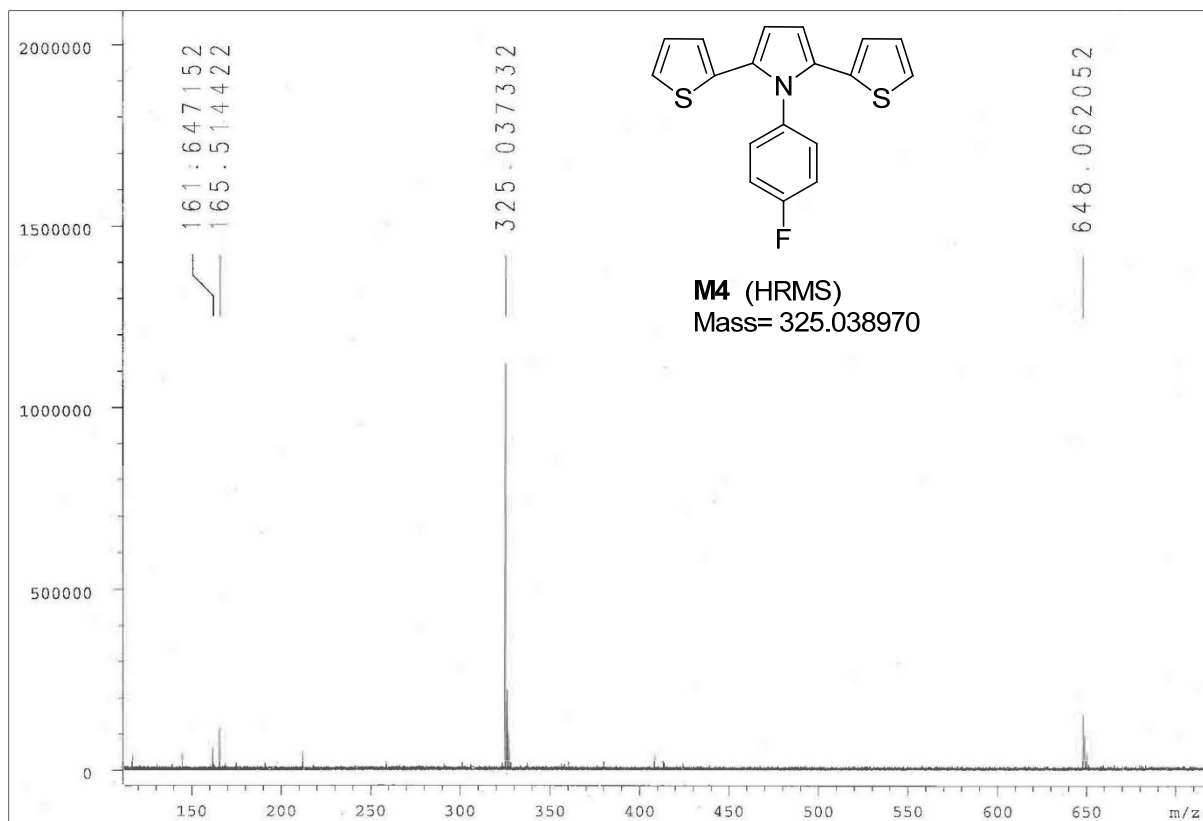


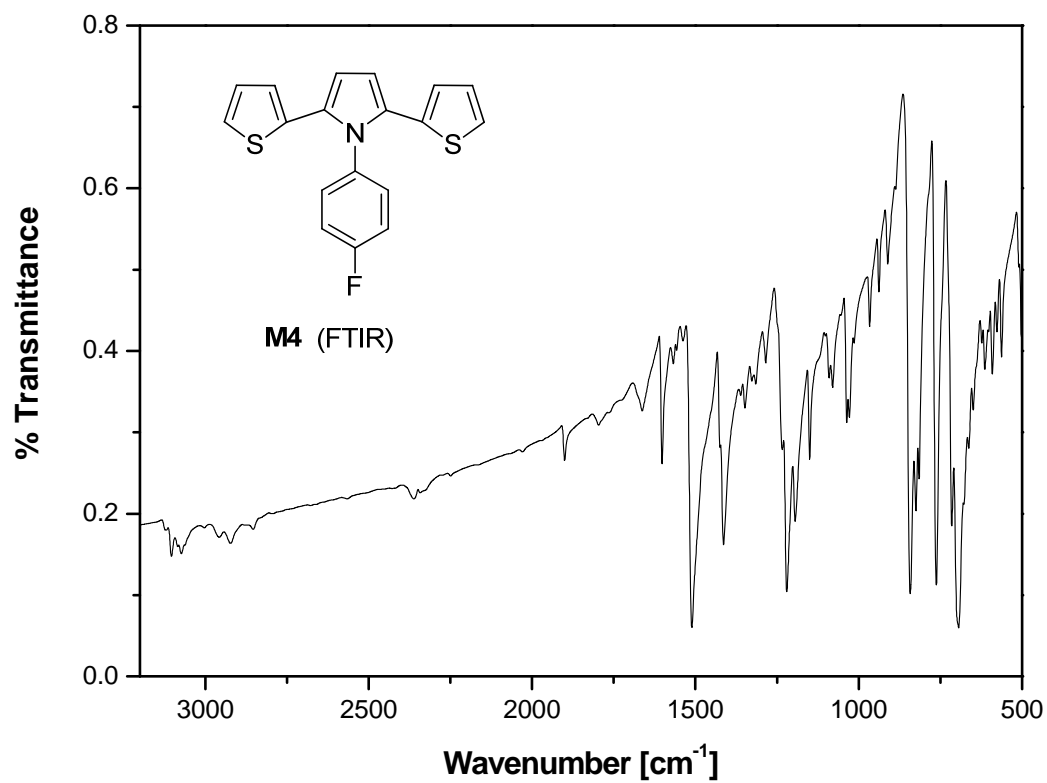


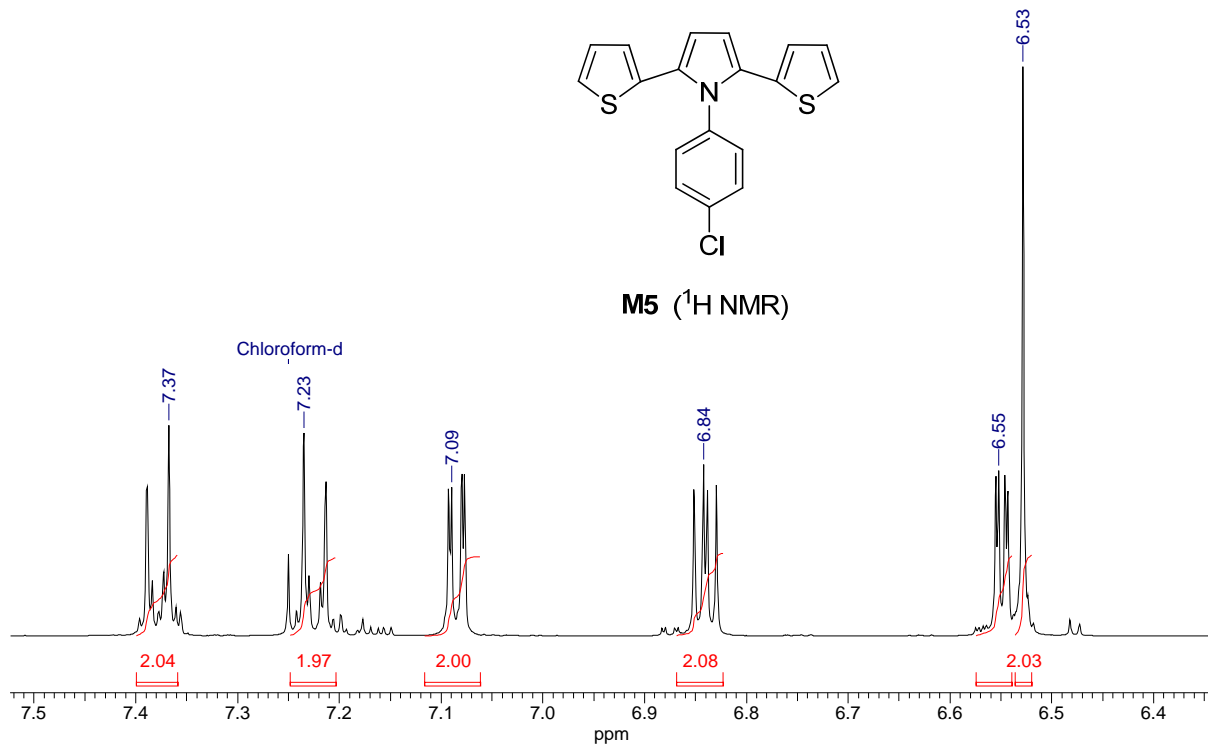
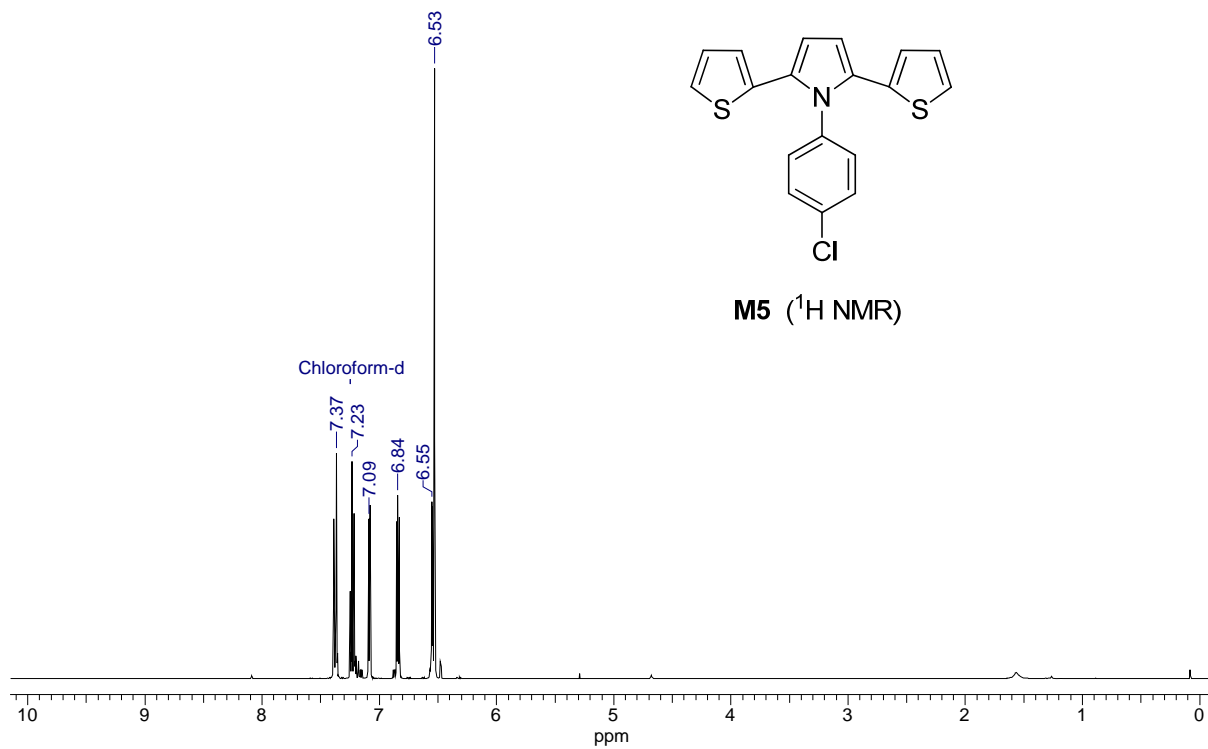


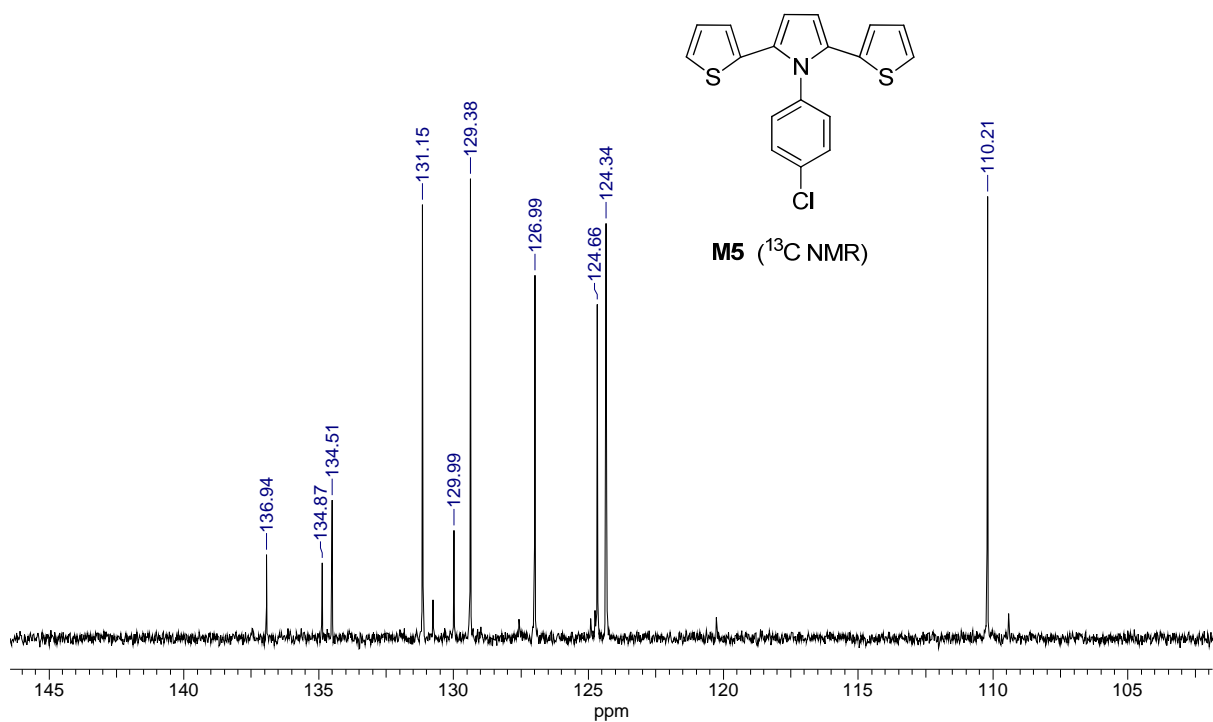
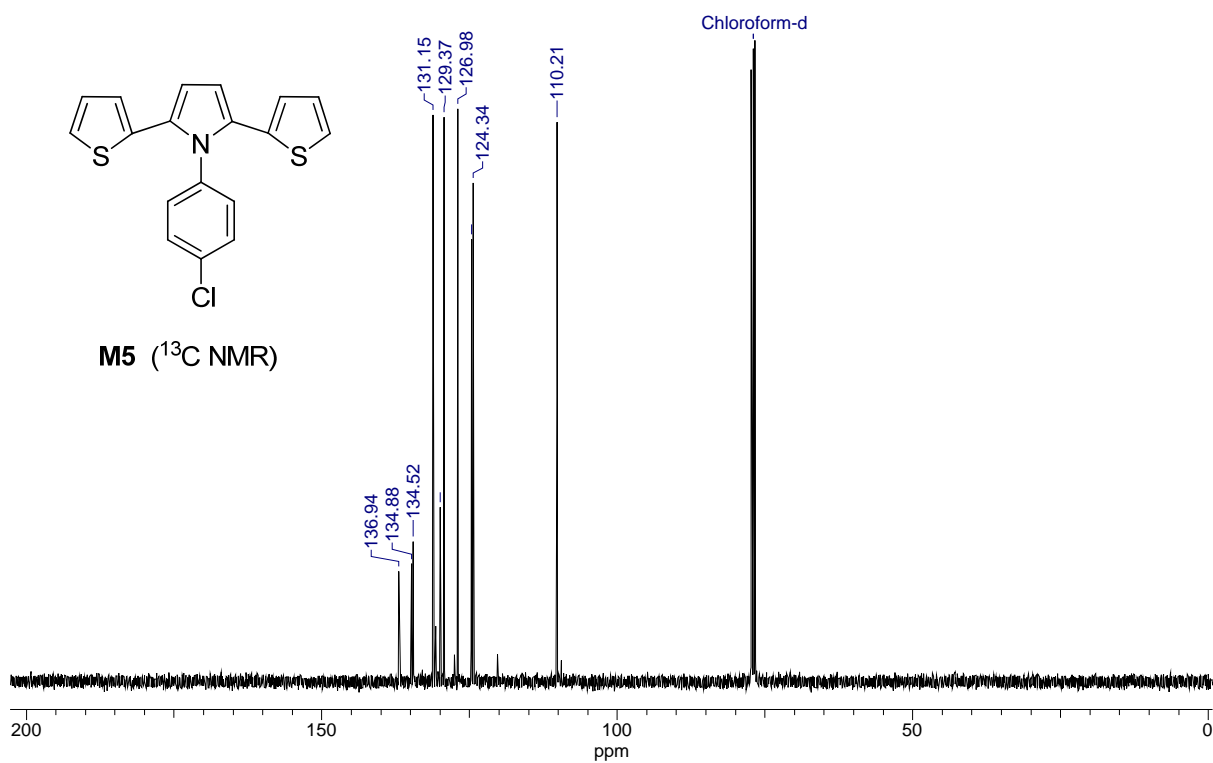


Analytical data of the compounds

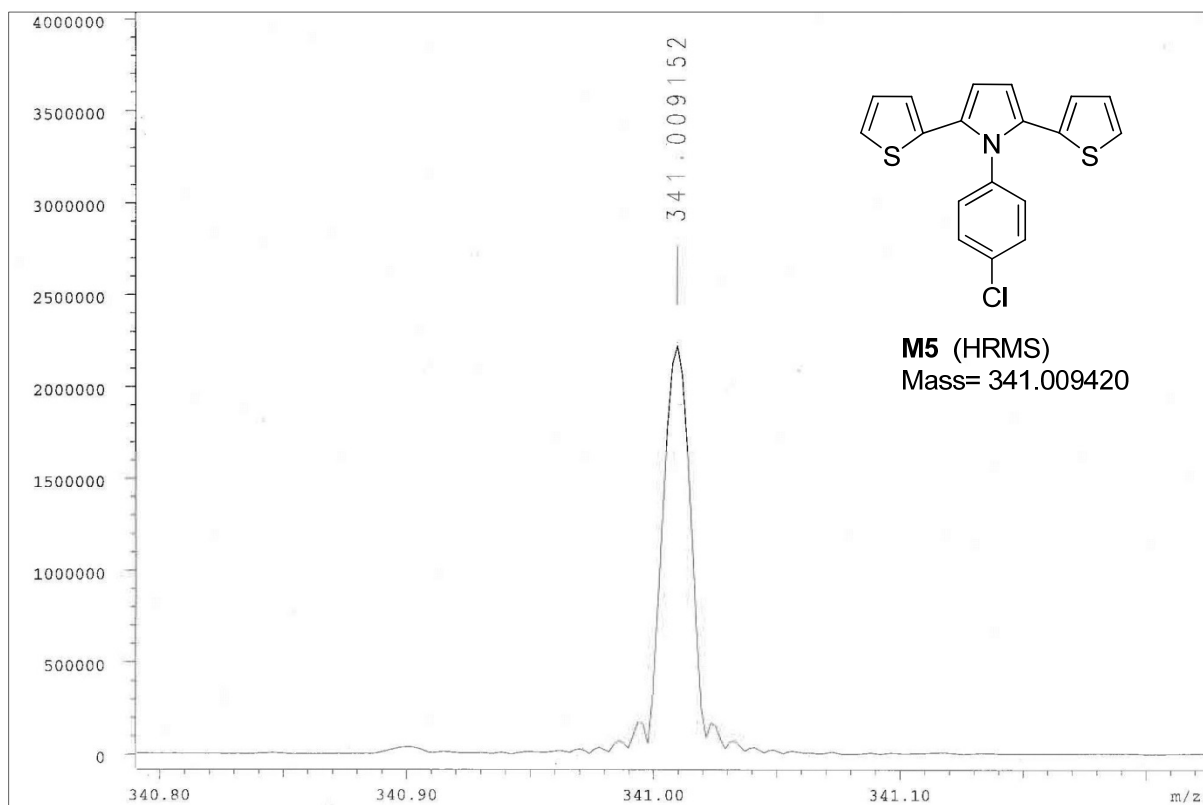
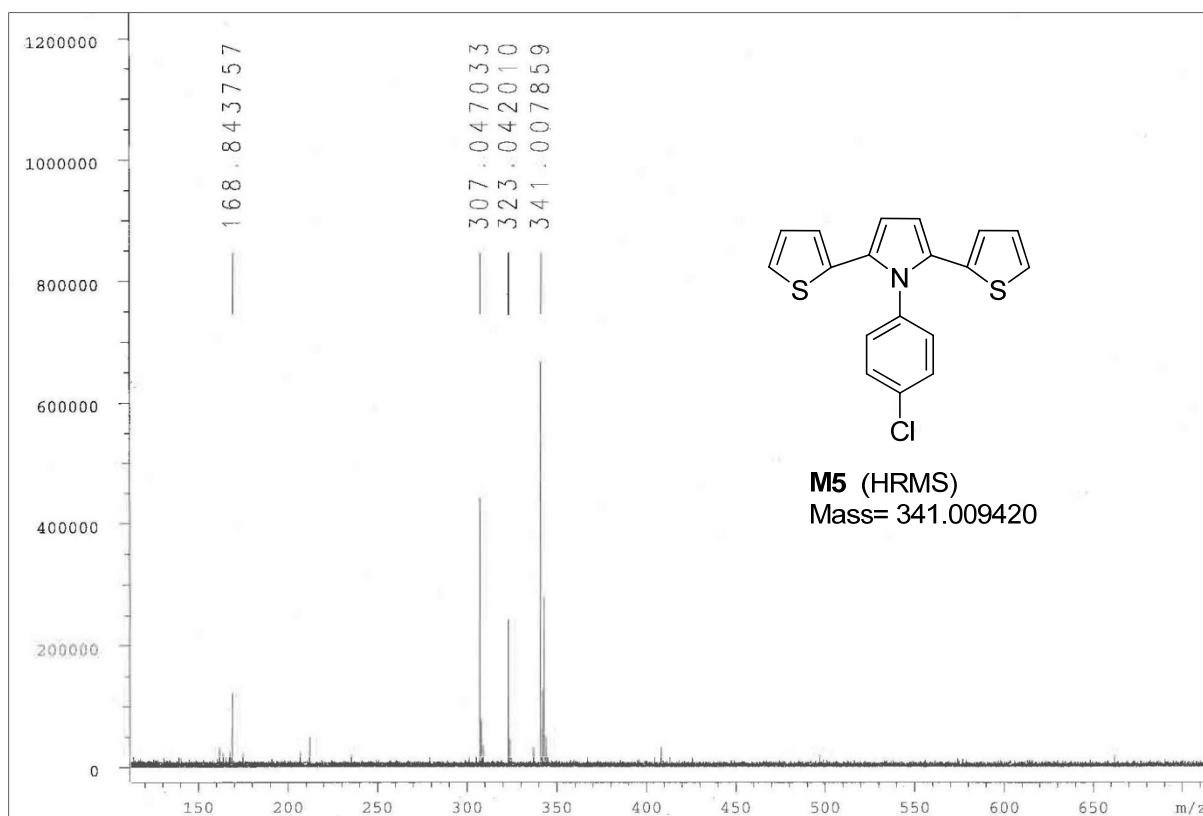


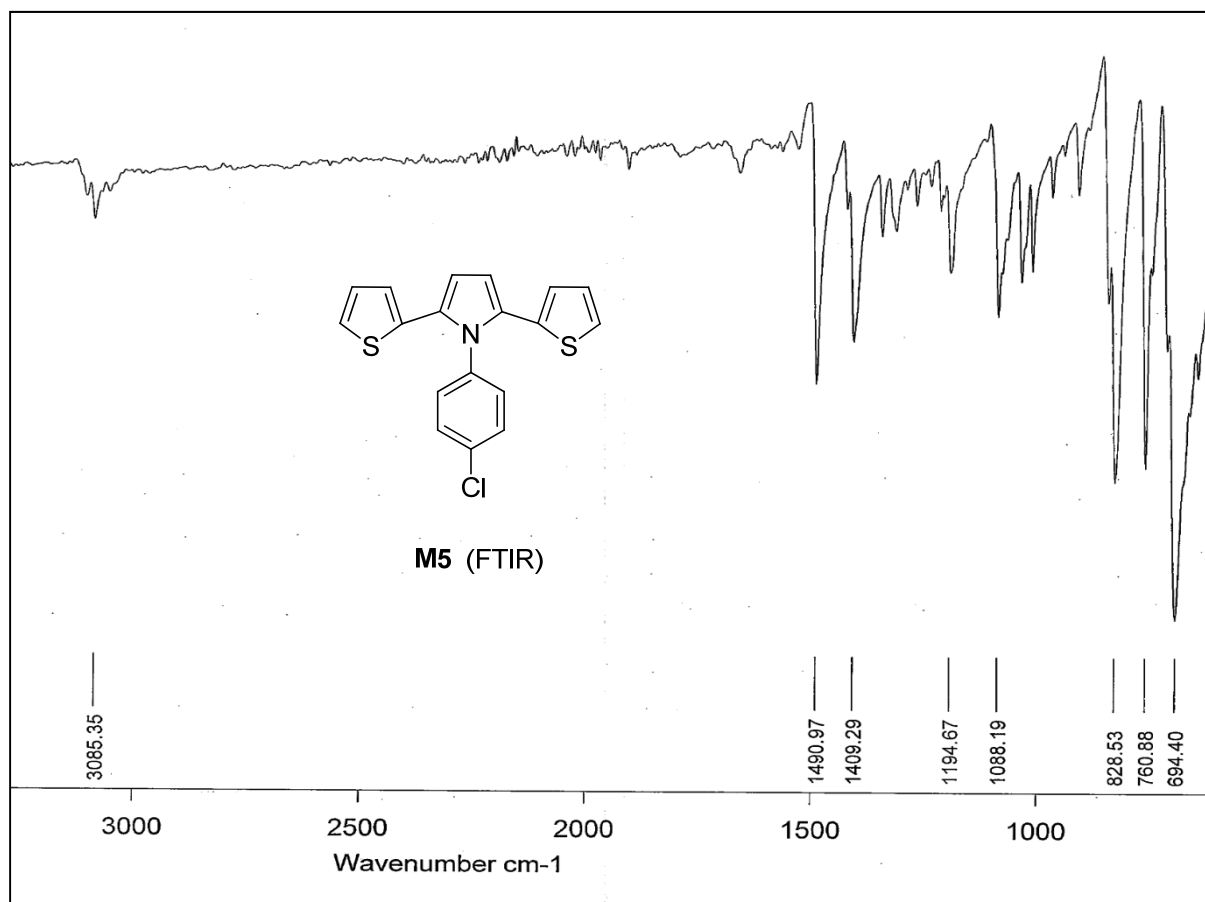


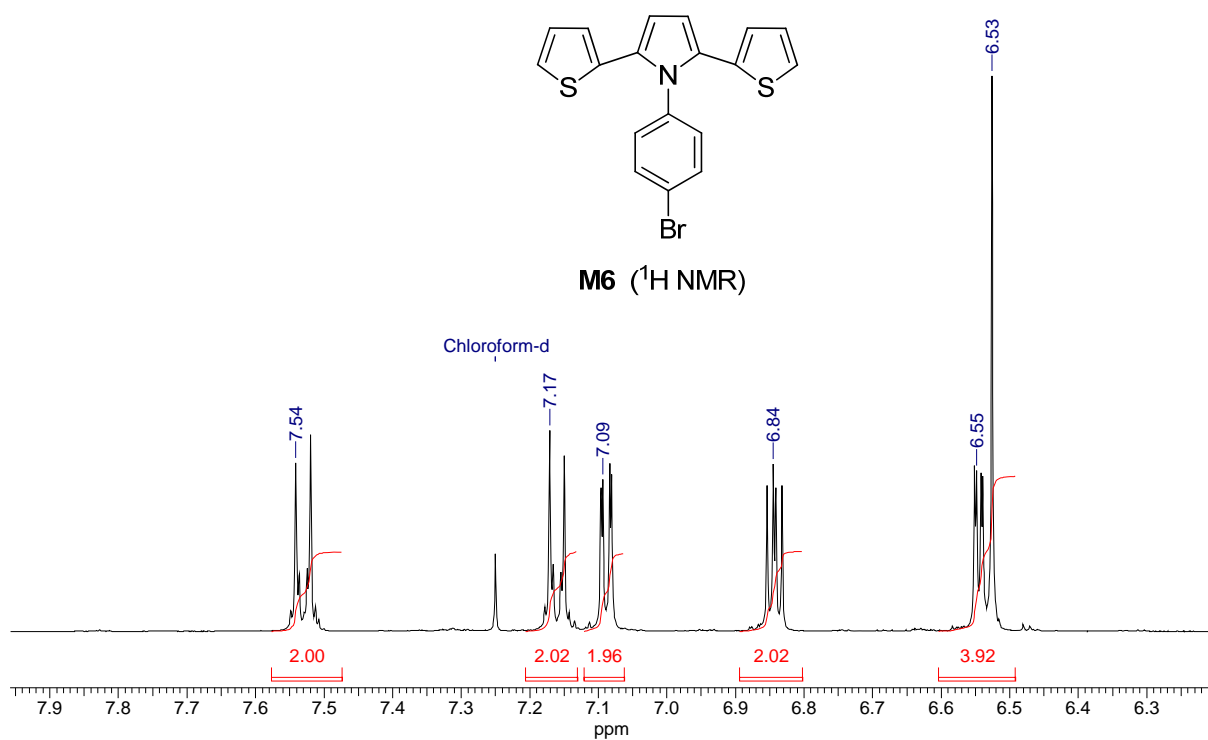
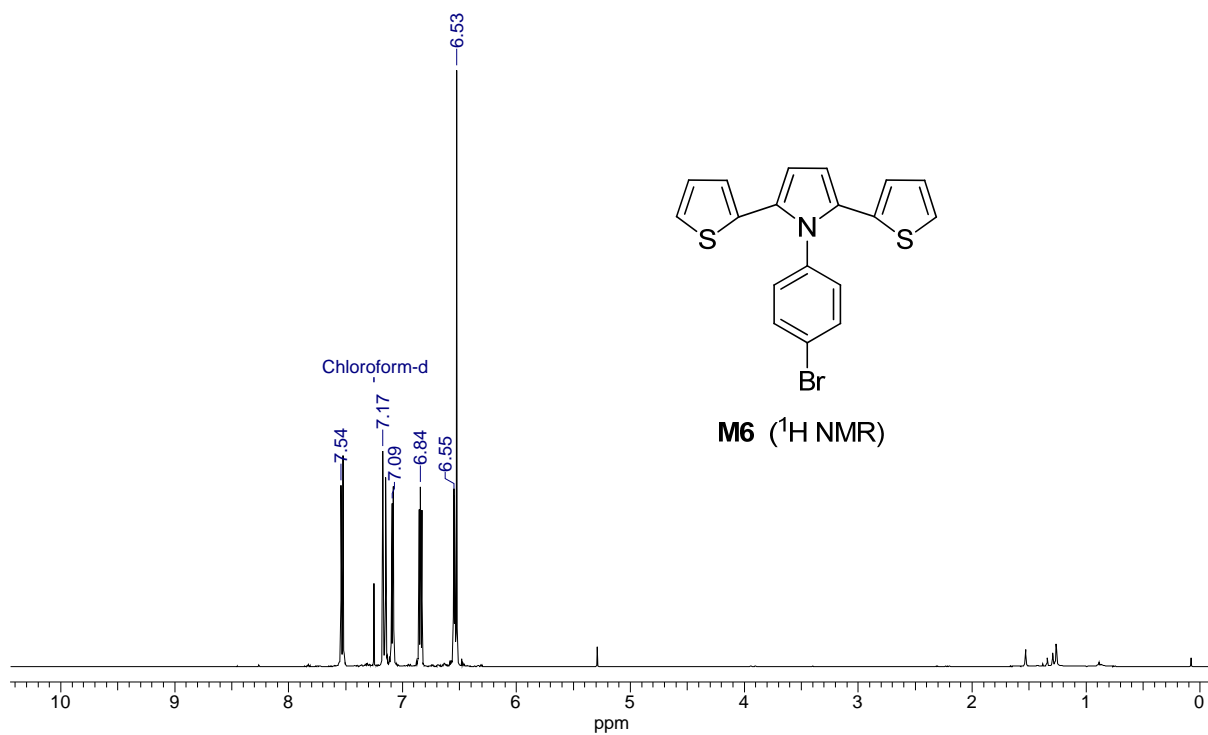


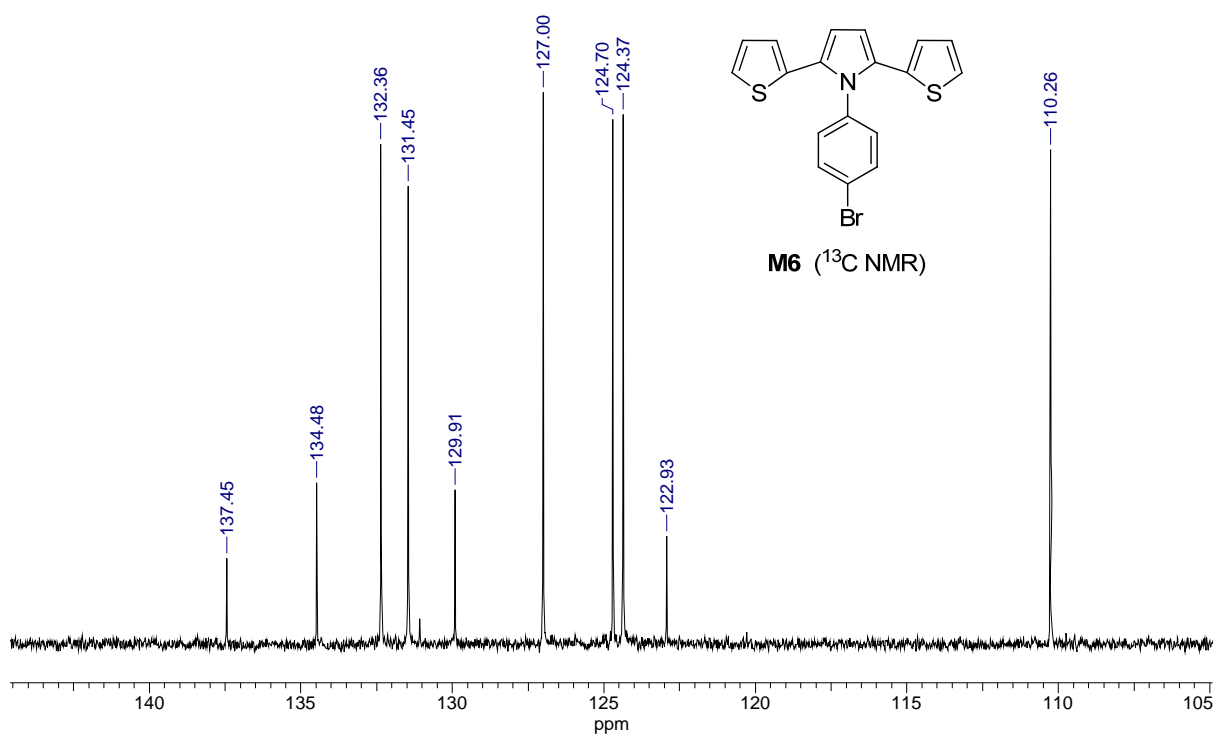
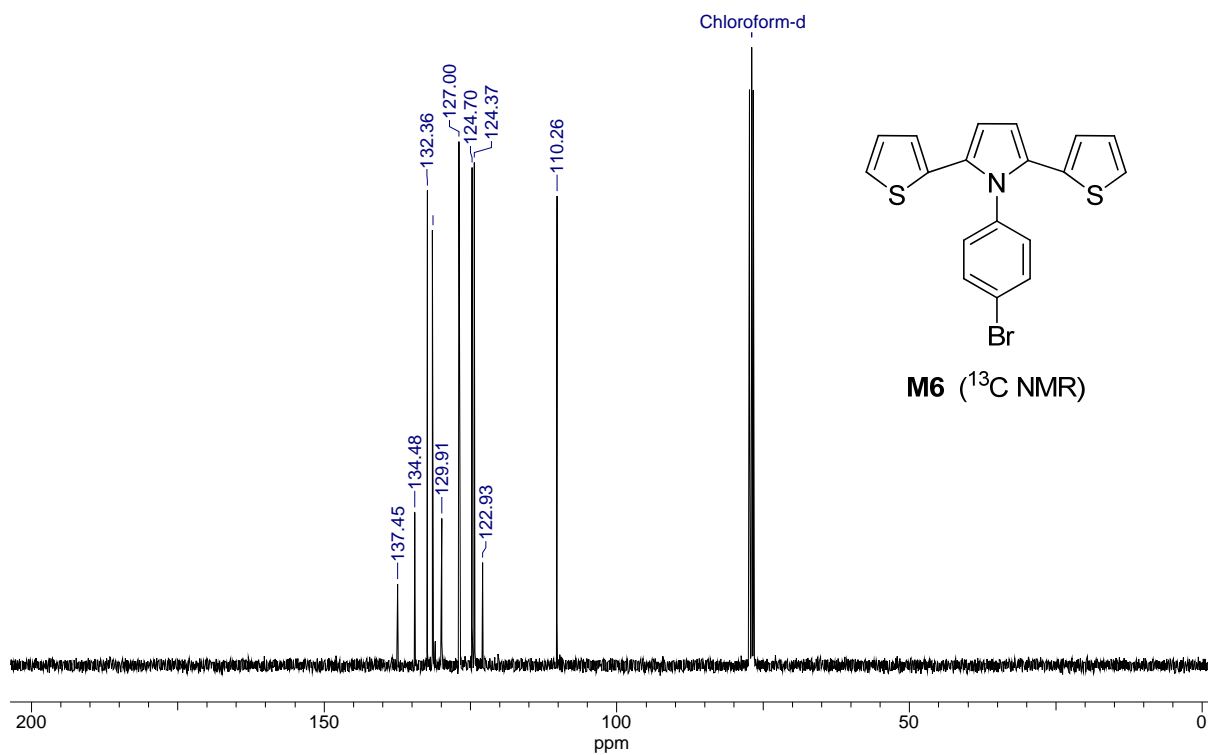


Analytical data of the compounds

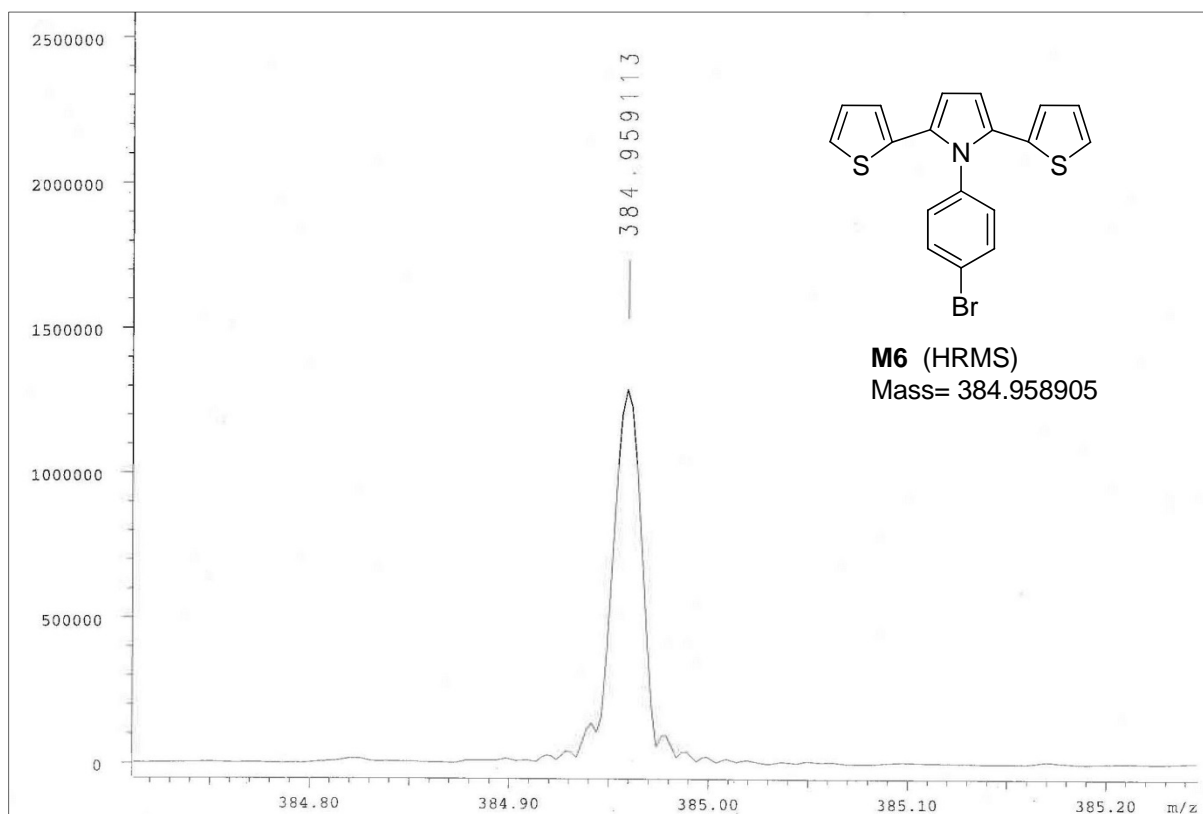
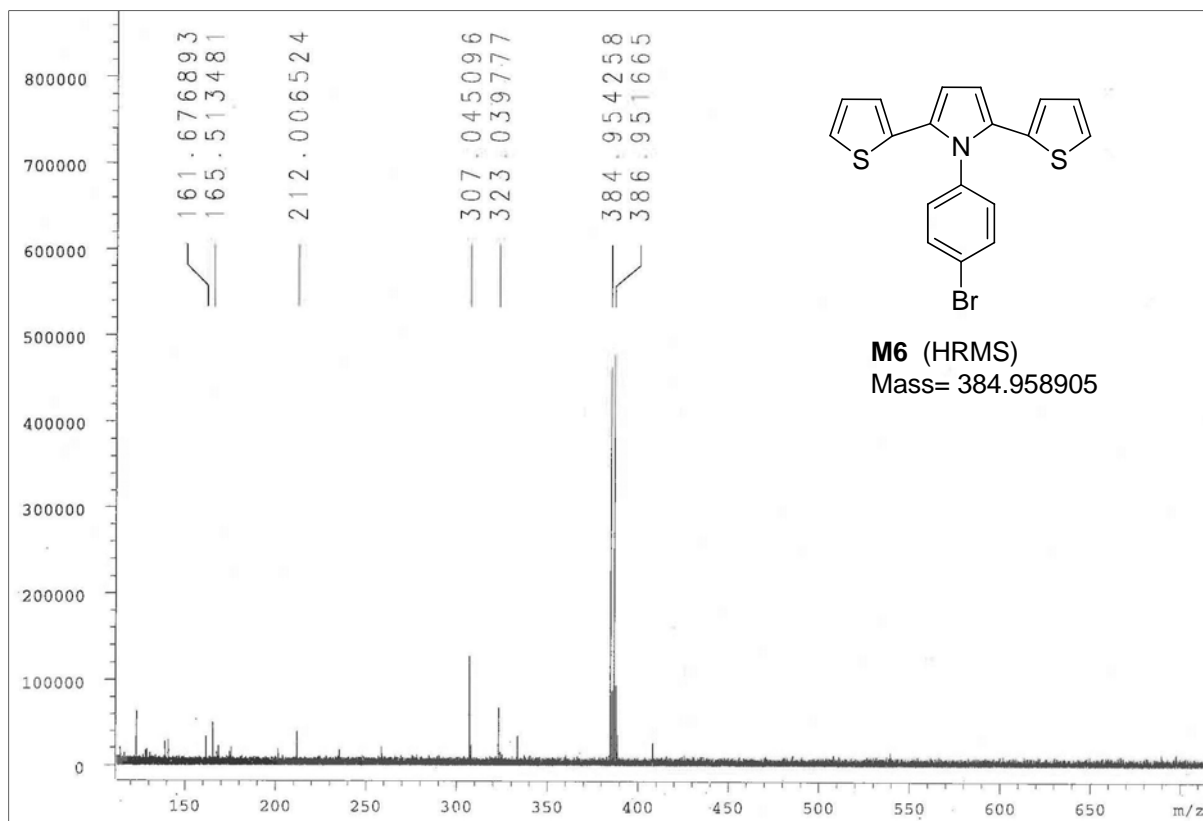


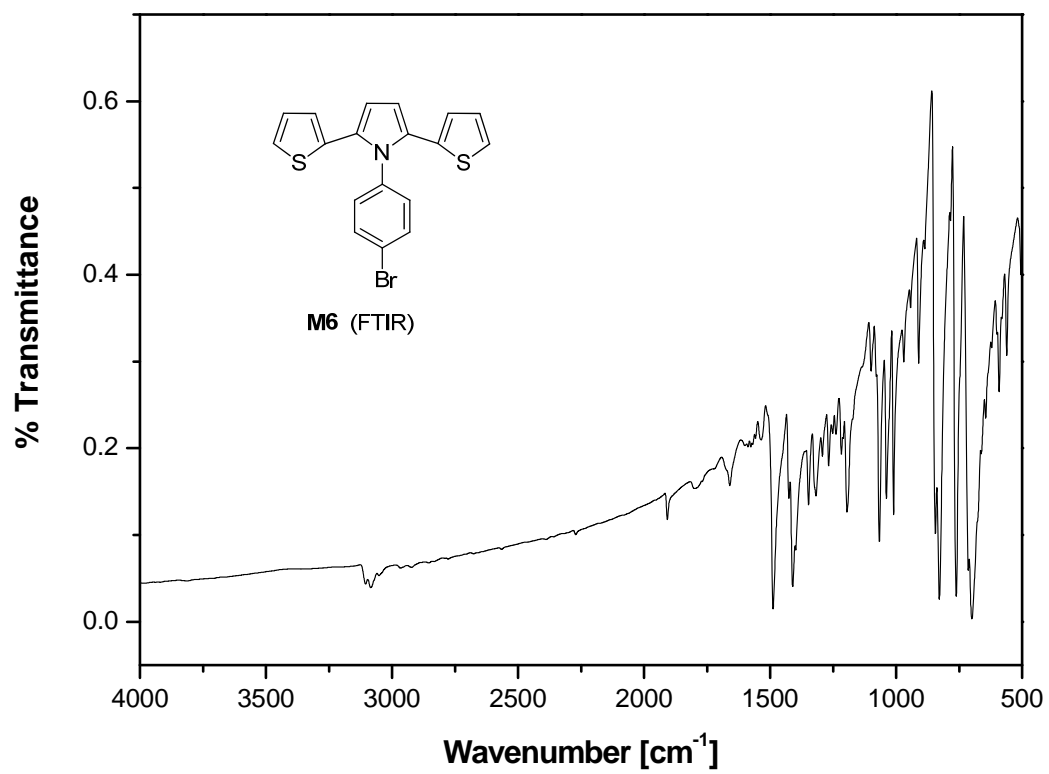


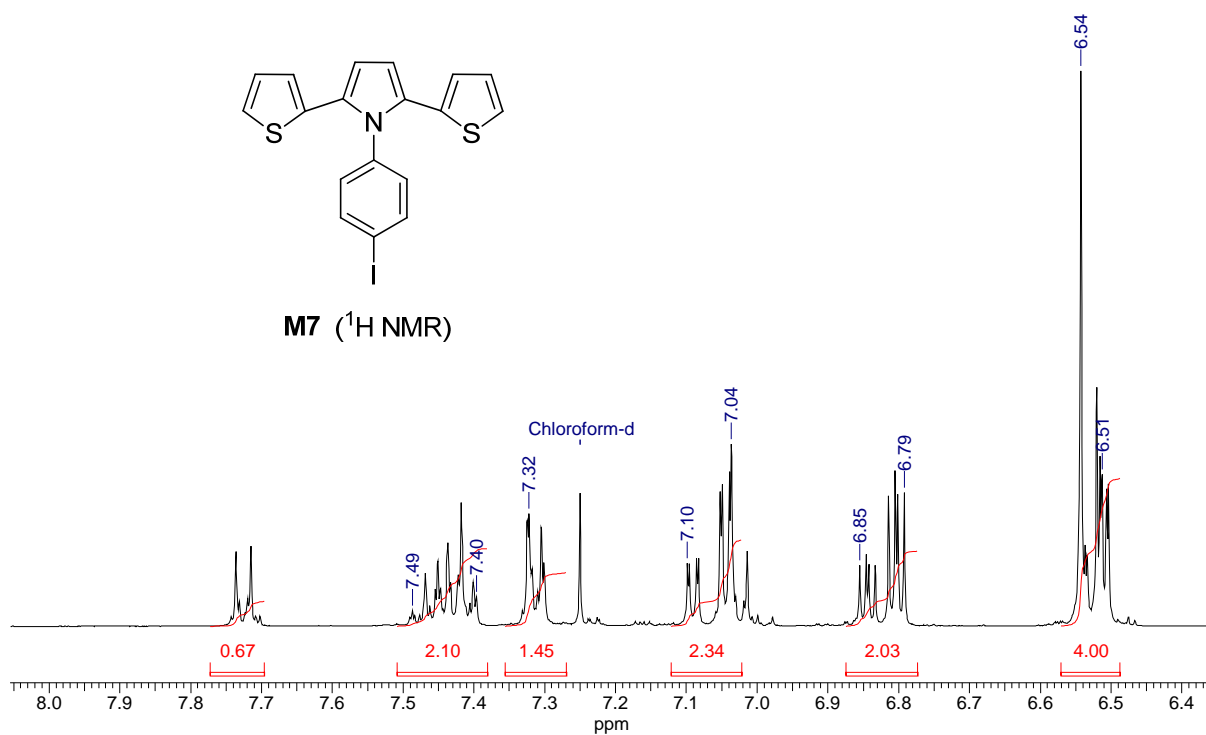
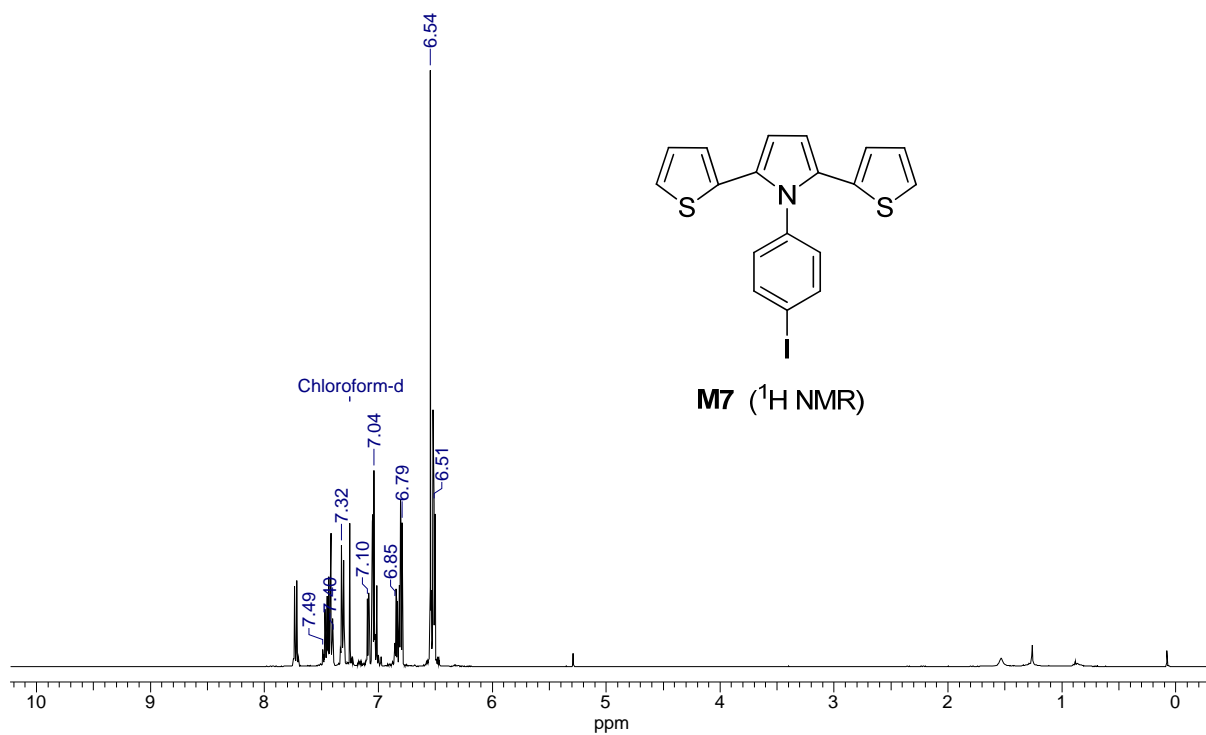


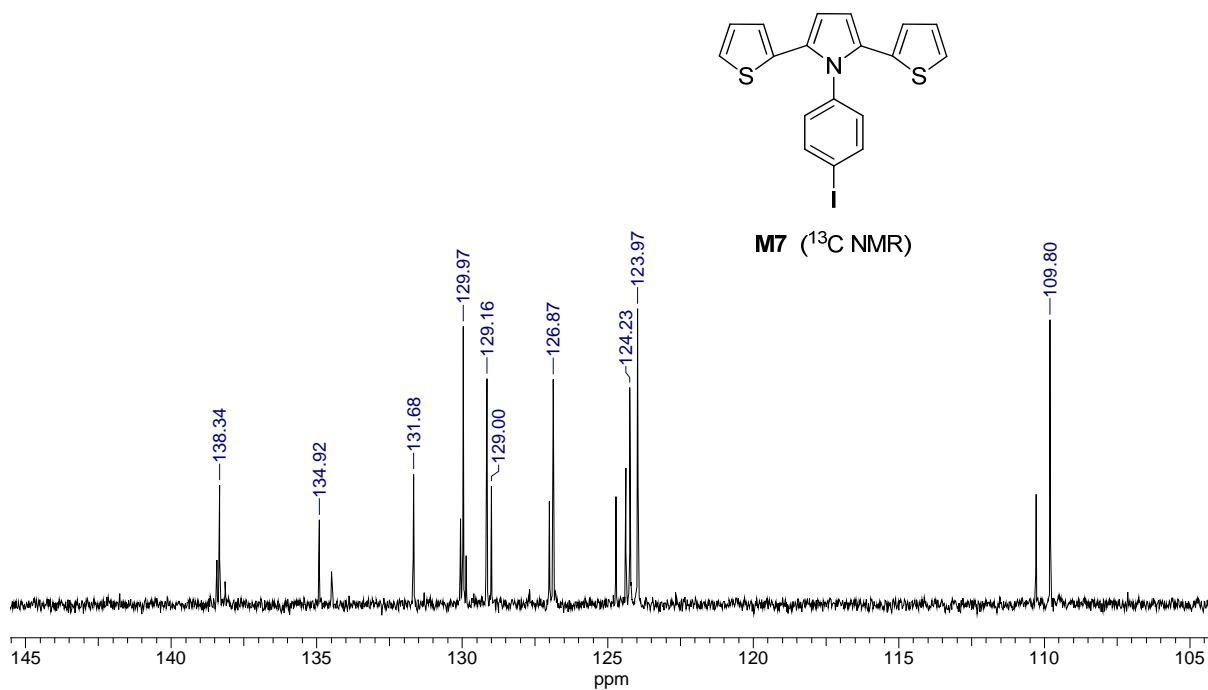
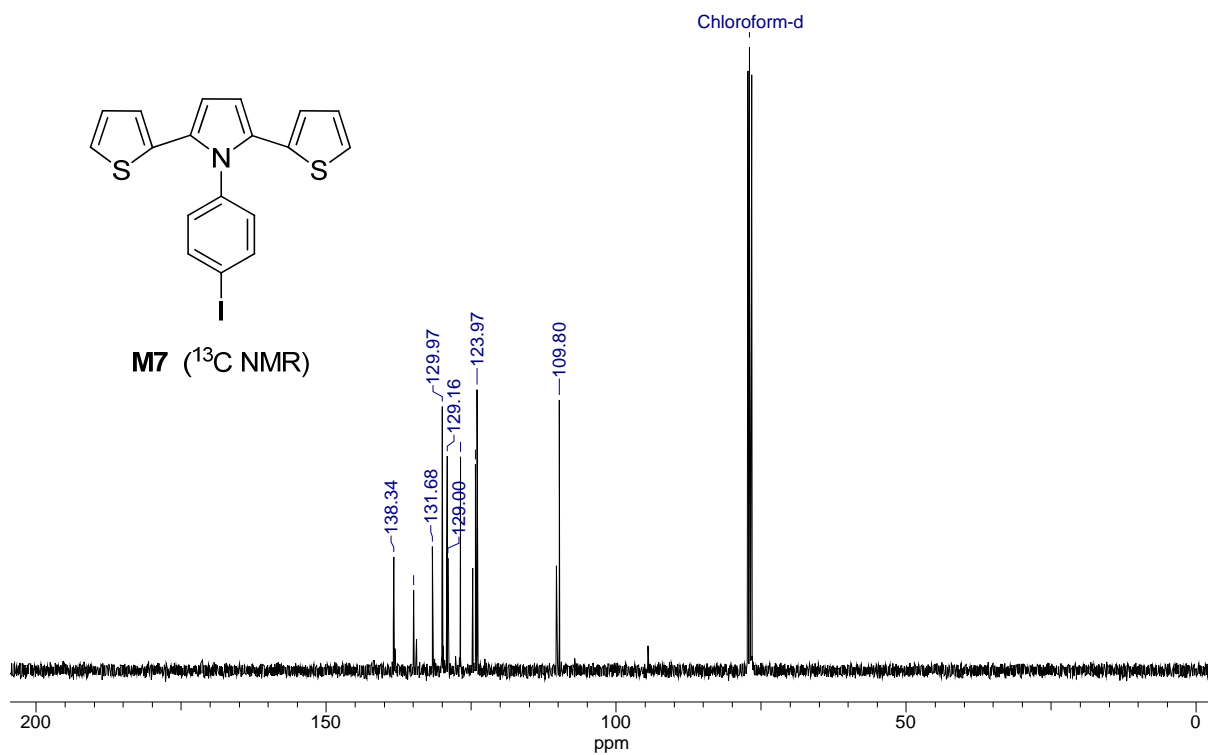


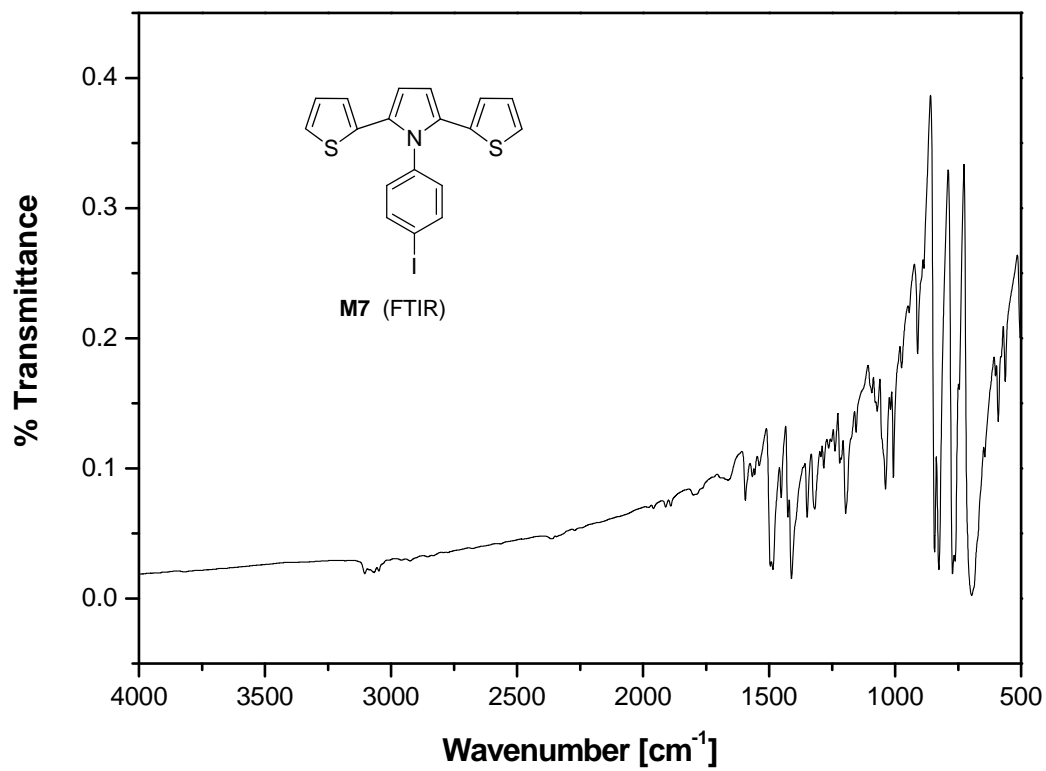
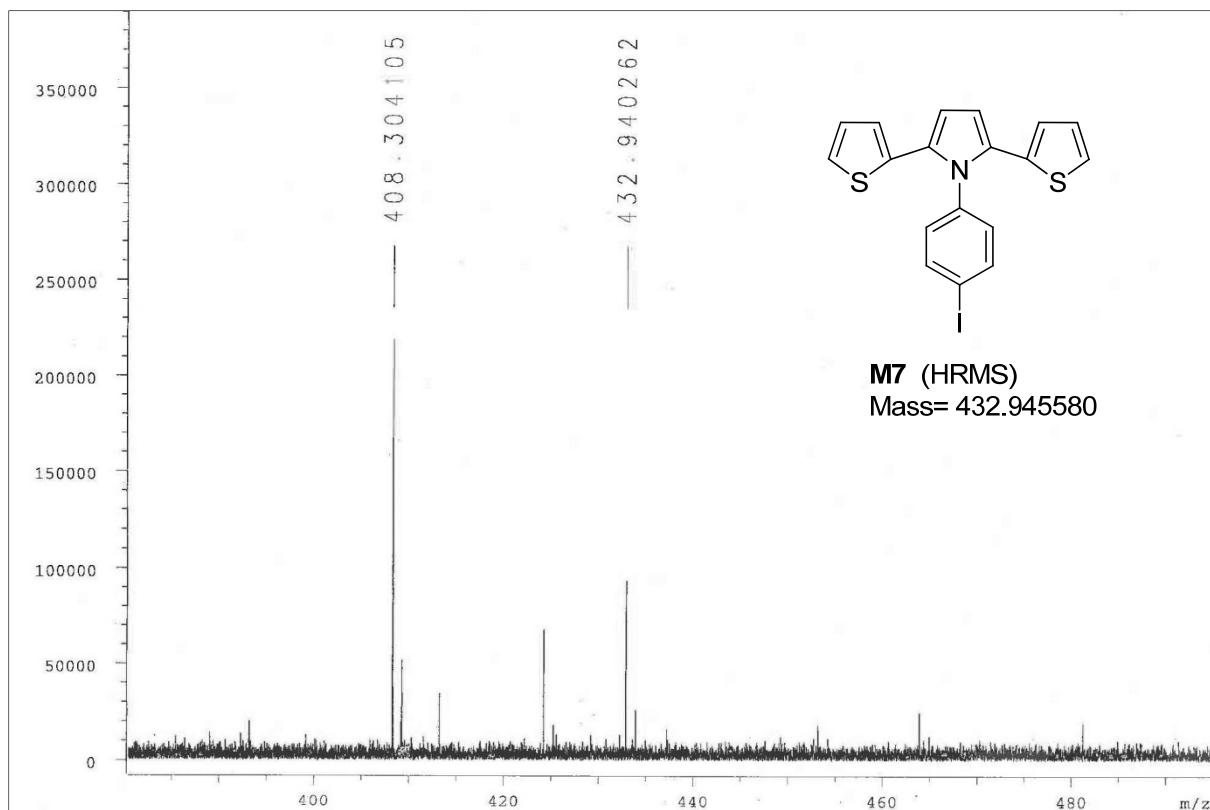
Analytical data of the compounds

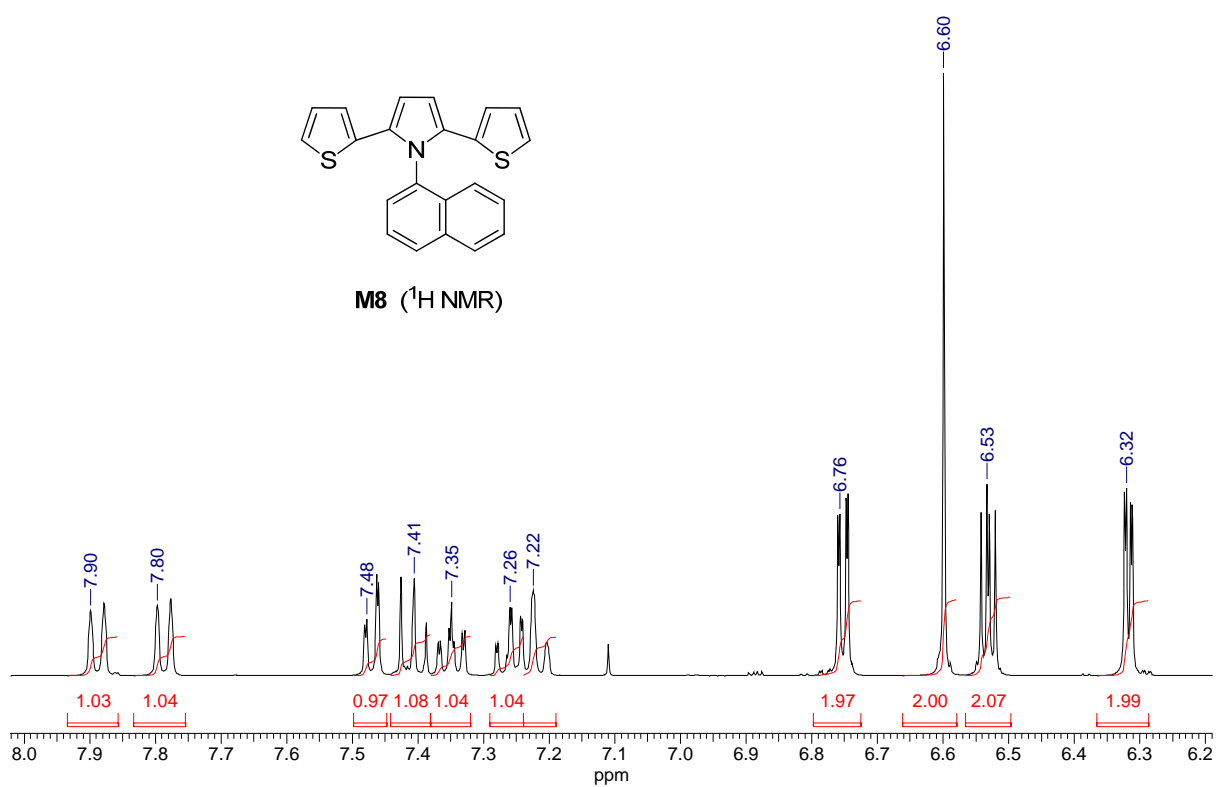
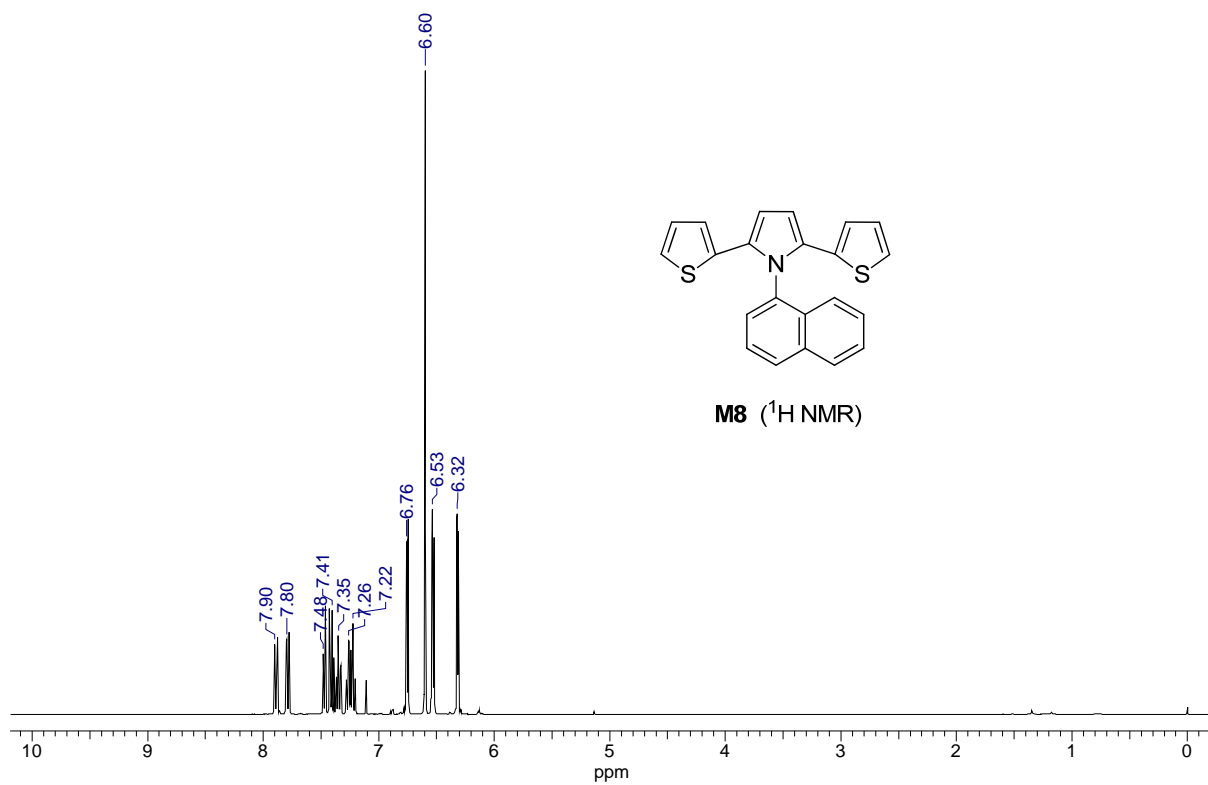


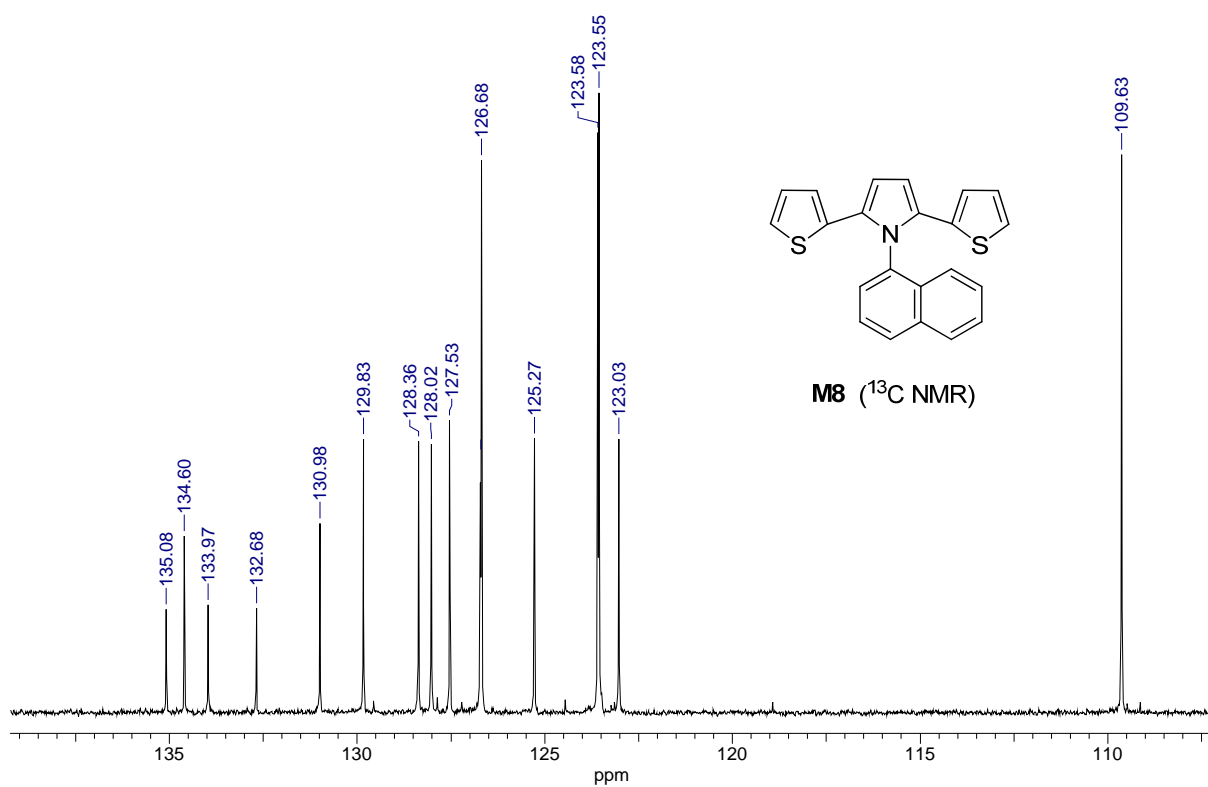
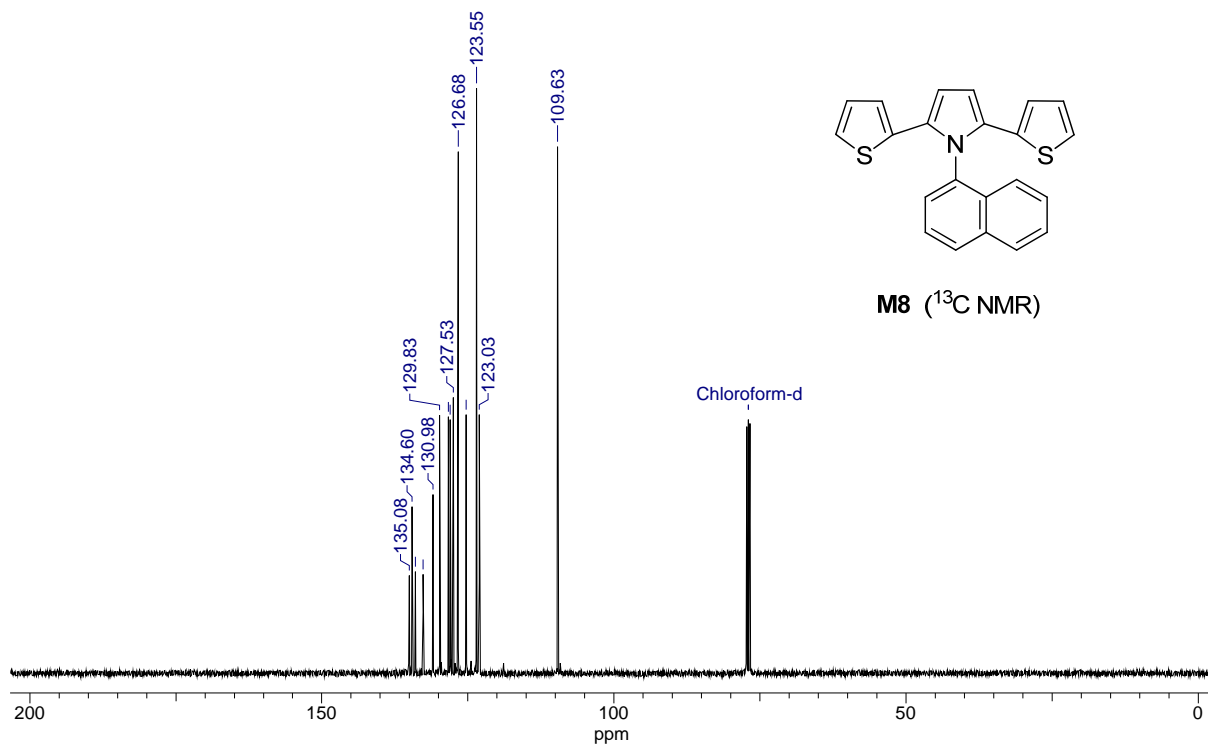


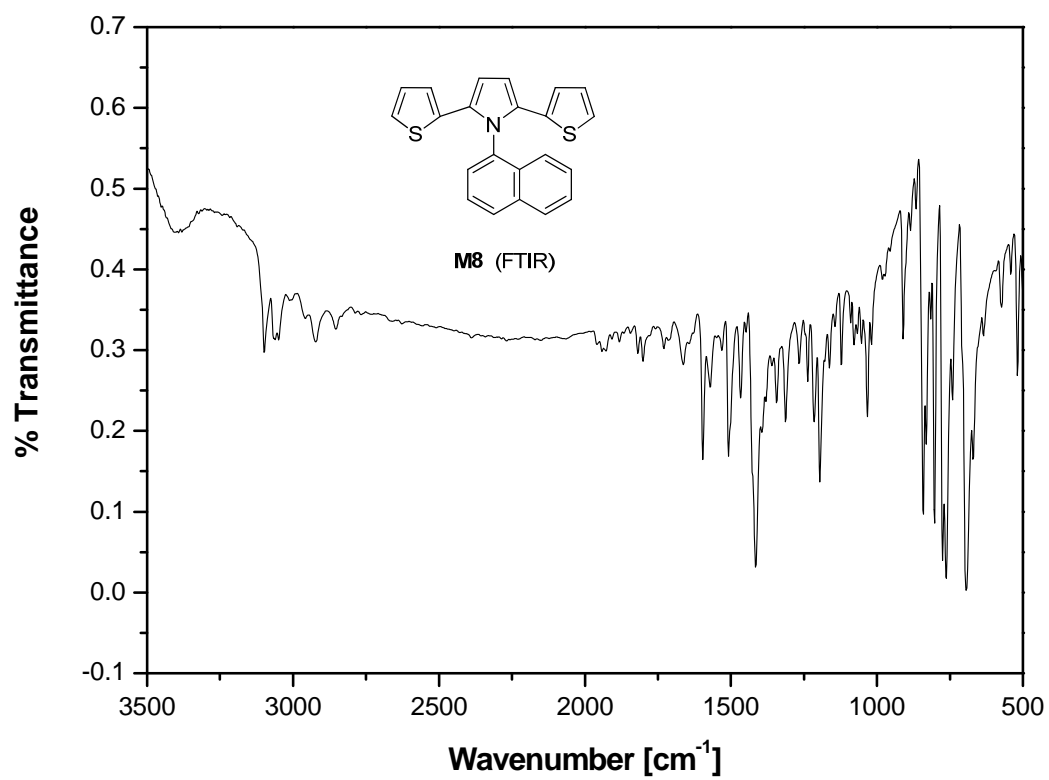
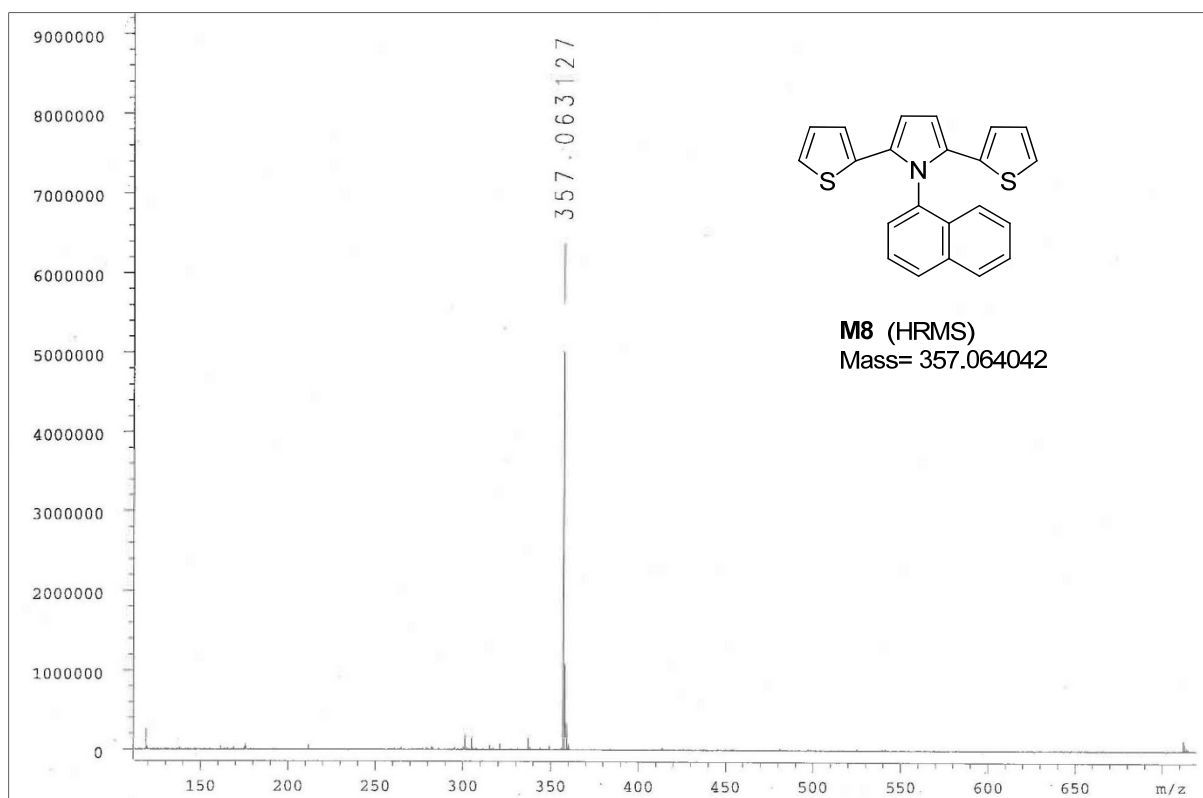


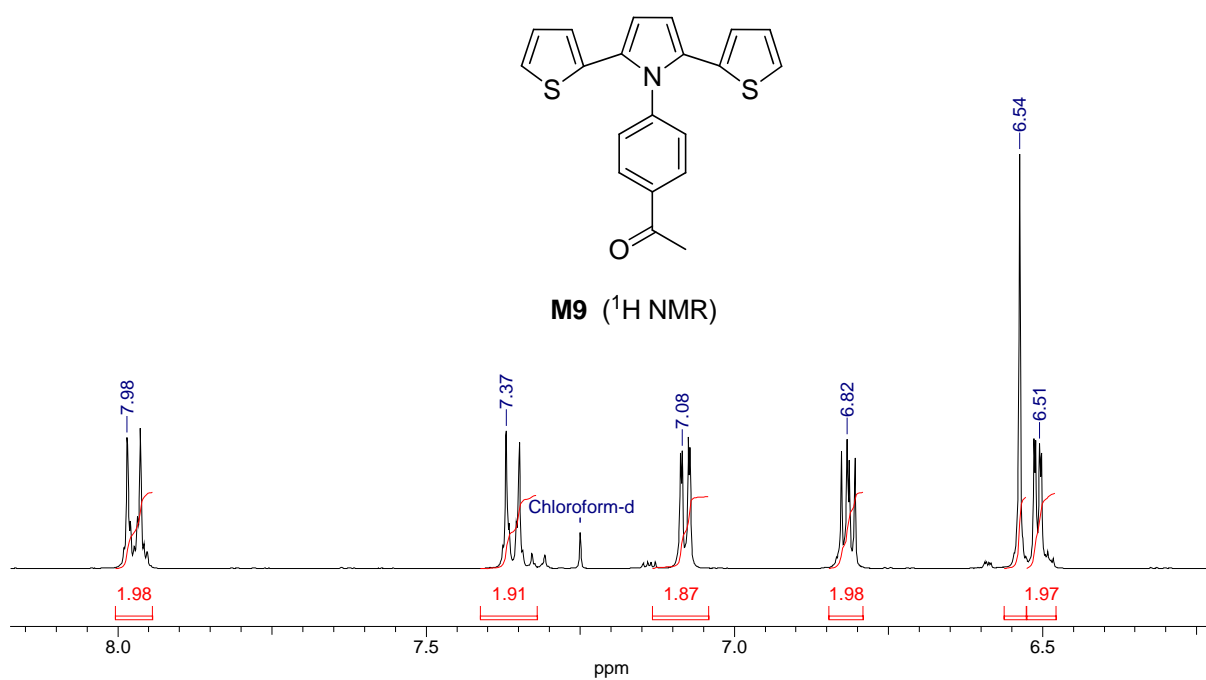
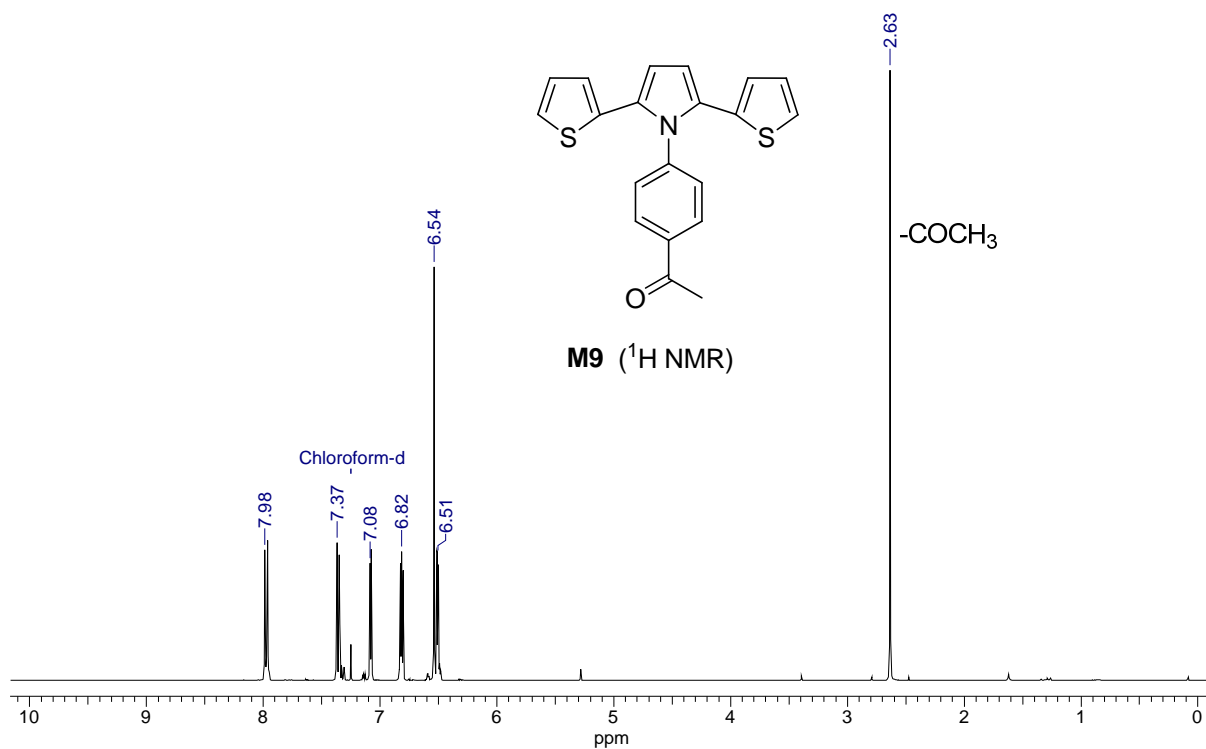


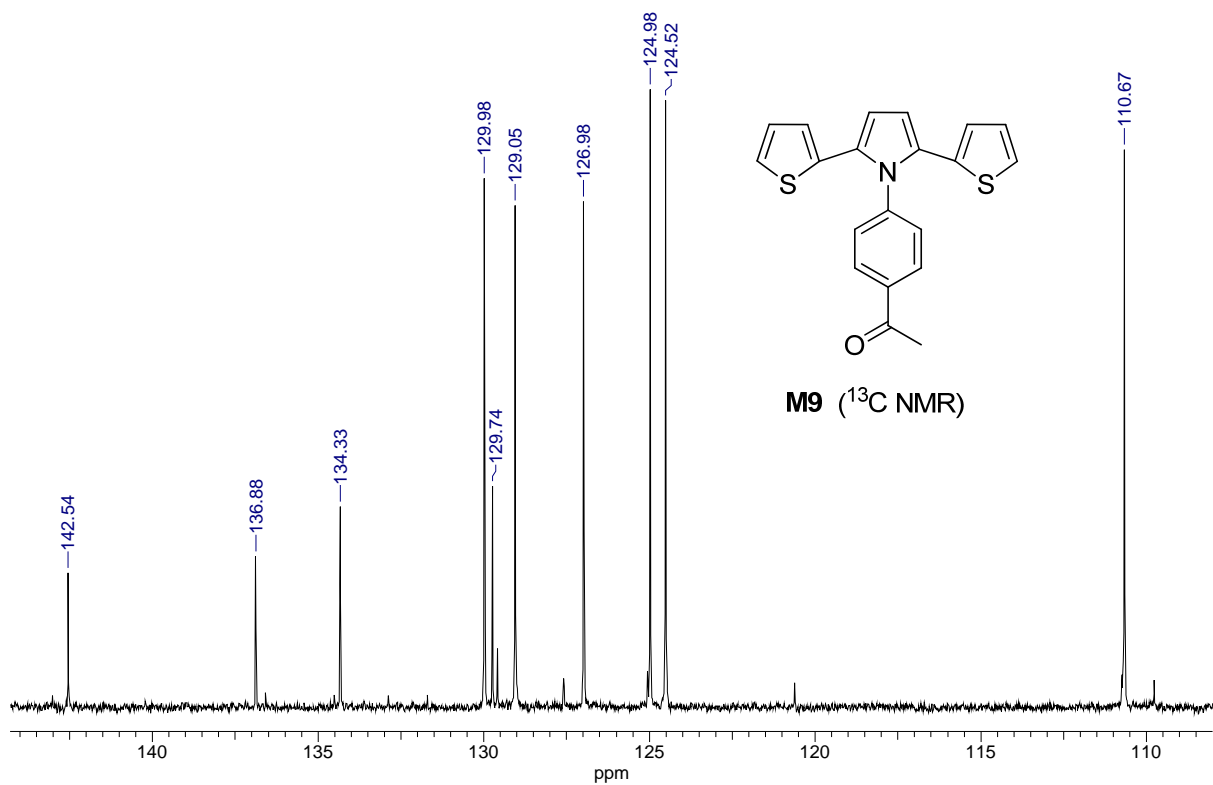
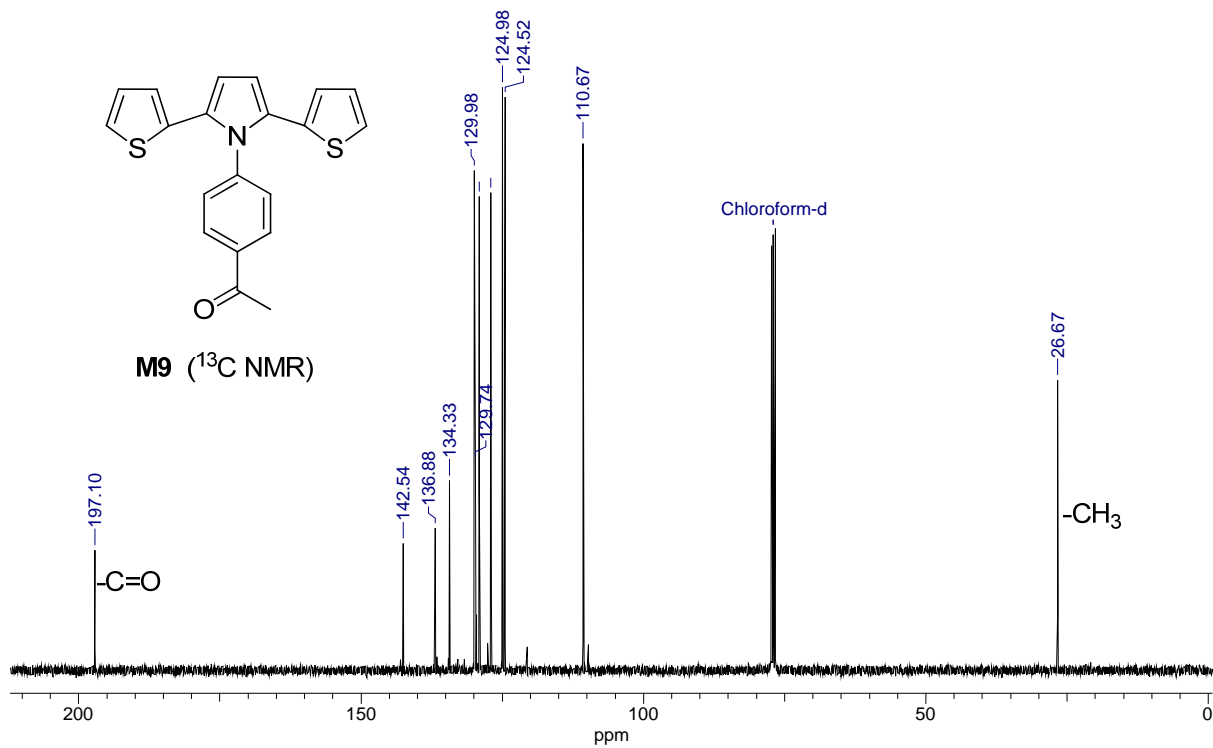




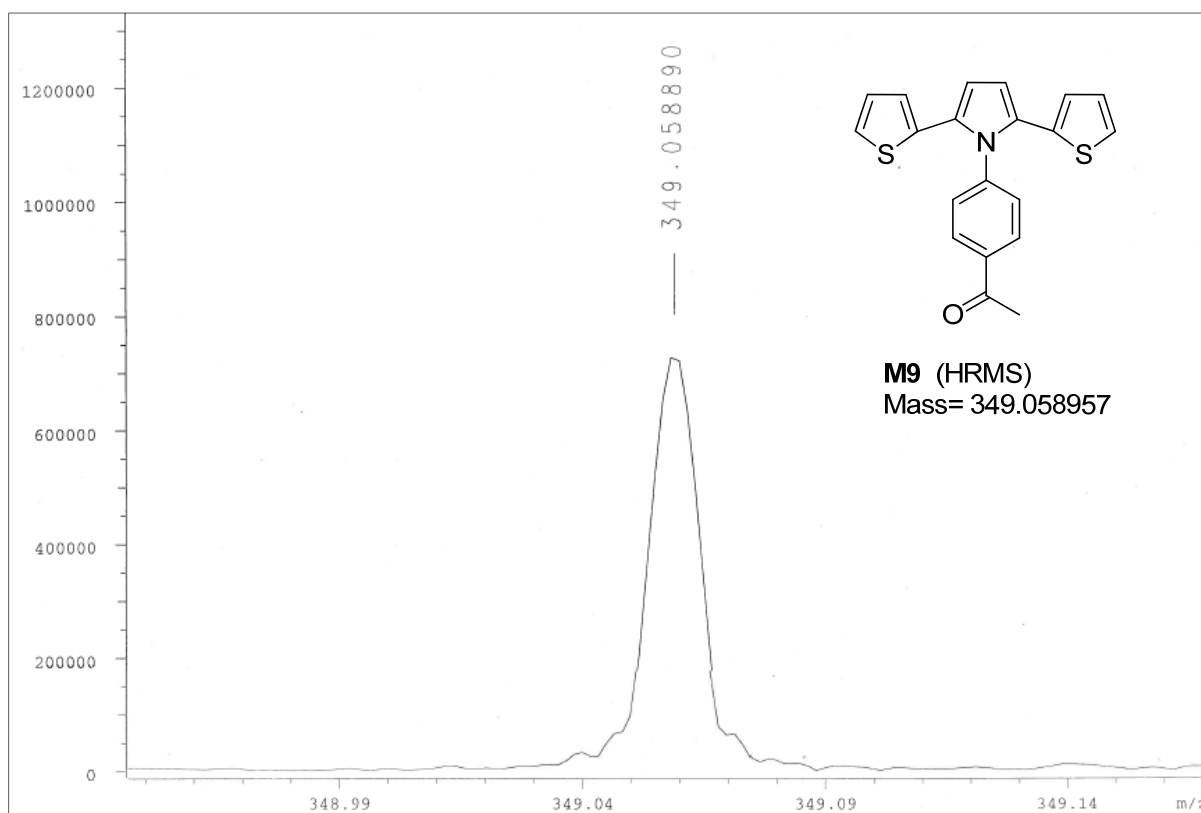
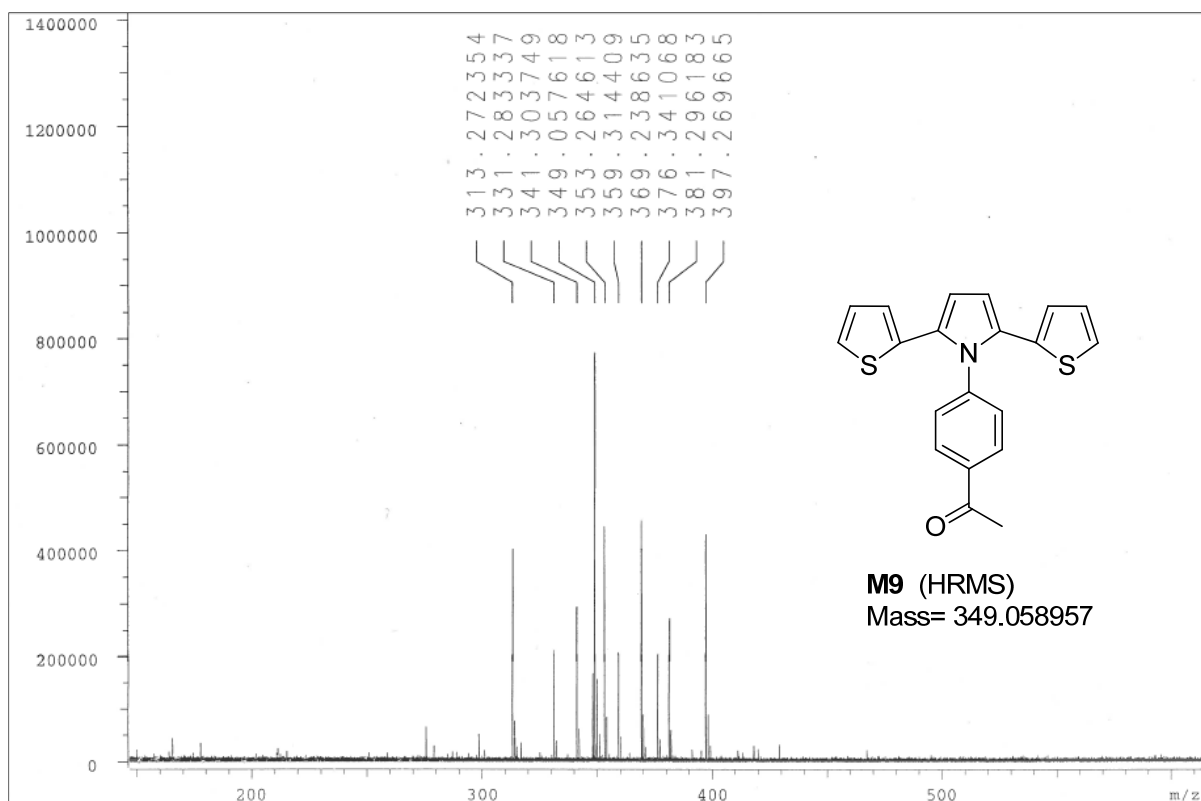


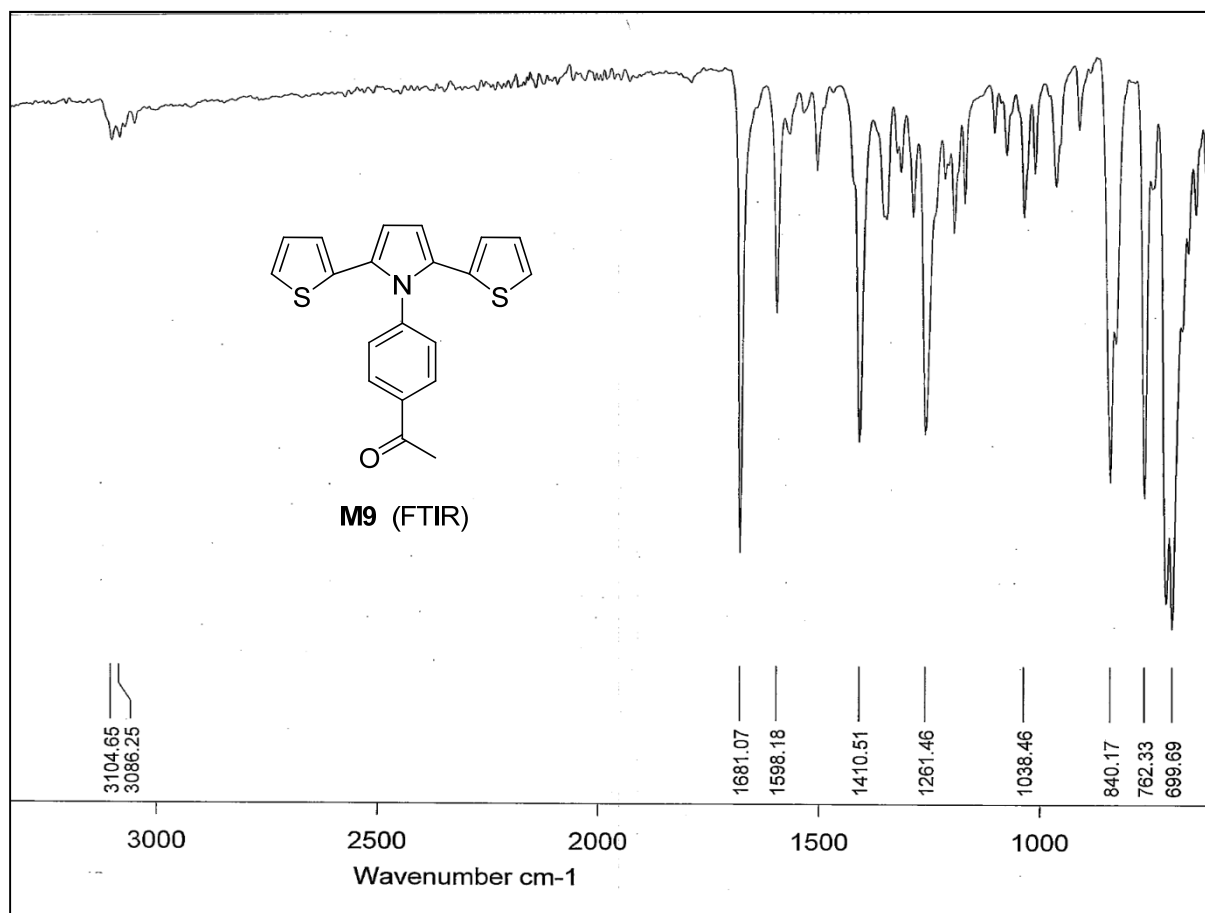


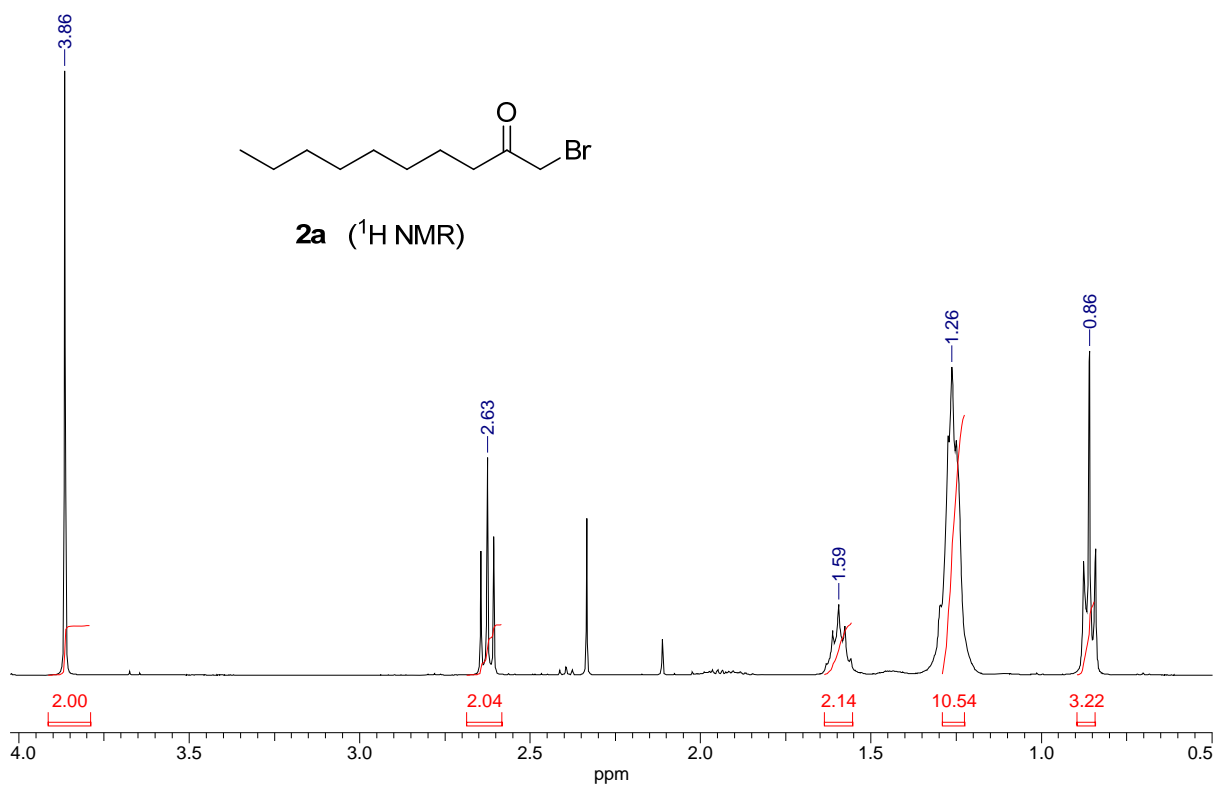
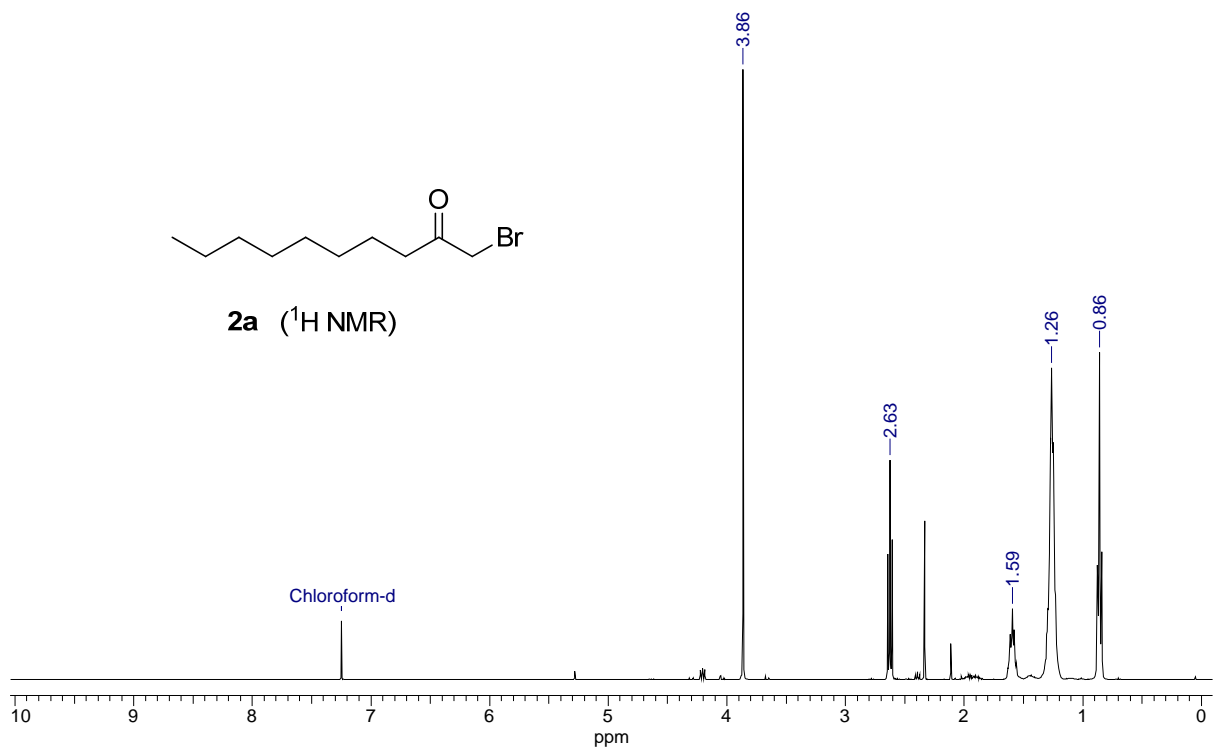


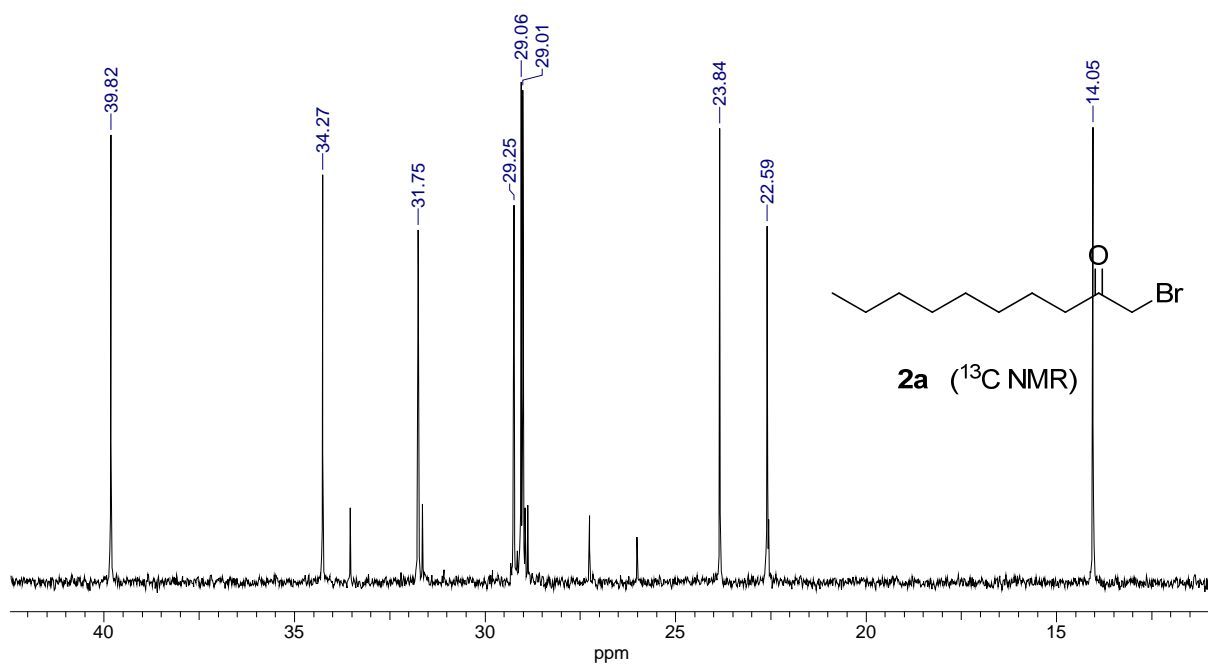
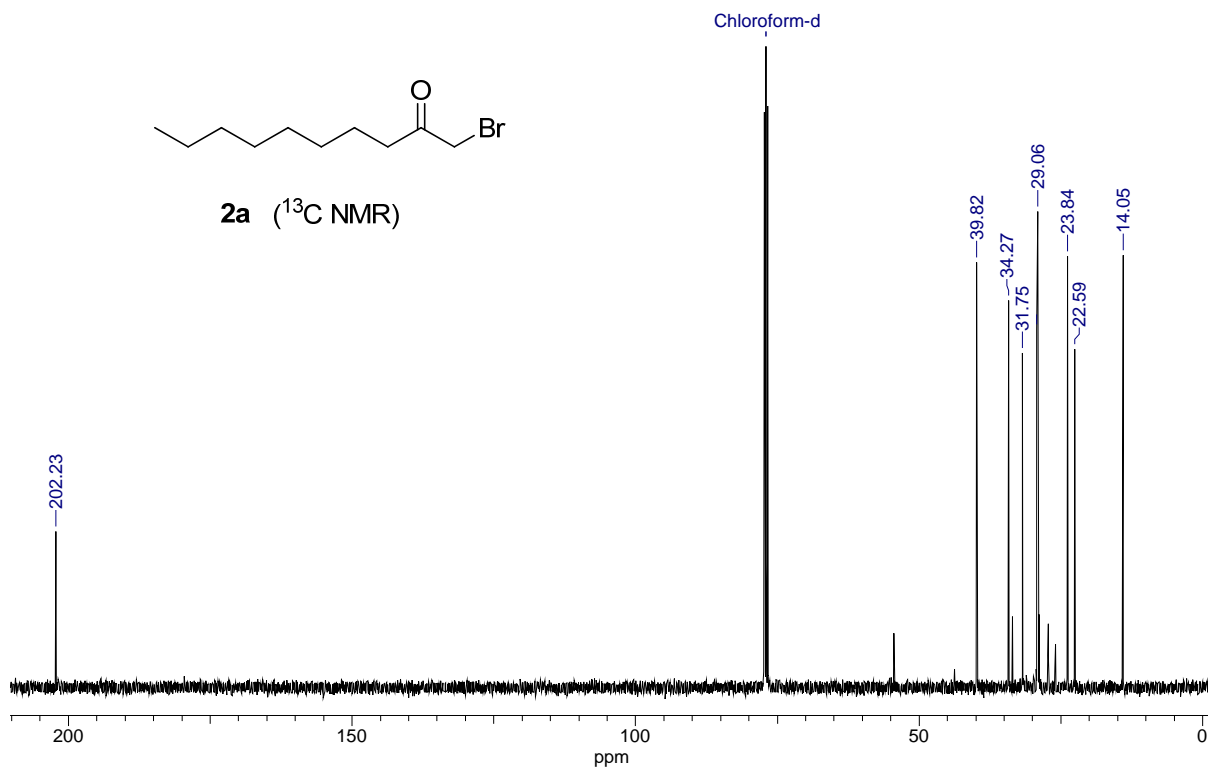


Analytical data of the compounds

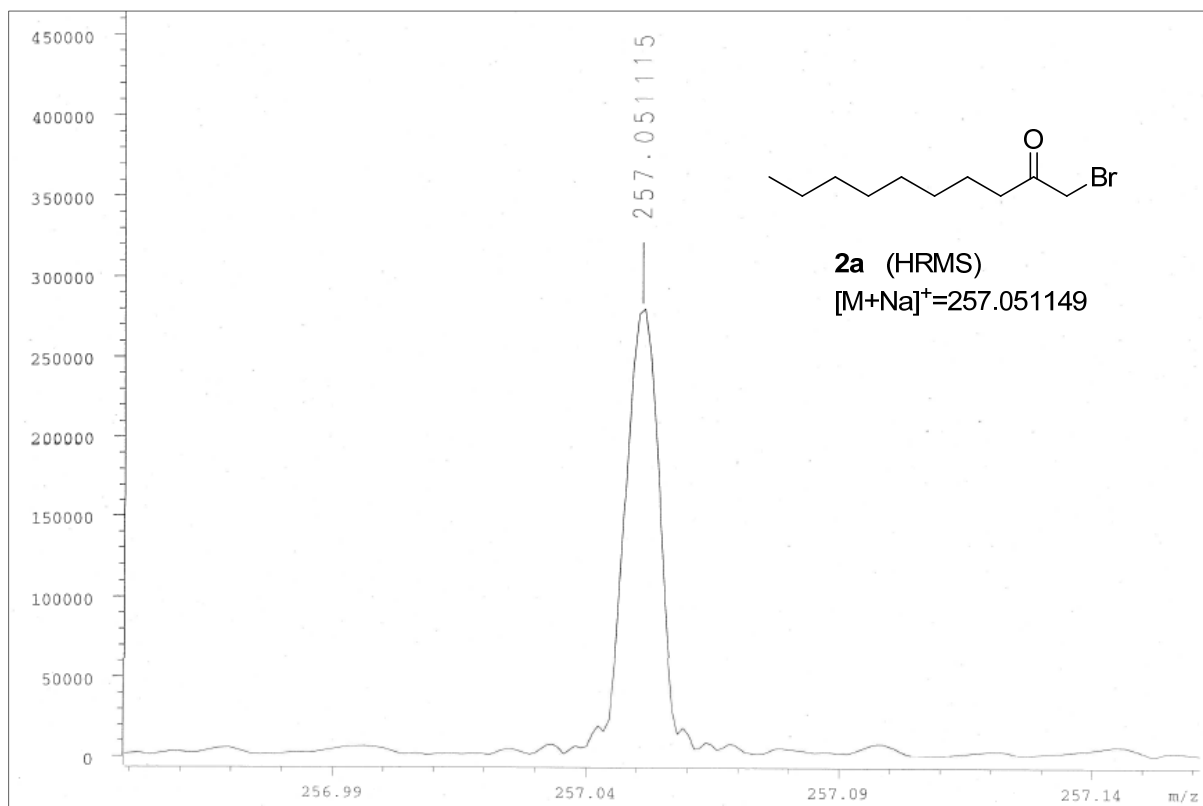
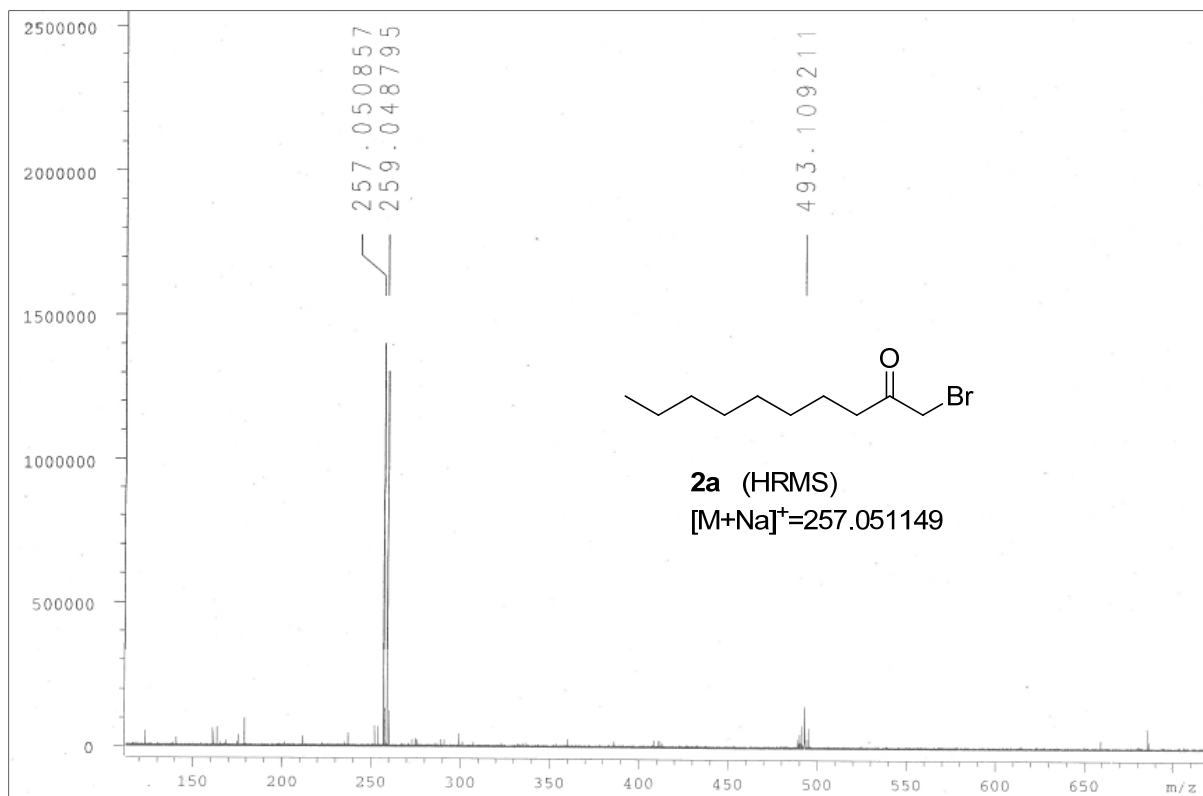


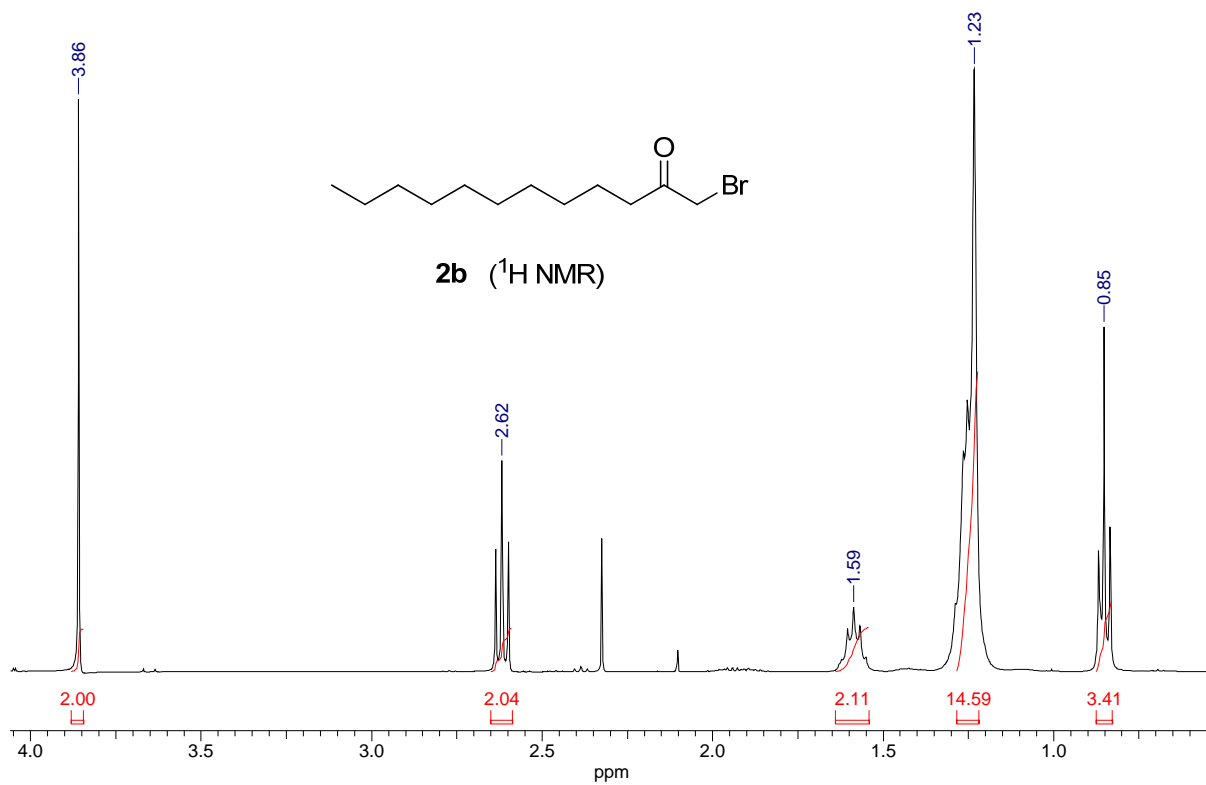
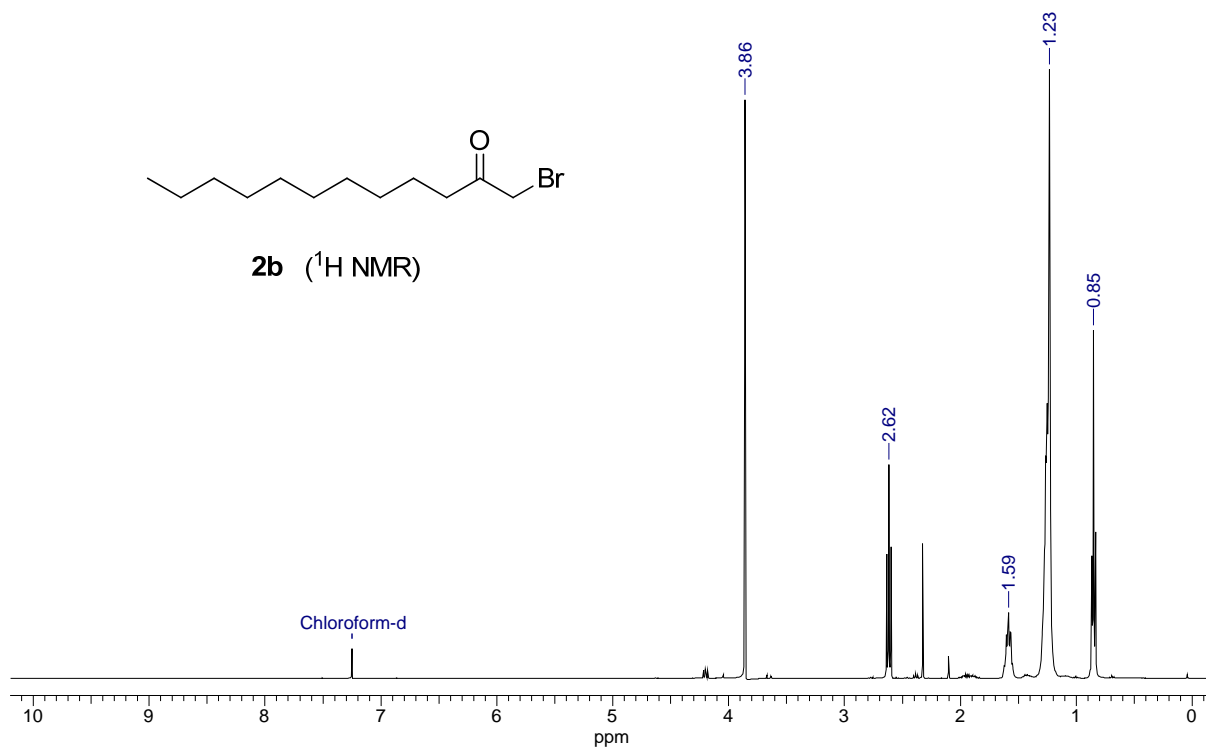


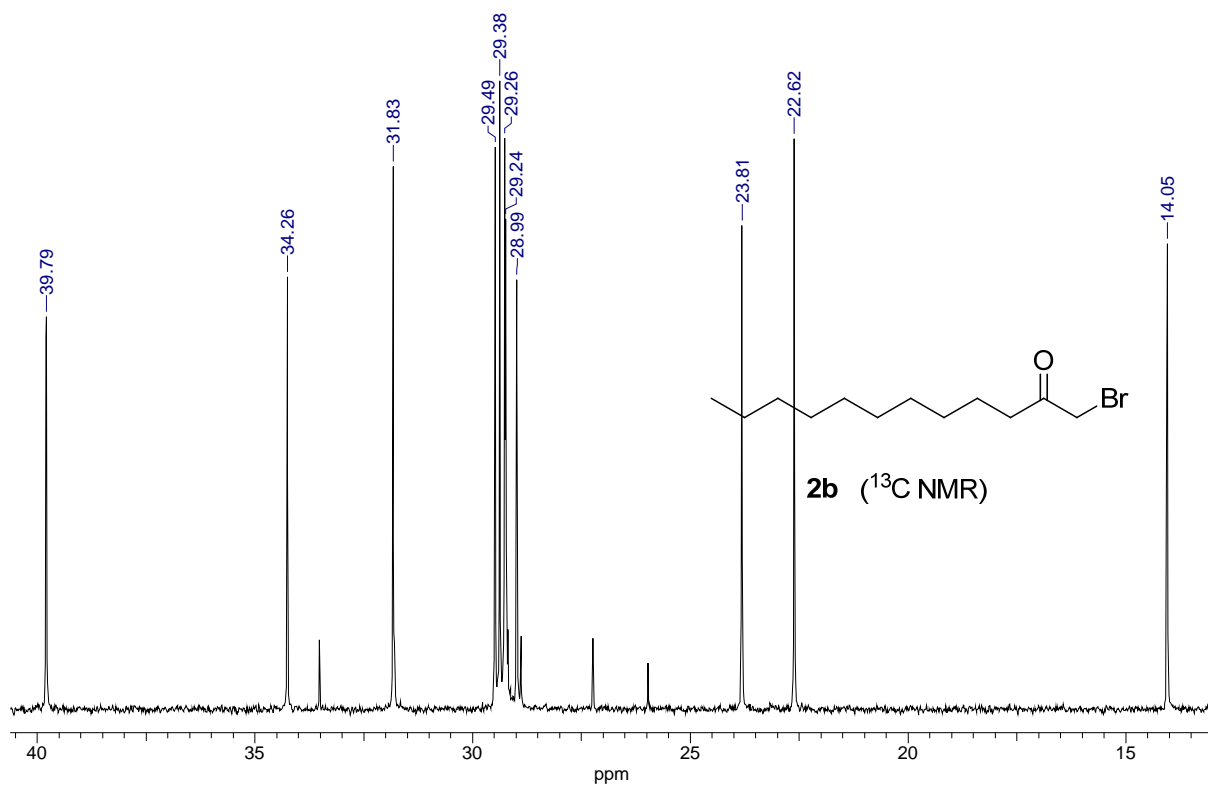
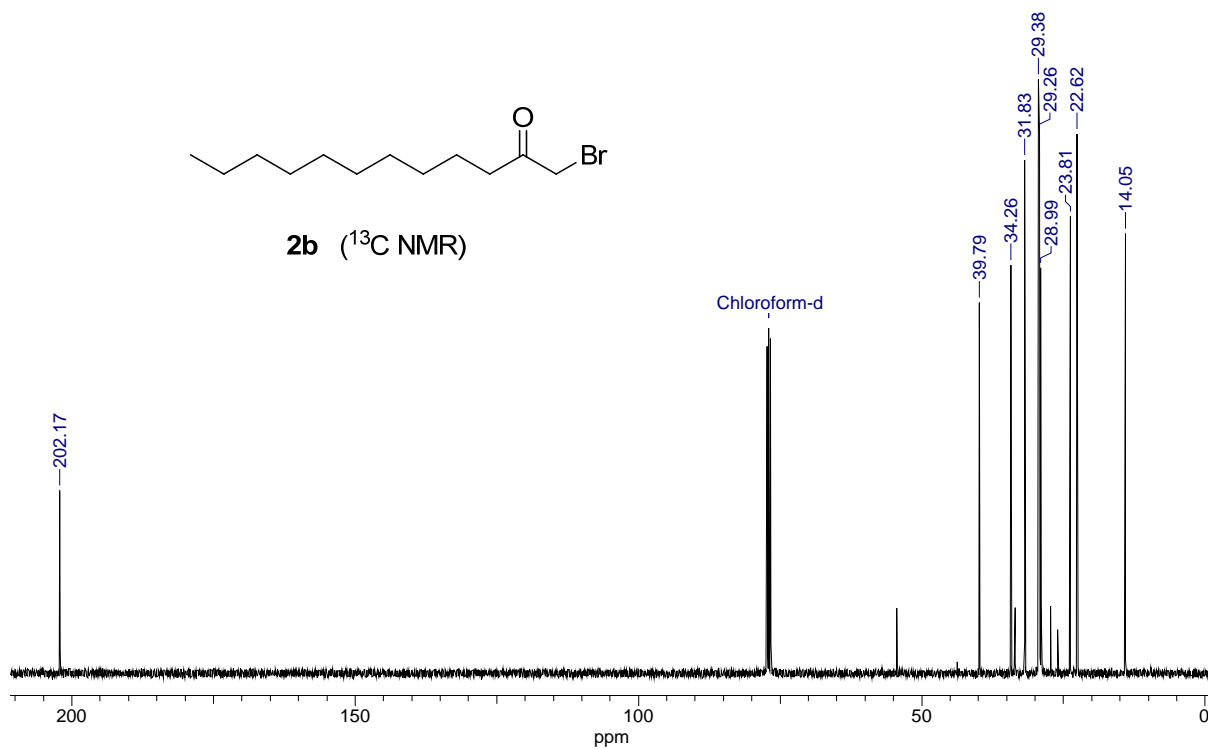




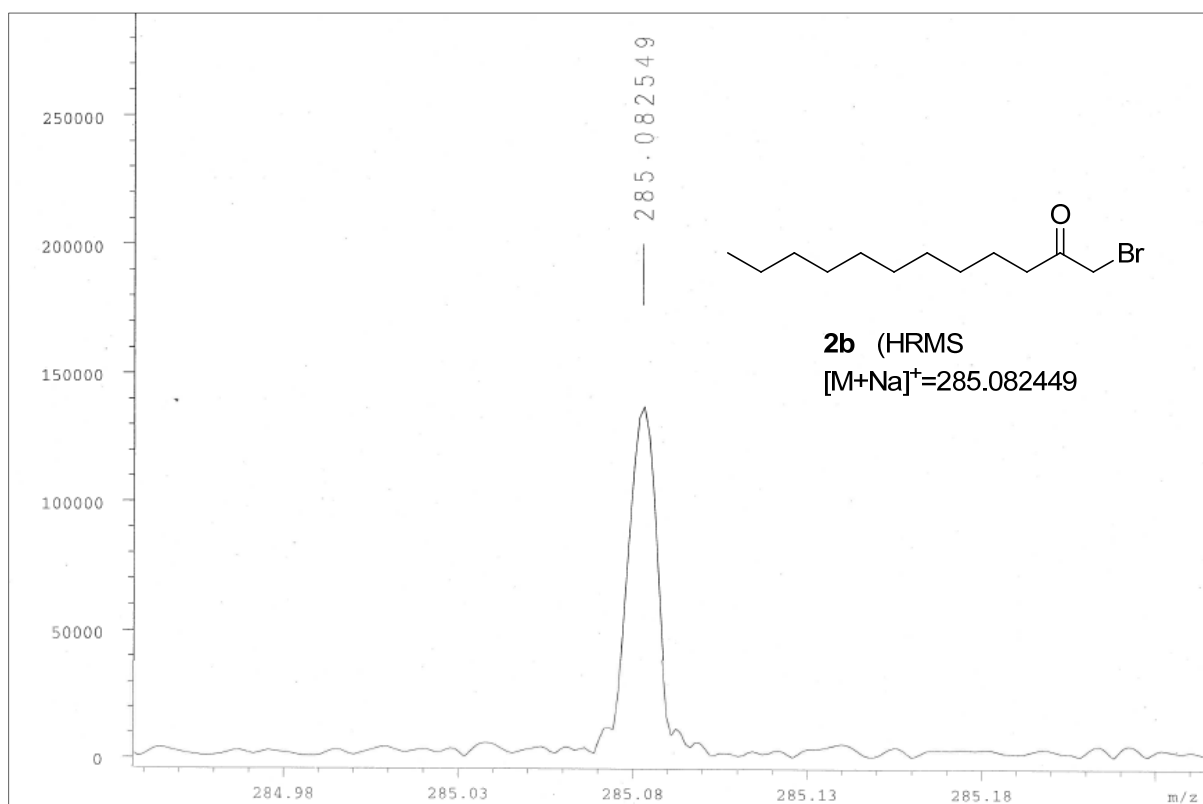
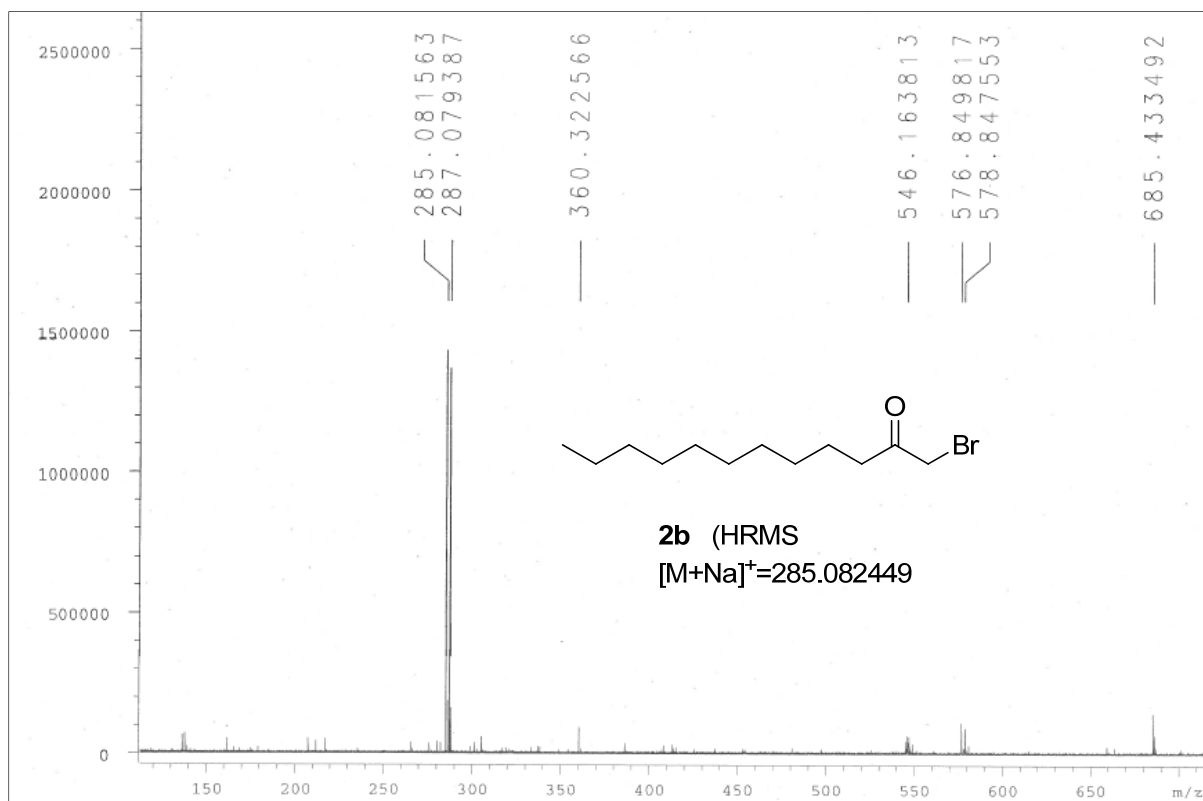
Analytical data of the compounds

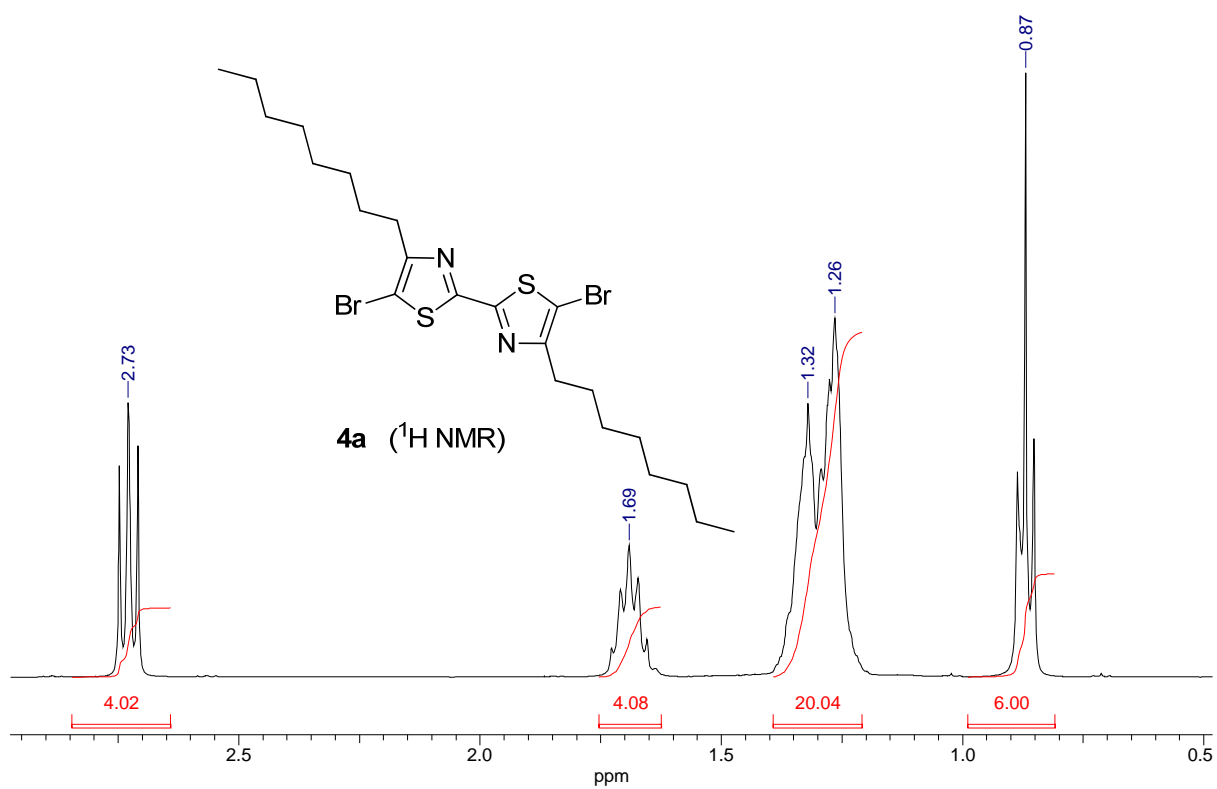
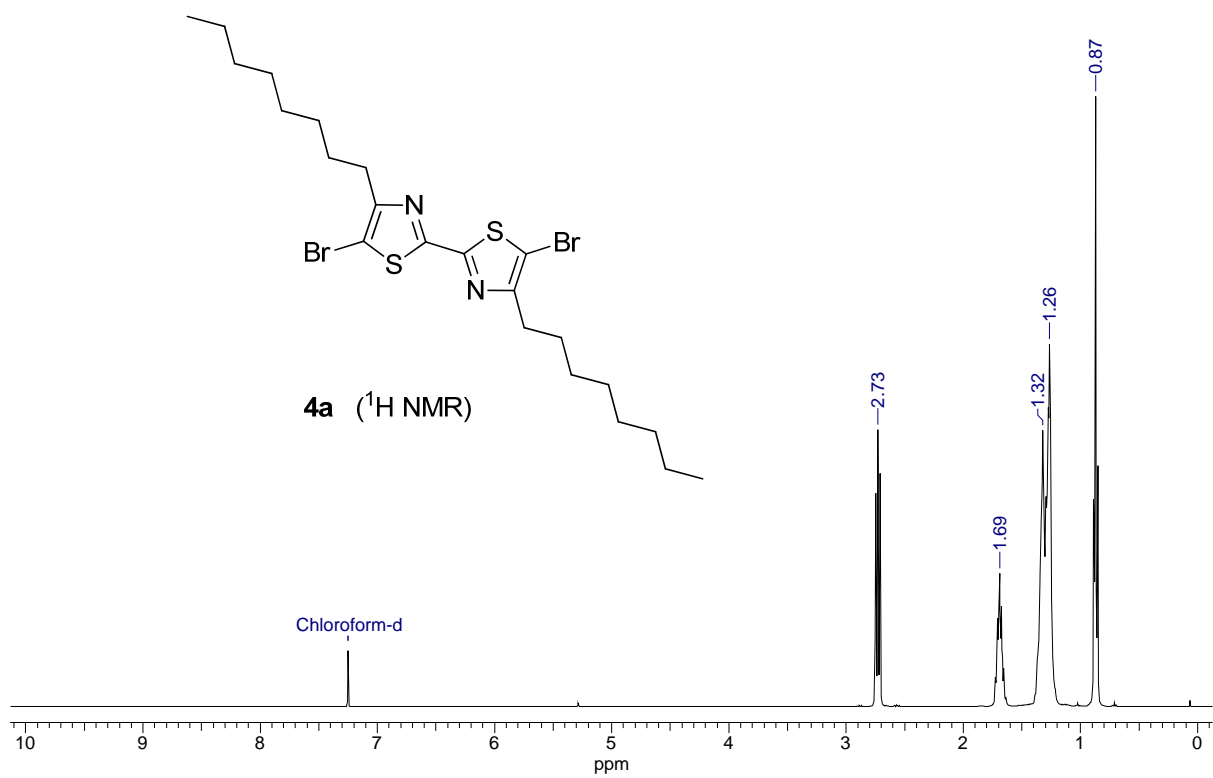


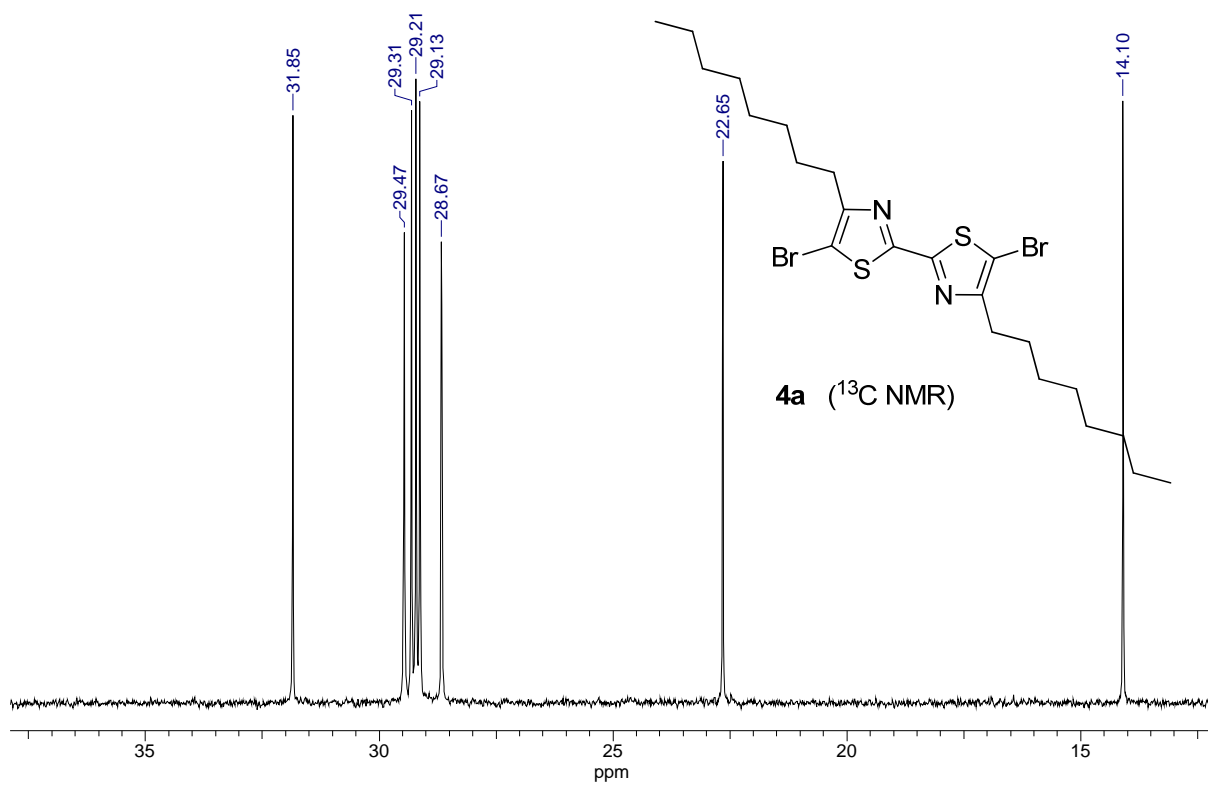
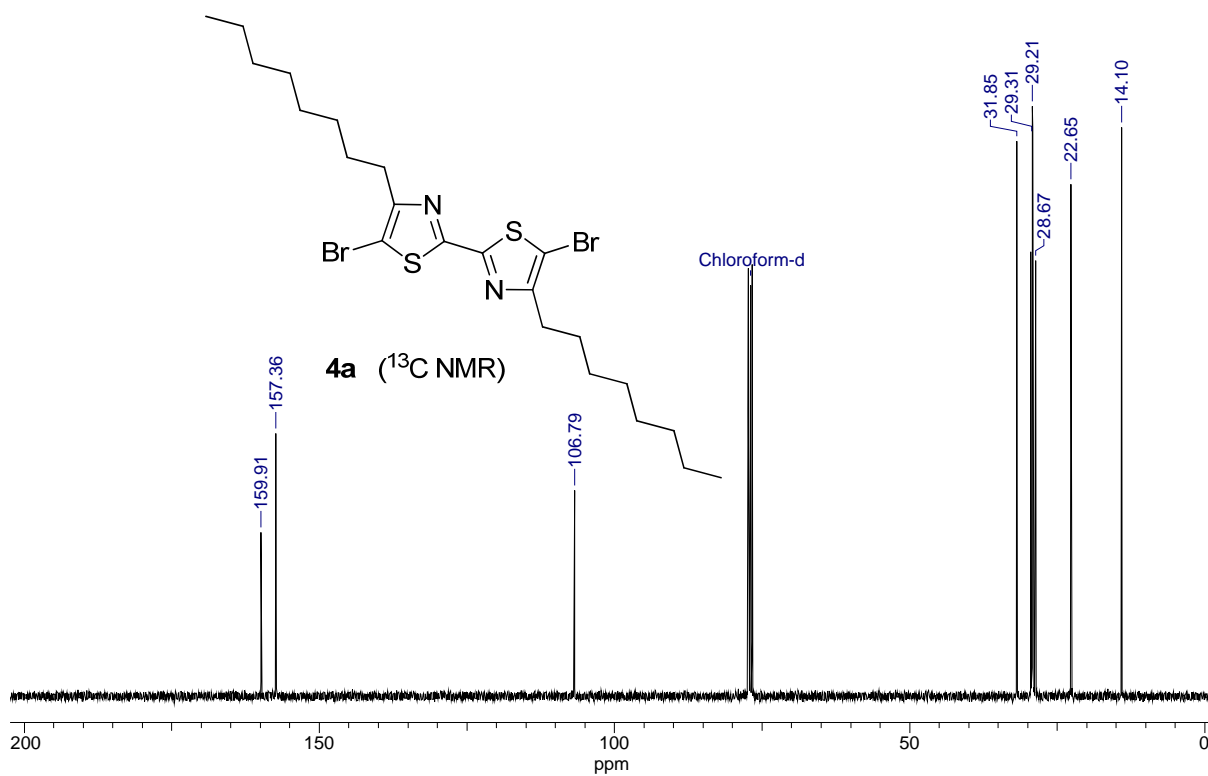


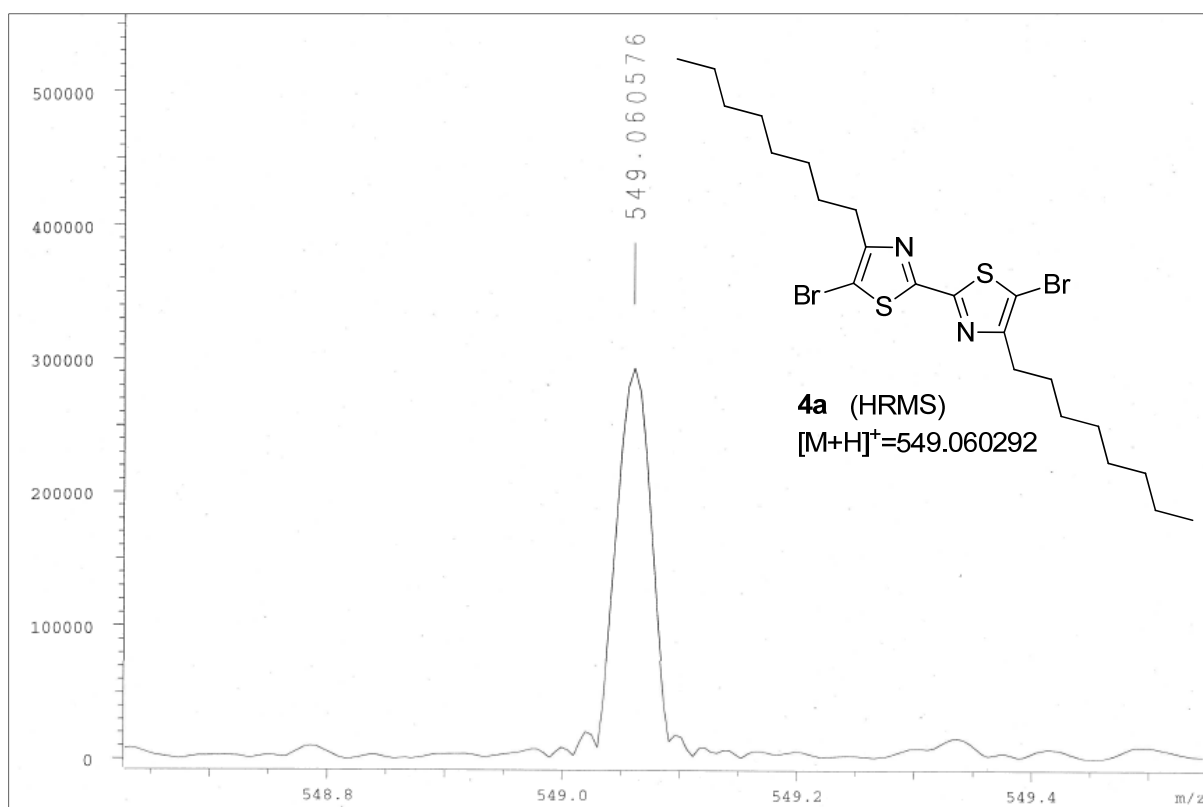
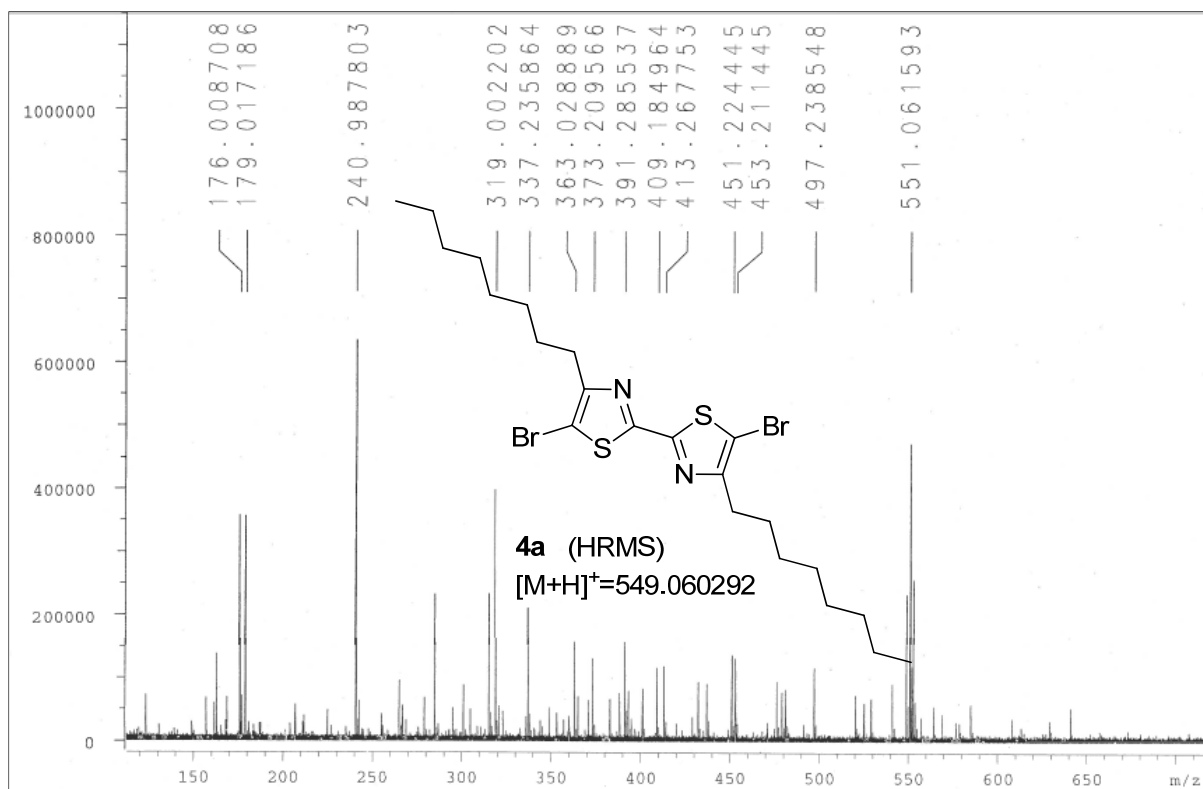


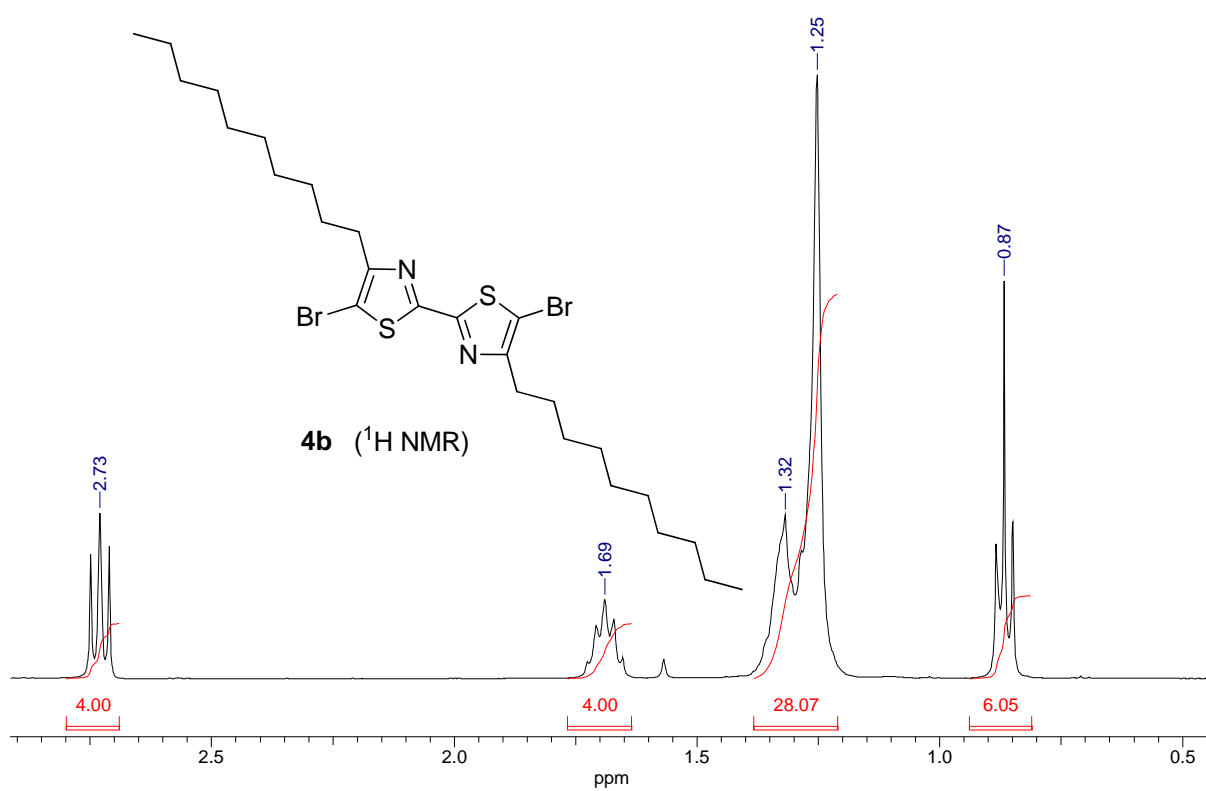
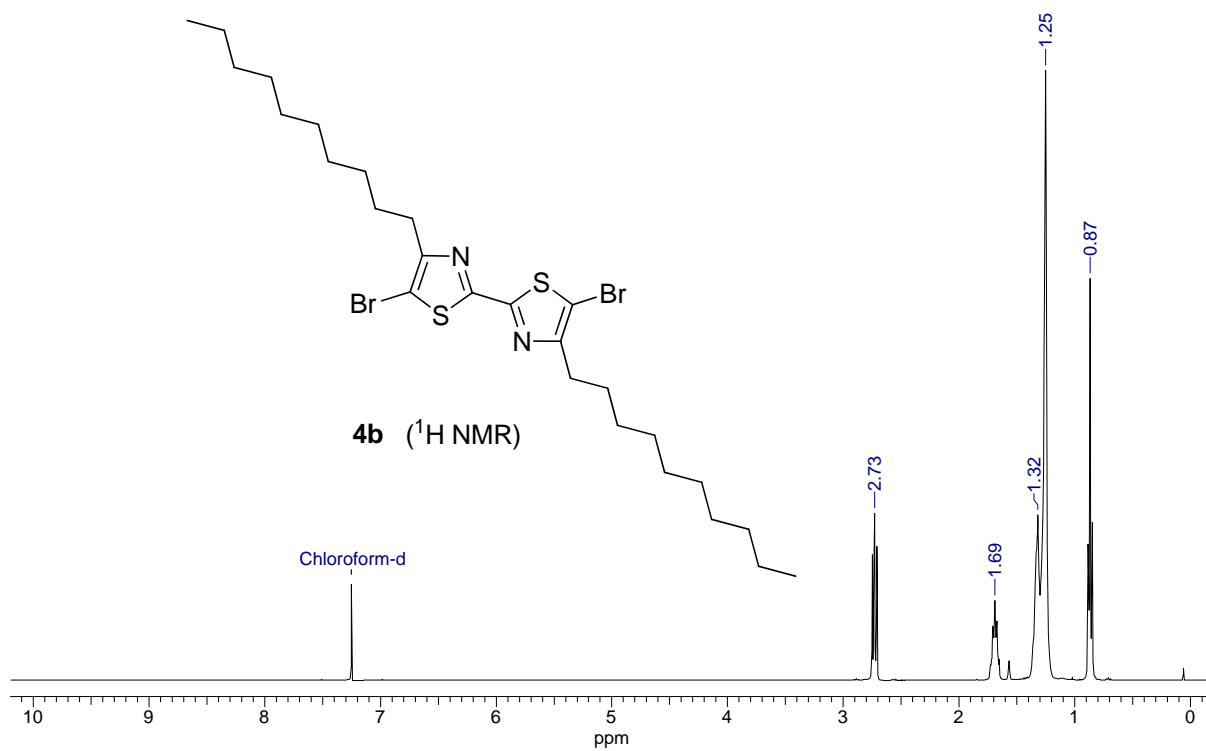
Analytical data of the compounds

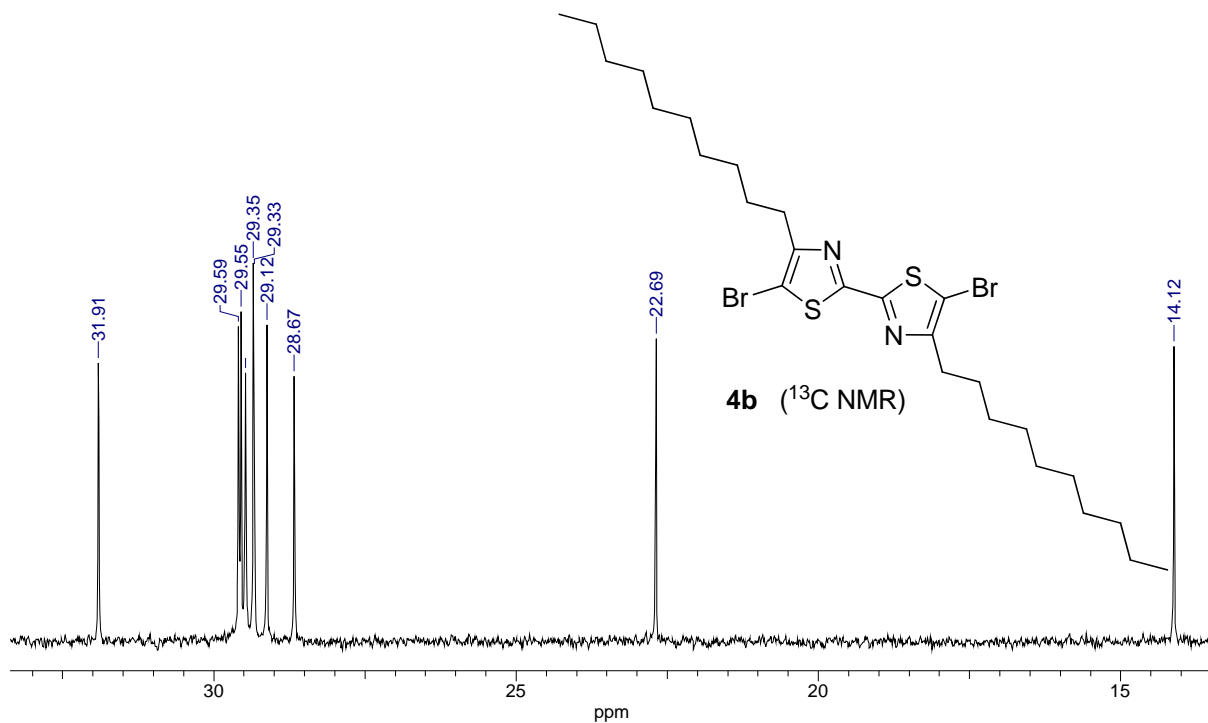
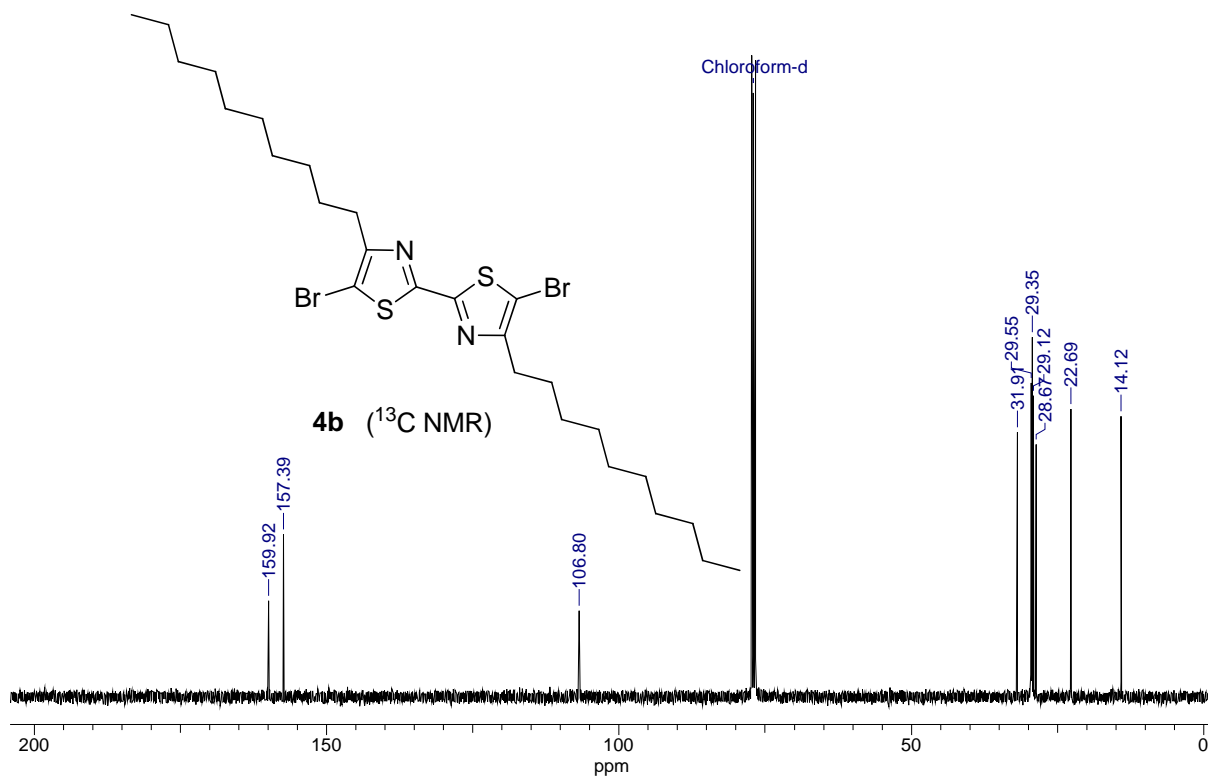


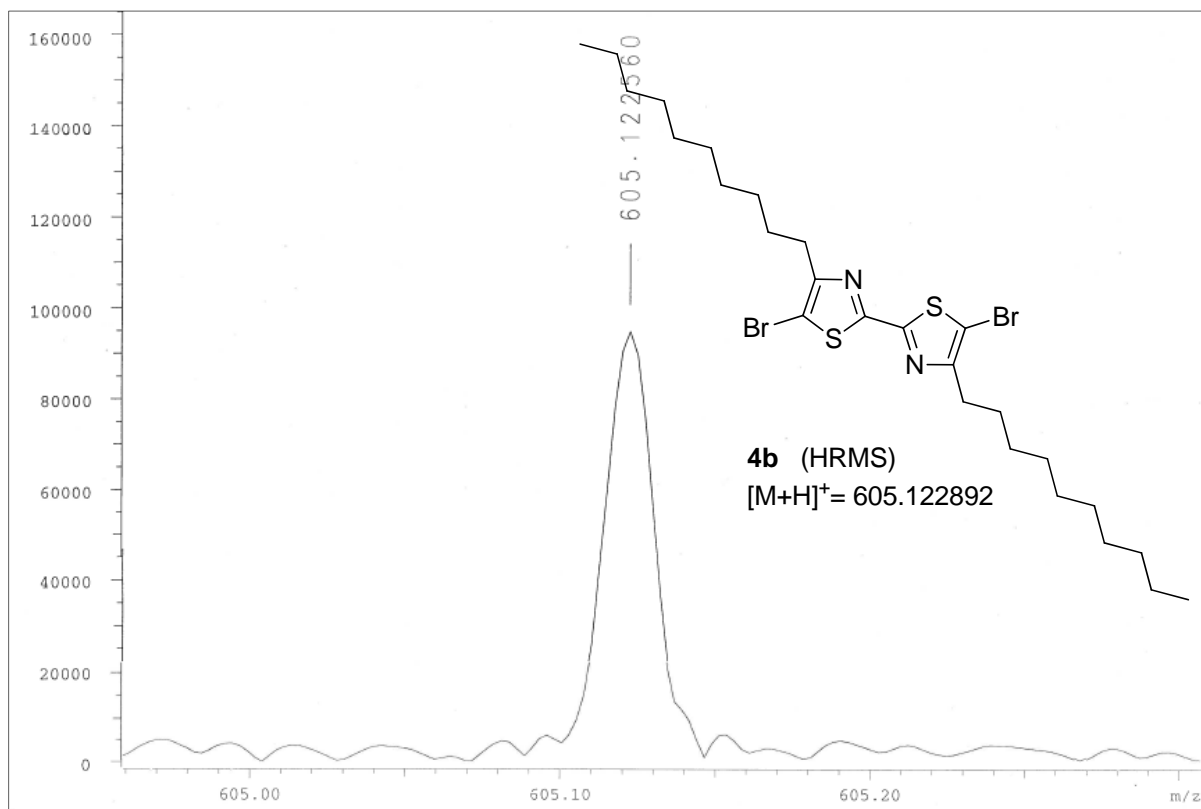
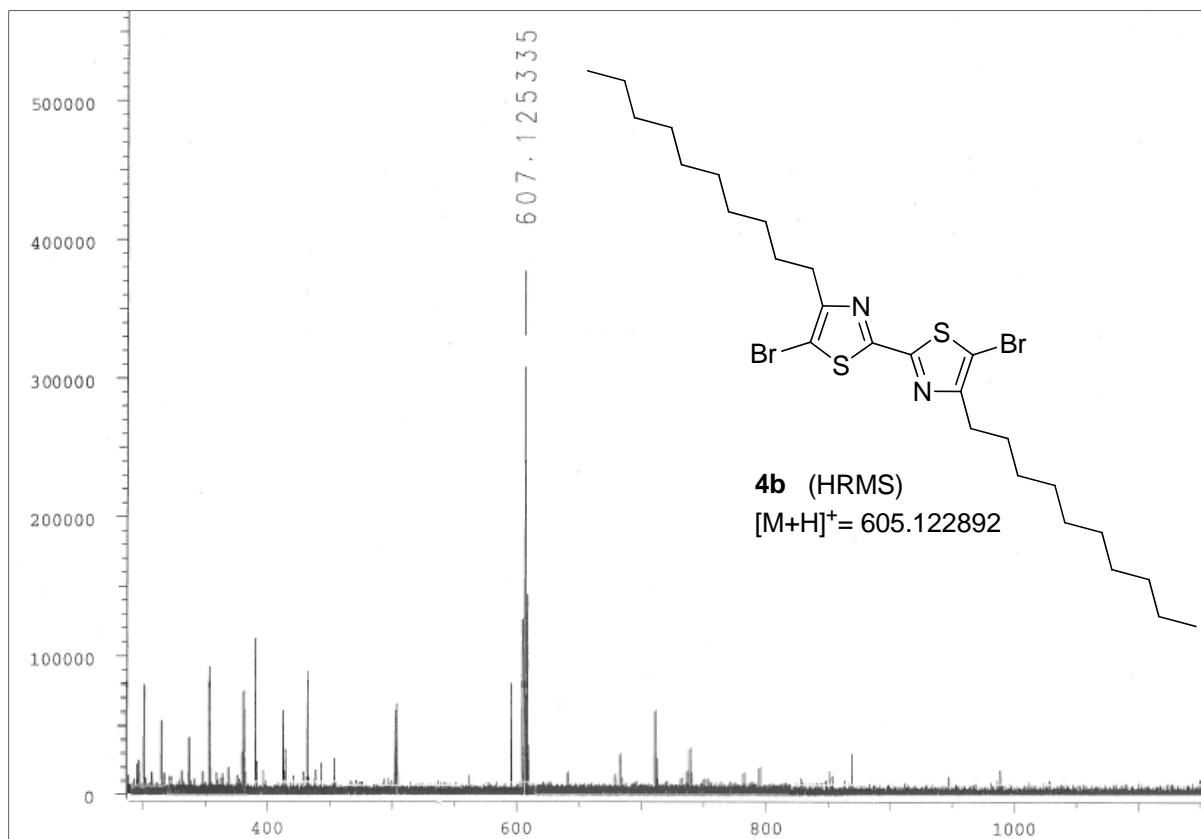












References

- [1] U. Nations and E. programme. *Food waste facts*. Available: <http://www.unep.org/wed/2013/quickfacts/>
- [2] M. S. Reid, M. J. C. Rhodes, and A. C. Hulme, "Changes in Ethylene and Co₂ during Ripening of Apples," *Journal of the Science of Food and Agriculture*, vol. 24, pp. 971-979, 1973.
- [3] G. Korotcenkov, *Chemical Sensors: Comprehensive sensor technologies*: Momentum Press, 2011.
- [4] K. Persaud and G. Dodd, "Analysis of Discrimination Mechanisms in the Mammalian Olfactory System Using a Model Nose," *Nature*, vol. 299, pp. 352-355, 1982.
- [5] J. V. Hatfield, P. Neaves, P. J. Hicks, K. Persaud, and P. Travers, "Towards an Integrated Electronic Nose Using Conducting Polymer Sensors," *Sensors and Actuators B-Chemical*, vol. 18, pp. 221-228, Mar 1994.
- [6] A. Pavlou, A. P. Turner, and N. Magan, "Recognition of anaerobic bacterial isolates in vitro using electronic nose technology," *Lett Appl Microbiol*, vol. 35, pp. 366-9, 2002.
- [7] A. P. Turner and N. Magan, "Electronic noses and disease diagnostics," *Nat Rev Microbiol*, vol. 2, pp. 161-6, Feb 2004.
- [8] A. K. Pavlou, N. Magan, D. Sharp, J. Brown, H. Barr, and A. P. Turner, "An intelligent rapid odour recognition model in discrimination of *Helicobacter pylori* and other gastroesophageal isolates in vitro," *Biosens Bioelectron*, vol. 15, pp. 333-42, Oct 2000.
- [9] A. Hulancki, S. Glab, and F. Ingman, "Chemical sensors definitions and classifications," *International union of pure and applied chemistry*, vol. 63, pp. 1247-1250, 1991.
- [10] H. E. Endres and S. Drost, "Optimization of the Geometry of Gas-Sensitive Interdigital Capacitors," *Sensors and Actuators B-Chemical*, vol. 4, pp. 95-98, May 1991.
- [11] A. Oprea, J. Courbat, N. Barsan, D. Briand, N. F. de Rooji, and U. Weimar, "Temperature, humidity and gas sensors integrated on plastic foil for low power applications," *Sensors and Actuators B-Chemical*, vol. 140, pp. 227-232, 2009.
- [12] A. Bearzotti, V. Foglietti, G. Polzonetti, G. Iucci, A. Furlani, and M. V. Russo, "Investigations on the response to humidity of an interdigitated electrode structure coated with iodine doped polyphenylacetylene," *Materials Science and Engineering B-Solid State Materials for Advanced Technology*, vol. 40, pp. 1-4, Aug 1996.
- [13] R. Zhou, A. Hierlemann, U. Weimar, and W. Gopel, "Gravimetric, dielectric and calorimetric methods for the detection of organic solvent vapours using poly(ether urethane) coatings," *Sensors and Actuators B-Chemical*, vol. 34, pp. 356-360, Aug 1996.
- [14] C. Hagleitner, A. Hierlemann, D. Lange, A. Kummer, N. Kerness, O. Brand, and H. Baltes, "Smart single-chip gas sensor microsystem," *Nature*, vol. 414, pp. 293-6, Nov 15 2001.
- [15] P. I. Neaves and J. V. Hatfield, "A New-Generation of Integrated Electronic Noses," *Sensors and Actuators B-Chemical*, vol. 27, pp. 223-231, Jun 1995.
- [16] A. C. Partridge, M. L. Jansen, and W. M. Arnold, "Conducting polymer-based sensors," *Materials Science & Engineering C-Biomimetic and Supramolecular Systems*, vol. 12, pp. 37-42, Aug 18 2000.
- [17] E. Schaller, J. O. Bosset, and F. Escher, "Instability of conducting polymer sensors in an electronic nose system," *Analisis*, vol. 28, pp. 217-227, Apr 2000.
- [18] J. Janata and M. Josowicz, "Conducting polymers in electronic chemical sensors," *Nature Materials*, vol. 2, pp. 19-24, Jan 2003.
- [19] H. Bai and G. Q. Shi, "Gas sensors based on conducting polymers," *Sensors*, vol. 7, pp. 267-307, Mar 2007.
- [20] P. D. Harris, W. M. Arnold, M. K. Andrews, and A. C. Partridge, "Resistance characteristics of conducting polymer films used in gas sensors," *Sensors and Actuators B-Chemical*, vol. 42, pp. 177-184, Aug 1997.

- [21] E. Krivan, C. Visy, R. Dobay, G. Harsanyi, and O. Berkesi, "Irregular response of the polypyrrole films to H₂S," *Electroanalysis*, vol. 12, pp. 1195-1200, Oct 2000.
- [22] F. Musio, M. E. H. Amrani, and K. C. Persaud, "High-Frequency Ac Investigation of Conducting Polymer Gas Sensors," *Sensors and Actuators B-Chemical*, vol. 23, pp. 223-226, Feb 1995.
- [23] F. Musio and M. C. Ferrara, "Low frequency a.c. response of polypyrrole gas sensors," *Sensors and Actuators B-Chemical*, vol. 41, pp. 97-103, Jun 30 1997.
- [24] N. Barsan, D. Koziej, and U. Weimar, "Metal oxide-based gas sensor research: How to?," *Sensors and Actuators B-Chemical*, vol. 121, pp. 18-35, Jan 30 2007.
- [25] G. F. Fine, L. M. Cavanagh, A. Afonja, and R. Binions, "Metal Oxide Semi-Conductor Gas Sensors in Environmental Monitoring," *Sensors*, vol. 10, pp. 5469-5502, Jun 2010.
- [26] C. A. Papadopoulos, D. S. Vlachos, and J. N. Avaritsiotis, "A new planar device based on Seebeck effect for gas sensing applications," *Sensors and Actuators B-Chemical*, vol. 34, pp. 524-527, Aug 1996.
- [27] N. Rao, C. M. Vandendriek, and J. Shoonman, "Taguchi-Type Nox Gas Sensors Based on Semiconducting Mixed Oxides," *Solid State Ionics*, vol. 59, pp. 263-270, Feb 1993.
- [28] J. Huusko, V. Lantto, and H. Torvela, "TiO₂ Thick-Film Gas Sensors and Their Suitability for No(X) Monitoring," *Sensors and Actuators B-Chemical*, vol. 16, pp. 245-248, Oct 1993.
- [29] D. Kohl, L. Heinert, J. Bock, T. Hofmann, and P. Schieberle, "Systematic studies on responses of metal-oxide sensor surfaces to straight chain alkanes, alcohols, aldehydes, ketones, acids and esters using the SOMMSA approach," *Sensors and Actuators B-Chemical*, vol. 70, pp. 43-50, Nov 1 2000.
- [30] G. Eranna, B. C. Joshi, D. P. Runthala, and R. P. Gupta, "Oxide materials for development of integrated gas sensors - A comprehensive review," *Critical Reviews in Solid State and Materials Sciences*, vol. 29, pp. 111-188, 2004.
- [31] K. Hauffe, "The Application of the Theory of Semiconductors to Problems of Heterogeneous Catalysis," *Advances in Catalysis*, vol. 7, pp. 213-257, 1955.
- [32] N. Barsan and U. Weimar, "Conduction model of metal oxide gas sensors," *Journal of Electroceramics*, vol. 7, pp. 143-167, Dec 2001.
- [33] N. Barsan and U. Weimar, "Understanding the fundamental principles of metal oxide based gas sensors; the example of CO sensing with SnO₂ sensors in the presence of humidity," *Journal of Physics-Condensed Matter*, vol. 15, pp. R813-R839, May 28 2003.
- [34] J. Getino, L. Ares, J. I. Robla, M. C. Horrillo, I. Sayago, M. J. Fernandez, J. Rodrigo, and J. Gutierrez, "Environmental applications of gas sensor arrays: combustion atmospheres and contaminated soils," *Sensors and Actuators B-Chemical*, vol. 59, pp. 249-254, Oct 19 1999.
- [35] M. Hubner, N. Barsan, and U. Weimar, "Influences of Al, Pd and Pt additives on the conduction mechanism as well as the surface and bulk properties of SnO₂ based polycrystalline thick film gas sensors," *Sensors and Actuators B-Chemical*, vol. 171, pp. 172-180, Aug-Sep 2012.
- [36] G. Sakai, N. Matsunaga, K. Shimano, and N. Yamazoe, "Theory of gas-diffusion controlled sensitivity for thin film semiconductor gas sensor," *Sensors and Actuators B-Chemical*, vol. 80, pp. 125-131, Nov 20 2001.
- [37] D. Koziej, K. Thomas, N. Barsan, F. Thibault-Starzyk, and U. Weimar, "Influence of annealing temperature on the CO sensing mechanism for tin dioxide based sensors-Operando studies," *Catalysis Today*, vol. 126, pp. 211-218, Aug 15 2007.
- [38] M. Tiemann, "Porous metal oxides as gas sensors," *Chemistry-a European Journal*, vol. 13, pp. 8376-8388, 2007.
- [39] C. K. Chiang, C. R. Fincher, Y. W. Park, A. J. Heeger, H. Shirakawa, E. J. Louis, S. C. Gau, and A. G. Macdiarmid, "Electrical-Conductivity in Doped Polyacetylene," *Physical Review Letters*, vol. 39, pp. 1098-1101, 1977.

- [40] H. Shirakawa, E. J. Louis, A. G. Macdiarmid, C. K. Chiang, and A. J. Heeger, "Synthesis of Electrically Conducting Organic Polymers - Halogen Derivatives of Polyacetylene, (Ch)X," *Journal of the Chemical Society-Chemical Communications*, pp. 578-580, 1977.
- [41] R. W. C. Li, L. Ventura, J. Gruber, Y. Kawano, and L. R. F. Carvalho, "A selective conductive polymer-based sensor for volatile halogenated organic compounds (VHOC)," *Sensors and Actuators B-Chemical*, vol. 131, pp. 646-651, May 14 2008.
- [42] O. Y. Posudievsky, N. V. Konoschuk, A. L. Kukla, A. S. Pavluchenko, Y. M. Shirshov, and V. D. Pokhodenko, "Comparative analysis of sensor responses of thin conducting polymer films to organic solvent vapors," *Sensors and Actuators B-Chemical*, vol. 151, pp. 351-359, Jan 28 2011.
- [43] P. N. Bartlett and S. K. Lingchung, "Conducting Polymer Gas Sensors .2. Response of Polypyrrole to Methanol Vapor," *Sensors and Actuators*, vol. 19, pp. 141-150, Aug 15 1989.
- [44] X. P. Chen, C. K. Y. Wong, C. A. Yuan, and G. Q. Zhang, "Impact of the functional group on the working range of polyaniline as carbon dioxide sensors," *Sensors and Actuators B-Chemical*, vol. 175, pp. 15-21, Dec 2012.
- [45] X. P. Chen, C. A. Yuan, C. K. Y. Wong, H. Y. Ye, S. Y. Y. Leung, and G. Q. Zhang, "Molecular modeling of protonic acid doping of emeraldine base polyaniline for chemical sensors," *Sensors and Actuators B-Chemical*, vol. 174, pp. 210-216, Nov 2012.
- [46] T. Y. Wei, P. H. Yeh, S. Y. Lu, and Z. Lin-Wang, "Gigantic Enhancement in Sensitivity Using Schottky Contacted Nanowire Nanosensor," *Journal of the American Chemical Society*, vol. 131, pp. 17690-17695, Dec 9 2009.
- [47] X. P. Chen, L. Shen, C. A. Yuan, C. K. Y. Wong, and G. Q. Zhang, "Molecular model for the charge carrier density dependence of conductivity of polyaniline as chemical sensing materials," *Sensors and Actuators B-Chemical*, vol. 177, pp. 856-861, Feb 2013.
- [48] M. Gerard, A. Chaubey, and B. D. Malhotra, "Application of conducting polymers to biosensors," *Biosens Bioelectron*, vol. 17, pp. 345-359, May 2002.
- [49] D. T. McQuade, A. E. Pullen, and T. M. Swager, "Conjugated polymer-based chemical sensors," *Chemical Reviews*, vol. 100, pp. 2537-2574, Jul 2000.
- [50] N. Gupta, S. Sharma, I. A. Mir, and D. Kumar, "Advances in sensors based on conducting polymers," *Journal of Scientific & Industrial Research*, vol. 65, pp. 549-557, Jul 2006.
- [51] P. N. Bartlett, P. B. M. Archer, and S. K. Lingchung, "Conducting Polymer Gas Sensors .1. Fabrication and Characterization," *Sensors and Actuators*, vol. 19, pp. 125-140, Aug 15 1989.
- [52] A. F. Diaz and J. A. Logan, "Electroactive Polyaniline Films," *Journal of Electroanalytical Chemistry*, vol. 111, pp. 111-114, 1980.
- [53] D. Kumar and R. C. Sharma, "Advances in conductive polymers," *European Polymer Journal*, vol. 34, pp. 1053-1060, Aug 1998.
- [54] S. Uemura, T. Nakahira, and N. Kobayashi, "Photopolymerization of aniline derivatives by photoinduced electron transfer for application to image formation," *Journal of Materials Chemistry*, vol. 11, pp. 1585-1589, 2001.
- [55] X. Y. Gong, L. M. Dai, A. W. H. Mau, and H. J. Griesser, "Plasma-polymerized polyaniline films: Synthesis and characterization," *Journal of Polymer Science Part a-Polymer Chemistry*, vol. 36, pp. 633-643, Mar 1998.
- [56] Y. P. Shen, J. Z. Sun, J. G. Wu, and Q. Y. Zhou, "Synthesis and characterization of water-soluble conducting polyaniline by enzyme catalysis," *Journal of Applied Polymer Science*, vol. 96, pp. 814-817, May 5 2005.
- [57] C. Weder, "Organometallic conjugated polymer networks," *Journal of Inorganic and Organometallic Polymers and Materials*, vol. 16, pp. 101-113, Jun 2006.
- [58] T. Okada, T. Ogata, and M. Ueda, "Synthesis and characterization of regiocontrolled poly(2,5-di-n-butoxy-1,4-phenylene) by oxovanadium-catalyzed oxidative coupling polymerization," *Macromolecules*, vol. 29, pp. 7645-7650, Nov 18 1996.

- [59] V. V. Abalyaeva and O. N. Efimov, "Electrochemical formation of conducting polymer coating on porous p- and n-silicon substrates," *Polymers for Advanced Technologies*, vol. 11, pp. 69-74, Feb 2000.
- [60] A. P. Malinauskas and T. S. Kress, "Effects of Chemical Phenomena on Lwr Severe Accident Fission-Product Behavior," *Nuclear Safety*, vol. 32, pp. 56-64, Jan-Mar 1991.
- [61] N. Toshima and S. Hara, "Direct Synthesis of Conducting Polymers from Simple Monomers," *Progress in Polymer Science*, vol. 20, pp. 155-183, 1995.
- [62] R. H. Baughman, J. L. Bredas, R. R. Chance, R. L. Elsenbaumer, and L. W. Shacklette, "Structural Basis for Semiconducting and Metallic Polymer Dopant Systems," *Chemical Reviews*, vol. 82, pp. 209-222, 1982.
- [63] M. Salmon, K. K. Kanazawa, A. F. Diaz, and M. Krounbi, "A Chemical Route to Pyrrole Polymer-Films," *Journal of Polymer Science Part C-Polymer Letters*, vol. 20, pp. 187-193, 1982.
- [64] A. Malinauskas, "Chemical deposition of conducting polymers," *Polymer*, vol. 42, pp. 3957-3972, Apr 2001.
- [65] W. Schuhmann, C. Kranz, H. Wohlschlager, and J. Strohmeier, "Pulse technique for the electrochemical deposition of polymer films on electrode surfaces," *Biosens Bioelectron*, vol. 12, pp. 1157-1167, Dec 30 1997.
- [66] G. J. Cruz, J. Morales, M. M. CastilloOrtega, and R. Olayo, "Synthesis of polyaniline films by plasma polymerization," *Synthetic Metals*, vol. 88, pp. 213-218, Jun 1997.
- [67] Q. L. Hao, V. Kulikov, and V. A. Mirsky, "Investigation of contact and bulk resistance of conducting polymers by simultaneous two- and four-point technique," *Sensors and Actuators B-Chemical*, vol. 94, pp. 352-357, Oct 1 2003.
- [68] J. M. G. Laranjeira, W. M. deAzevedo, and M. C. U. deAraujo, "A conductimetric system based on polyaniline for determination of ammonia in fertilizers," *Analytical Letters*, vol. 30, pp. 2189-2209, 1997.
- [69] R. Noufi, A. J. Frank, and A. J. Nozik, "Stabilization of N-Type Silicon Photoelectrodes to Surface Oxidation in Aqueous-Electrolyte Solution and Mediation of Oxidation Reaction by Surface-Attached Organic Conducting Polymer," *Journal of the American Chemical Society*, vol. 103, pp. 1849-1850, 1981.
- [70] R. Noufi and D. Tench, "High-Efficiency Gaas Photoanodes," *Journal of the Electrochemical Society*, vol. 127, pp. 188-190, 1980.
- [71] R. A. Bull, F. R. Fan, and A. J. Bard, "Polymer-Films on Electrodes .13. Incorporation of Catalysts into Electronically Conductive Polymers - Iron Phthalocyanine in Polypyrrole," *Journal of the Electrochemical Society*, vol. 130, pp. 1636-1638, 1983.
- [72] A. Delcourt-Lancon, "Electrochemical analysis supported by macro and microelectrode array," Ph. D., Chemistry, Durham University, Durham, 2011.
- [73] Allen J. Bard and L. R. Faulkner, "Electrochemical Methods: Fundamentals and Applications," in *Electrochemical Methods: Fundamentals and Applications*, ed New York: John Wiley & Sons Inc., 2001, p. 231.
- [74] E. Laviron, "Theoretical Study of a Reversible Reaction Followed by a Chemical Reaction in Thin-Layer Linear Potential Sweep Voltammetry," *Journal of Electroanalytical Chemistry*, vol. 39, pp. 1-&, 1972.
- [75] R. F. Lane and A. T. Hubbard, "Electrochemistry of Chemisorbed Molecules .2. Influence of Charged Chemisorbed Molecules on Electrode-Reactions of Platinum Complexes," *Journal of Physical Chemistry*, vol. 77, pp. 1411-1421, 1973.
- [76] S. M. Sayyah, S. S. Abd El-Rehim, and M. M. El-Deeb, "Electropolymerization of pyrrole and characterization of the obtained polymer films," *Journal of Applied Polymer Science*, vol. 90, pp. 1783-1792, Sep 17 2003.

- [77] M. Zhou and J. Heinze, "Electropolymerization of pyrrole and electrochemical study of polypyrrole. 2. Influence of acidity on the formation of polypyrrole and the multipathway mechanism," *Journal of Physical Chemistry B*, vol. 103, pp. 8443-8450, Oct 7 1999.
- [78] A. Ajayaghosh, "Donor-acceptor type low band gap polymers: polysquaraines and related systems," *Chemical Society Reviews*, vol. 32, pp. 181-191, Jul 2003.
- [79] J. L. Bredas and G. B. Street, "Polarons, Bipolarons, and Solitons in Conducting Polymers," *Accounts of Chemical Research*, vol. 18, pp. 309-315, 1985.
- [80] A. J. Heeger, "Charge Storage in Conducting Polymers - Solitons, Polarons, and Bipolarons," *Polymer Journal*, vol. 17, pp. 201-208, 1985.
- [81] J. L. Bredas, B. Themans, J. G. Fripiat, J. M. Andre, and R. R. Chance, "Highly Conducting Polyparaphenylene, Polypyrrole, and Polythiophene Chains - an Abinitio Study of the Geometry and Electronic-Structure Modifications Upon Doping," *Physical Review B*, vol. 29, pp. 6761-6773, 1984.
- [82] G. Crecelius, M. Stamm, J. Fink, and J. J. Ritsko, "Asf5-Doped Polyparaphenylene - Evidence for Polaron and Bipolaron Formation," *Physical Review Letters*, vol. 50, pp. 1498-1500, 1983.
- [83] D. Moses, A. Denenstien, J. Chen, A. J. Heeger, P. Mcandrew, T. Woerner, A. G. Macdiarmid, and Y. W. Park, "Effect of Nonuniform Doping on Electrical Transport in Trans-(Ch)X - Studies of the Semiconductor-Metal Transition," *Physical Review B*, vol. 25, pp. 7652-7660, 1982.
- [84] A. G. MacDiarmid, "'Synthetic metals': A novel role for organic polymers (Nobel lecture)," *Angewandte Chemie-International Edition*, vol. 40, pp. 2581-2590, 2001.
- [85] S. Holdcroft and B. L. Funt, "Preparation and Electrocatalytic Properties of Conducting Films of Polypyrrole Containing Platinum Microparticulates," *Journal of Electroanalytical Chemistry*, vol. 240, pp. 89-103, Jan 25 1988.
- [86] G. W. Lu, L. T. Qu, and G. Q. Shi, "Electrochemical fabrication of neuron-type networks based on crystalline oligopyrene nanosheets," *Electrochimica Acta*, vol. 51, pp. 340-346, Oct 10 2005.
- [87] J. Reemts, J. Parisi, and D. Schlettwein, "Electrochemical growth of gas-sensitive polyaniline thin films across an insulating gap," *Thin Solid Films*, vol. 466, pp. 320-325, Nov 1 2004.
- [88] J. H. Cho, J. B. Yu, J. S. Kim, S. O. Sohn, D. D. Lee, and J. S. Huh, "Sensing behaviors of polypyrrole sensor under humidity condition," *Sensors and Actuators B-Chemical*, vol. 108, pp. 389-392, Jul 22 2005.
- [89] S. T. McGovern, G. M. Spinks, and G. G. Wallace, "Micro-humidity sensors based on a processable polyaniline blend," *Sensors and Actuators B-Chemical*, vol. 107, pp. 657-665, Jun 29 2005.
- [90] S. Brady, K. T. Lau, W. Megill, G. G. Wallace, and D. Diamond, "The development and characterisation of conducting polymeric-based sensing devices.," *Synthetic Metals*, vol. 154, pp. 25-28, Sep 22 2005.
- [91] M. S. Silverstein, H. W. Tai, A. Sergienko, Y. L. Lumelsky, and S. Pavlovsky, "PolyHIPE: IPNs, hybrids, nanoscale porosity, silica monoliths and ICP-based sensors," *Polymer*, vol. 46, pp. 6682-6694, Aug 8 2005.
- [92] L. Ruangchuay, A. Sirivat, and J. Schwank, "Selective conductivity response of polypyrrole-based sensor on flammable chemicals," *Reactive & Functional Polymers*, vol. 61, pp. 11-22, 2004.
- [93] H. G. O. Sandberg, T. G. Backlund, R. Osterbacka, S. Jussila, T. Makela, and H. Stubb, "Applications of an all-polymer solution-processed high-performance, transistor," *Synthetic Metals*, vol. 155, pp. 662-665, Dec 15 2005.
- [94] D. Li, Y. D. Jiang, Z. M. Wu, X. D. Chen, and Y. R. Li, "Self-assembly of polyaniline ultrathin films based on doping-induced deposition effect and applications for chemical sensors," *Sensors and Actuators B-Chemical*, vol. 66, pp. 125-127, Jul 25 2000.
- [95] N. M. Ratcliffe, "Polypyrrole-Based Sensor for Hydrazine and Ammonia," *Analytica Chimica Acta*, vol. 239, pp. 257-262, Dec 3 1990.

- [96] J. M. Slater and E. J. Watt, "Examination of Ammonia Poly(Pyrrole) Interactions by Piezoelectric and Conductivity Measurements," *Analyst*, vol. 116, pp. 1125-1130, Nov 1991.
- [97] N. E. Agbor, M. C. Petty, and A. P. Monkman, "Polyaniline Thin-Films for Gas-Sensing," *Sensors and Actuators B-Chemical*, vol. 28, pp. 173-179, Sep 1995.
- [98] F. Selampinar, L. Toppare, U. Akbulut, T. Yalcin, and S. Suzer, "A Conducting Composite of Polypyrrole .2. As a Gas Sensor," *Synthetic Metals*, vol. 68, pp. 109-116, Jan 1995.
- [99] K. H. An, S. Y. Jeong, H. R. Hwang, and Y. H. Lee, "Enhanced sensitivity of a gas sensor incorporating single-walled carbon nanotube-polypyrrole nanocomposites," *Advanced Materials*, vol. 16, pp. 1005-+, Jun 17 2004.
- [100] N. V. Bhat, A. P. Gadre, and V. A. Bambole, "Investigation of electropolymerized polypyrrole composite film: Characterization and application to gas sensors," *Journal of Applied Polymer Science*, vol. 88, pp. 22-29, Apr 4 2003.
- [101] J. Elizalde-Torres, H. L. Hu, and A. Garcia-Valenzuela, "NO₂-induced optical absorbance changes in semiconductor polyaniline thin films," *Sensors and Actuators B-Chemical*, vol. 98, pp. 218-226, Mar 15 2004.
- [102] G. F. Li, M. Josowicz, J. Janata, and S. Semancik, "Effect of thermal excitation on intermolecular charge transfer efficiency in conducting polyaniline," *Applied Physics Letters*, vol. 85, pp. 1187-1189, Aug 16 2004.
- [103] S. V. Mello, P. Dynarowicz-Latka, A. Dhanabalan, R. F. Bianchi, R. Onmori, R. A. J. Janssen, and O. N. Oliveira, "Langmuir and Langmuir-Blodgett films from the N-hexyl-pyrrole-thiophene (AB) semi-amphiphilic copolymer," *Colloids and Surfaces a-Physicochemical and Engineering Aspects*, vol. 198, pp. 45-51, Feb 18 2002.
- [104] V. C. Nguyen and K. Potje-Kamloth, "Electrical and chemical sensing properties of doped polypyrrole/gold Schottky barrier diodes," *Thin Solid Films*, vol. 338, pp. 142-148, Jan 29 1999.
- [105] M. K. Ram, O. Yavuz, and M. Aldissi, "NO₂ gas sensing based on ordered ultrathin films of conducting polymer and its nanocomposite," *Synthetic Metals*, vol. 151, pp. 77-84, May 31 2005.
- [106] C. N. Van and K. Potje-Kamloth, "Electrical and NO_x gas sensing properties of metallophthalocyanine-doped polypyrrole/silicon heterojunctions," *Thin Solid Films*, vol. 392, pp. 113-121, Jul 23 2001.
- [107] D. Xie, Y. D. Jiang, W. Pan, D. Li, Z. M. Wu, and Y. R. Li, "Fabrication and characterization of polyaniline-based gas sensor by ultra-thin film technology," *Sensors and Actuators B-Chemical*, vol. 81, pp. 158-164, Jan 5 2002.
- [108] N. V. Bhat, A. P. Gadre, and V. A. Bambole, "Structural, mechanical, and electrical properties of electropolymerized polypyrrole composite films," *Journal of Applied Polymer Science*, vol. 80, pp. 2511-2517, Jun 24 2001.
- [109] H. Yoon, M. Chang, and J. Jang, "Sensing behaviors of polypyrrole nanotubes prepared in reverse microemulsions: Effects of transducer size and transduction mechanism," *Journal of Physical Chemistry B*, vol. 110, pp. 14074-14077, Jul 27 2006.
- [110] L. Ruangchuay, A. Sirivat, and J. Schwank, "Electrical conductivity response of polypyrrole to acetone vapor: effect of dopant anions and interaction mechanisms," *Synthetic Metals*, vol. 140, pp. 15-21, Jan 6 2004.
- [111] R. Back and R. B. Lennox, "Electrochemical Investigation of Novel Polymerizable Thiophene Ferrocene Conjugates," *Langmuir*, vol. 8, pp. 959-964, Mar 1992.
- [112] S. Cosnier, M. Fontecave, D. Limosin, and V. Nivière, "A poly(amphiphilic pyrrole)-flavin reductase electrode for amperometric determination of flavins," *Analytical Chemistry*, vol. 69, pp. 3095-3099, Aug 1 1997.
- [113] C. J. Pickett and K. S. Ryder, "Bioinorganic Reaction Centers on Electrodes - Modified Electrodes Possessing Amino-Acid, Peptide and Ferredoxin-Type Groups on a Poly(Pyrrole) Backbone," *Journal of the Chemical Society-Dalton Transactions*, pp. 2181-2189, Jul 21 1994.

- [114] H. K. Youssoufi, M. Hmyene, F. Garnier, and D. Delabouglise, "Cation Recognition Properties of Polypyrrole 3-Substituted by Azacrown Ethers," *Journal of the Chemical Society-Chemical Communications*, pp. 1550-1552, Oct 21 1993.
- [115] G. Zotti, G. Schiavon, S. Zecchin, A. Berlin, A. Canavesi, and G. Pagani, "Self-assembly and electropolymerization of pyrrole- and bithiophene-n-hexyl-ferrocene molecules on ITO electrodes.," *Synthetic Metals*, vol. 84, pp. 239-240, Jan 1997.
- [116] G. Zotti, S. Martina, G. Wegner, and A. D. Schluter, "Well-Defined Pyrrole Oligomers - Electrochemical and Uv Vis Studies," *Advanced Materials*, vol. 4, pp. 798-801, Dec 1992.
- [117] W. Tenhoeve, H. Wynberg, E. E. Havinga, and E. W. Meijer, "Substituted 2,2'-5',2''-5'', 2('X3)-5('X3), 2('X4)-5('X4), 2('X5)-5('X5), 2('X6)-5('X6), 2('X7)-5('X7), 2('X8)-5('X8), 2('X9)-5('X9), 2('X10)-Undecithiophenes - the Longest Characterized Oligothiophenes," *Journal of the American Chemical Society*, vol. 113, pp. 5887-5889, Jul 17 1991.
- [118] J. P. Ferraris and G. D. Skiles, "Substitutional Alloys of Organic Polymeric Conductors," *Polymer*, vol. 28, pp. 179-182, Feb 1987.
- [119] J. P. Ferraris and M. D. Newton, "Electrochemical and Optical-Properties of Thiophene Alkylheteroaromatic Copolymers," *Polymer*, vol. 33, pp. 391-397, 1992.
- [120] H. J. Kooreman and H. Wynberg, "Chemistry of Polythienyls .3. Synthesis of Terthienyls," *Recueil Des Travaux Chimiques Des Pays-Bas*, vol. 86, pp. 37-&, 1967.
- [121] J. Kagan and S. K. Arora, "2,5-Di(2'-Thienyl)Furan and an Improved Synthesis of Alpha-Terthienyl," *Heterocycles*, vol. 20, pp. 1941-1943, 1983.
- [122] H. Wynberg and J. Metselaar, "A Convenient Route to Polythiophenes," *Synthetic Communications*, vol. 14, pp. 1-9, 1984.
- [123] W. Y. Leung and E. Legoff, "A Facile Synthesis of 1,4-Diketones from Organo-Lithium Reagents and N,N,N',N'-Tetramethylsuccinamide," *Synthetic Communications*, vol. 19, pp. 787-792, 1989.
- [124] L. F. Schweiger, K. S. Ryder, D. G. Morris, A. Glidle, and J. M. Cooper, "Strategies towards functionalised electronically conducting organic copolymers," *Journal of Materials Chemistry*, vol. 10, pp. 107-114, 2000.
- [125] V. Amarnath, D. C. Anthony, K. Amarnath, W. M. Valentine, L. A. Wetterau, and D. G. Graham, "Intermediates in the Paal-Knorr Synthesis of Pyrroles," *Journal of Organic Chemistry*, vol. 56, pp. 6924-6931, Nov 22 1991.
- [126] A. A. Athawale and M. V. Kulkarni, "Polyaniline and its substituted derivatives as sensor for aliphatic alcohols," *Sensors and Actuators B-Chemical*, vol. 67, pp. 173-177, Aug 10 2000.
- [127] T. Y. Lee and Y. B. Shim, "Direct DNA hybridization detection based on the oligonucleotide-functionalized conductive polymer," *Analytical Chemistry*, vol. 73, pp. 5629-5632, Nov 15 2001.
- [128] M. A. Rahman, P. Kumar, D. S. Park, and Y. B. Shim, "Electrochemical sensors based on organic conjugated polymers," *Sensors*, vol. 8, pp. 118-141, Jan 2008.
- [129] M. A. Rahman, M. S. Won, H. H. Kwon, J. H. Yoon, D. S. Park, and Y. B. Shim, "Water sensor for a nonaqueous solvent with poly(1,5-diaminonaphthalene) nanofibers," *Analytical Chemistry*, vol. 80, pp. 5307-5311, Jul 15 2008.
- [130] M. J. A. Shiddiky, M. A. Rahman, and Y. B. Shim, "Hydrazine-catalyzed ultrasensitive detection of DNA and proteins," *Analytical Chemistry*, vol. 79, pp. 6886-6890, Sep 1 2007.
- [131] G. G. Mcleod, M. G. B. Mahboubianjones, R. A. Pethrick, and S. D. Watson, "Synthesis, Electrochemical Polymerization and Properties of Poly(2,5-Di-(2-Thienyl)-Pyrrole)," *Polymer*, vol. 27, pp. 455-458, Mar 1986.
- [132] A. A. Athawale, M. V. Kulkarni, and V. V. Chabukswar, "Studies on chemically synthesized soluble acrylic acid doped polyaniline," *Materials Chemistry and Physics*, vol. 73, pp. 106-110, Jan 2 2002.
- [133] K. Yakushi, L. J. Lauchlan, T. C. Clarke, and G. B. Street, "Optical Study of Polypyrrole Perchlorate," *Journal of Chemical Physics*, vol. 79, pp. 4774-4778, 1983.

- [134] J. P. Ferraris and T. R. Hanlon, "Optical, Electrical and Electrochemical Properties of Heteroaromatic Copolymers," *Polymer*, vol. 30, pp. 1319-1327, Jul 1989.
- [135] Z. Q. Hu, M. H. Wang, S. J. Li, X. Y. Liu, and J. H. Wu, "Ortho alkyl substituents effect on solubility and thermal properties of fluorenyl cardo polyimides," *Polymer*, vol. 46, pp. 5278-5283, Jun 27 2005.
- [136] A. J. B. Loman, L. Vanderdoes, A. Bantjes, and I. Vulic, "Effect of Methyl-Groups on the Thermal-Properties of Polyesters from Methyl-Substituted 1,4-Butanediols and 4,4'-Biphenyldicarboxylic Acid," *Journal of Polymer Science Part a-Polymer Chemistry*, vol. 33, pp. 493-504, Feb 1995.
- [137] Y. Martele, V. Van Speybroeck, M. Waroquier, and E. Schacht, "Thermodegradable polycarbonates: Effect of substituents on the degradation temperature," *E-Polymers*, Nov 14 2002.
- [138] J. R. Reynolds, A. D. Child, J. P. Ruiz, S. Y. Hong, and D. S. Marynick, "Substituent Effects on the Electrical-Conductivity and Electrochemical Properties of Conjugated Furanyl Phenylene Polymers," *Macromolecules*, vol. 26, pp. 2095-2103, Apr 12 1993.
- [139] R. D. McCullough, "The chemistry of conducting polythiophenes," *Advanced Materials*, vol. 10, pp. 93-+, Jan 22 1998.
- [140] S. Allard, M. Forster, B. Souharce, H. Thiem, and U. Scherf, "Organic semiconductors for solution-processable field-effect transistors (OFETs)," *Angewandte Chemie-International Edition*, vol. 47, pp. 4070-4098, 2008.
- [141] Z. N. Bao, "Materials and fabrication needs for low-cost organic transistor circuits," *Advanced Materials*, vol. 12, pp. 227-+, Feb 3 2000.
- [142] Z. N. Bao, Y. Feng, A. Dodabalapur, V. R. Raju, and A. J. Lovinger, "High-performance plastic transistors fabricated by printing techniques," *Chemistry of Materials*, vol. 9, pp. 1299-8, Jun 1997.
- [143] Z. N. Bao, J. A. Rogers, and H. E. Katz, "Printable organic and polymeric semiconducting materials and devices," *Journal of Materials Chemistry*, vol. 9, pp. 1895-1904, Sep 1999.
- [144] J. Bharathan and Y. Yang, "Polymer electroluminescent devices processed by inkjet printing: I. Polymer light-emitting logo," *Applied Physics Letters*, vol. 72, pp. 2660-2662, May 25 1998.
- [145] F. Garnier, R. Hajlaoui, A. Yassar, and P. Srivastava, "All-Polymer Field-Effect Transistor Realized by Printing Techniques," *Science*, vol. 265, pp. 1684-1686, Sep 16 1994.
- [146] H. Pan, Y. Wu, Y. Li, P. Liu, B. S. Ong, S. Zhu, and G. Xu, "Benzodithiophene copolymer - A low-temperature, solution-processed high-performance semiconductor for thin-film transistors," *Advanced Functional Materials*, vol. 17, pp. 3574-3579, Nov 23 2007.
- [147] M. I. Heeney, C. Bailey, K. Genevicius, M. I. Shkunov, D. Sparrowe, S. Tierney, R. Wagner, W. M. Zhang, M. L. Chabinyk, R. J. Kline, M. D. McGehee, and M. F. Toney, "Liquid-crystalline semiconducting polymers with high charge-carrier mobility," *Nature Materials*, vol. 5, pp. 328-333, Apr 2006.
- [148] Y. N. Li, Y. L. Wu, P. Liu, M. Birau, H. L. Pan, and B. S. Ong, "Poly(2,5-bis(2-thienyl)-3,6-dialkylthieno[3,2-b]thiophene)s-high-mobility semiconductors for thin-film transistors," *Advanced Materials*, vol. 18, pp. 3029-+, Nov 17 2006.
- [149] J. Li, F. Qin, C. M. Li, Q. L. Bao, M. B. Chan-Park, W. Zhang, J. G. Qin, and B. S. Ong, "High-performance thin-film transistors from solution-processed dithienothiophene polymer semiconductor nanoparticles," *Chemistry of Materials*, vol. 20, pp. 2057-2059, Mar 25 2008.
- [150] M. Heeney, C. Bailey, K. Genevicius, M. Shkunov, D. Sparrowe, S. Tierney, and I. McCulloch, "Stable polythiophene semiconductors incorporating thieno[2,3-b]thiophene," *Journal of the American Chemical Society*, vol. 127, pp. 1078-1079, Feb 2 2005.
- [151] H. Sirringhaus, R. J. Wilson, R. H. Friend, M. Inbasekaran, W. Wu, E. P. Woo, M. Grell, and D. D. C. Bradley, "Mobility enhancement in conjugated polymer field-effect transistors through chain alignment in a liquid-crystalline phase," *Applied Physics Letters*, vol. 77, pp. 406-408, Jul 17 2000.

- [152] B. S. Ong, Y. L. Wu, P. Liu, and S. Gardner, "High-performance semiconducting polythiophenes for organic thin-film transistors," *Journal of the American Chemical Society*, vol. 126, pp. 3378-3379, Mar 24 2004.
- [153] I. Osaka, G. Sauve, R. Zhang, T. Kowalewski, and R. D. McCullough, "Novel thiophene-thiazolothiazole copolymers for organic field-effect transistors," *Advanced Materials*, vol. 19, pp. 4160-+, Dec 3 2007.
- [154] D. Sainova, S. Janietz, U. Asawapirom, L. Romaner, E. Zojer, N. Koch, and A. Vollmer, "Improving the stability of polymer FETs by introducing fixed acceptor units into the main chain: Application to poly(alkylthiophenes)," *Chemistry of Materials*, vol. 19, pp. 1472-1481, Mar 20 2007.
- [155] T. Yamamoto, M. Arai, H. Kokubo, and S. Sasaki, "Copolymers of thiophene and thiazole. Regioregulation in synthesis, stacking structure, and optical properties," *Macromolecules*, vol. 36, pp. 7986-7993, Oct 21 2003.
- [156] W. J. Li, H. E. Katz, A. J. Lovinger, and J. G. Laquindanum, "Field-effect transistors based on thiophene hexamer analogues with diminished electron donor strength," *Chemistry of Materials*, vol. 11, pp. 458-465, Feb 1999.
- [157] S. J. Coats and H. H. Wasserman, "The Conversion of Alpha-Bromo-Beta-Dicarbonyls to Vicinal Tricarbonyls Using Dimethyldioxirane and Base," *Tetrahedron Letters*, vol. 36, pp. 7735-7738, Oct 16 1995.
- [158] A. V. R. Rao, A. K. Singh, K. M. Reddy, and K. Ravikumar, "Regioselective Free-Radical Cyclization - a General-Method for the Synthesis of the Spiro[4.4]Nonane System of Fredericamycin-A," *Journal of the Chemical Society-Perkin Transactions 1*, pp. 3171-3175, Dec 21 1993.
- [159] X. X. Shi and L. X. Dai, "Mild Halogenation of Stabilized Ester Enolates by Cupric Halides," *Journal of Organic Chemistry*, vol. 58, pp. 4596-4598, Aug 13 1993.
- [160] K. Tanemura, T. Suzuki, Y. Nishida, K. Satsumabayashi, and T. Horaguchi, "A mild and efficient procedure for alpha-bromination of ketones using N-bromosuccinimide catalysed by ammonium acetate," *Chemical Communications*, pp. 470-471, Feb 21 2004.
- [161] K. Hakam, M. Thielmann, T. Thielmann, and E. Winterfeldt, "Reactions with Indole-Derivatives .55. An Enantiodivergent Route to Both Vincamine Enantiomers," *Tetrahedron*, vol. 43, pp. 2035-2044, 1987.
- [162] W. Ogilvie and W. Rank, "Thermolysis of Geminal Diazides - a Novel Route to 1,3,4-Oxadiazoles," *Canadian Journal of Chemistry-Revue Canadienne De Chimie*, vol. 65, pp. 166-169, Jan 1987.
- [163] P. Dowd, C. Kaufman, and P. Kaufman, "Beta-Methylene-D,L-Asparagine," *Journal of Organic Chemistry*, vol. 50, pp. 882-885, 1985.
- [164] S. S. Arbuji, S. B. Waghmode, and A. V. Ramaswamy, "Photochemical alpha-bromination of ketones using N-bromosuccinimide: a simple, mild and efficient method," *Tetrahedron Letters*, vol. 48, pp. 1411-1415, Feb 19 2007.
- [165] I. Pravst, M. Zupan, and S. Stavber, "Halogenation of ketones with N-halosuccinimides under solvent-free reaction conditions," *Tetrahedron*, vol. 64, pp. 5191-5199, May 26 2008.
- [166] B. Das, K. Venkateswarlu, G. Mahender, and L. Mahender, "Studies on novel synthetic methodologies, part 59. A simple and efficient method for alpha-bromination of carbonyl compounds using N-bromosuccinimide in the presence of silica-supported sodium hydrogen sulfate as a heterogeneous catalyst," *Tetrahedron Letters*, vol. 46, pp. 3041-3044, Apr 25 2005.
- [167] H. M. Meshram, P. N. Reddy, K. Sadashiv, and J. S. Yadav, "Amberlyst-15((R))-promoted efficient 2-halogenation of 1,3-keto-esters and cyclic ketones using N-halosuccinimides," *Tetrahedron Letters*, vol. 46, pp. 623-626, Jan 24 2005.

- [168] D. Yang, Y. L. Yan, and B. Lui, "Mild alpha-halogenation reactions of 1,3-dicarbonyl compounds catalyzed by Lewis acids," *Journal of Organic Chemistry*, vol. 67, pp. 7429-7431, Oct 18 2002.
- [169] H. M. Meshram, P. N. Reddy, P. Vishnu, K. Sadashiv, and J. S. Yadav, "A green approach for efficient alpha-halogenation of beta-dicarbonyl compounds and cyclic ketones using N-halosuccinimides in ionic liquids," *Tetrahedron Letters*, vol. 47, pp. 991-995, Feb 6 2006.
- [170] J. C. Lee, J. Y. Park, S. Y. Yoon, Y. H. Bae, and S. J. Lee, "Efficient microwave induced direct alpha-halogenation of carbonyl compounds," *Tetrahedron Letters*, vol. 45, pp. 191-193, Jan 1 2004.
- [171] A. Bekaert, O. Provot, O. Rasolojaona, M. Alami, and J. D. Brion, "N-Methylpyrrolidin-2-one hydrotribromide (MPHT) a mild reagent for selective bromination of carbonyl compounds: synthesis of substituted 2-bromo-1-naphtols," *Tetrahedron Letters*, vol. 46, pp. 4187-4191, Jun 13 2005.
- [172] G. K. S. Prakash, R. Ismail, J. Garcia, C. Panja, G. Rasul, T. Mathew, and G. A. Olah, "alpha-Halogenation of carbonyl compounds: halotrimethylsilane-nitrate salt couple as an efficient halogenating reagent system," *Tetrahedron Letters*, vol. 52, pp. 1217-1221, Mar 16 2011.
- [173] A. T. Khan, M. A. Ali, P. Goswami, and L. H. Choudhury, "A mild and regioselective method for alpha-bromination of beta-keto esters and 1,3-diketones using bromodimethylsulfonium bromide (BDMS)," *Journal of Organic Chemistry*, vol. 71, pp. 8961-8963, Nov 10 2006.
- [174] E. H. Kim, B. S. Koo, C. E. Song, and K. J. Lee, "Halogenation of aromatic methyl ketones using Oxone (R) and sodium halide," *Synthetic Communications*, vol. 31, pp. 3627-3632, 2001.
- [175] S. I. Zavyalov and N. E. Kravchenko, "Influence of Urea on the Bromination of Methyl Alkyl Ketones," *Bulletin of the Academy of Sciences of the Ussr Division of Chemical Science*, vol. 32, pp. 1324-1324, 1983.
- [176] M. Gaudry and A. Marquet, "Enolisation des cetonnes dissymetriques-III ☆: Acces facile aux bromomethylcetonnes par bromation en presence de methanol," *Tetrahedron*, vol. 26, pp. 5611-5615, 1970.
- [177] M. D. Curtis, J. I. Nanos, and M. D. McClain, "Thiazole polymers and method of producing same," United states of America Patent, 1994.
- [178] J. Y. Liu, R. Zhang, I. Osaka, S. Mishra, A. E. Javier, D. M. Smilgies, T. Kowalewski, and R. D. McCullough, "Transistor Paint: Environmentally Stable N-alkyldithienopyrrole and Bithiazole-Based Copolymer Thin-Film Transistors Show Reproducible High Mobilities without Annealing," *Advanced Functional Materials*, vol. 19, pp. 3427-3434, Nov 9 2009.
- [179] P. A. Lieberzeit, C. Palfinger, F. L. Dickert, and G. Fischerauer, "SAW RFID-Tags for Mass-Sensitive Detection of Humidity and Vapors," *Sensors*, vol. 9, pp. 9805-9815, Dec 2009.
- [180] I. M. Steinberg and M. D. Steinberg, "Radio-frequency tag with optoelectronic interface for distributed wireless chemical and biological sensor applications," *Sensors and Actuators B-Chemical*, vol. 138, pp. 120-125, Apr 24 2009.
- [181] R. Byrne and D. Diamond, "Chemo/bio-sensor networks," *Nature Materials*, vol. 5, pp. 421-424, Jun 2006.
- [182] O. Atsushi and Y. Kentaro, "A temperature-managed traceability system using RFID tags with embedded temperature sensors," *Nec Technical Journal*, vol. 1, pp. 82-86, May 2006.
- [183] S. Zampolli, I. Elmi, E. Cozzani, G. C. Cardinali, A. Scorzoni, M. Cicioni, S. Marco, F. Palacio, J. M. Gomez-Cama, I. Sayhan, and T. Becker, "Ultra-low-power components for an RFID Tag with physical and chemical sensors," *Microsystem Technologies-Micro-and Nanosystems-Information Storage and Processing Systems*, vol. 14, pp. 581-588, Apr 2008.
- [184] R. A. Potyrallo and W. G. Morris, "Multianalyte chemical identification and quantitation using a single radio frequency identification sensor," *Analytical Chemistry*, vol. 79, pp. 45-51, Jan 1 2007.
- [185] D. R. Thevenot, K. Toth, R. A. Durst, and G. S. Wilson, "Electrochemical biosensors: Recommended definitions and classification," *Analytical Letters*, vol. 34, pp. 635-659, 2001.

- [186] D. R. Thevenot, K. Toth, R. A. Durst, and G. S. Wilson, "Electrochemical biosensors: recommended definitions and classification," *Biosens Bioelectron*, vol. 16, pp. 121-131, Jan 2001.
- [187] J. P. Chambers, B. P. Arulanandam, L. L. Matta, A. Weis, and J. J. Valdes, "Biosensor recognition elements," *Current Issues in Molecular Biology*, vol. 10, pp. 1-12, 2008.
- [188] J. Niazi. *Overview, history & types of biosensors*. Available: http://myweb.sabanciuniv.edu/javed/files/2009/10/JHNiazi_Introductory-Week-Overview-history-types-of-biosensors.pdf
- [189] A. F. Collings and F. Caruso, "Biosensors: recent advances," *Reports on Progress in Physics*, vol. 60, pp. 1397-1445, Nov 1997.
- [190] S. Cosnier, "Biomolecule immobilization on electrode surfaces by entrapment or attachment to electrochemically polymerized films. A review," *Biosens Bioelectron*, vol. 14, pp. 443-456, May 31 1999.
- [191] S. Choi and J. Chae, "A Physisorbed Interface Design of Biomolecules for Selective and Sensitive Protein Detection," *Jala*, vol. 15, pp. 172-178, Jun 2010.
- [192] A. P. Henderson, C. Bleasdale, W. Clegg, and B. T. Golding, "2,6-diarylaminotetrahydropyrans from reactions of glutaraldehyde with anilines: Models for biomolecule cross-linking," *Chemical Research in Toxicology*, vol. 17, pp. 378-382, Mar 2004.
- [193] N. J. Geddes, E. M. Paschinger, D. N. Furlong, F. Caruso, C. L. Hoffmann, and J. F. Rabolt, "Surface Chemical Activation of Quartz-Crystal Microbalance Gold Electrodes - Analysis by Frequency Changes, Contact-Angle Measurements and Grazing Angle Ftir," *Thin Solid Films*, vol. 260, pp. 192-199, May 15 1995.
- [194] T. Wink, S. J. vanZuilen, A. Bult, and W. P. vanBennekom, "Self-assembled monolayers for biosensors," *Analyst*, vol. 122, pp. R43-R50, Apr 1997.
- [195] P. Pelosi, "Perireceptor events in olfaction," *Journal of Neurobiology*, vol. 30, pp. 3-19, May 1996.
- [196] H. Breer, "Olfactory receptors: molecular basis for recognition and discrimination of odors," *Anal Bioanal Chem*, vol. 377, pp. 427-433, Oct 2003.
- [197] J. Pevsner, V. Hou, A. M. Snowman, and S. H. Snyder, "Odorant-Binding Protein - Characterization of Ligand-Binding," *Journal of Biological Chemistry*, vol. 265, pp. 6118-6125, Apr 15 1990.
- [198] M. Dalmonte, M. Centini, C. Anselmi, and P. Pelosi, "Binding of Selected Odorants to Bovine and Porcine Odorant-Binding Proteins," *Chemical Senses*, vol. 18, pp. 713-721, Dec 1993.
- [199] M. F. Herent, S. Collin, and P. Pelosi, "Affinities of nutty and green-smelling pyrazines and thiazoles to odorant-binding proteins, in relation with their lipophilicity," *Chemical Senses*, vol. 20, pp. 601-608, Dec 1995.
- [200] J. S. Kim, B. Lagel, E. Moons, N. Johansson, I. D. Baikie, W. R. Salaneck, R. H. Friend, and F. Cacialli, "Kelvin probe and ultraviolet photoemission measurements of indium tin oxide work function: a comparison," *Synthetic Metals*, vol. 111, pp. 311-314, Jun 1 2000.
- [201] B. E. Conway, Mathieso.Jg, and H. P. Dhar, "Orientation Behavior of Adsorbed Pyridine and Pyrazine at Mercury-Water Interface in Relation to Solution Thermodynamic Properties," *Journal of Physical Chemistry*, vol. 78, pp. 1226-1234, 1974.
- [202] V. Lazarescu, "Adsorption of Pyrazine on Au(111) and Ag(111) - on the Role of the Electronic Factor," *Surface Science*, vol. 335, pp. 227-234, Jul 20 1995.
- [203] A. Iannelli, A. G. Brolo, D. E. Irish, and J. Lipkowski, "Electrochemical and Raman spectroscopic studies of pyrazine adsorption at the Au(210) electrode surface," *Canadian Journal of Chemistry-Revue Canadienne De Chimie*, vol. 75, pp. 1694-1702, Nov 1997.

List of Publications

Journal Papers

Sudam Pandule, Alexandru Oprea, Nicolae Barsan, Udo Weimar, Krishna Persaud. “Synthesis of Poly-[2, 5-di(thiophen-2-yl)-1*H*-pyrrole] derivatives and the effects of the substituents on their properties”. *Accepted with revision to Synthetic Metals*

D. Briand, F. Molina-Lopez, A. Vasquez Quintero, G. Mattana, N.F. de Rooij, E. Danesh, K. Persaud, **S. Pandule**, U. Altenberend, A. Oprea, N. Barsan, U. Weimar, E.C.P. Smits, M. Koetse, J.F.M. Schram, R.H.C.A.T. Lelieveld, R.H.L. Kusters, J. van den Brand. “Printed Multi-Sensor Platform and its Integration into RFID Labels for Perishable Goods Monitoring”. *In preparation for the volume dedicated to IMCS 2014 of the Sensors and Actuators B: Chemical*

Sudam Pandule, Alexandru Oprea, Nicolae Barsan, Udo Weimar, Krishna Persaud. “Optical, Electrical, Thermal and Chemical gas sensing properties of Poly-[1-(naphthalen-1-yl)-2,5-di(thiophen-2-yl)-1*H*-pyrrole]”. *Ready to submit to Journal of Macromolecular Science, Part A*

Sudam Pandule, Alexandru Oprea, Nicolae Barsan, Udo Weimar, Krishna Persaud. “Comparative studies on the halogenated derivatives of Poly-[2, 5-di(thiophen-2-yl)-1*H*-pyrrole]”. *Manuscript under preparation*

Conferences Participations

Sudam Pandule, “Synthesis and polymerization of new dithienyl pyrrole derivatives and their applications in chemical gas sensors”, ChemCYS 2014, 12th Chemistry conference for Young Scientists, Blankenberge, Belgium, 27-28 Feb. 2014 (Poster Presentation)

Sudam Pandule, Alexandru Oprea, Nicolae Barsan, Udo Weimar, Krishna Persaud, “Synthesis of poly-(dithienyl pyrrole) derivatives and its copolymers for chemical gas sensing applications ”, Doktorandentreffen der Gassensorik/Gasmesstechnik, Tübingen, Germany, 19-20 Sept. 2013, (Oral Presentation)

Sudam Pandule, Elena Tuccori, Alexandru Oprea, Nicolae Barsan, Udo Weimar, Krishna Persaud, “Biosensors based on pig odorant binding proteins and their characterization using Kelvin probe method”, Workshop on Material Science & Technology, Bari, Italy, 18th Jan. 2012 (Poster Presentation)

Congress of the European Chemoreception Research Organisation, ECRO 2011, Manchester, UK, 7-10 Sept. 2011 (Participation)

GOSPEL workshop on gas sensors based on semiconducting metal oxides: basic understanding and applications, Tübingen, Germany, 6-7 June 2011 (Participation)

Curriculum Vitae

Sudam S. Pandule

Date of Birth : 22nd April 1985
Marital status : Married
Nationality : Indian
Permanent Address : At-Bhavadi, Post-Hiradgaon, Tal-Shrigonda, Dist-Ahmednagar,
Maharashtra, India-413 701.
E-mail : sudampandule@gmail.com

Education

- **Ph. D., Pursuing since March 2011**
 - Department of Chemistry, Institute of Physical & Theoretical Chemistry, University of Tübingen, Germany and School of Chemical Engineering and Analytical Science, The University of Manchester, UK.
 - Thesis Title: Organic receptors for chemical sensors realized on flexible substrates
 - Supervisors: Dr. Nicolae Barsan, Prof. Dr. Udo Weimar, Prof. Dr. Krishna Persaud
- **Master of Science, Organic Chemistry, 2005-2007**
 - University of Pune, India
 - Grade: First class
- **Bachelor of Science, Chemistry, 2002-2005**
 - University of Pune
 - Grade: First class with distinction

Work Experience

- Research Chemist at Innovation Centre, TATA Chemical Ltd. Pune, India. April 2010 to Feb. 2011

- Research Chemist at Dept. of Organic synthesis, Chembiotek Research International Pvt. Ltd. Pune, India. June 2007 to March 2010